UNIVERSITY *of the*
WESTERN CAPE

Faculty of Natural Sciences

Department of Earth Science

Characterization of flowpaths to improve the prediction of vegetation impacts on hydrological processes in semi-arid mountainous catchments of the Cape Fold Belt.

By

Faith Tatenda Jumbi

A thesis submitted in fulfilment of the requirements for the degree of Doctor of Philosophy

Supervisors

Prof D. Mazvimavi

Dr. J Glenday

November 2021

Characterization of flowpaths to improve the prediction of vegetation impacts on hydrological processes in semi-arid mountainous catchments of the Cape Fold Belt.

Keywords
Groundwater

Surface water

Connectivity

Soil water content

Landcover change

Palmiet

Black wattle

Isotope hydrology

Physico-chemistry

Hydrological modelling

ABSTRACT

Characterization of flowpaths to improve the prediction of vegetation impacts on hydrological processes in semi-arid mountainous catchments of the Cape Fold Belt

Faith Jumbi

Ph.D. Thesis, Earth Science Department, University of the Western Cape

Mountainous areas are important water sources in many landscapes. An understanding of how mountainous catchments function is important particularly in semi-arid areas, where water shortages are prevalent. In addition to climate and physiographic factors, the hydrological responses of mountainous catchments can be influenced by land uses and land cover types. Although the general effects of land use and land cover types on hydrological processes are known, prediction of the specific effects in a given catchment is still problematic. This study characterized flowpaths, and hydrological responses to different land cover types in a semi-arid, mountainous Kromme River catchment (Eastern Cape province of South Africa), located in the Cape Fold Mountains of the Table Mountain Group (TMG) geological region. This was done to improve the simulation of vegetation impacts on processes through a customized data-informed model structure. Hydrological processes and flowpaths were characterized using streamflow data, deep and shallow groundwater levels, environmental isotopes, and hydrochemistry data. The data collected was then used to inform a distributed structure in the MIKE SHE modelling platform for simulation of processes. Selected scenarios of possible changes in areas invaded by wattle trees (*Acacia mearnsii*) in different locations in the catchment were modeled with 10 years of climate data. Key results from the study are summarized below.

Kromme has both steep areas (mountainous terrain) and flat floodplain areas with significant alluvial deposits, therefore processes varied due to the diversity of topographic characteristics, geomorphological factors and precipitation inputs. Surface and subsurface flows from perennial tributaries, originating in the mountains, were significant in recharging the central valley floodplain alluvial aquifer and maintaining streamflow in the main channel even during dry periods. Furthermore, the floodplain alluvial aquifers made significant contributions to catchment storage and outflows as shown by hydrometric data. Tracer patterns confirmed this by indicating continuous groundwater contribution to surface flows. Chemical separations from snapshot samples showed that the alluvial aquifer contributes high proportions of flow to the river (contributions up to 96% during dry periods). Low average annual runoff coefficients (0.09) implied large ET withdrawals from dominant flowpaths and/or storage in inactive groundwater as the catchment was monitored in a

relatively dry period. Isotope tracer samples showed that water in the main channel became increasingly enriched moving downstream likely due to evaporation, but showed depletion in areas where mountain tributaries discharge into the main river. Water from tributaries was depleted due to contributions from the fractured TMG bedrock aquifer. This indicated the importance of surface and subsurface contributions from the mountains that recharge the alluvial aquifer and contribute to river flows.

Soil water content varied significantly under the three monitored land cover types in the floodplain namely black wattle (*Acacia mearnsii*), palmiet (*Prionium serratum*), and grass (*Pennisetum clandestinum spp*). In general, rainfall of 30 mm/day was required for significant changes in soil water content (SWC) to be observed across all sites. High SWC was observed at the palmiet site than at the wattle and grass sites. The least SWC was observed at the wattle site due to high transpiration rates associated with black wattle trees. Shallow groundwater levels were within 2 m of the ground surface for prolonged periods in areas with palmiet and grass and below 3 m in areas under black wattle trees. The water table at the wattle site remained below piezometer depths (3 m), only responding after high intensity events (> 40 mm/day).

Simulated results of land cover scenarios for the period 2008-2018 showed a reduction in streamflow and the drawdown of the alluvial aquifer due to increased transpiration rates by woody alien trees. Results indicated that clearing of floodplain black wattle and allowing the regeneration of palmiet could increase groundwater levels by 13%, baseflow by 9% and total outflow by 5%. Simulation results also indicated that ET and streamflow responses to a specific land cover type was not uniformly proportional to the unit area occupied by the land cover but depended greatly on the specific location of the land cover type within the catchment. Alien invading woody species were shown to have increased transpiration and reduced runoff per unit area of cover in riparian areas (0.35 and 0.36 Mm^3/year respectively) compared to drier upland areas (0.09 and 0.07 Mm^3/year respectively).

November 2021

DECLARATION

I, Faith Tatenda Jumbi declare that **"*Characterization of flowpaths to improve the prediction of vegetation impacts on hydrological processes in semi-arid mountainous catchments of the Cape Fold Belt*"** is my work that has not been submitted for any other assessment or degree at another university or academic institution. I also declare that all other sources and quotes used have been indicated and acknowledged by complete references.

Full Name: Faith Tatenda Jumbi

Signature 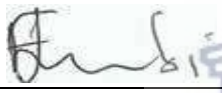 **Date** November 2021

ACKNOWLEDGEMENTS

I would like to thank the following people and organizations for their support during my Ph.D. journey. Without their patience, guidance, and support, this thesis would not have materialized. I owe them my deepest gratitude.

- Research Promoters-Professor Dominic Mazvimavi and Dr Julia Glenday, it was a privilege to have you both as my promoters. I will never forget your unwavering support and your dedication to my work. Thank you for guiding me through this journey; your encouragement and total commitment to my work is greatly appreciated.
- Research Funding-Water Research Commission.
- Research Facilitation- SAEON, Living Lands, and UWC.
- Data-ARC, SAWS, and DWA.

I would also like to thank my family for moral support with special mention to Trevor, Tafadzwa and Kunashe Jumbi; Ivy, Sonia and Eugine Mataramvura, and Plaxedes Jumbi. My friends Paul Chikunichawa, Caroline Haparimwi, Errol Malijani, Nompumelelo Mobe, Caroline Nyangumbe, Yonela Mkunyana, Nolusindisiso Ndara, Zanele Ntshidi, Mandla Dlamini, Retang Mokua, and Siyamthanda Gxokwe; thank you for always being there for me. You made this journey bearable.

Above all, I thank the Lord Almighty for making this dream a reality in his perfect time. *Oluwamoyebo* (God has brought titles), *Oluwamakinde* (God has brought us victory).

DEDICATION

To all women out there pursuing careers in science "*Do not fear difficult moments. The best comes from them*" (Rita Levis-Montalcini).

TABLE OF CONTENTS

LIST OF FIGURES

LIST OF TABLES

LIST OF ABBREVIATIONS

ARC:	Agricultural Research Council
CL:	Chloride
EC:	Electrical conductivity
ET:	Evapotranspiration
PET:	Potential evapotranspiration
PCA:	Principal Component Analysis
HAND:	Height above the nearest drainage
GLUE:	Generalized likelihood uncertainty Estimation
SAWS:	South Africa Weather Services
WMO:	World Meteorological Organization
ORP:	Oxidation-reduction potential
GMWL:	Global meteoric water line
LMWL:	Local meteoric water line
LEL:	Local evaporation line
TMG:	Table Mountain Group
TWI:	Topographic wetness index
CRNT:	Current vegetation cover scenario
PMFP:	Floodplain palmiet cover scenario
WTFP:	Floodplain wattle cover scenario
WTALL:	Maximum wattle invasion scenario

GLOSSARY OF TERMS

Alluvial aquifer	A body of sediment deposited in floodplains and river channels that hold groundwater
Bedrock aquifer	A body of hard or porous rock that holds groundwater usually confined between layers. Water moves through fractures and cracks or the porous rock.
Cape Fold Belt	A belt of mountains formed from the folded and faulted sedimentary rocks by tectonic convergence at plate margins in the Western and Eastern parts of South Africa
Dominant flowpath	The largest contributor to mean annual runoff leaving the catchment
Flood peak	The crest or the highest value of an inflow at any point in the river channel
Floodplain	A flat land adjacent to a river stretching from the banks of a channel to an enclosing valley wall, this area tends to be inundated during high flows
Interflow	Water moving laterally in the vadose zone
Land use	The management of the earth surface, human inputs and utilisation.
Land cover	The biophysical state of the surface and upper subsurface.
Piezometer	A small diameter borehole used to measure groundwater levels
Riparian zone	An area near the channels, this includes the floodplains, extending further into the dry lands. The riparian zone functioning is assumed to be highly influenced by the wetland
Recession	The depletion of streamflow during dry spells or periods of little or no precipitation
Sub-Surface Water	Water beneath the ground surface

CHAPTER 1: INTRODUCTION

1.1 Background

Mountainous areas are major sources of freshwater globally. Mountains supply freshwater by generating substantial streamflow and these areas are especially important in semi-arid and arid regions that are highly susceptible to water shortages and increasing conflicts over water use and allocation (Viviroli et al., 2011, 2007; Viviroli and Weingartner, 2004). In humid areas, mountainous areas are known to contribute 20-50% of regional river flows, whilst in semi-arid and arid regions they contribute 50-90% (Viviroli et al., 2011). Physiographic features of mountainous areas, such as high elevations and deeply incised narrow valleys, influence complex meteorological patterns (von Freyberg, 2015). High altitudes in mountainous catchments result in low temperatures and therefore low evapotranspiration rates (Wilson and Guan, 2013, 2004). Due to orographic effects, mountains generally receive more precipitation compared to surrounding lowlands (Burke, 2009; Wilson and Guan, 2013, 2004). As precipitation rates and intensities are high in the mountains, a larger proportion becomes runoff (McDonnell and Kendall, 1992; Wenninger et al., 2008).

Runoff formation in mountainous catchments is, however, a complex phenomenon that needs an understanding of how rainfall is partitioned into surface and sub-surface flows at different spatial and temporal scales (Becker, 2005). Knowledge of flowpaths can give an idea of the catchment's residence time (Grande et al., 2020; Zhou et al., 2021), runoff source areas (Wenninger et al., 2008) and connectivity between hillslopes and floodplain plains (Ochoa et al., 2013; Okin et al., 2015). A diversity of flowpaths may be dominant at different spatial and temporal scales as the underlying geology and the complex topographic properties give rise to different response characteristics in various topographic landscape units such as plateaus, cliffs, and hillslopes (Savenije, 2010). In the past, runoff generation mechanisms and the associated flowpaths have mainly been investigated in headwater catchments in humid environments (Becker, 2005; James and Roulet, 2009; Penna et al., 2011; Zhao et al., 2019). Our understanding of these processes in semi-arid catchments at the meso-scale is still inadequate, particularly in mountainous areas. Studies of runoff generation processes, streamflow characteristics, and water sources in semi-arid mountainous catchments have been limited due to topographic complexities, inaccessibility and climatic factors. Given the heterogeneous and episodic rainfall, and surface flows, long datasets and/or multiple data types (groundwater levels, soil moisture etc.) are needed to gain insights about processes in semi-arid catchments. In general, several studies in semi-arid catchments have found that groundwater or subsurface flow contributions (60-90%) can dominate long-term average

runoff (Hrachowitz et al., 2011; Saraiva Okello et al., 2018; Wenninger et al., 2008). However, there is significant variability in the proportion of subsurface flows across catchments.

The Kromme catchment which lies in the Eastern Cape Province in South Africa was selected as a case study site to gain insights into the hydrological functioning of a mountainous catchment in a semi-arid setting. The Kromme catchment is regionally important for water supply as it supplies water to the Nelson Mandela Metropolitan (NMM) which has been experiencing severe water shortages since 2010. The Kromme forms part of the Cape Fold Belt which is a series of mountains in the western and eastern parts of South Africa formed from the folding and faulting of sedimentary rocks by tectonic convergence at plate margins (Colvin et al., 2009; Xu et al., 2009). The Table Mountain Group (TMG) is one of the dominant formations within the Cape Supergroup. Groundwater occurs due to the dominance of faults and fractures in the TMG which influence dynamic processes of aquifer storage, recharge and discharge in catchments (Roets et al., 2008; Xu et al., 2009). Previous studies in some parts of the TMG have shown that groundwater is discharged through valley bottom wetlands, seeps, springs, and as baseflow in river channels indirectly via alluvial aquifers or where the river intersects the bedrock (Colvin et al., 2003; Roets et al., 2008). Other TMG studies have shown that significant portions of river flows are from interflow from the soil/rock interface or the highly fractured bedrock (Lin et al., 2007; Xu et al., 2009). Interflow also contributes significant portions of water to wetlands in valley bottoms and recharge to alluvial aquifers (Roets et al., 2008; Smith and Tanner, 2019; Xu et al., 2009).

The hydrological responses of mountainous catchments are also influenced by land use and land cover types dominant in a catchment and/or changes thereof (Viviroli and Weingartner, 2004). Land use and land cover changes are common across the globe, for example, encroachment of the riparian zones by alien woody species has become a problem in many countries e.g. willows (*Salix spp*) in Australia, salt cedar (*Tamarix spp*) in America and the black wattle (*Acacia mearnsii*) in South Africa (Doody et al., 2011; Huxman et al., 2005; Le Maitre et al., 2015). In the Kromme catchment, the Australian black wattle predominantly invaded riparian areas where soil water is readily available (Rebelo et al., 2015) and competes aggressively with the native vegetation such as fynbos, palmiet, and grass (Chamier et al., 2012; Rebelo et al., 2015). This has resulted in the loss of indigenous palmiet (*Prionium serratum*) wetlands. Previous work has shown considerably higher water use by Acacia species invasions compared to the indigenous fynbos and grass they often replace. These plants cause lowering of water tables and reducing groundwater discharge to rivers as well as altering subsurface flow connectivity between hillslopes and streams (Dye and Jarmain, 2004; Galatowitsch and Richardson, 2005; Görgens and Van Wilgen, 2004; Le Maitre et al.,

2015, 2000; Rebelo et al., 2015). Clearing of alien woody species often results in increases in groundwater recharge and river flows (Albhaisi et al., 2013; Moyo et al., 2009; Scanlon et al., 2005). Most of the previous work has examined changes in river flows after clearing without including the impacts on soil water content and groundwater (Görgens and Van Wilgen, 2004; Le Maitre et al., 2015). Furthermore, there is a gap in the scientific understanding of effects of the mosaic of land use and land cover changes on hydrological responses at medium to large spatial scales at which most water resources management decisions are made (Le Maitre et al., 2015; Nolin, 2012; Sanyal et al., 2014). The extrapolation of results from studies in small mountainous catchments to large catchments with combinations of significant upstream headwater, hillslopes and valley bottoms is likely to be problematic.

Numerous methods have been adopted to characterize processes, each of which gives specific insights into water storage, sources, interactions, and the spatio-temporal variations in hydrological processes under various climatic conditions and at different spatial scales. In addition to classical hydrometric techniques, isotope tracers have been useful in providing new insights into the hydrological functioning of catchments. Tracers complement other hydrological methods to characterize sources, flowpaths, and water residence times (Wenninger et al., 2008). Furthermore, the spatiotemporal variability of tracer patterns can be used meaningfully to quantify runoff components (Camacho Suarez et al., 2015; Hugenschmidt et al., 2014; Wenninger et al., 2008) and parameterize hydrological models (Saraiva Okello et al., 2018). In addition to isotopes, geochemical tracers such as electrical conductivity (EC) have also been used to improve hydrological process understanding (Penna et al., 2014).

To gain further insights into the hydrological functioning of mountainous areas and responses to selected scenarios of land use and land cover types particularly at large spatial scales, hydrological modelling presents a useful tool in this context. However, hydrological modelling is challenging particularly in mountainous catchments due to the pronounced temporal and spatial heterogeneity and in most cases, the lack of both hydrological and meteorological data to force and validate models (Hood and Hayashi, 2015). Most observation networks are inadequate to capture the heterogeneity (Morán-Tejeda et al., 2015). At the same time, as computing power increases, models are becoming more sophisticated with codes and routines being added to represent processes at finer scales (Orth et al., 2015). Such developments have given rise to debates regarding whether increased sophistication in a model necessarily results in improved performance or if the solution lies in the choice of structure used and how it represents internal processes (Gharari et al., 2014; McMillan et al., 2011; Orth et al., 2015; Savenije, 2009).

The problems associated with finding the most appropriate model structure for particular processes are due to the lack of understanding of the differences between the models and how they represent processes, resulting in the indiscriminate use of models with predefined structures (Clark et al., 2008). To avoid this, available data can be used for a systematic analysis to get indications of patterns and thresholds for the occurrence of certain processes. These patterns and thresholds can then be used in the development of the model structure (McMillan et al., 2011). For example, an analysis of baseflow recession can be used to assess the influence of storage on the catchment outflow and in turn inform the decision on the type and number of reservoirs to use in the model. Furthermore, the temporal variation of baseflow recession can be a good indicator of evapotranspiration (ET) effects on storage (Clark et al., 2011; McMillan et al., 2011). Additionally, isotope and geochemical tracers can be used to quantify runoff components from different sources (Camacho Suarez et al., 2015). Such knowledge can be used to improve how internal processes are represented in model structures as well as the validation of simulated results. Most studies of this nature have focused on first order headwater catchments, wet environments, with relatively little research on meso-scale catchments in arid semi-arid mountainous environments.

1.2 Research Aim

The overall aim of this study is to improve the understanding of streamflow generation, flowpaths, and vegetation impacts on hydrological responses in semi-arid, meso-scale, mountainous catchments.

1.3 Study Objectives

The study specifically seeks to:

- Determine streamflow characteristics and dominant flowpaths linking landscape units in a semi-arid mountainous catchment of the Cape Fold Belt.
- Assess the temporal variation in patterns of soil water content and water table responses to rainfall under three vegetation types: indigenous palmiet (*Prionium serratum*), invasive black wattle trees (*Acacia mearnsii*), and grassland (*Pennisetum clandestinum spp*).
- Improve hydrological process understanding from the spatio-temporal variability of water chemistry and tracer patterns in a semi-arid mountainous catchment.
- Assess the potential impacts of selected likely scenarios of future land cover change on the hydrological response of a semi-arid meso-scale, mountainous catchment.

1.4 Thesis Layout

This thesis comprises 8 chapters with Chapter 1, 2, 3 and 8 presenting the introduction, literature review, description of the study area and conclusions respectively. Chapters 4 to 7 each cover one of the research objectives. These chapters have been written following the format for scientific journal papers with the ultimate intention that each of these chapters will be submitted for publication with minor modifications. Thus each chapter has sections expected in a journal paper such as abstract, introduction, methods, results and discussion. Because of the format used, there is some slight repetition of the description of study area in chapters 4 to 7.

Chapter 1 gives a general introduction of the thesis highlighting the background, justification and significance of the study.

Chapter 2 presents a review of the literature which elaborates on the research gaps and explores some of the methods used to investigate the research gaps.

Chapter 3 describes the study area and research design.

Chapter 4 characterizes dominant flowpaths and describes the spatial and temporal variability of streamflow characteristics in the Kromme catchment.

Chapter 5 presents the spatio-temporal patterns of floodplain soil water content and water table responses to rainfall under different vegetation types.

Chapter 6 focuses on improving hydrological process understanding from the spatio-temporal variability of water chemistry and tracer patterns from different sources in the catchment.

Chapter 7 presents the structuring of a distributed hydrological model using decisions made from field data and simulation of impacts of selected vegetation types on hydrological processes.

Chapter 8 gives a synthesis of the main research findings, over-arching conclusions, and recommendations for further work.

CHAPTER 2: LITERATURE REVIEW

2.1 Introduction

This chapter presents a review of topics related to characterization and simulation of hydrological processes in semi-arid, meso-scale mountainous catchments. Understanding hydrological processes in catchments enables improved conceptualization of processes. The conceptualized processes can then be translated into predictive models for streamflow estimation under different scenarios of land use and land cover types as well as climatic conditions. In turn, this will inform appropriate water resource management strategies for sustainable ecosystems and future water security, particularly in semi-arid mountainous catchments. Separate research components that describe flowpaths and connectivity between different topographic landscape units, streamflow characteristics, and land use and land cover impacts are addressed in the following sections. Furthermore, an overview of methods for characterization of processes to gain insights into the hydrological functioning of catchments such as the classic hydrometric methods, isotope tracers, and hydrological modelling is also given.

2.2 Hydrological process understanding in mountainous catchments

A mountain is defined as a portion of the earth's crust which is elevated and rising abruptly by at least 300 m from its surrounding area, comprising steep slopes and characterised by distinct variations in local climate from the valley bottom to its summit (Barry and Price, 1981). Mountainous catchments are major sources of water supply across the world (Viviroli et al., 2011). They are biodiversity centres utilized by more than one billion people around the world for ecosystem goods and services (Viviroli and Weingartner, 2004). Some of the critically important mountain regions for water supply are the Eastern Arc Mountains (Iddi, 1998), Andes and the Rocky Mountains (Kohler and Maselli, 2009) Drakensburg and Cape Fold escarpments in South Africa (Colvin et al., 2009; Taylor et al., 2016; Xu et al., 2009). In South Africa, the Cape Fold Belt is one of the most important sources of fresh water in the Western and Eastern parts of the country.

2.2.1 The Cape Fold Belt and Table Mountain Group

The Cape Fold belt in South Africa comprises a series of mountain ranges (peaks reaching up to 2250 m.a.s.l) formed from the folded and faulted sedimentary rocks due to tectonic convergence at plate margins (Colvin et al., 2009; Xu et al., 2009). The Cape Fold Belt region is made up of a few geologic formations collectively known as the Cape Supergroup; the Table Mountain Group

(TMG) is one formation within the Cape Supergroup. The TMG is the dominant remaining geology of the mountains whereas the other overlying groups have largely eroded away on high terrain and are mostly found in the valleys. The dominance of faults and fractures in the TMG influences aquifer storage, recharge and discharge in catchments within the TMG aquifer zone (Roets et al., 2008; Xu et al., 2009). Groundwater from the high yielding TMG fractured sandstones is crucial for water supply in the arid and semi-arid areas of the Cape region (Xu et al., 2009). Previous studies in TMG regions have shown that groundwater is generally discharged through valley bottom wetlands, seeps, springs, and as baseflow in river channels indirectly via alluvial aquifers or where rivers intersect the bedrock (Colvin et al., 2009; Midgley and Scott, 1994; Roets et al., 2008). Fractured rock aquifer systems are complex to conceptualize. Flow direction has been shown to be dynamic and controlled by the geological structure and nature of the fractures and faults (Xu et al., 2009, 2002). Due to differences in uplifted fault blocks and the hardness of other TMG layers, the main valley also varies in width. Some areas have wide widths (>1km wide) whilst other sections are narrow (100-500m). Previous research in the TMG indicated that interflow from the highly fractured bedrock and soil-bedrock interface contributes significantly (>50%) to streamflow and wetland hydrographs (Midgley and Scott, 1994; Roets et al., 2008; Xu et al., 2002). However, determining the nature of flowpaths in these catchments is difficult due to the non-uniformity of fractures (Xu et al., 2009) but understanding these flowpaths, sources and runoff generation is crucial for strategic management of water resources in mountainous catchments.

2.2.2 Hydrological process understanding in semi-arid mountainous catchments.

Mountainous catchments generally receive more precipitation than surrounding lowlands, making them important freshwater sources particularly in arid and semi-arid areas where water availability is limited (Burke, 2009). A combination of features result in the relatively high rainfall and runoff production in mountains compared to lower terrain. Physiographic features of mountainous areas, such as high elevations and deeply incised narrow valleys, influence complex meteorological patterns (Viviroli et al., 2003; von Freyberg, 2015). Rainfall patterns are characterized by high-intensity storm events. As precipitation intensities are higher in the mountains, a larger proportion becomes runoff received by the rivers, thereby sustaining ecosystems, agriculture as well as surrounding industries in lowlands (Burke, 2009). Depending on catchment size, different processes and flowpaths may be dominant at different scales and times in these catchments. In a multi-scale study, McGlynn et al. (2004) found that riparian areas were consistent streamflow sources in small headwater catchments, whilst in larger

catchments, contribution to streamflow from the valley bottom areas was only after high rainfall events. Surface and shallow subsurface runoff has been generally observed as first order determinants of streamflow generation patterns for micro-scale headwater catchments (<1km^2); whilst in meso-scale catchments (>10km^2), rainfall spatial distribution is a major controlling factor (Uhlenbrook et al., 2004). Meso-scale mountainous catchments can comprise both steep headwater areas and sometimes sizeable floodplains, including a range of topographic and geologic features with different response characteristics. As such, as catchment scales increase, there is a possibility of an increasing proportion of groundwater from the bedrock to total catchment outflows (Orlova and Branfireun, 2014). In these mountainous catchments, the bedrock is either porous and/or highly fractured, the soils are usually thin and fast draining. There is therefore increased percolation into bedrock aquifers and contributions from the bedrock aquifers recharge the alluvial aquifer and contribute to catchment outflows, with estimated values of 10-70% of recharge or outflow (Katsuyama et al., 2010; Stoelzle et al., 2020; Welch and Allen, 2012).

In humid regions, mountains supply 20-50% of the total discharge whilst in arid and semi-arid areas, they supply 50-95% (Viviroli and Weingartner, 2004). Understanding hydrological processes in mountainous areas particularly in semi-arid regions is challenging. This is because arid and semi-arid regions are prone to droughts and floods sometimes as a consequence of global change drivers such as climate and land-use and land cover changes (Misra, 2014). Therefore, resource management in most semi-arid mountainous catchments in Southern Africa suffers from a general lack of process knowledge (Hughes, 2007). The structurally complex geology and rugged terrain in mountainous catchments limits access to establish monitoring networks thereby limiting the availability of data needed to improve and validate models and improve our process understanding (Somers and McKenzie, 2020).

There are limited studies on runoff generation processes, streamflow characteristics, and water sources in semi-arid catchments, due to topographic complexities and climatic factors. Nevertheless, studies that exist show that more than 60% of long-term average runoff comes from groundwater or subsurface flowpaths contributing large portions of outflow in mountainous catchments. For example Yeh et al. (2014) showed mountain aquifers contributed up to 83% of streamflow whilst direct rainfall accounted for 17% in a semi-arid catchment. Zhou et al. (2015) found that baseflow accounted for up to 67% of runoff in the meso-scale Shule catchment in the Qilian Mountains (northern China). Wenninger et al. (2008) suggested that

almost 90 % of contributions to river flows were from groundwater during the dry season in a semi-arid catchment in South Africa (Weatherly). In another study in the semi-arid Kaap catchment in South Africa, groundwater contributed between 64-98% to the total runoff in the catchment depending on the season (Camacho Suarez et al., 2015). In other studies i.e. semi-arid Makanya catchment in Tanzania, results showed that surface and shallow subsurface runoff dominated after storms (Mul et al., 2009, 2008). Some studies have shown that runoff generation is mainly a result of "new water" displacing "old water" that has been stored in the catchment even in storm events (Ala-aho et al., 2018; Midgley and Scott, 1994). In the Jonkershoek catchment, South Africa, peak flows were found to be mostly old water getting pushed into the stream (i.e. new water from the rain enters soil and rock fractures further up and pushes out the older water to the river) despite Jonkershoek being quite a steep, mountainous catchment (Midgley and Scott, 1994). Other studies have indicated that streamflow is dominated by delayed interflow during dry periods while during wet months, direct runoff was the major contributor to streamflow (Bosch et al., 2017; Jovanovic and Clercq, 2012). In addition to physiographic factors and climate, streamflow in a catchments is also influenced by land use and land cover types and changes thereof (Morán-Tejeda et al., 2015).

2.3 Vegetation impacts on hydrological processes and responses

Schulze (2000) defines land use as the management of the earth's surface, human inputs, and utilization, whilst land cover is the biophysical state of the surface and upper subsurface. Hydrological processes are sensitive to, and influenced by, land use and land cover types and changes thereof (Warburton, 2012). Rainfall received in a catchment is partitioned into various fluxes and pathways via processes such as infiltration, evapotranspiration (ET), and runoff influenced by land use and land cover types amongst other factors. The extent to which land cover types influence hydrological responses depends not only on the spatial area covered, but also the location of the land cover type within the catchment (Le Maitre et al., 2015). General impacts are determined by size, woodiness, leafy-ness, root depth and stand density, which affect canopy interception, soil properties and infiltration, total water use and the seasonal pattern of use from groundwater and soil. The density of vegetation and composition as well as the different structural groups of plants present (herbaceous, shrubs, trees, etc.) has been found to influence catchment-scale hydrological process and hence ecosystem functions, such as the dynamics of droughts, generation of floods, and groundwater recharge (Nijzink et al., 2016).

Changes in land cover types, such as woody plant clearing or woody plant invasion in areas previously dominated by grass and other herbaceous species, can have impacts on both floodplain subsurface hydraulic processes and soil moisture dynamics (Wang et al., 2012; Zhang et al., 2020). The monitoring of soil moisture dynamics provides insights into patterns of infiltration, storage, and percolation as well as vegetation water uptake in the active root zone. Soils can play a fundamental role to improve the understanding of interactions between groundwater and surface water as they store water, control residence times as well as the partitioning of hydrological flowpaths in a landscape (Kellner and Hubbart, 2016; le roux et al., 2015). Monitoring changes in soil moisture, as well as the water table, gives insights into larger-scale processes of ET (evapotranspiration), storage, and recharge (Legates et al., 2011; Wang et al., 2012). For example, McMillan et al. (2011) inferred the rate of drainage and water retention processes as well as ET from monitoring and analysing soil wetting and drying after rainfall events. Understanding soil moisture dynamics give insights into the hydrological response of a landscape to impacts of different land cover types (Burke, 2009).

Invasive alien woody species are a common cause of land cover change in South Africa and particularly known to have high water use compared to indigenous vegetation (Calder and Dye, 2001; Le Maitre et al., 2015). Black wattle *(Acacia mearnsii)* is one type of alien woody plant in South Africa used for timber and other commercial purposes, which has rapidly spread beyond planted areas (Moyo et al., 2009). Black wattle invades riparian areas in most cases, where soil moisture is readily available (Dye and Jarmain, 2004) and competes with the native vegetation such as fynbos, palmiet, and grass communities. Black wattle alters the catchment's hydrological regime and ecosystem function by increased rates of evapotranspiration, lowering of water tables, and reduction in streamflow and recharge rates (Dye and Jarmain, 2004; Galatowitsch and Richardson, 2005; Görgens and Van Wilgen, 2004; Le Maitre et al., 1999). In some cases, after clearing the woody alien species, groundwater recharge and river flows increased (Albhaisi et al., 2013; Moyo et al., 2009).

Several studies in South Africa have investigated the impacts of woody alien plants on hydrological processes in invaded catchments (Le Maitre et al., 2015, 2000; Morris et al., 2011; Moyo et al., 2009). Reductions in river flows following alien woody species invasions in the Western Cape and KwaZulu Natal provinces were quantified and showed reductions ranging from 55% to 82% respectively (Chamier et al., 2012). In areas such as Mpumalanga and parts of the Eastern Cape, some rivers dried up following establishment of plantations or invasions

(Chamier et al., 2012). Clearing of invasive trees saves water but actual volumes depend on the species water use, location in the landscape, and the water use characteristics of vegetation established after clearing (Doody et al., 2011). For example in two semi-arid areas in the USA and Australia, studies showed that high ET rates due to alien invasive trees (salt cedars and willows respectively) in riparian areas negatively affected groundwater and river flows. Nevertheless, the same study also showed that some indigenous vegetation had similar ET rates as the invaders (Doody et al., 2011). Efforts are being made worldwide to restore degraded river systems (Kurth et al., 2015; Kurth and Schirmer, 2014; Muhar et al., 2016). In South Africa, the Working for Water Programme was established to control the impacts of invasive alien plants on ecosystems and water resources in particular (McConnachie et al., 2012). However, further research is still needed to support informed decision making for such programmes.

The majority of studies on impacts of land use and land cover change on hydrological processes have only considered reductions in river flows, but have not explicitly shown the impacts on shallow and deep groundwater levels (Görgens and Van Wilgen, 2004; Gyamfi et al., 2016; Le Maitre et al., 2015). In some arid and semi-arid settings, studies have shown that additional water supply can be found from groundwater contributions in riparian and floodplain areas after clearing invasive species (Dye and Jarmain, 2004; Salemi et al., 2012). Plants of the same species use more water in riparian areas where it is readily available than in uplands and dry areas (Le Maitre et al., 2015). Therefore, the impacts of land use and land cover changes on groundwater levels especially in floodplain and riparian zones where invasions have greater impacts need to be considered.

The impact of changes in land cover types on hydrological processes can be monitored and assessed with relative ease at small scales, compared to large catchment scales where the distinction of impacts from individual changes becomes difficult. Studies in land cover change scenarios often utilize models to assess the projected likely hydrological response of catchments (Aduah et al., 2017; Gyamfi et al., 2016). This can be achieved by simulating scenarios of land use and land cover change using hydrological models with structures that are sensitive to cover changes and which can conceptualize and adequately represent hydrological processes (Devia et al., 2015). This is however, challenging as both hydrological and meteorological data to drive the models are limited particularly in mountainous areas (Viviroli et al., 2011), whilst the heterogeneity and complexity of processes in these areas require high-resolution models that are data demanding. The majority of such modelling studies have shown that different changes in

land use and land cover contributed to various effects in the annual water yield and ET in the respective catchments i.e. the White Volta Basin in West Africa (Awotwi et al., 2015), Kromme catchment, South Africa (Cornelius et al., 2019; Rebelo, 2012) and Mngeni, Luvuvu and Upper Breede catchments, South Africa (Warburton, 2012). The location of a land cover change in a catchment is crucial when evaluating impacts of land cover change on runoff and groundwater per unit area of change i.e. riparian vs. dryland. Le Maitre et al. (2015) showed that woody alien invasive plants have greater impacts in riparian settings where water is not limited and the water tables is shallow compared to upland invasions. In their study, invasive trees of the same species used 1.5–2.0 times more water in riparian areas than in upland (drier) areas. Warburton (2012) also concluded that streamflow contributions in response to a specific land cover type were not equally proportional to the unit area occupied but was dependant on the location of the land cover within the catchment.

Similar to any other landscape, mountainous catchments are sensitive to land use, land cover and changes thereof (Morán-Tejeda et al., 2015). Mountainous catchments can include small floodplain areas and although they are not extensive spatially, land cover change in them can be important. Some of the valley bottoms in mountainous catchments comprise floodplain wetlands, however, these wetlands are diminishing due to land use and land cover change (Vörösmarty et al., 2010). For example, historically, the Kromme valley bottom was dominated by *Prionium serratum* (palmiet) wetlands but due to the encroachment of the black wattle *(Acacia mearnsii)*, these wetlands have been degraded. Palmiet is a wetland plant regarded as an environmental engineer because of its extensive root system that reduces the velocity of flow in channels and trapping sediments thereby stabilizing the channels and reducing sedimentation in dams respectively (Sieben, 2012). Land cover changes such as degradation of palmiet wetlands either by alien encroachment or removal for agriculture results in the destabilization of the river channels. In general, the overall response of a catchment is therefore influenced by the spatial distribution of land cover types and changes thereof in the entire catchment as well as the balancing or cancelling effects of those land use and land cover types (Sanyal et al., 2014).

2.4 Monitoring and characterization of hydrological processes

Management of water resources requires accurate analysis and understanding of hydrological processes in a catchment (Soulsby et al., 2016; Wenninger et al., 2008). This is achieved through various methods including hydrological modelling. However, reliable hydrological modelling

requires data for validation, which may not always be available. Furthermore, measured streamflow data alone may not always be sufficient for model validation (Eckhardt, 2005). Sound knowledge of internal processes becomes important. Numerous methods have been adopted to characterize and quantify hydrological processes, each of which gives specific insights into water storage, sources, hydrochemistry, interactions, mixing, etc. Such methods and techniques include hydrometry, geophysics, and tracer experiments (Tetzlaff et al., 2010). Each method has strengths and weaknesses in terms of the scale of application, cost, and the quality of information it can yield. Therefore, many researchers have adopted the multi-method approach to get a comprehensive understanding of the system (Böhme et al., 2016; Madlala et al., 2019; Ramatsabana et al., 2019).

2.4.1 Use of tracers in catchment-scale hydrology

Tracers have been very useful in providing new insights into the hydrological functioning of catchments. They were introduced to complement other hydrological methods and have been useful in hydrograph separation (Gou et al., 2018; Saraiva Okello et al., 2018), determination of water age (Lutz et al., 2018), water sources, flowpath characterization (Correa et al., 2017; Wenninger et al., 2008; Zhou et al., 2015) and until recently, calibration and validation of models (Camacho Suarez et al., 2015; Mosquera et al., 2018). Table 2.1 shows various applications for natural tracers in catchments.

Table 2.1: Tracers and their typical application

Tracer	Application
Temperature	Determine exchange between groundwater and surface water
$\delta^{18}O$, $\delta^{2}H$	Source identification, residence time, recharge rate estimation
Chloride	Deep drainage, mineralization
pH	Origin of runoff components
EC	Origin of runoff components, flowpath length, evaporation processes

(Adopted from Aurecon, 2011)

Environmental isotopes of water, $\delta^{2}H$ (deuterium) and $\delta^{18}O$ are conservative natural tracers which can be used to trace flowpaths. A conservative isotope does not decay or react with other minerals. Their compositions in water change with mixing of water from different sources and from evaporative separation only. They are not affected or changed by interactions with rock minerals and other aquifer materials, thereby allowing the determination of sources in a sample (Vitvar and Aggarwal, 1998). In a river channel, the isotope compositions reflect the inputs from

different sources and any evaporative enrichment occurring along the course of the river. The local and global meteoric water lines (empirical relationship between $\delta^{2}H$ and $\delta^{18}O$ of precipitation) are used to detect evaporative enrichment (fractionation) of different water samples (Midgley and Scott, 1994). Water samples plotting on the meteoric line are assumed to be of atmospheric origin and not altered by other processes, such as open water evaporation, evapotranspiration from soil storage, or mixing with evaporation enriched water. Sources of groundwater can be deduced by analysing where they plot in relation to the meteoric water line. If the isotopic concentration of a groundwater sample plots on or close to the line of precipitation, it means the sample is of meteoric origin, indicating relatively direct groundwater recharge from rainfall, without significant evaporation during storage in a surface water body or soil (Dansgaard, 1964).

Geochemical tracers such as electrical conductivity (EC) and major ions have also been used alone or in combination with stable isotopes to gain insights and improve hydrological process understanding (Camacho Suarez et al., 2015; Penna et al., 2015). EC is non-conservative, which means it will not only give transport, source, and flowpath information, but reactive processes as well (Singha et al., 2011). Spatial variation of EC values in different water bodies are then used to deduce recharge and discharge relationships, as well as sources (Maurya et al., 2011; Song et al., 2006). In some cases, EC is a better alternative tracer to isotopes for process-based hydrological understanding through flow partitioning and hydrological modelling applications. This is because EC can be monitored continuously at higher temporal resolutions using in-situ logging instruments compared to water isotopes which require relatively expensive off-site processing of samples with laboratory instruments (Mosquera et al., 2018).

Many hydrological studies in semi-arid mountainous regions have used isotopes and geochemical tracers to provide insights into the hydrological functioning of catchments. These studies have generally found that, overall, runoff in these environments is dominated by subsurface flow contributions predominantly generated from groundwater with contributions of up to 98% in some cases (Camacho Suarez et al., 2015; Gibson et al., 2016; Guo et al., 2017; Wenninger et al., 2008; Zhou et al., 2015). However, the roles and contributions of different subsurface flow paths (interflow, shallow and deep groundwater) and event response flow contributions vary from catchment to catchment. Tracers are invaluable in identifying and quantifying runoff components which is important in hydrological process understanding particularly in cases where hydrometric data alone is insufficient. Several studies have therefore

acknowledged the importance of combining isotopes and hydrometric data to determine runoff generation in ways that would not have been possible when using just one method (Klaus and McDonnell, 2013; Laudon et al., 2004; Mcdonnell et al., 1999). Studies have tested that using both methods enables the estimation of residence times, and determination of origins and magnitudes of runoff components at different scales (Mul et al., 2009, 2008; Uhlenbrook et al., 2002).

Precise quantification of runoff components remain uncertain at large spatial scales, however, the general patterns and interactions of runoff components at different timescales (event and seasonal) can be identified. There are challenges associated with the application of tracers particularly in semi-arid settings which generally have high inter annual variability and flashy streamflow responses, lack of surface runoff in some cases, and the presence of deep groundwater resources, and high evaporation rates (Camacho Suarez et al., 2015; Hrachowitz et al., 2011; Jackson et al., 2008). Challenges are also experienced in meso-scale, mountainous catchments due to spatial variability; for example getting representative end-member samples for hydrograph separation given the high spatial and temporal heterogeneity. Other studies have therefore, used different indices to identify end members (McGuire and McDonnell, 2010; Ocampo et al., 2006). For example McGuire and McDonnell, (2010) identified hydromorphic soil characteristics that help to identify controlling end-members. Ocampo et al. (2006) used well levels to justify using one pre-event end-member (two-component hydrograph separation) as well data suggested that only one subsurface storage was active during events in a Western Australia agricultural watershed. In a semi-arid Makanya catchment, Tanzania, the applicability of using isotope tracers in identifying the runoff sources at different scales (0.3 km^2 and 26 km^2), was tested (Mul et al., 2008; 2009). However, isotope tracer results were ambiguous (Mul et al., 2008). Their study further showed that hydrograph separation could be applied at smaller scales where spatial variability could be neglected compared to large scales. For a comprehensive understanding of catchment processes, it becomes important to integrate tracer data and classical hydrometric measurements.

2.5 Hydrological Modelling

2.5.1 Development of conceptual models in mountainous catchments

In order to have an accurate conceptualization of hydrological processes in a catchment, a sound knowledge of catchment internal processes is essential. Using diagnostic patterns of soil moisture, streamflow, groundwater, and isotope data, processes such as streamflow generation and dominant hydrological flowpaths can be determined (Clark et al., 2008; Hrachowitz and

Clark, 2017; McMillan et al., 2011). Data analyses involves the assessment of particular responses from available data to infer the occurrence of certain phenomena i.e. assessment of subsurface soil moisture responses (saturation and drainage) to infer on evapotranspiration under different conditions (McMillan et al., 2011). Timing differences between rainfall and streamflow peaks can be analysed to assess subsurface flow responses (slow or quick flow) (Glenday, 2015). Using such information, a conceptual model of catchment processes is developed which will then be translated to a numerical model to simulate processes and test different hypotheses.

Using a conceptual model developed, a catchment can be divided into landscape units with distinct hydrological responses in preparation for numerical modelling (Fenicia et al., 2011; H. Gao et al., 2014). This is because many physical processes that occur in the landscapes have a high correlation with the topographic position of the unit in the landscape (Weiss, 2001). Therefore, units are derived primarily based on topography, but other attributes such as geology, slope, and land use can also be considered (Savenije, 2010). Using the knowledge of the catchment hydrological behaviour, the dominant processes are represented for each landscape unit. Savenije (2010) proposes that in general, storage excess subsurface flow dominates hillslopes; plateaus have vertical drainage thereby recharging the deep groundwater store; and riparian areas are dominated by subsurface drainage and saturation excess overland flow. Flowpaths are therefore, dominant at different spatial scales depending on the landscape unit (Savenije, 2010). Most of these processes are however dependant on precipitation thresholds (Clark et al., 2011).

2.5.2 Catchment scale model structure, data needs, and data availability.

The use of process-oriented models to predict responses of catchments to anticipated scenarios is one of the most adopted methods in hydrology (Morán-Tejeda et al., 2015; Viviroli et al., 2011). Hydrological models are simplified representations of processes to predict system behaviour, future scenarios, and gain insights into the hydrological functioning of catchments. Models are intended for many functions which could be investigative or operational (Montanari et al., 2013). Since the development of the first models i.e. the rational method for peak discharge (Mulvany, 1850) there has been an abundance of models developed which can be used to test different hypotheses (Clark et al., 2011).

There are different types of models ranging from empirical, conceptual to physically based models. Their classification is based on the physical principles applied, parameterization, and input data required (Todini, 2007). Purely empirical models do not always explicitly take into account internal processes; they provide behaviour based on observed numerical relationships without attempting to describe the physical mechanisms generating them. They are data-driven with equations derived from past data on a catchment's inputs and outputs, rather than beginning from quantitative conceptions about physical laws and processes that have been derived externally. Empirical models can have high predictive power in some settings, but low to no explanatory power for investigative changes (Beven, 2001). Conceptual models aim to describe components of catchment hydrological processes. Parameters are assessed through calibration and field data and some empirical equations are used in these models (Fenicia et al., 2011). Physically-based models allow the discretization of a catchment in a distributed or semi-distributed way whilst taking into account the finite equations that represent processes and components of the hydrological cycle (Beven, 1982; Islam, 2015). Input parameters are physical properties of parts of the catchment that could, in theory, be measured in the field. Physically-based models often include a greater number of parameters than other model types and are usually data intensive due to their complex structures.

A model structure is a representation of the catchment's organization and how the different parts are connected (Blöschl et al., 2008). To identify the most appropriate model structure to apply for a given problem, an understanding of differences between model structures is needed (Clark et al., 2008). In fixed modelling approaches, a predefined model structure is selected and various parameter values are calibrated to improve the fit of the model output to the observations from the catchment. Often this relies on model structures that have been built into available software programs, such as SWAT (Arnold et al., 1998), MIKE-SHE (Refsgaard and Storm, 1996) and ACRU (Schulze, 1995). Sometimes the model structure selection is based on data available for the catchment and the understanding of processes, but it may also be driven by the modeller's familiarity with the structure and associated software (McMillan et al., 2011).

The major disadvantage of using fixed approaches is that the model structure selected may not realistically represent dominant processes for the catchments they are being applied to. This results in poor model performance, numerical errors, and ultimately ill-informed decisions based on unreliable simulated outputs (Refsgaard and Hansen, 2010). Beven (2001) emphasized the notion that different processes are important and active at various spatial and temporal scales for various catchments (uniqueness of place). Hence flexible modelling was proposed as a

solution to the problems associated with fixed structure (one size fits all) modelling approaches (Fenicia et al., 2011). The advantage of using a flexible structure is that different hypotheses can be tested using similar or varying model structures (Clark et al., 2008; Fenicia et al., 2008). Furthermore, this approach allows for the comprehensive testing of the different model components on how they represent processes (H. Gao et al., 2014; Gharari et al., 2014; Savenije, 2010). This can be achieved by developing a model structure using information gathered from field data to constrain the model (Mockler et al., 2016). Emphasis has been placed on targeted use of field data and information from the conceptual model to make decisions and inform the model structure, instead of choosing a pre-existing structure independently from the catchment conceptualisation to then be parameterized using available data (McMillan et al., 2011; Glenday, 2015).

Based on a review of several existing modelling platforms such as SWAT (Arnold et al., 1998) and ACRU (Schulze, 1995), the MIKE SHE (Refsgaard and Storm, 1996) modelling platform was selected for use in this study. The MIKE SHE model is an example of a mostly physically-based model that can simulate processes such as surface and subsurface water flow, evapotranspiration, and the complex interactions between groundwater and surface water (Prucha et al., 2016). It can simulate water quality, management and water use related operations, including but not limited to, irrigation and water control structures. However, the model can be set up in varying levels of complexity (lumped, semi-distributed, or distributed) depending on the intended use and data availability thereby allowing the testing of different hypotheses. MIKE SHE includes channel routing, overbank flooding and allows runoff routing across catenas of hydrological response units thereby considering infiltration of flow along the flowpath across different units. Some models do not allow this but instead route the runoff from each modelled unit in parallel to the river channel (Glenday, 2015).

2.5.3 Predictive uncertainty in hydrological modelling

The majority of research in hydrological modelling aims to represent processes occurring at scales of interest which are often difficult or impossible to measure (Beven and Young, 2013; Tanner et al., 2015). Models are then parameterized and calibrated to fit the catchment properties where they are applied. This can lead to uncertainty issues. Problems of uncertainty emanate from a variety of sources: errors in the input data used (could be either incomplete or with flaws), upscaling or downscaling of parameter sets used, and limited knowledge of the catchment's dominant processes (Beven and Young, 2013; Tanner et al., 2015). Input variables are available as point measurements that must be extrapolated for use in the model, land use

and land cover data and soils information can be aggregated as well for the model. Uncertainties also arise from data used in calibration and validation such as streamflow data.

There are several techniques available that can be used to assess uncertainty in hydrological modelling exercises such as Parameter Solution (van Griensven and Meixner, 2007) and Generalized Likelihood Uncertainty Estimation (Beven and Binley, 1992) or accepting sets of parameters that fall within acceptable ranges in a goodness-of-fit measure or acceptable thresholds set (Fenicia et al., 2008). Thresholds can be determined in consideration of the desired use of the model outputs and informed by literature or available data.

2.6 Conclusion

The review of literature highlighted the significance of mountainous catchments for water supply particularly in semi-arid environments where conflicts regarding water use and allocation are increasing. Furthermore, the review highlighted the numerous methods that can be employed to characterize and simulate hydrological responses to different vegetation types. The aim and objectives of this study were formulated based on this review of literature.

CHAPTER 3: DESCRIPTION OF THE STUDY AREA AND RESEARCH DESIGN

3.1 Introduction

The Kromme catchment (Figure 3.1) which lies in the Eastern Cape Province in South Africa was selected as a case study site to gain insights into the hydrological functioning of mountainous catchments in semi-arid regions. The Kromme catchment supplies water to Nelson Mandela Metropolitan (NMM) which has been experiencing severe water shortages since 2010. The Kromme comprises both steep areas and floodplains with significant alluvial deposits and alluvial aquifers therefore presenting an opportunity to study the link between these landscape units and how processes vary due to a broad diversity of topographic characteristics, geomorphological types, precipitation inputs, and land use and land cover types. Different land use and land cover types were hypothesized to influence its hydrological functioning, particularly riparian invasion by black wattle (*Acacia mearnsii*) trees which affect streamflow and recharge processes.

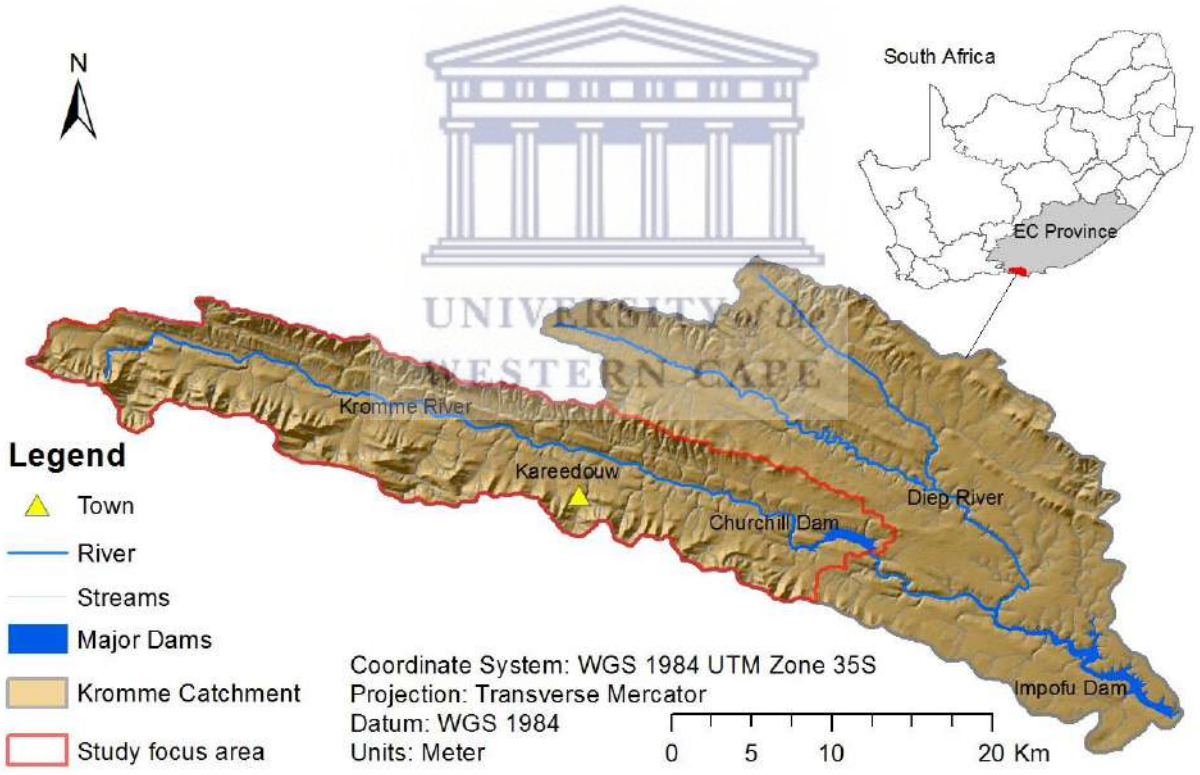

Figure 3.1: The Kromme Catchment and study area, showing major towns and dams.

The Kromme River (Figure 3.1) is bordered by the Suuranys (inland) and the Tsitsikamma (coastal) mountains with elevations of ±1050 metres above sea level (m.a.s.l) and ±1500 m.a.s.l. respectively (Mander et al., 2010). The river drains through a narrow valley between the two mountain ranges which are narrow and steep making their structure unique due to the geological uplifting and folding which took place millions of years ago (Powell and Mander, 2009). The catchment area of the Kromme River catchment is approximately 1560km² from

its headwaters to the estuary (McConnachie et al., 2012). The river starts at an altitude of 550 m.a.s.l. and becomes an estuary draining into the Indian Ocean through St Francis Bay after 100 km (Mander et al., 2010). The focus area for this study is 360 km² from the headwaters to Churchill Dam (Figure 3.1).

3.2 Climate

Rainfall in the Kromme catchment is highly variable with a mean annual of approximately 600 mm/year (Figure 3.2). Rainfall in this catchment has become more variable and decreased over time (Rebelo, 2012). Annual rainfall can be high as 1200 mm/year and as low as 300-400 mm/year. Although rainfall is unpredictable and falls anytime of the year, in the long-term data, most rainfall is received in autumn (February to April) and spring (August to October) compared to summer and winter. Furthermore, rainfall is unevenly distributed spatially within the catchment increasing from inland towards the coast (Lynch, 2004). Data collection took place during the most severe drought in over 30 years. The year 1984 was the driest in the region whilst 2016 and 2017 were third and second driest respectively. The Kromme has mean annual evaporative demand of approximately 1400 mm/year to 1800 mm/year and a mean annual runoff of 75 mm/year. The variability of rainfall gives rise to extremely variable runoff regimes. Average minimum temperatures range from 4-16°C whilst average maximum temperatures fluctuate between 22 and 29 °C throughout the year. Average potential evapotranspiration rates are high in summer and autumn, and lowest in winter (Figure 3.2).

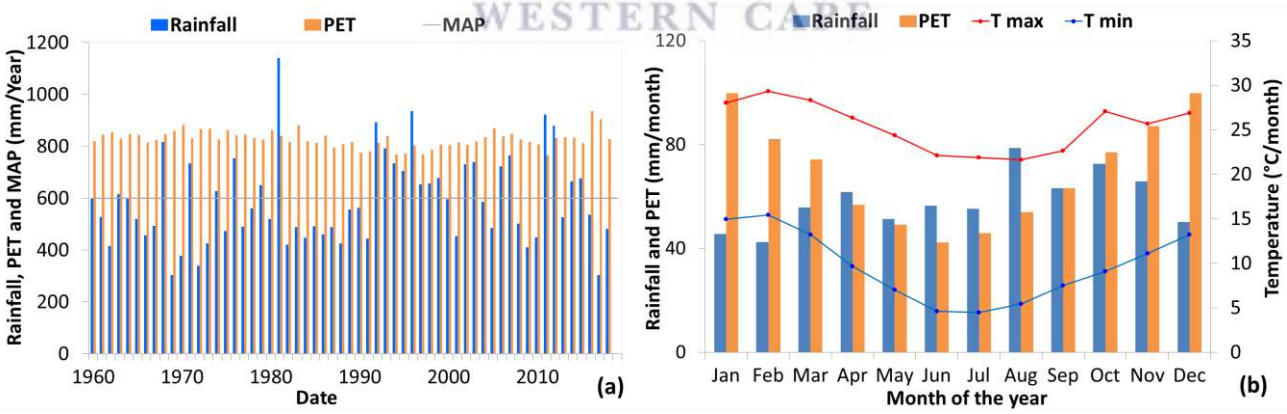

Figure 3.2: Rainfall, PET, MAP from 1960 to 2018 (a) and (b) Rainfall, PET, and minimum and maximum temperatures for the different months of the year

3.3 Geology and Topography

The geology of the Kromme catchment is shown in Figure 3.3. This catchment falls within the Cape Fold mountain region of South Africa which runs for approximately 1000 km in an east to west direction. The Cape Fold Belt comprises a series of mountain ranges with peaks reaching up to 2250 m.a.s.l. and formed from the folded and faulted sedimentary and partially

metamorphosed rocks due to tectonic convergence at plate margins (Colvin et al., 2009; Xu et al., 2009). The region is made up of a few geologic formations collectively known as the Cape Supergroup which consists of quartzitic sandstones and shale. One formation dominant within the Cape Supergroup is the Table Mountain Group (TMG) (Diamond, 2014). The dominance of faults and fractures in the TMG influences dynamic processes of aquifer storage, recharge and discharge in catchments within the TMG aquifer zone (Roets et al., 2008; Xu et al., 2009). The intense folding in the Cape Fold belt resulted in a trellis drainage pattern. The TMG lithology also comprises shales with low permeability which creates aquicludes.

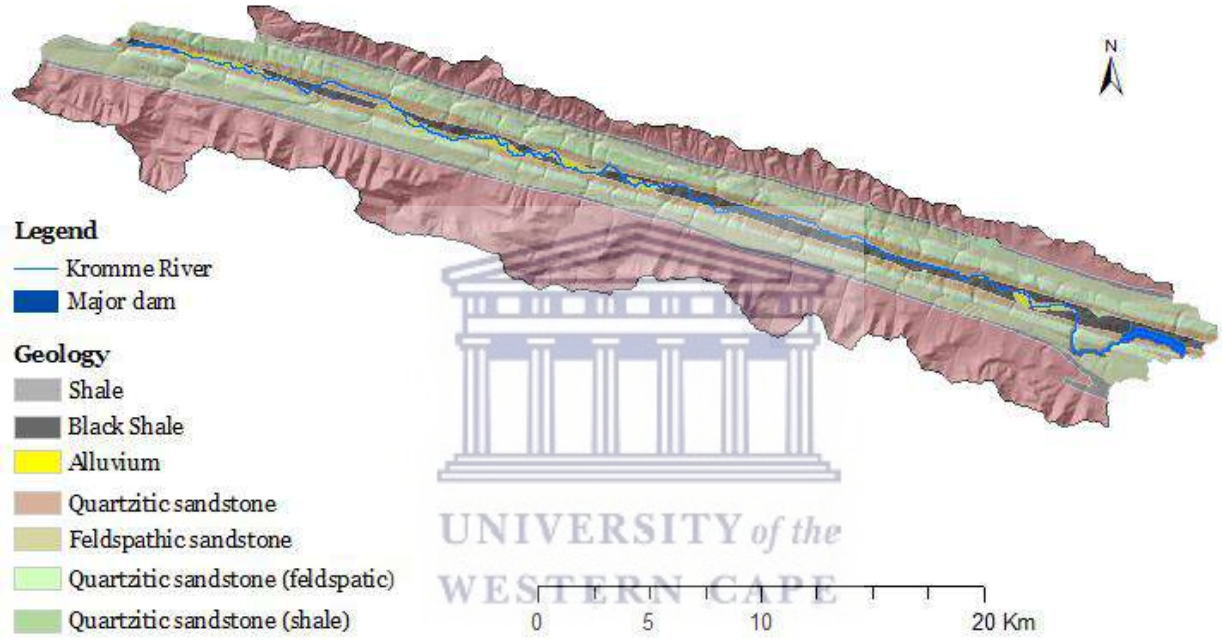

Figure 3.3: Geology of the Kromme Catchment dominated by sandstones and shale

The hydrogeology of the catchment is strongly influenced by the TMG sandstones which are an important groundwater source (water-bearing fractured quartzitic sandstones) although the yield may be highly variable (Xu et al., 2009). The yield is determined by the presence of fractures and faults. Although there are no data on proportions of groundwater contribution to streamflow, estimates show that baseflow is significant (mean of 57% of MAR) indicating a substantial role of groundwater fluxes in this catchment (Rebelo, 2012). Groundwater from the high yielding TMG fractured sandstones is crucial for water supply in the arid and semi-arid areas of the Cape region (Xu et al., 2009). The Peninsula and Nardouw are the two major quartzite formations both known to have aquifers (Xu et al., 2009). The Peninsula forms the mountain top outcrops which are fractured therefore would be recharge zones and some springs are formed at the interface of the Peninsula aquifer and Cedarberg shale aquicludes. The Kromme River central valley has alluvium above a Bokkeveld shale layer bordered by outcroppings of the Nardouw formation at the margins and Peninsula at the mountain tops.

There may not be direct feedbacks or contributions from the Nardouw and Peninsula formations, however, the tributaries discharge water from the high yielding Peninsula into the main valley. A number of alluvial fans are evident on the valley floor where the mountain tributaries join the main river. These fans are hydrologically relevant as they promote groundwater recharge. They act as buffers whereby water coming from the tributary catchments spreads and infiltrates on the fan, reducing the chances of it reaching the main river channel directly as surface flow (Rebelo, 2012; Smith and Tanner, 2019). They also act as controls on valley bottom wetlands by limiting their extent (Haigh et al., 2008).

The topography is extremely variable and altitude ranges from 0 to 1500 m.a.s.l (Figure 3.4). The topography of the Kromme comprises both steep mountainous terrain and floodplains with significant alluvial deposits. Similar to the topography, slopes in the catchment are also variable ranging from 20%-30% (north facing) and 25%-60% (south-facing) (Haigh et al., 2002). The upper part of the Kromme valley floor has a longitudinal slope of 0.6% and a regional slope of 0.35%.

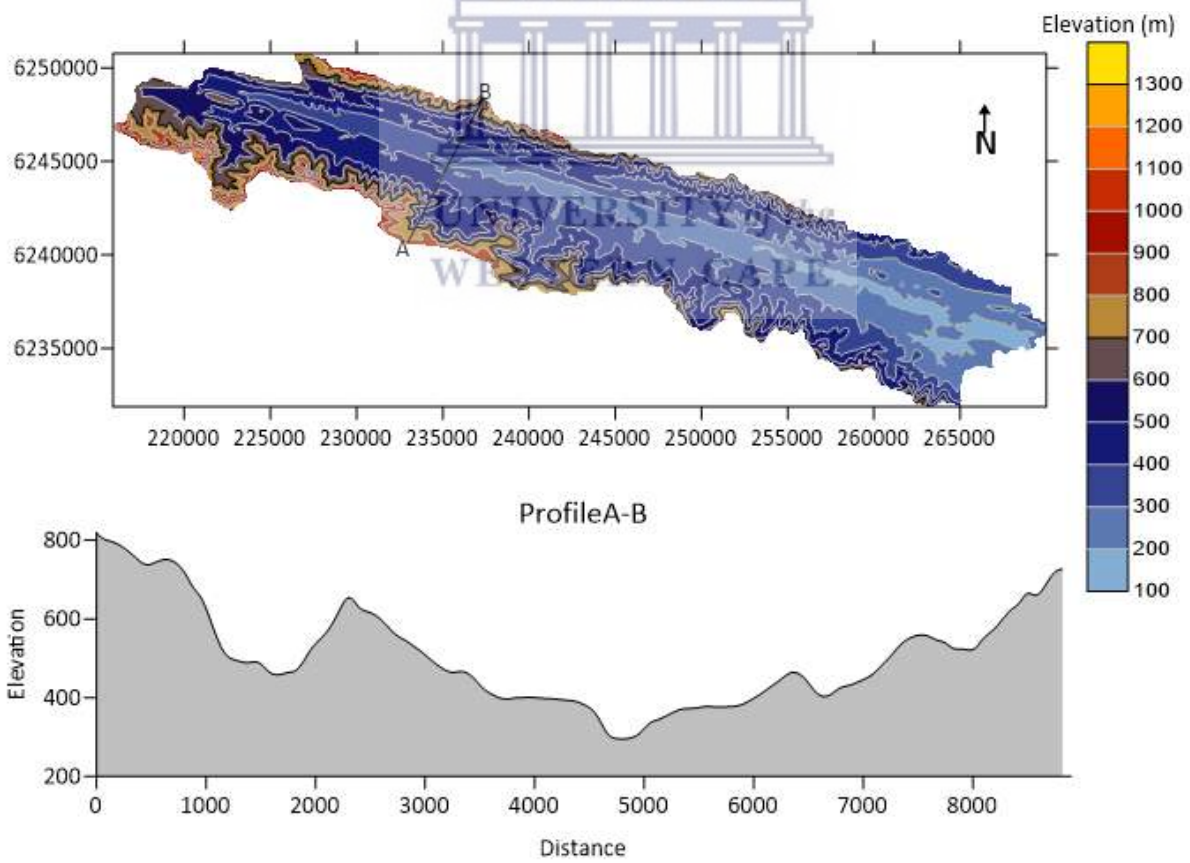

Figure 3.4: The topography of the Kromme catchment showing steep slopes in the upper parts of the catchment.

Soils in the catchment are shallow particularly on the mountain slopes. In the lower slopes of the landscape, the soils are structured and dark whilst slopes higher up the mountains comprises acidic and nutrient-poor soils. The soils are a result of the weathering of quartzite sandstone and the shale (Powell and Mander, 2009). Due to the shallow soils characteristic of the mountain slopes and the low water-use of fynbos, groundwater recharge is perceived to be high despite the low average amounts of rainfall received in the catchment.

3.4 Spatial distribution of the major land use types

Land uses in the catchment consist of intensive fruit, vegetable, and livestock farming including irrigated pasture for dairy (Rebelo, 2012) (Figure 3.5). The largest town in the catchment is Kareedouw with a population of approximately 1000 people (Rebelo, 2012). There is one major impoundment (Churchill dam) and several small farm dams in the study focus area. Farm dams used for irrigation are recharged by tributary streams and water abstracted directly from the river.

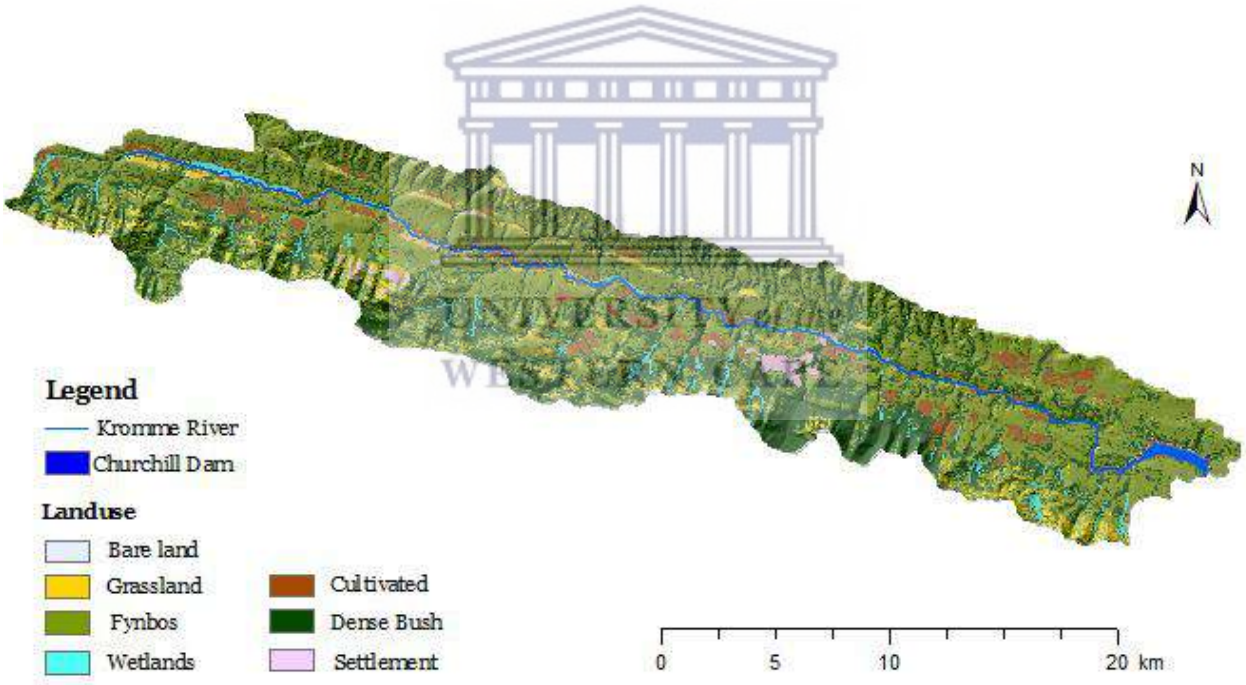

Figure 3.5: Land use types found in the Kromme Catchment

There is intensive fruit, vegetable and livestock farming in the floodplain of the Kromme River. Although farmlands cover approximately 28 000 hectares of the landscape with livestock and commercial fruits, large areas of natural vegetation still exist. The headwaters in the Kromme catchment are dominated by indigenous vegetation, primarily fynbos. The valley bottoms as well as a few other upslope parts of the catchment are dominated by wetlands which have suffered severe degradation as active farming in the wetlands is conducted. Valley bottom wetlands are dominated by palmiet (*Prionium serratum*) which is a wetland plant that usually

dominates fluvial river systems in landscapes underlain by quartzitic bedrock particularly in the Eastern and Western Cape provinces of South Africa. The Kromme catchment has been heavily transformed by agriculture and alien invasion particularly in riparian areas. Woody alien plant invasion in the Kromme catchment began in the 1930s resulting in deterioration of wetland health since then (Rebelo, 2012).

3.5 Spatial distribution of vegetation types in the Kromme Catchment

Fynbos is the dominant vegetation type in the area, particularly on mountainous areas and high plateaus not utilized for agriculture due to nutrient poor soils (Figure 3.6) (Mander et al., 2010; Mucina and Rutherford, 2006). Fynbos has been severely degraded due to grazing and managed burning on the lower mountain slopes. Thickets of indigenous trees occupy small sections in the lower mountain slopes and riparian areas where nutrient rich soils occur (Mucina and Rutherford, 2006). Indigenous forest is also found in the narrow mountain kloofs. Other areas have shale renosterveld, grassland and forest (Mucina and Rutherford, 2006). There are also irrigated pastures and apple orchards (Figure 3.6). Kromme has large permanent wetlands which are dominated by palmiet (*Prionium serratum)* with smaller patches of reeds, sedges, grasses, and ferns (Haigh, et al., 2002).

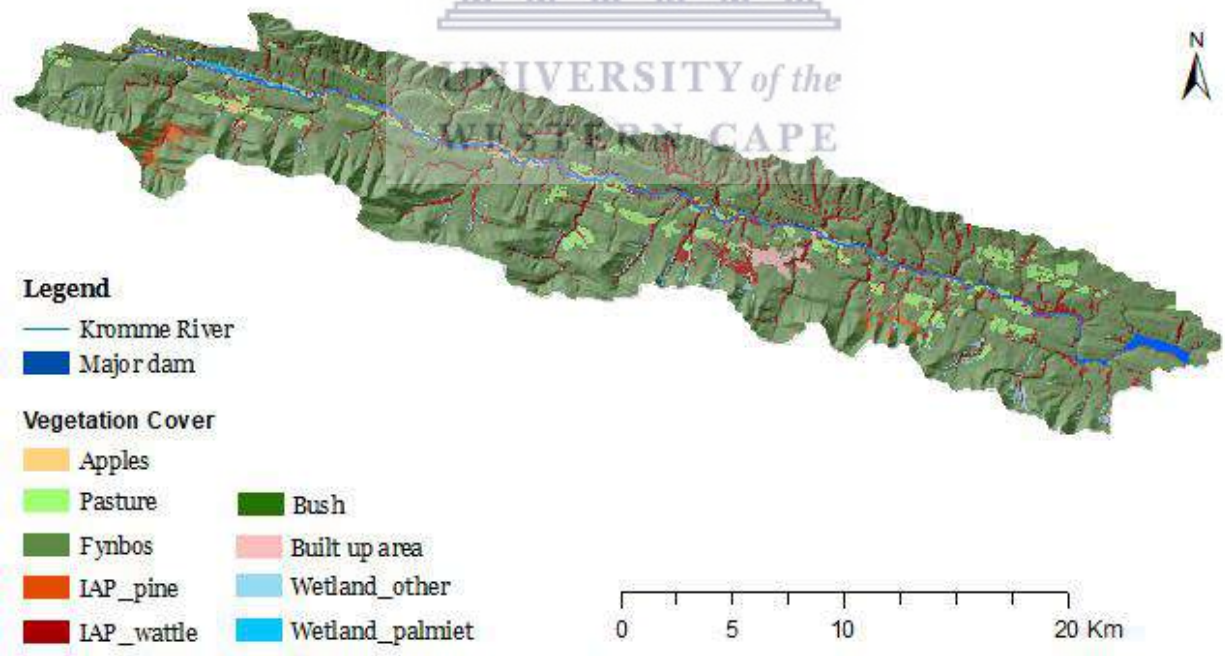

Figure 3.6: Vegetation types found in the Kromme Catchment

Land cover conversion has mostly been floodplain cultivation and the growth of dense stands of invasive trees, predominantly in riparian areas (Figure 3.6) (Mander et al., 2010; Rebelo, 2012). Alien trees are known to use more water than indigenous vegetation as well as being

responsible for the collapse of palmiet wetlands (Rebelo, 2012). The trees have invaded different parts of the catchment such as mountain slopes, wetlands but predominant in riparian areas where water is readily available. Dominant invasive alien trees in the catchment are black wattle (*Acacia mearnsii*) and pines (*Pinus pinaster*). Isolated populations of blackwood (*A. melanxylon*), silky hakea (*Hakea sericea*), gum (*Eucalyptus spp.*), and rooikrans (*A. cyclops*) are also present (Rebelo, 2012). In the 1980s, more than 60% of the Kromme catchment was invaded by alien trees (Carpenter 1999), however, due to clearing efforts by farmers as well as the Working for Water Programme, alien expansion has not increased in coverage but rather decreased (McConnachie et al., 2012).

3.6 Drainage and hydrology

The Kromme drainage follows a trellis pattern influenced by the folding and faulting of the Cape Fold Belt geology. There are six major and five minor tributaries that join the main river from the southern Tsitsikamma Mountain range, and seven large and numerous minor tributaries entering from the drier northern Suuranys Mountain range (Haigh et al., 2002). Groundwater from both the bedrock and alluvial aquifers maintain perennial to near perennial streamflow in the main channel and the mountain tributary streams. Groundwater recharge is estimated to be high largely because mountain slopes are characterised by shallow soils and the dominant fynbos vegetation has low water use (Rebelo, 2012).

The Kromme River discharges into the Churchill and Impofu dams (capacity: 35 710 106 m^3) (Haigh et al., 2008). These major dams cover 7.3 km^2 (0.9% of the catchment). The dams supply water to the Nelson Mandela Metropolitan (approximately 90 million m^3 per year) (Mander et al., 2010). Farm dams are not prevalent in this catchment with a few covering 0.3% of the catchment area (2.8 km^2). Discharge from the Kromme catchment varies significantly due to the high inter-annual variability of rainfall. The mean annual runoff of Kromme River catchment is ±75 mm/year approximately 11% of the estimated mean annual rainfall received in the catchment (Middleton & Bailey 2008).

Water demands are increasing inside the catchment and surrounding areas due to the growing human population. Changes in land use and cover types in the catchment impact hydrological processes. Understanding the impacts of changes in land and water management on the water security of the Kromme catchment therefore, becomes imperative.

3.7 Research design

The general approach for field data collection used in this study will be outlined in this chapter because it is relevant across objectives; however, specific methods for each objective will be described in detail in subsequent chapters. The focus area of the study was the Kromme upper catchment down to the Churchill Dam (Figure 3.7).

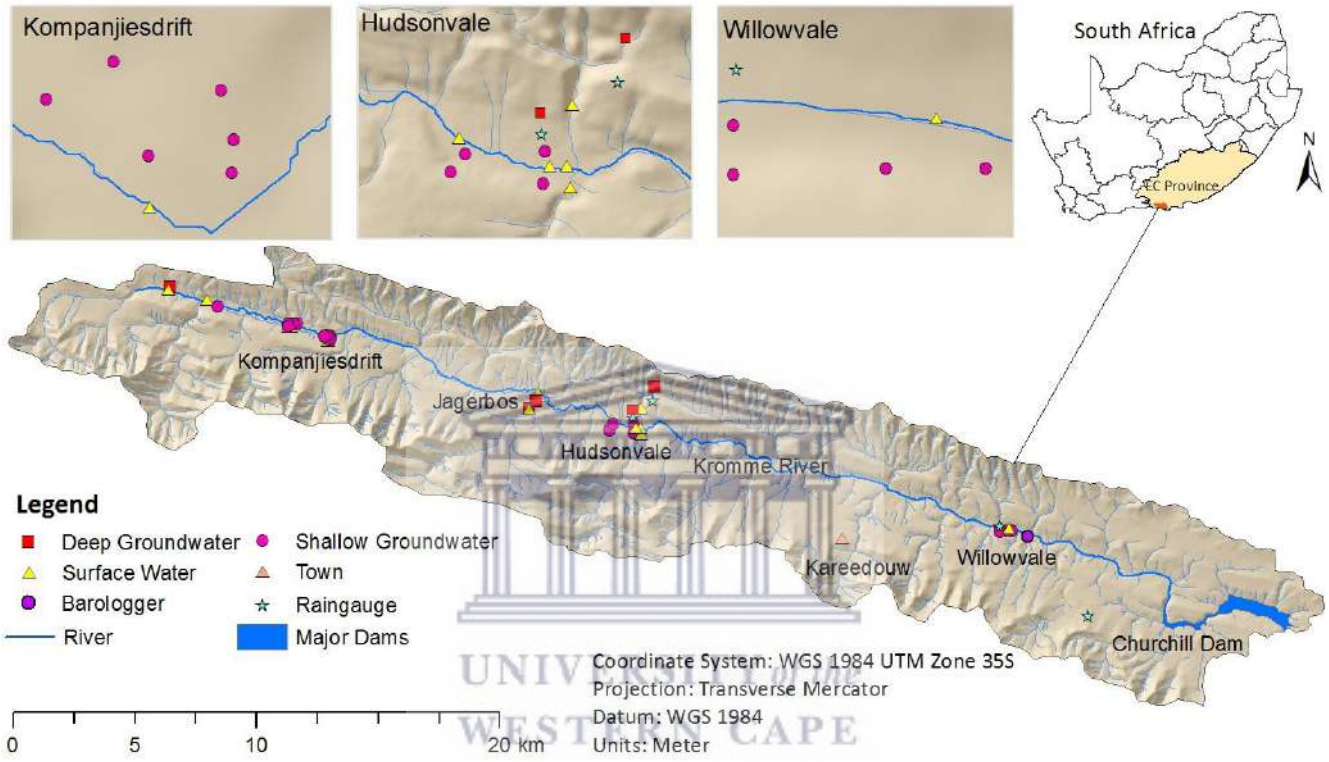

Figure 3.7: Map of Kromme Catchment showing the study focus area and monitoring sites.

To characterize the spatiotemporal variability of water sources, flowpaths and streamflow generation patterns, various hydrometric data were collected continuously by installed equipment from April 2017 to December 2019. Field visits were done every 2-3 months to download data and for routine sampling. Stream water levels were measured at selected sites along the main channel (upper, middle and lower parts of the catchment) and two tributaries (one from the drier Suuranys Mountains and the other from the wetter Tsitsikamma Mountains). Rainfall data were obtained from four tipping bucket rain gauges installed at both high and low elevation areas with loggers recording event-based rainfall (calibrated to 0.2 mm) and temperature. Long term data sets were obtained from the Agricultural Research Council (ARC) and the South African Weather Services (SAWS) for the Kareedouw and Churchill dam weather stations. Quality control on weather data was done by the supplying agencies.

Shallow and deep groundwater levels were monitored to assess recharge mechanisms as well as to understand interactions between groundwater and surface water in the catchment. Herein, shallow groundwater refers to subsurface water from the alluvial aquifer monitored in piezometers (<4 m) in the floodplain, whilst deep groundwater refers to subsurface water from bedrock aquifers monitored from boreholes. Shallow groundwater level dynamics were monitored in 20 piezometers from April 2017 to December 2019 at three sites (Figure 3.7) These sites were an upstream site near a palmiet wetland in the floodplain (Kompanjiesdrift), then midway down the catchment at an actively farmed site with some remnant wetland area (Hudsonvale), and a site at the lower parts of the catchment with a large mature stand of black wattle and an area that has been cleared of wattle, where palmiet wetland is re-establishing (Willowvale). Sites for piezometers were selected based on their location in the floodplain as well as the above ground land cover type dominant at each site. The depths and number of piezometers installed was dependent on site accessibility and depth to refusal. Deep groundwater level dynamics were monitored in boreholes (one in the upper part of the catchment and two in the middle part of the catchment), using Solinst level loggers (logging at one-hour intervals). Water quality parameters were measured manually at each site and samples collected for lab analyses. Locations, names and sites codes used in this study are given in Table 3.1. and 3.2. The same site codes are used throughout subsequent chapters.

Table 3.1: Upper catchment monitoring site names and codes used in the study.

Site Name	Code	Site Type	Instrument		Elevation		Depth
					Ground	Bottom	
Kompanjiesdrift	KDBH*	Borehole	AT	PT	437.4		33
	KDRV*	River	MM				
	KGRV*	River	AT	PT	396.3		
	KPZA	Piezometer	MM	SG	343. 7	341. 9	1.8
	KPZB	Piezometer	MM	SG	342.3	340.7	1.6
	KPZC	Piezometer	MM	SG	344.3	340.6	3.7
	KPZD	Piezometer	MM	SG	344.3	341.1	3.2
	KPZE	Piezometer	MM	SG	344.1	341	3.1
	KPZF	Piezometer	MM	SG	341.3	339.3	2
	KPZG	Piezometer	MM	SG	339.97	337. 5	2.5
	KPZH	Piezometer	MM	SG	339.5	337.6	1.9
	KPZI	Piezometer	MM	SG	341.96	340.7	1.2

*Sites established by Smith and Tanner (2019), SG-Staff Gauge, PT-Pressure Transducer, AT-Automated and MM-Manual.

Table 3.2: Midcatchment site names and codes used in the study.

Site Name	Code	Site Type	Instrument		Elevation		Depth
					Ground	Bottom	
DT Jagerbos	JBHU	Borehole	AT	PT	295.8		30
	JBHL	Borehole	AT	PT	286.7		100
Hudsonvale	HV BR	River	MM				
	HV GB	River	AT	PT	255.3		
	HVPK BH	Borehole	MM	SG			
	HVPK SP	Seep	MM				
	HVPZ1	Piezometer	MM	SG	258.9	257.8	1.12
	HVPZ2	Piezometer	MM	SG	259.1	257.7	1.35
	HVPZ3	Piezometer	MM	SG	262.4	260.3	2.1
	HVPZ4	Piezometer	MM	SG	262.8	261.1	1.8
	HVPK	Tributary	AT	PT	290.9		
	Witels TB	Tributary	AT	PT	257.8		
Willowvale	WV RV	River	AT	PT	176. 4		
	WT PZ1	Piezometer	AT	PT	179.2	176.1	3.1
	WT PZ2	Piezometer	MM	SG	177.9	176.9	1.0
	WT PZ3	Piezometer	MM	SG	178.2	176.6	1.59
	PM PZ4	Piezometer	AT	PT	180.5	177.9	2.63
	GS PZ6	Piezometer	MM	SG	181.2	179.3	1.9
	GS PZ7	Piezometer	MM	SG	181.6	178.4	3.15

SG-Staff Gauge, PT-Pressure Transducer, AT-Automated and MM-Manual

CHAPTER 4: STREAMFLOW CHARACTERISTICS AND DOMINANT FLOWPATHS LINKING LANDSCAPE UNITS IN A SEMI-ARID, MOUNTAINOUS CATCHMENT OF THE CAPE FOLD BELT.

4.1 ABSTRACT

Improving our understanding of streamflow characteristics, water storage, and flowpaths in mountainous regions is important as mountains play an important role in delivering water to lowlands, particularly in semi-arid areas. Conceptual and physical understanding of catchment function can be built from analyses of hydrometric data of various types and scales. This chapter characterizes water sources, flowpaths, and streamflow characteristics in a semi-arid, mountainous Kromme catchment in Eastern Cape Province of South Africa. Precipitation, soil moisture, groundwater levels and streamflow data were analysed to identify patterns that indicate the occurrence and/or dominance of certain processes, responses, and flowpaths. The goal of the study was to use available data to build a conceptual model of the catchment which would ultimately be used for numerical modelling. The results demonstrated how the catchment responds differently to rainfall events across seasons and intensities. Steep and rocky areas that make up much of the Kromme catchment contributed significant flood peaks after high-intensity storms. Surface and subsurface flows were significant in recharging the floodplain alluvial aquifer as well as maintaining streamflow during dry periods. Average annual runoff coefficients were low implying large ET withdrawals from dominant flowpaths and/or storage in inactive groundwater (coefficients are less than 10% meaning that more than 90% of precipitation inputs may be lost to ET). Quick and slow flow responses after rainfall events indicated the dominance of both surface and subsurface flowpaths after storm events. The Kromme catchment has a sizeable floodplain with large alluvial aquifers, which make significant contributions to catchment storage and outflows. Overall, the catchment streamflow was sustained by baseflow (for >60% of the time). Recession patterns showed that the channel receives flow from different storages such as the alluvial and bedrock aquifers and flowpaths at different rates with maximum recession periods up to 22 days indicative of interflow dominance and floodplain drainage. Throughout the monitoring period, the river system was gaining flow at the different sites during both low and high flow conditions. Groundwater and stream water level data indicated that the channel was gaining from the mountain bedrock through tributary flows and from the alluvial aquifer. A conceptual model of flowpaths and processes at the catchment scale is presented. This research helps to improve the understanding of catchment scale hydrological processes in semi-arid meso-scale mountainous environments.

4.2 INTRODUCTION

Mountainous areas are important water sources that sustain surrounding ecosystems, agriculture, and industries, particularly in arid and semi-arid regions (Viviroli et al., 2011, 2003). An assessment by Vivirolli and Weingarther (2004) revealed that 90% of the total estimated freshwater in all rivers globally comes from mountainous areas. Understanding hydrological processes in these catchments can contribute significantly to sustainable management of water resources, however the majority of research to date has focused on small headwater catchments particularly in humid areas (Xing et al., 2015; Zhao et al., 2019).

Multiple features and processes contribute to the dominant hydrological role of mountains. Mountainous catchments often receive more precipitation than surrounding lowlands, particularly in arid and semi-arid areas (Burke, 2009). Complex meteorological patterns in these catchments are influenced by physiographic features such as high elevation peaks and deeply incised narrow valleys (Concern, 2014; Washington, 1996). Groundwater from these catchments has also been shown to contribute significantly to streamflow (Wilson and Guan, 2013). Notable contributions to streamflow, and/or floodplain storage, can come through the bedrock because soils and alluvium are generally thin or non-existent in steep mountainous terrain (Graham et al., 2010; Mueller et al., 2013).

Semi-arid mountainous catchments exhibit high variability in streamflow characteristics in both space and time which makes prediction of these characteristics challenging (Bafitlhile and Li, 2019). This is partly due to paucity of hydrological data and complexity of runoff generating processes, particularly when spatial scales of analysis increase (Hood and Hayashi, 2015). A diversity of flowpaths may be dominant at different spatial and temporal scales as the underlying geology and the complex topographic properties give rise to different response characteristics in various locations (Savenije, 2010). Knowledge of flowpaths can give an idea of the catchment's residence time (Grande et al., 2020; Zhou et al., 2021), runoff source areas (Wenninger et al., 2008), and connectivity between hillslopes and floodplains (Ochoa et al., 2013; Okin et al., 2015).

Runoff generation mechanisms and the associated flowpaths, have been mainly investigated in headwater catchments in humid areas (Becker, 2005; James and Roulet, 2009; Penna et al., 2011; Zhao et al., 2019). Understanding of these processes in semi-arid catchments at the meso-scale is still inadequate, particularly in mountainous areas. Some studies have indicated that pre-event or old water dominates hydrographs in these catchments (Camacho Suarez et al.,

2015; Wenninger et al., 2008). Under dry conditions, due to very low antecedent moisture conditions, the hydrograph does not reveal immediate response to rainfall events as storage deficits will be high (James and Roulet, 2009). Furthermore, process observation and simulation studies done at the meso-scale in semi-arid environments have observed seasonal patterns in flowpath connectivity between land units, showing evidence of threshold dependence in some cases (Bracken et al., 2013; McGuire and McDonnell, 2010; Ochoa et al., 2013; Poeppl et al., 2019). Other studies have shown variable patterns of connectivity between streams and alluvial aquifers (Keene et al., 2007; Raiber et al., 2019) and significant differences in these patterns during droughts (Raiber et al., 2019). During dry periods, connectivity between land units is maintained by subsurface flows, i.e. between uplands and mountain front plains (Ocampo et al., 2006), and between floodplains and river channels (Keene et al., 2007; Raiber et al., 2019). Antecedent soil moisture conditions and magnitude of rainfall received have been further shown to control hydrological connectivity between land units (McGuire and McDonnell, 2010) as well as controlling runoff generation at the catchment scale (James and Roulet, 2009). These responses depend on rainfall characteristics, land use, topography, and the underlying geology.

This study investigates the spatiotemporal variability of streamflow characteristics, water sources, and flowpaths in the upper Kromme catchment, a semi-arid, meso-scale (360 km^2) catchment in the Cape Fold Belt of South Africa. In the semi-arid Cape region of South Africa, mountain ranges in the Cape Fold Belt are the headwaters of almost all rivers and dominate the water supply system with peaks reaching up to 2250 m.a.s.l (Colvin et al., 2009; Xu et al., 2009). The Kromme is dominated by Table Mountain Group (TMG) quartzitic sandstones and shales, and comprises both steep mountainous terrain and floodplains with significant alluvial deposits and alluvial aquifers. Groundwater from the high yielding TMG fractured quartzitic sandstones is crucial for water supply in the arid and semi-arid areas of the Cape region (Xu et al., 2009). A previous study in the Kromme upper catchment showed that subsurface flow comes out of tributary catchments via alluvial fans and recharges the alluvial aquifer supporting the floodplain wetland (Smith and Tanner, 2019). Furthermore, groundwater from the mountain bedrock was discharged into tributaries, even during dry periods water appeared to still move through alluvial deposits along the drainage line to reach the floodplain. The study by Smith and Tanner (2019), focused on a small area covering one tributary however, similar results were expected as the Kromme catchment comprises many tributaries discharging into the main river directly and/or via alluvial fans. Studies in some parts of the TMG have indicated that groundwater is discharged through valley bottom wetlands, seeps, and as baseflow in river channels indirectly via alluvial aquifers or where the river channels cut directly into the bedrock (Colvin et al., 2009).

In the Kromme catchment, as reported elsewhere in the Cape Fold Belt TMG region (Midgley and Scott, 1994; Roets et al., 2008; Xu et al., 2009), interflow from the highly fractured surface rock layers and soil-bedrock interface is expected to be a significant source of water discharging into wetlands, floodplain aquifers, and tributaries and the main river. Interflow also contributes significant portions of water to wetlands in valley bottoms and recharge to alluvial aquifers facilitated by the steep slopes and thin coarse grained soils characteristic of these catchments (Roets et al., 2008; Smith, 2019; Xu et al., 2002). Similar to the neighbouring Baviaanskloof catchment (Glenday, 2015), the Kromme has coarse alluvial deposits and a generally low gradient, therefore the floodplain is expected to slow down flows or reduce the intensity of flooding due to channel roughness and floodplain infiltration.

Most work in the TMG has, however, overlooked some features common to the region's catchments at larger scales, such as the typical floodplain areas between parallel mountain ridges; their flowpath connectivity to the mountains and their role in the hydrology of meso-scale catchments. The objective of this chapter is therefore to characterize the spatiotemporal variability in water sources, flowpaths, and streamflow characteristics in the Kromme catchment through interpretation of hydrometric data.

4.3 MATERIALS AND METHODS

4.3.1 Study site

Detailed descriptions of location, geology, land use, and other physiographic characteristics of the Kromme catchment are presented in Chapter 3. To characterize the spatiotemporal variability in water sources, flowpaths and streamflow characteristics, rainfall, groundwater and streamflow data was used. Data was obtained from rain gauges and weather stations owned by the Agricultural Research Council (ARC), the South African Weather Services (SAWS), and the Department of Water and Sanitation (DWS) at Kareedouw and Cape St Francis (by Churchill dam) (Figure 4.1). Data were also collected for surface and groundwater monitoring sites in the upper part of the catchment established by Smith and Tanner (2019). Additional monitoring sites were established for this study to capture the spatiotemporal variability of processes at the catchment scale, shown in Figure 4.1. The study focus area was the Kromme upper catchment up to Churchill dam (360 km^2) (Figure 4.1).

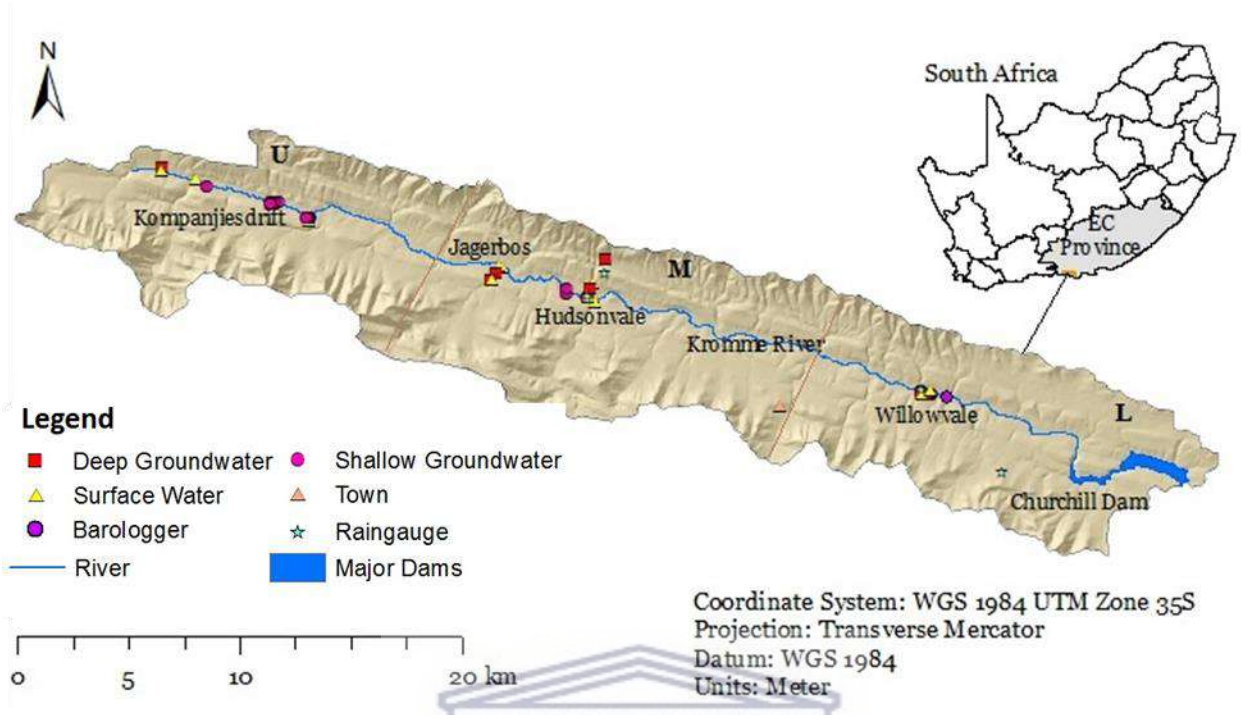

Figure 4.1: Map of Kromme Catchment showing established monitoring sites for rainfall, streamflow and groundwater. The focus area is divided into three sections: U-Upper catchment (Kompanjiesdrift), M-mid catchment (Hudsonvale), and L-lower catchment (Willowvale).

4.3.2 Data collection procedures

To characterize processes and response patterns, rainfall, temperature, and surface and groundwater levels were logged continuously by installed equipment from April 2017 to December 2019. Field visits were done every 2-3 months to download data and do routine sampling. Rainfall data were obtained from four tipping bucket rain gauges installed at both high and low elevation areas for the measurement of event-based rainfall (calibrated to 0.2 mm) and temperature. High elevation rain gauges were installed at 481 and 382 m.a.s.l. at the northern and southern mountain ranges respectively. Sites higher than 500 m.a.s.l. could not be reached to install rain gauges due to inaccessibility. The floodplain rain gauges were installed at 262 and 182 m.a.s.l. (Figure 4.1).

Twenty piezometers were installed to monitor groundwater levels in the floodplain to compare fluctuations with surface water elevations. Sites for piezometers were selected based on their location in the floodplain as well as the above ground land cover type dominant at each site. Piezometers were installed at three sites (Figure 4.1): Kompanjiesdrift, an upstream site near a palmiet wetland in the floodplain; Hudsonvale (midway down the catchment), an actively farmed site with some remnant wetland area; and Willowvale, a site in the lower part of the

catchment with a large mature stand of black wattle and an area that has been cleared of wattle, where palmiet wetland is re-establishing. The depths and number of piezometers installed was dependent on site accessibility and depth to auger refusal. Eighteen piezometers were manually monitored due to financial constraints (two to three month intervals) whilst two were equipped with Solinst level loggers logging at 30-minute intervals from April 2017 to December 2019.

At Kompanjiesdrift, the upper catchment site, nine piezometers were installed in the floodplain adjacent to a gabion weir which was built to prevent further erosion of the wetland by the Working for Water Programme of South Africa. At Hudsonvale, the midcatchment site, four piezometers were installed. Two piezometers were installed inside the wetland and the other two were installed outside the wetland in the floodplain. At Willowvale, the lower catchment site, seven piezometers were installed. Three piezometers were installed in one transect in the black wattle stand, two piezometers were installed in the regenerating palmiet patch and two piezometers in the re-establishing grass area. This was done to compare the variability in groundwater levels at the different locations.

Deep groundwater was monitored at privately-owned boreholes courtesy of willing farm owners. To monitor groundwater level dynamics, water level loggers (Solinst, logging at one-hour intervals) were installed in boreholes; one in the upper part of the catchment, at Kromdraai (KDBH), and two in the middle part of the catchment, at Jagerbos. Stream water levels were measured at three sites along the main channel in upper, middle and lower parts of the catchment (Figure 4.1). Sites along the main river were selected in areas with palmiet wetlands, alien trees and/or where tributaries join the main channel. Water levels were also measured at two tributaries, one from the drier Suuranys Mountains (HVPK site) and the other from the wetter Tsitsikamma Mountains (Witels), to monitor the variability of flows from the two mountain ranges. Sites for water level and river flow measurements were selected using the World Meteorological guidelines whereby channels should be free of aquatic plants, water flow confined to a single channel, and regular profiles with stable banks (World Meteorological Organization, 2008). However aquatic plants, splitting of the main channel and off-channel pools along floodplains were frequently encountered during site selection campaigns, thereby restricting the majority of sampling sites to gabion structures and bridges that provide artificial control sections.

River water levels were measured using pressure transducers (Solinst level loggers) logging at 30-minute intervals. The data were compensated for atmospheric pressure using a barometer

logging at 30-minute intervals at the Willowvale site. Table 4.1 shows monitoring sites and contributing catchment area for each site. River water level data were then used to estimate streamflow based on rating curves (Cornelius et al., 2019). Rating curves were derived from channel cross-section data and manual flow measurements taken under different conditions. The channel cross-sections were surveyed at Witels, HVPK (tributaries), Kompanjiesdrift, Hudsonvale, and Willowvale (main river), using a GeoMax Zenith20 differential GPS, with a GNSS Base RTK Rover system. Flow measurements were done using a flow meter (OTT MF pro) at equally spaced points across the channel (0.5 m intervals). For the determination of Manning's n roughness coefficients, measured flow, slope, and wetted cross-sectional area were used. The topographic surveys also allowed for the assessment of surface vs. groundwater levels at the different sites. The majority of analyses were done using data at daily time steps, however in order to characterize the variability of some processes and responses hourly data was used.

Table 4.1: Monitoring locations and their catchment areas

Site name	Site type	Catchment area (km²)	Equipment		Duration
Kromdraai	Main river	15	BH,WQ	(MM)	Aug 2018 to Dec 2019
Krugersland	Main river	37	PZ,WQ,SF	(MM)	Aug 2018 to Dec 2019
Kompanjiesdrift	Main river	49	PZ,WQ	(MM)	Apr 2017 to Dec 2019
Hudsonvale	Main river	152	PZ,RN,WQ,SF	(AT)	Apr 2017 to Dec 2019
Jagerbos	Main river	135	BH,WQ	(MM)	May 2018 to Dec 2019
Witels	Tributary	18	WQ,SF	(AT)	Apr 2017 to May 2018
HVPK	Tributary	3	BH,RN,WQ,SF	(AT)	Apr 2017 to Dec 2019
Willowvale	Main river	278	PZ,RN,WQ,SF	(AT)	Apr 2017 to Dec 2019

Borehole-BH, Piezometer-PZ, Rainfall-RN, Water quality-WQ, Surface flow-SF, Manual Measurements-MM, Automated-AT

4.3.3 Data analysis

Several analyses were performed on data collected during the monitoring period from April 2017 to December 2019. In this study, a rainfall event was defined ≥2 mm in a day. Heavy storms were defined as events when rainfall received was ≥30 mm/day. A streamflow response to a rainfall event was defined as starting with a 20% increase in flow within 24 hours and ending when the flow decline over a 24 hour period was less than 10% in comparison to flow during the previous hour. Precipitation and streamflow data were also used to estimate runoff coefficients, and thresholds for streamflow initiation for the whole catchment and tributary sub catchments. Contributing areas to monitoring sites are given in Table 4.1. To calculate runoff coefficients,

spatially averaged rainfall for the contributing catchment area of each monitored site was used and streamflow volumes were converted to depths (mm). Spatially averaged rainfall for each sub catchment area considered was estimated using time series rain gauge data and the Lynch (2004) surfaces of median monthly precipitation (Cornelius et al., 2019). The mean monthly rainfall surface estimated by Lynch (2003) was extracted for all grid cells where installed rainfall driver stations were located using Thiessen polygons and zonal statistics. The surface was produced at a regional scale with a relatively coarse spatial resolution at a regional scale. Surfaces were used to interpolate spatially averaged rainfall for a time series record for areas of interest (Cornelius et al., 2019). PET was estimated from daily temperature data using the Hargreaves and Samani (1985) method and scaled up using the Schulze et al. (2007) PET surfaces and station time series data for sub catchment units of interest (Cornelius et al., 2019). The Hargreaves and Samani (1985) method was used to estimate PET as it only requires daily mean minimum and maximum temperature data as well as solar radiation and has demonstrated accuracy for arid climates (Nóia Júnior et al., 2019). The same scaling method used for rainfall scaling was applied for PET using Schulze et al. (2007) PET surfaces to estimate spatial climate parameters by applying season varying scaling factors to driver station time-series data. Patching was done for gaps in the record using rainfall or PET monthly ratios for closely correlated stations that are within 30 km of a driver station with a minimum of 5 years of 5 overlap.

Flow duration curves (FDC) which show the percentage of time a particular discharge was equalled or exceeded as a cumulative frequency curve were constructed for all sites where flow was measured. To estimate baseflow, the digital filter method was adopted from Eckhardt (2005). The method involved the use of a two parameter digital filter on time series daily flow data, separating quick and slow portions of the total flow to approximate baseflow contributions.

$$b_t = \frac{(1 - BFI_{max})ab_{t-1} + (1 - \mathrm{a})BFI_{max\,Qt}}{1 - aBFI_{max}} \qquad (4.1)$$

Where

b_t = baseflow portion of the daily flow (m^3/s) for time step t

t = time step number (days)

t-1 = previous day

a = filter parameter derived by recession analysis

BFI_{max} = filter parameter (maximum value of baseflow index)

Q_t = total daily flow (m^3/s) for time step t

The baseflow index was calculated using equation 4.2 below where N is the total number of days in the observed flow record.

$$BFI = \frac{\sum_{t=1}^{N} b_t}{\sum_{t=1}^{N} Q_t} \quad (4.2)$$

The BFI_{max} cannot be estimated before the separation in many instances, however, there are BFI_{max} values proposed by Eckhardt (2005) that can be used (linked to the hydrogeological characteristics of the catchment). Proposed values for BFI_{max} are 0.25 and 0.80 for perennial streams with hard rock and porous aquifers respectively whilst 0.50 was proposed for ephemeral streams with porous aquifers (Eckhardt, 2005). Recession analysis was performed to get the filter parameter/recession constant a. Values for the recession constant a varies from zero to one giving an indication of flow depletion rate at each site (Mazvimavi et al., 2003). The recession analysis was performed using observed data from April 2017 to December 2019. The Kromme catchment has no defined rainfall seasonality, therefore the master recession curves (Tallaksen, 1995) could not be applied for this catchment. Streamflow recession was therefore described using equations 4.3 and 4.4 (Chapman, 1999).

$$Q_b = Q_0\, e^{-b/\tau} = Q_0\, a^b \quad (4.3)$$

$$a = 1/\tau \quad (4.4)$$

Q_b = flow in m³/s at time b after event recession started in days

Q_0 = flow at the beginning of the recession in m³/s

a = recession constant

b = time since recession started (days)

τ = groundwater storage turnover time

The recession analysis was performed for periods when streamflow declined for at least five consecutive days, excluding the first two days after a rainfall event, until the day before the next rainfall event (adapted from Glenday, 2015). Recession curves were plotted for d_{Q_r}/d_t vs. Q_r, where $Q_r$is receding streamflow and t is time using Rupp and Selker (2006) accumulated volume method. The recession constant a value was derived from the best fit linear regression exponential equation. The average response time in storage was given by $1/a$.

4.4 Systematic data analyses to infer on the occurrence of processes

Using data collected from April 2017 to December 2019, a systematic analysis was performed for the description of catchment processes and connectivity between land units. This was done following data analyses recommended by McMillan et al. (2011) and Clark et al. (2011). A summary of the analyses done is given in Table 4.2 and further descriptions are given thereafter.

Table 4.2: Summary of analyses performed on available data to infer and/or indicate the occurrence of dominant patterns or processes- Adopted from Glenday (2015) and McMillan et al. (2011).

Scale	Data	Data analysis	Interpretation of process
Tributary	SW, P	Determination of thresholds for streamflow initiation and duration of flow	Surface and subsurface contributions to tributary flows are indicated by timing between rainfall events, flow peaks and response shape.
Main Channel	GW, SW	Comparison of elevation differences between alluvial groundwater level and surface and water elevation	Channels lose water to ET and bed infiltration which may recharge the alluvial aquifer or channels may gain from the alluvial aquifer, and groundwater from mountain bedrock discharge. When the river water elevation is above the groundwater level elevation, the river reach will be losing and vice versa.
Alluvial aquifer	GW, P	Analysis of timing in groundwater level change and peak timing after a rainfall event	Responsiveness indicates notable local recharge through direct infiltration, percolation and/or flow to the site. No response or long lags shows net recharge is not significant and could be affected notably by ET.
Catchment	SW, P	Analysis of streamflow peak timing after a storm	Slow time to peak may indicate ET impacts on contributing flowpaths. Quick time to peak indicates dominance of surface runoff and event water to streamflow.
Catchment	SW, P	Analysis of quick and slow response flowpaths (numerical filter applied to hydrograph)	Relative dominance of surface vs. subsurface flowpaths. Variability in slow flow (baseflow) indicates variability in aquifer storage.
Catchment	SW, P	Calculation of average annual runoff coefficients	Low ratios may indicate large ET withdrawals from the dominant flowpaths in the catchment and/or storage in inactive groundwater

SW - surface water, P - precipitation, GW groundwater, ET evapotranspiration

The timing of streamflow peaks after rainfall events was used to infer lengths of flowpaths. To determine aquifer-channel connectivity, river water levels and water tables at sites close to each other were plotted together to determine when and where groundwater levels were above or below surface water levels and river thalweg elevation. When the water table is above the river channel thalweg, the stream may be gaining from the groundwater storage. If the water table is below the thalweg, then the channel may be losing water to groundwater (Banks et al., 2011). However, other factors may also be at play, i.e. water from a river that goes into the bed and banks may also be used quickly by riparian vegetation and may never make it to the groundwater table or lost from very high evaporation off the water surface and wetlands at certain times. When the groundwater level is above the channel bed level, it is not always guaranteed that there will be groundwater inflow into the channel. However, the Kromme floodplain alluvial material is mostly sandy, coarse material therefore, the assumption is that when the groundwater level in the alluvial aquifer is above the channel elevation (m.a.s.l.) it is likely that the alluvial aquifer will be discharging into the river.

For deep groundwater levels, the connection with surface water is not always easy to determine. When there is no direct physical contact between the channel and the bedrock layer being measured, there can still be an indirect connection. Groundwater from the bedrock aquifer would either have to come out in a spring and flow on the surface to the main channel and/or could recharge the alluvial aquifer, if they are connected, which could then discharge into the river. The relative elevations of the water table at different sites in this study are being used to point out what is possible. Multiple observations such as the texture of the material, timing and magnitude of rise are used to support process conceptualization.

Changes in floodplain shallow and deep groundwater levels in response to rainfall, as well as the lag times for peaks, were also analysed. After a rainfall event, if there was no change in groundwater levels, this would indicate that either there might not have been any significant recharge because the event was too small or the soil was too dry. If there was a change, then recharge could be attributed to quick and shorter surface and/or subsurface flowpaths. Longer lag times are a result of travel times, linked to flowpath length and subsurface material properties. The magnitudes of water level change can also be influenced by ET. Much of the Kromme floodplain is dominated by invasive tree species, particularly black wattle (*Acacia mearnsii*), which has higher water use than indigenous vegetation therefore, high rates of ET were expected (Doody et al., 2011; Le Maitre et al., 2015).

4.5 RESULTS

4.5.1 Rainfall

Mean annual rainfall in the Kromme catchment is approximately 600 mm/year; however there was high inter-annual variability, with annual values ranging from 300 to 1200 mm/year between 1960 and 2019 (Figure 4.2b). There are no strongly defined wet and dry seasons, therefore rainfall events occur any time of the year (Figure 4.2a). The long-term average shows more rainfall in spring (August to October) and the least rainfall in summer (Figure 4.2c) (Nsor and Gambiza, 2013), however individual years show significant variation from this pattern (Figure 4.2c).

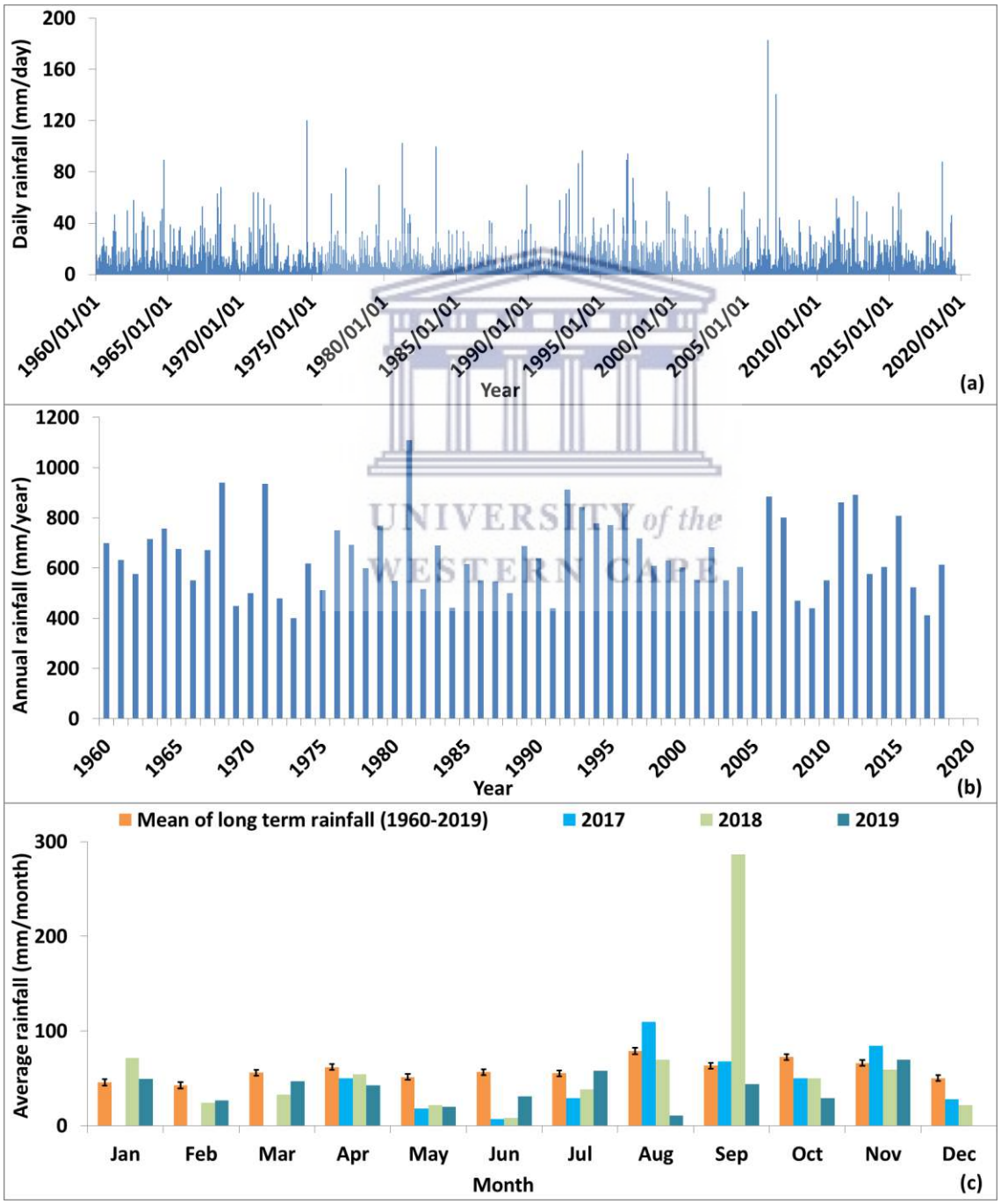

Figure 4. 2: Variations in long term (a) daily, (b) annual and (c) average monthly rainfall

Data collection took place during the most severe drought in over 50 years. The year 1973 was the driest in the record whilst 2016 was second driest (Figure 4.2b). Typical lengths of dry spells in the analysed long term record (1960-2019) were on average 20 days. Exceptional dry spells were recorded in June and July 2000 (44 days), June and July 2019 (41 days), and February to March 2012 (35 days). Dry spells were often experienced in winter (June and July) and summer (particularly in December). Exceptional rainfall events were experienced in August 2006, March 2007 and September 2018 characterised by daily rainfall amounts of 182, 140 and 87 mm respectively (Figure 4.2a). During the monitoring period (April 2017 and December 2019), the largest daily rainfall events observed were in September 2017 (34 mm/day), September 2018 (88 mm and 46 mm/day consecutively), November 2018 (19 mm/day), and November 2019 (53 mm/day).

A comparison of monthly rainfall during the study period with the long-term mean monthly rainfall (Figure 4.2c) shows that the long term mean monthly rainfall is higher than monthly rainfall between 2017 and 2019 except for a few months i.e. August 2017 and September 2018. Based on this comparison, it shows that the catchment was monitored during a relatively dry period. During the monitoring period (2017-2019), the year 2018 was the wettest (555 mm/year) whilst 2017 was the driest of the three years (450 mm/year).

4.5.2 Evapotranspiration

Estimated monthly PET rates for the Kromme catchment are shown in Figure 4.3 below.

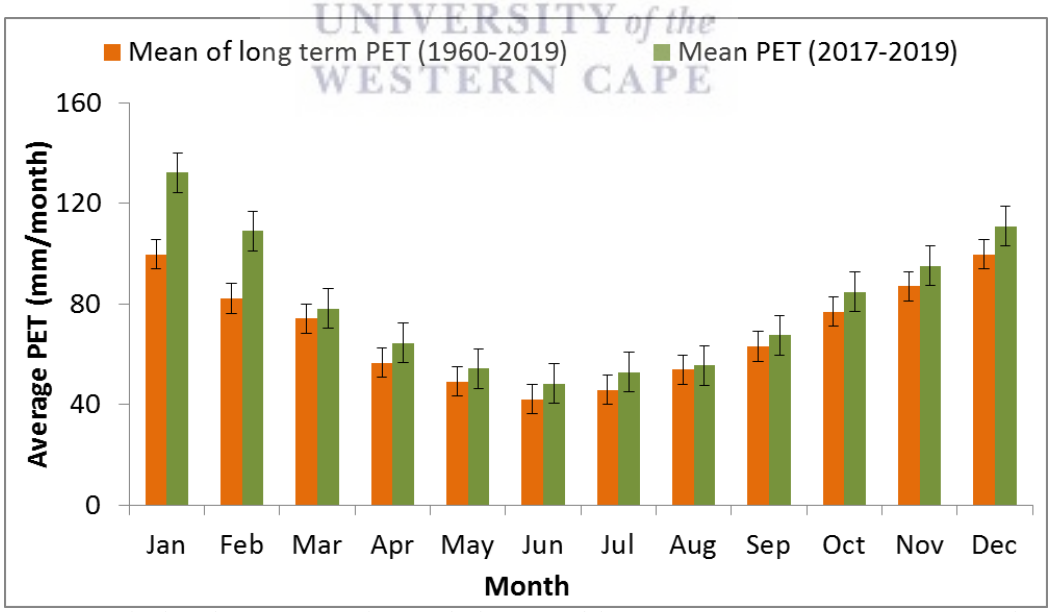

Figure 4. 3: Variation between estimated short and long term PET averages. Green bars show average PET during the monitoring period whilst orange shows the long term average.

A comparison of monthly reference potential evapotranspiration rates during the study period (2017-2019) with the long-term monthly averages (1960-2019) shows that evapotranspiration demand during the study period was generally higher than the long-term averages(Figure 4. 3).

4.5.3 A comparison of flow characteristics observed across sites in the catchment

4.5.3.1 A generalized description of variation of flows over time

The catchment was monitored during a relatively dry period with most (98%) of the mean daily flows below 1 m^3/s (Figures 4.4). The catchment was very dry during the lead up period before April 2017, when monitoring began; the soil moisture and alluvial groundwater storage was depleted, therefore received precipitation inputs replenished the storage and some were lost to evapotranspiration. The streamflow responses to rainfall events in April-August 2017 were lower than they were later on in the observation period (Figures 4.4). The observed discharge during the monitoring period (April 2017 to December 2019) was characterized by long periods of low flows and a few short wet periods (Figure 4.4). There was a general decline in water levels as well as flow volumes from April to August 2017 and from June to August 2018 as well as between September and December 2019 (Figure 4.4). However, Willowvale (lower part of the catchment) responded to some of the events during the dry period from September to December 2019 (Figure 4.4).

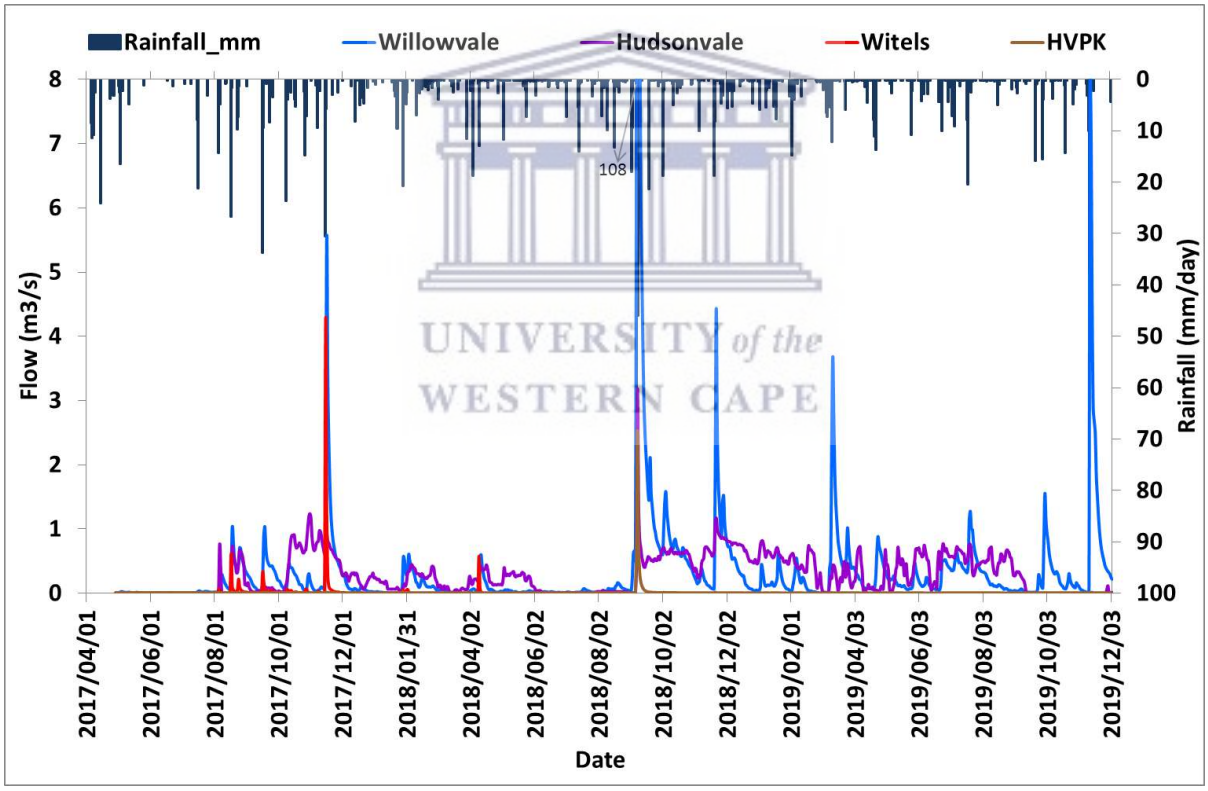

Figure 4.4: Monitored streamflow locations including the main river (Willowvale and Hudsonvale) and tributaries (Witels and HVPK). Witels record ends in August 2018.

Assessments of surface hydrographs for the monitored sites in the catchment show various response patterns to precipitation inputs (Figure 4.4). Observed streamflow showed fast responses to storms >10 mm/day, with relatively less pronounced responses to light or moderate rainfall <5 mm/day. The catchment seldom responded to precipitation inputs of less than 5 mm/day unless there were a series of cumulative events before. Approximately 25 rainfall events

of more than 10 mm/day were recorded during the monitoring period of which 15 of them coincided with discernible peak flow responses. Some of the major events observed were in November 2017 (31 mm/day), September 2018 (87 mm/day and 46 mm/day consecutively) and November 2019 (53 mm/day). The largest event that did not coincide with a streamflow peak during the observation period was 16 mm/day (3 May 2017) indicating the effects of interception and soil storage on streamflow during dry periods when storages are depleted. The extreme storm event, on the 7th and 8th of September 2018, resulted in a peak daily flow (108 m^3/s) at the Willowvale site downstream. Sometimes large events that followed a long dry period yielded relatively low runoff response i.e. 16 July 2017 rainfall event of 21 mm/day after 64 consecutive days (received < 1 mm/day of rainfall).

Overall, for most of the monitored sites, hydrographs show sharp peak and sharp recession curves. This could be indicative of the dominance of surface water and shallow subsurface water pushed through by event water. Sustained flows during long dry spells (April-August 2017 and June-August 2018) indicated the possibility of prolonged baseflow contributions from the alluvial and bedrock aquifers. Streamflow variability during low flow periods is commonly indicative of variability in contributing aquifer storages.

4.5.3.2 An event based analysis of flow variation per site

In 2017 when monitoring started, after storm events of 42 mm/day and 40 mm/day in consecutive months (16 August and 15 September 2017), Willowvale and Hudsonvale reached peak flows after 48 hours of each event whilst the southern tributary (Witels) reached its peak in 24 hours. In November 2017, following the storm event of 48 mm/day on the 14th, significant responses were observed; Willowvale reached peak flows in 48 hours of the event and took approximately 21 days to recede back to pre-event flow. Streamflow at the Hudsonvale site in the main channel and northern tributary, HVPK, did not show notable responses to this event. The Witels tributary peaked a day after the event and receded to pre-event flow conditions within 14 days. For most of 2018 there were no notable responses to most rainfall events, even storms of up to 27 mm/day, until the heavy storm (134 mm over two days) on the 7th and 8th of September 2018. This event made September 2018 an exceptionally wet month in comparison to all the other months during the monitoring period. In response to this storm, all sites reached peak flows within two days of the event. Willowvale (lower catchment) had the highest peak (108 m^3/s) by the next day whilst Hudsonvale (mid-catchment) peak flow was 3 m^3/s. In 2019, only Willowvale (lower catchment) responded with notable peaks to most rainfall events >10 mm/day (Figure 4.4).

Overall, there were notable responses from the monitoring sites along the main channel and peak timing was often within 24 to 48 hours after an event, implying faster flowpaths such as surface runoff and push-through subsurface flow dominate the hydrograph during storm peak flow and recede to low flow conditions, where the streamflow was sustained by baseflow. Prolonged elevated flows after events, up to three weeks in some cases, indicated flow contributions from deeper, slower subsurface flowpaths, whilst delayed contributions within a few days after an event could have been from faster interflow. Sustained low flows during long dry spells i.e. July to September 2018 indicated prolonged baseflow contributions from the alluvial and bedrock aquifers. Streamflow variability during low flow periods was indicative of variability in contributing aquifer storages.

4.5.3.3 Monthly runoff variation per site

Monthly variation in runoff at all flow monitoring sites is shown in Figure 4.5. The catchment was monitored during a relatively dry period with most monthly flows below 12 mm/month. A comparison of monthly runoff at main river sites shows higher runoff per unit area at Hudsonvale site (midcatchment) compared to Willowvale site (lower catchment) overall (Figure 4.5a) than tributaries (Figure 4.5b). High runoff would be expected at Willowvale due to a larger contributing area (352 km^2). The average monthly runoff per unit area at Hudsonvale was 4.66 mm/month and 4.16 mm/month at Willowvale main river sites (2017-2019 monitoring period). The comparison of runoff per unit area for all sites monitored shows that on average the HVPK tributary, which had the smallest catchment area (3 km^2), produced more runoff per unit area than other sites. Flow at HVPK was less rainfall dependent and had more steady baseflow compared to the other sites. One explanation based on field observations could be constant contributions from the bedrock aquifer which does not pass a major alluvial deposit or a floodplain that could absorb it in that small catchment. Seeps discharging into tributaries were observed even during the drought in 2016 (scoping trips) and 2017 (when monitoring commenced). The average monthly runoff for tributaries Witels and HVPK were 6.04 mm/month and 10.6 mm/month respectively during the 2017-2019 monitoring period.
Overall, by the end of 2019, high runoff was recorded at HVPK (149 mm/month) (Figure 4.5b).

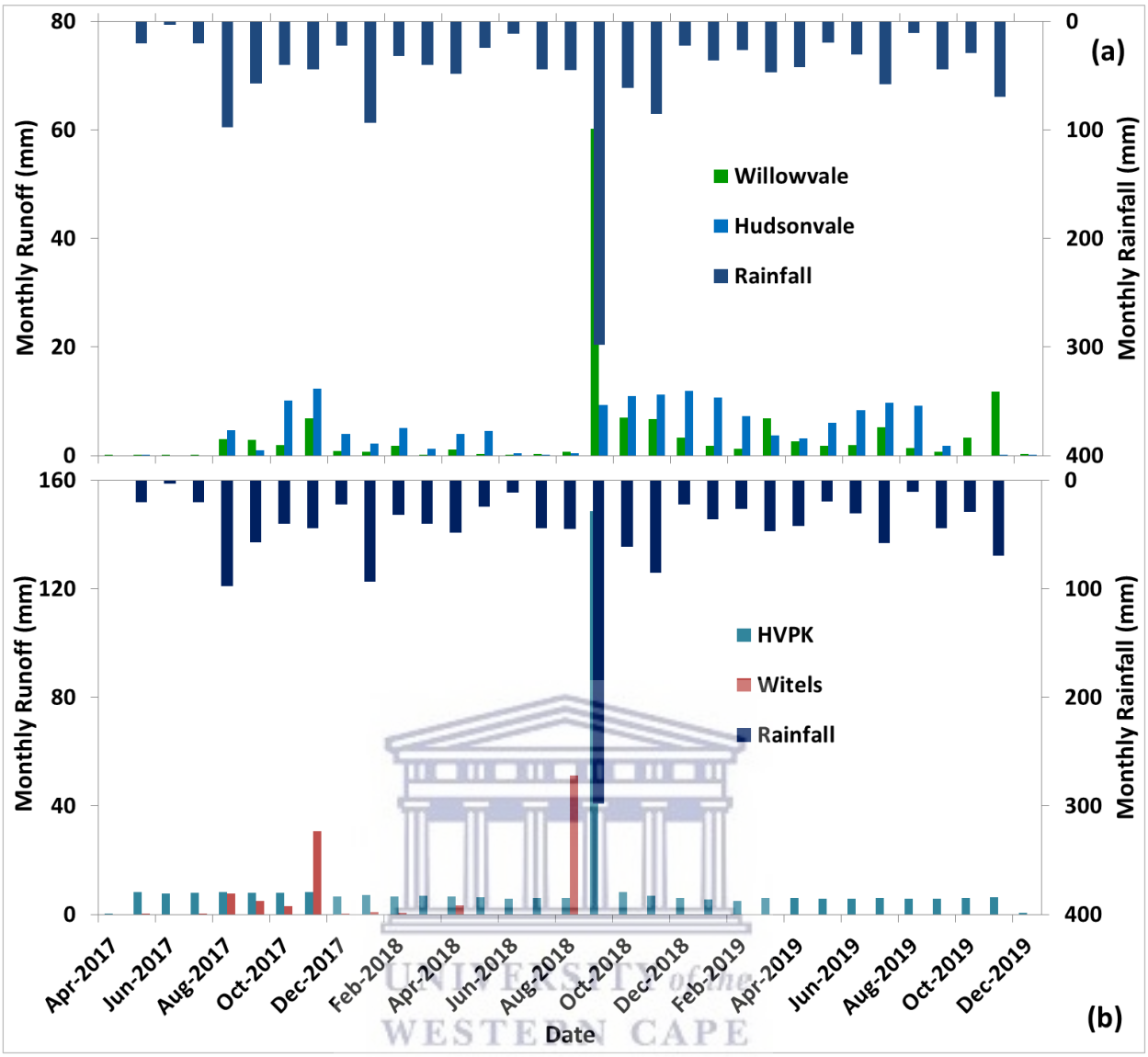

Figure 4.5: Monthly spatial rainfall and runoff observed at main channel (a) and tributary (b) sites. The record for Witels stopped in August 2018 as the level logger was lost during a flood.

4.5.4 Comparison of runoff coefficients across main channel sites and tributaries

Runoff coefficients (Table 4.3) were estimated to indicate the proportion of rainfall that was not lost to evapotranspiration or groundwater storage. The coefficients gave useful insights into patterns of runoff production in the catchment (Figure 4.6). A comparison across all monitored sites over the monitoring period (April 2017– December 2019) shows that the north facing mountain tributary (HVPK) has a higher runoff coefficient (0.26) than other sites (Table 4.3). This is a steep rocky tributary probably receiving groundwater discharge and flows that do not pass through any major alluvial deposits where they can be lost to infiltration. Furthermore, due to steep slopes, substantial amounts of rainfall form surface runoff that would increase runoff coefficients even without groundwater contribution. This tributary would therefore be expected to respond to most events compared to flatter main river sites with floodplain buffering.

Table 4.3: Runoff coefficients calculated flow monitoring sites (April 2017-December 2019).

Site	Duration (Years)	Area (km2)	Rainfall (mm)	Runoff (mm)	Runoff Coefficient
HVPK (Tributary)	2.7	3	641.6	290.3	0.26
Hudsonvale (Main River)	2.7	152	658.5	104.3	0.09
Willowvale (Main River)	2.7	278	655.8	99.9	0.09

Sites in the main valley (Hudsonvale and Willowvale), had low average runoff coefficients (0.09) during the monitoring period, despite some heavy storm events received (i.e. 134 mm in 48 hours in September 2018). The low runoff coefficients are however, not unusual for semi-arid catchments. The values were lower than the monitored tributaries due to steep slopes dominating a greater proportion of the tributary catchments which are expected to have runoff coefficients greater than the main channel sites that have floodplain buffers. The low coefficients were due to depleted storage and/or water lost to ET.

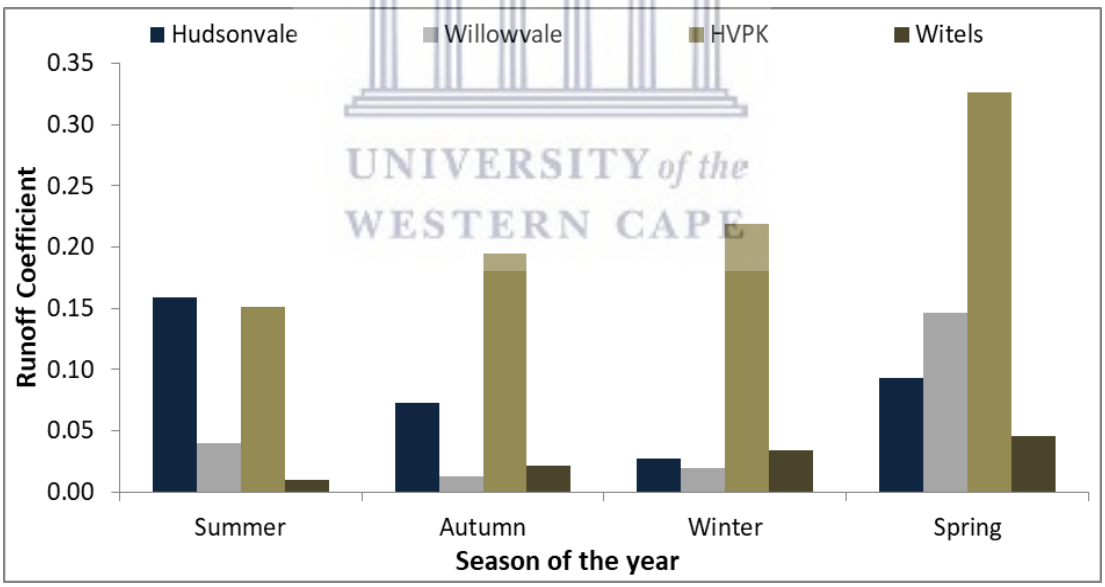

Figure 4.6: Calculated monthly runoff coefficients for all tributaries and main river sites

Overall, all sites except one tributary (HVPK) had runoff coefficients less than 10% indicating that over 90% of precipitation inputs received in this catchment are lost to ET and/or groundwater storage that is not connected to the river channel upstream of the monitored locations. An analysis of variation in runoff coefficients across two seasonal cycles during the monitored period showed no distinct seasonality (Figure 4.6), possibly because the catchment has no defined rainfall seasonality. However there was relatively high runoff observed in spring during the monitored period due to higher rainfall (Figure 4.6).

4.5.5 Variation in surface water flow duration at monitoring sites.

Flow duration curves for the period April 2017 to December 2019 were analysed and results are shown in Table 4.4 and Figure 4.7. The maximum runoff recorded at main river sites was 34 mm/day and 1.8 mm/day equalled or exceeded for 0.1% of the time at Willowvale and Hudsonvale respectively. The northern tributary HVPK had the highest runoff of 73 mm/day which was equalled or exceeded for 0.1% of the time (Table 4.4, Figure4.7). The catchment reaches or exceeds high flow rates for small proportions of the time as they are extreme flood events which rarely occur.

Table 4.4: Runoff magnitudes equalled or exceeded for selected percentiles

	Runoff (mm/day) at different frequencies of exceedance					
Site	**Max**	**5%**	**10%**	**25%**	**50%**	**75%**
Witels	51	0.25	0.12	0.02		
HVPK	73	0.31	0.27	0.25	**0.21**	0.2
Hudsonvale	1.8	0.44	0.39	0.3	**0.12**	0.006
Willowvale	34	0.37	0.22	0.11	**0.03**	0.008

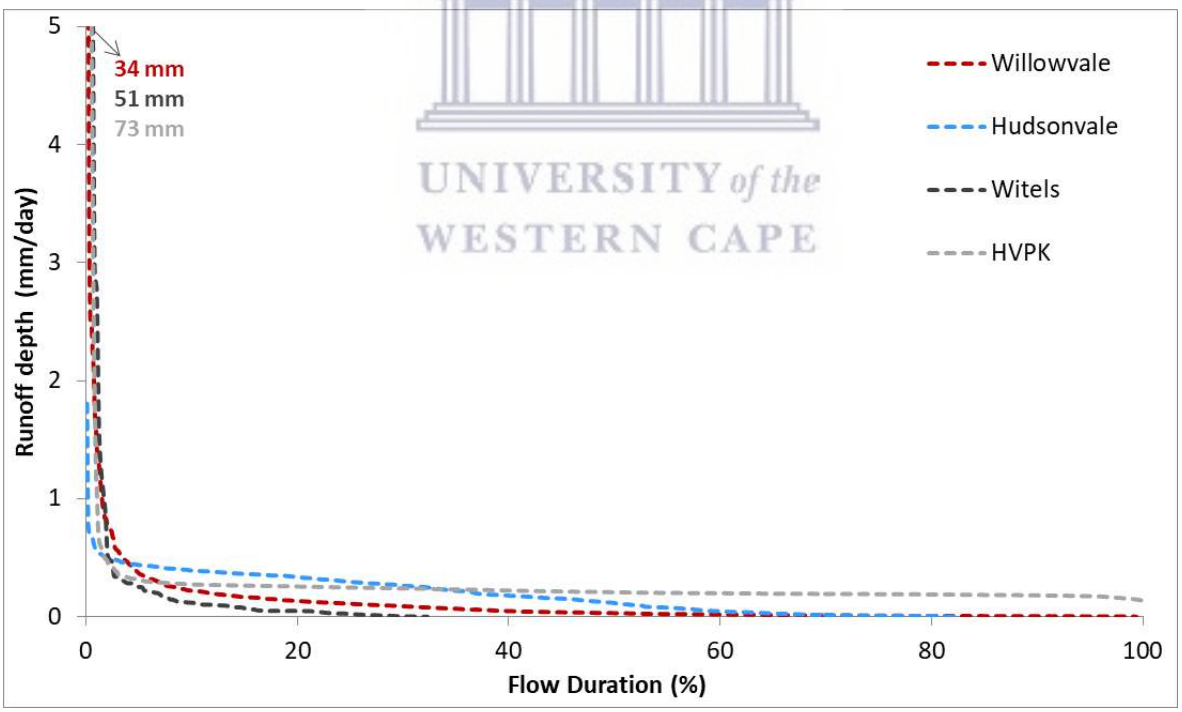

Figure 4.7: Flow duration curves for the period April 2017 to December 2019 for main channel (Willowvale and Hudsonvale) and tributaries (Witels and HVPK).

The runoff equalled or exceeded at 50% of the time was highest at HVPK (0.21 mm/day). Low flows were between 60-100% exceedance (Figure 4.7) showing that baseflows sustain river flows in this catchment. The shapes of the flow duration curves show high flows (flash floods) that last for short time durations (sharp/steep curve). Runoff curves for Willowvale and HVPK imply

perennial channels shown by 100% flow duration (Figure 4.7). The curves for Hudsonvale and Witels sites imply ephemeral flows (Figure 4.7). Overall, the flow duration curves are plotting at low flow values (below 0.5 mm/day for 95% exceedance) implying a relatively dry period in which case the catchment was sustained by base flows for the most part.

4.5.6 Flow recession analysis and baseflow estimation for observed flow

4.5.6.1 Flow recession analysis

Recession patterns characterized from streamflow time-series data to infer the dominance of drainage originating from different storages and flowpaths are shown in Figure 4.8. River stage and flow were measured at four sites in the catchment. The recession patterns and constants gave an idea of the different storages contributing to flow in the main channel and tributaries. Observed recession constants from the full record ranged from 0.7 to 0.9 (Figure 4.8). Witels had the lowest constant, however the record for Witels tributary was also short due to loss of the measuring pressure transducer at this site during a flood. Hudsonvale site in the main river had the highest recession constant whilst Willowvale and HVPK (main channel and tributary respectively) differed slightly.

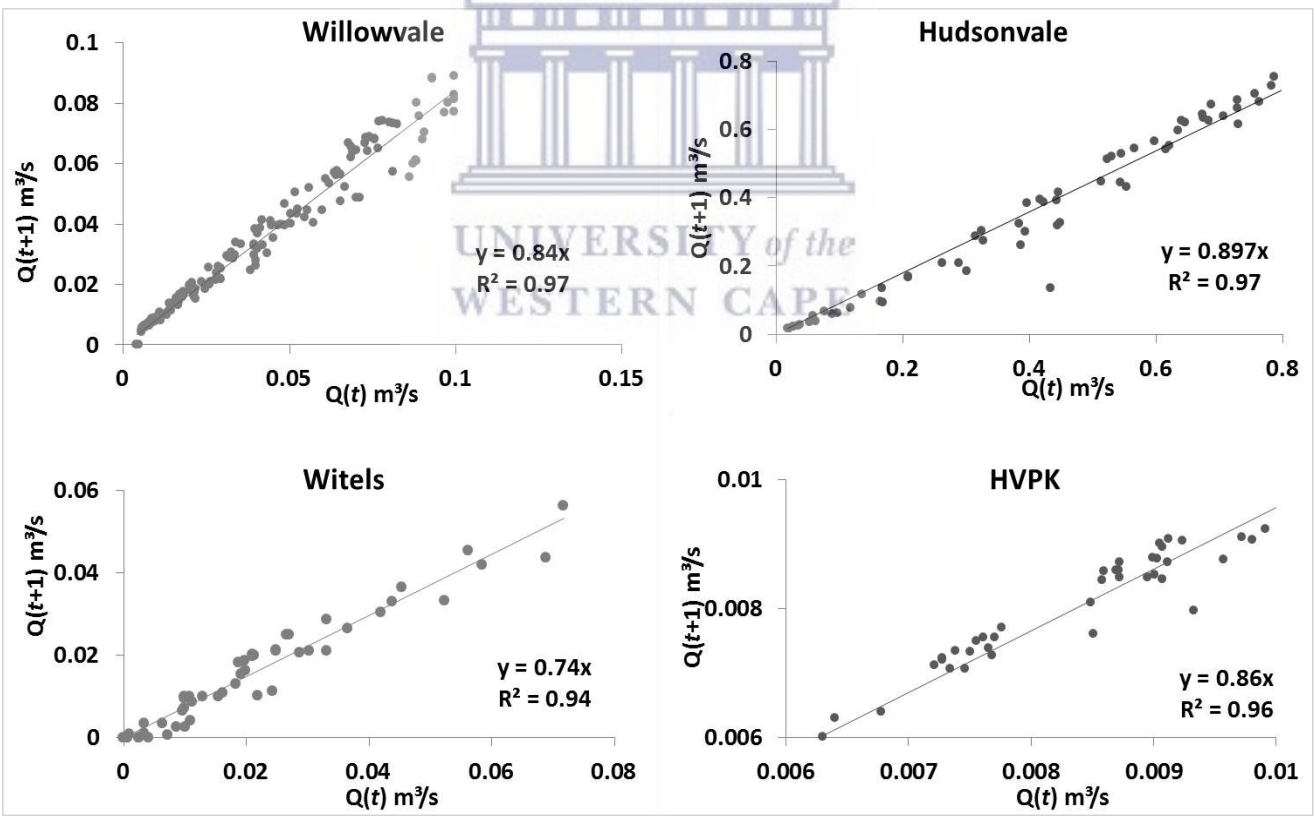

Figure 4. 8: Variation of recession patterns for the period April 2017 to December 2019.

Recession patterns from selected events from the observed streamflow record were analysed individually to check for differences in degree of linearity for the various rainfall events. The analyses of individual recession event degree of linearity were done for each site (Appendix

Figure A4.1). Different degrees of linearity of recession events indicated that delayed flows were likely coming from different storages with different drainage rates.

The degrees of linearity and slopes of the different recession events, per site (Appendix Figure A4.1) gave insights into the different likely storages contributing to baseflow per site. Observed relationships between Q ($t+1$) and Q (t) for the selected events showed different slopes and degrees of linearity for the analysed recession events ($n=12$) for Hudsonvale (midcatchment) and Witels (tributary). Willowvale (lower catchment) and HVPK (tributary), showed relatively similar recession shapes for all the recession events analysed which implies constant flow contributions and storage-outflow relationships. Storage-outflow relationships from the 12 events analysed differed due to event size, storage size, antecedent conditions and ET.

4.5.6.2 Baseflow estimation for observed flow

The baseflow estimate produced by applying the digital filter algorithm (Eckhardt, 2005) for the amount of flow reaching the catchment outlet via quick and slow pathways, is shown in Figure 4.9 for the HVPK (tributary) and Willowvale (main channel) sites.

Drought conditions over most of the monitoring period (from April to August 2017 and June to August 2018 as well as September to December 2019), meant that the short flow peaks from the few storms that occurred made up the bulk of the total flow. Since the Kromme catchment was monitored during a very dry period, baseflow sustained streamflow most of the time at both tributary and main river sites (Figure 4.9). During the period from April 2017 to December 2019, more than 60% of the total flow was baseflow which contributed more of the total flow than quickflow at both sites.

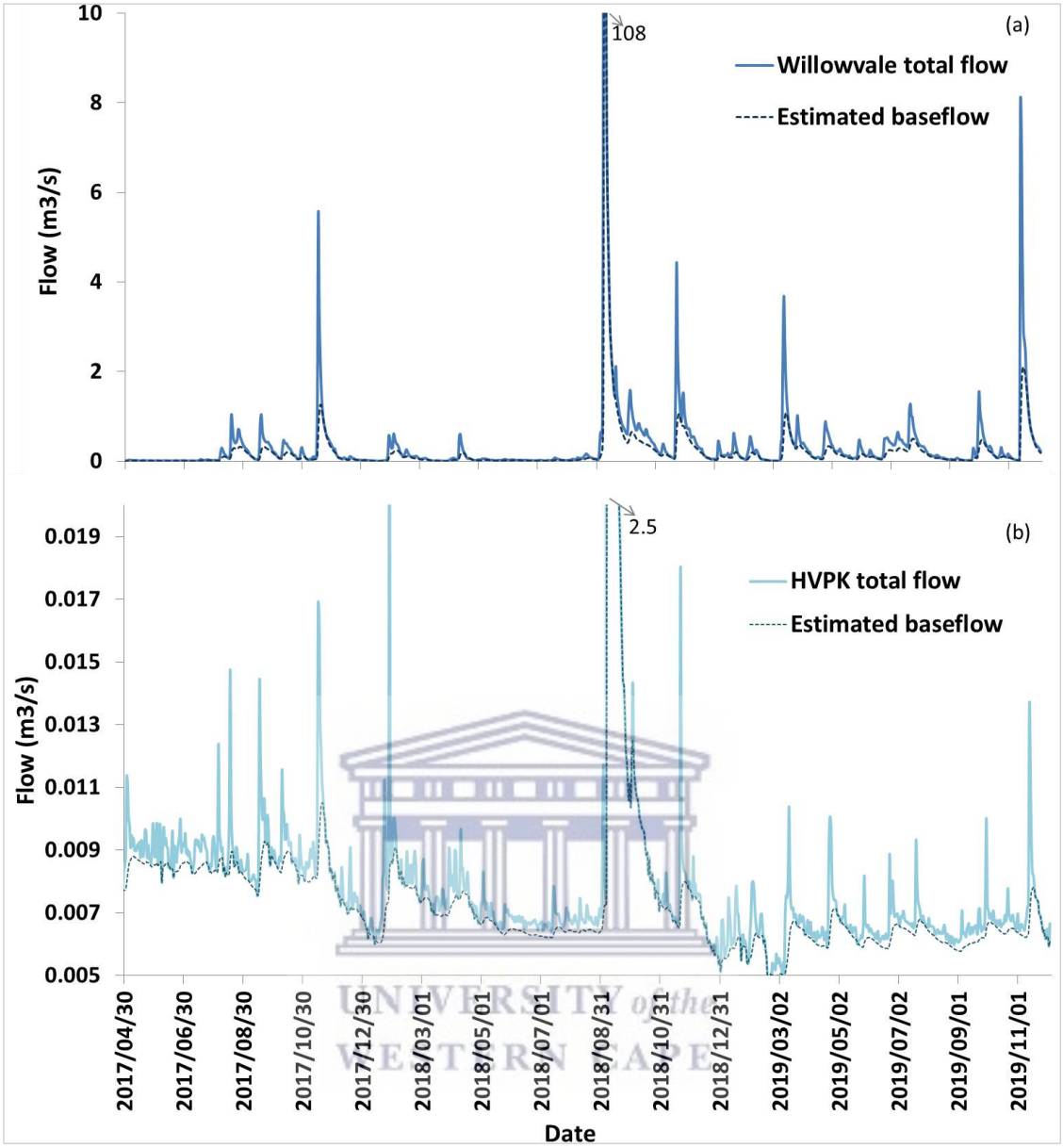

Figure 4.9: Observed streamflow and estimated baseflow at (a) Willowvale (main channel) and (b) HVPK (tributary) sites from April 2017 to December 2019.

To check if the baseflow portion, as separated using the Eckhardt (2005) two parameter numerical filter was showing a reasonable pattern in terms of peaks and recessions, the observed groundwater water levels in the floodplain alluvial aquifer were plotted together with the estimated baseflow time series (Figure 4.10). The estimated baseflow shows relatively similar patterns to the observed shallow groundwater time-series pattern. Unfortunately, due to equipment malfunction, there is no data for year 2017; however, the patterns are comparable to a certain extent between the estimated baseflow and the groundwater levels alluvial aquifer from the period when data was available.

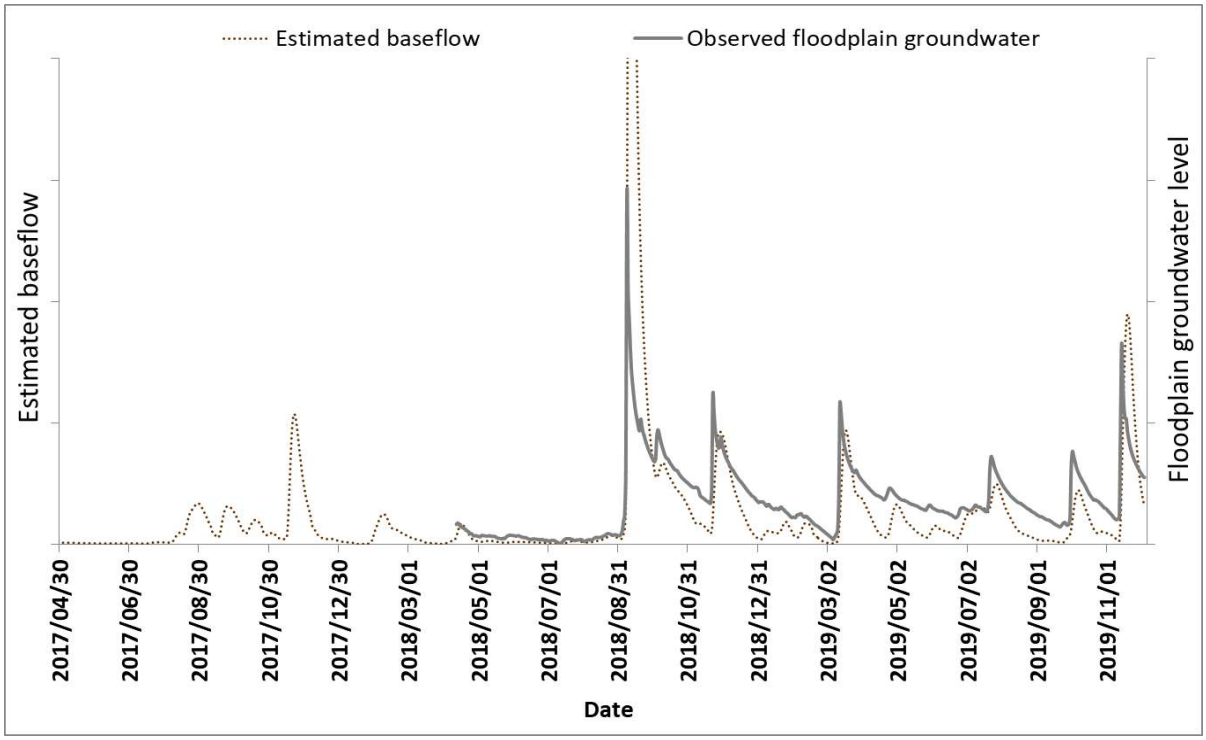

Figure 4.10: A comparison of patterns between estimated baseflow and observed groundwater level patterns at Willowvale site. Units are omitted as graph is comparing patterns only.

BFI values for Willowvale (lower catchment main river site) and HVPK (tributary) for different periods are shown in Table 4.5. BFI gave indications of groundwater discharge to rivers. From April 2017 to December 2019 baseflow sustained flows at Willowvale for approximately 50% of the time whilst at the tributary HVPK, baseflow contributions were higher (73%) than the main channel. The years 2017 and 2019 were relatively dry during the monitoring period, therefore baseflow proportions were high (55% and 95% for main river and tributary sites respectively). Groundwater discharge to the river plays an important part sustaining flows in this catchment.

Table 4. 5: Calculated BFI values for monitored sites

Site	Date/Year	total flow (m^3/s)	baseflow (m^3/s)	BFI
Willowvale	2017-2019	441.51	213.16	**0.48**
	2017	50.96	28.00	0.55
	2018	264.69	115.99	0.44
	2019	125.83	69.14	0.55
HVPK	2017-2019	12.14	8.87	**0.73**
	2017	2.21	2.10	0.95
	2018	7.68	4.63	0.60
	2019	2.25	2.14	0.95

4.5.7 Temporal variation in floodplain surface and groundwater linkages

Data on paired surface and groundwater levels (m.a.s.l.) at adjacent sites were compared to determine possible linkages between the floodplain alluvial aquifer and streamflow (Figures 4.11 to 4.16). Observed responses of the water table in the alluvial aquifer varied with location,

season, antecedent moisture conditions, and the magnitudes of rainfall events. Results will be presented per site (in order from upper to lower parts of the catchment).

4.5.7.1 Temporal variation in groundwater and surface water levels at upper catchment sites, Kromdraai and Kompanjiesdrift

Streamflow characteristics and groundwater levels at one of the upper catchment sites (Figure 4.11) were monitored courtesy of Smith and Tanner (2019).

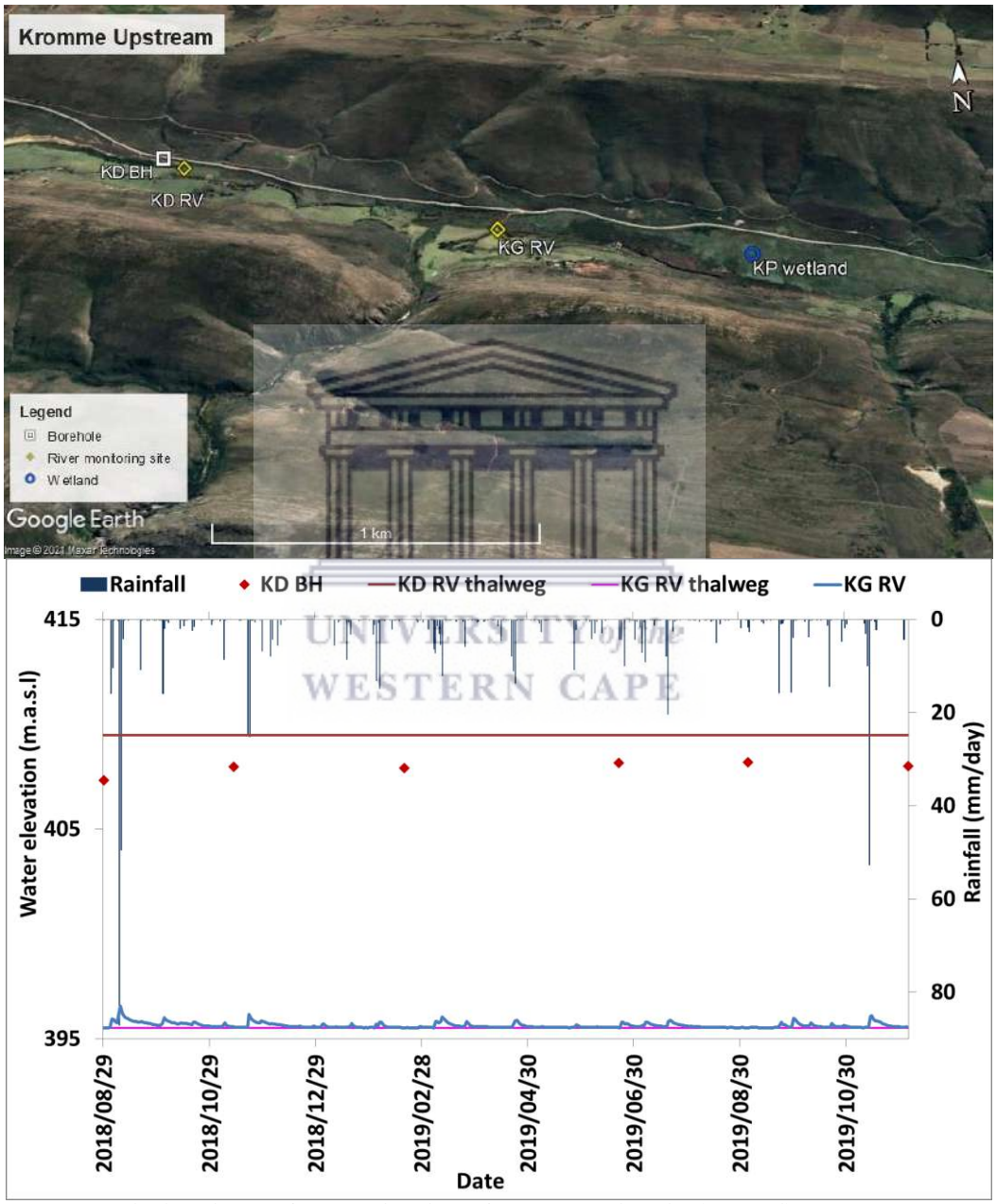

Figure 4.11: Variation in surface and subsurface water levels (m.a.s.l) at an upper catchment site. KD BH and KG RV represent the Kromdraai borehole and the Kromme River at Krugersland. Google earth image 2020 CNES/Airbus (Maxar Technologies, AfriGIS Pvt Ltd).

The water table for borehole (KD BH) at the Kromdrai site (KD) was lower than the adjacent river thalweg for all readings (Figure 4.11). This borehole is in Bokkeveld shale bedrock, which

may not be connected to the alluvial aquifer. Water stage at this site (Kromdraai) was not continuously monitored however, the channel had flow throughout the monitoring period. Although the water table in the borehole was lower than the adjacent river thalweg, it was difficult to ascertain if the river system was losing to groundwater due to the absence of shallow subsurface water level monitoring in the floodplain alluvial aquifer at this location.

The Kromme River at Krugersland (KG) where the Kompanjiesdrieft (KP) wetland starts (Figure 4.11) showed notable responses in channel stage only after rainfall events over 10 mm/day (Figure 4.11). Some of the observed responses to rainfall events were up to 0.6 m increase in river stage after an event. The river flow monitoring site (KG RV) is just after the confluence of the Kromme River and a tributary (Figure 4.11), therefore surface flows from the tributary contributes to river flows at this site.

Shallow groundwater levels (depths <4 m monitored in piezometers) in the upper catchment were monitored at Kompanjiesdrift (Figure 4.12). Piezometers at this site were installed adjacent to the river and close to a gabion weir which is downstream of a palmiet wetland (Figure 4.12). The highest water table was observed at KP PZA and KP PZB in February 2018 (Figure 4.12). KP PZA and KP PZB were the furthest piezometers from the main channel moving upslope (approximately 50 m), however, the high water table could have been due to their location in a ditch therefore, storm water may have accumulated in the ditch resulting in increased infiltration replenishing alluvial aquifer storage. KP PZA has one observation because a stone was inserted into the piezometer. Overall, the water table elevation at KP PZE (adjacent to channel) was on average, higher than the water table elevations at all the other piezometers, including KP PZD and KP PZH, even though they were all located closer to the channel than the rest of the piezometers (Figure 4.12).
The water table at piezometers KPZ E, G and H did not drop below piezometer bottom levels (3.1, 2.5 and 1.9 m respectively) during the dry period. The water table remained within 0-2 m of the ground surface at these points probably maintained by subsurface flows from the wetland.

Other piezometers KP PZD, KP PZF and KP PZI were dry during all field visits. Due to the absence of continuous time series recording instruments at this site, it is therefore difficult to ascertain if the water table never rose to piezometer depths in these piezometers. Piezometer KP PZ D was among the deepest piezometers at this site (3.2 m) and located less than 10 m from the channel, however the water table was below 3.2 m during all field campaigns. There were also potential flows from the mountain bedrock via the tributary into the alluvial aquifer that would influence the alluvial aquifer groundwater levels.

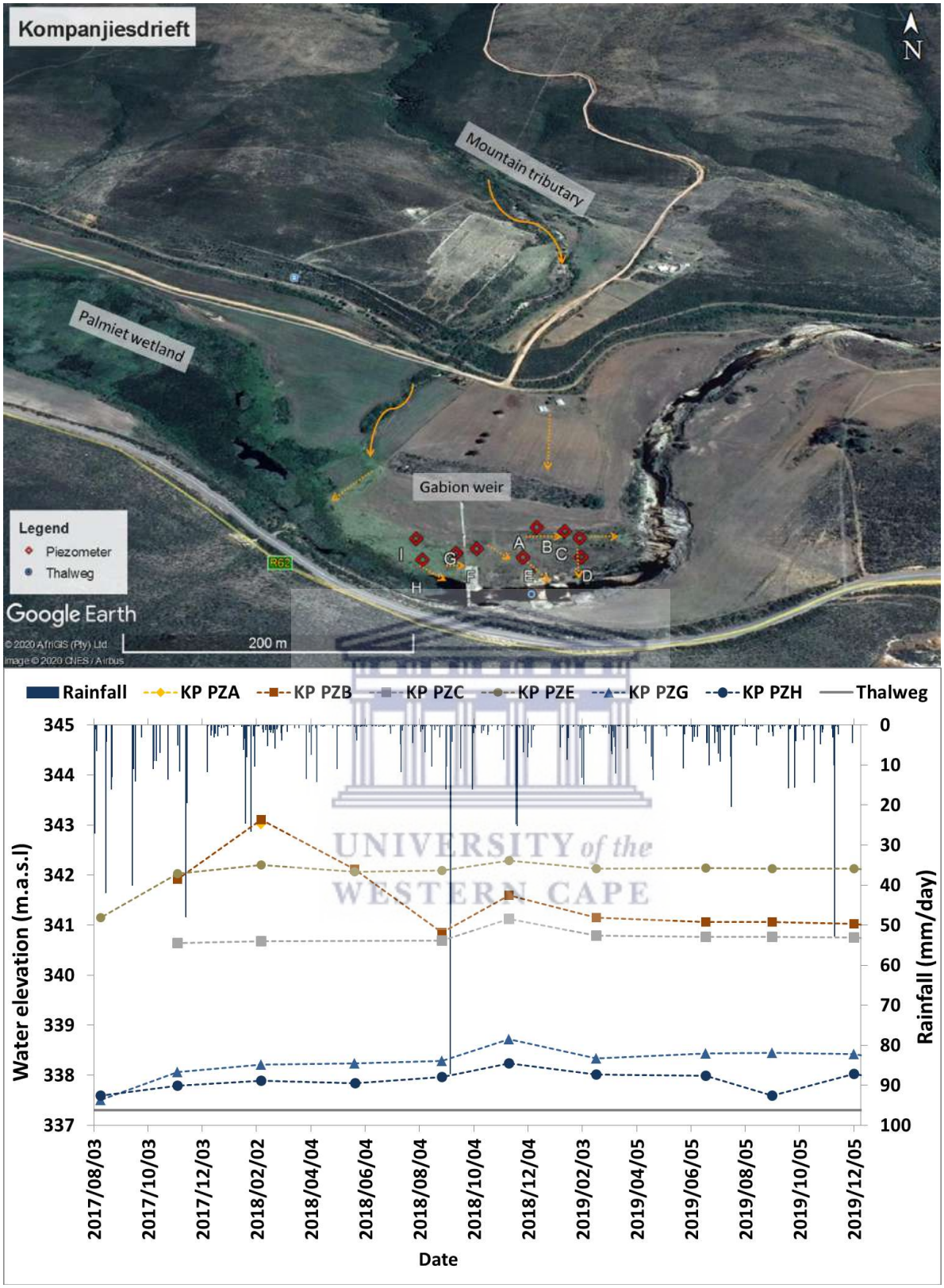

Figure 4.12: Water table responses to rainfall at the gabion site. KP PZ A-H are all piezometers monitored at Kompanjiesdrift site (monitored manually). Google earth image Airbus (2020 CNES/AfriGIS Pvt Ltd).

4.5.7.2 Temporal variation in water table responses to rainfall at the mid-catchment site, Jagerbos

Groundwater was monitored at two boreholes at Jagerbos (Figure 4.13). Both boreholes were not being used for water supply at the time of sampling therefore changes in water levels were all assumed to be due to natural processes.

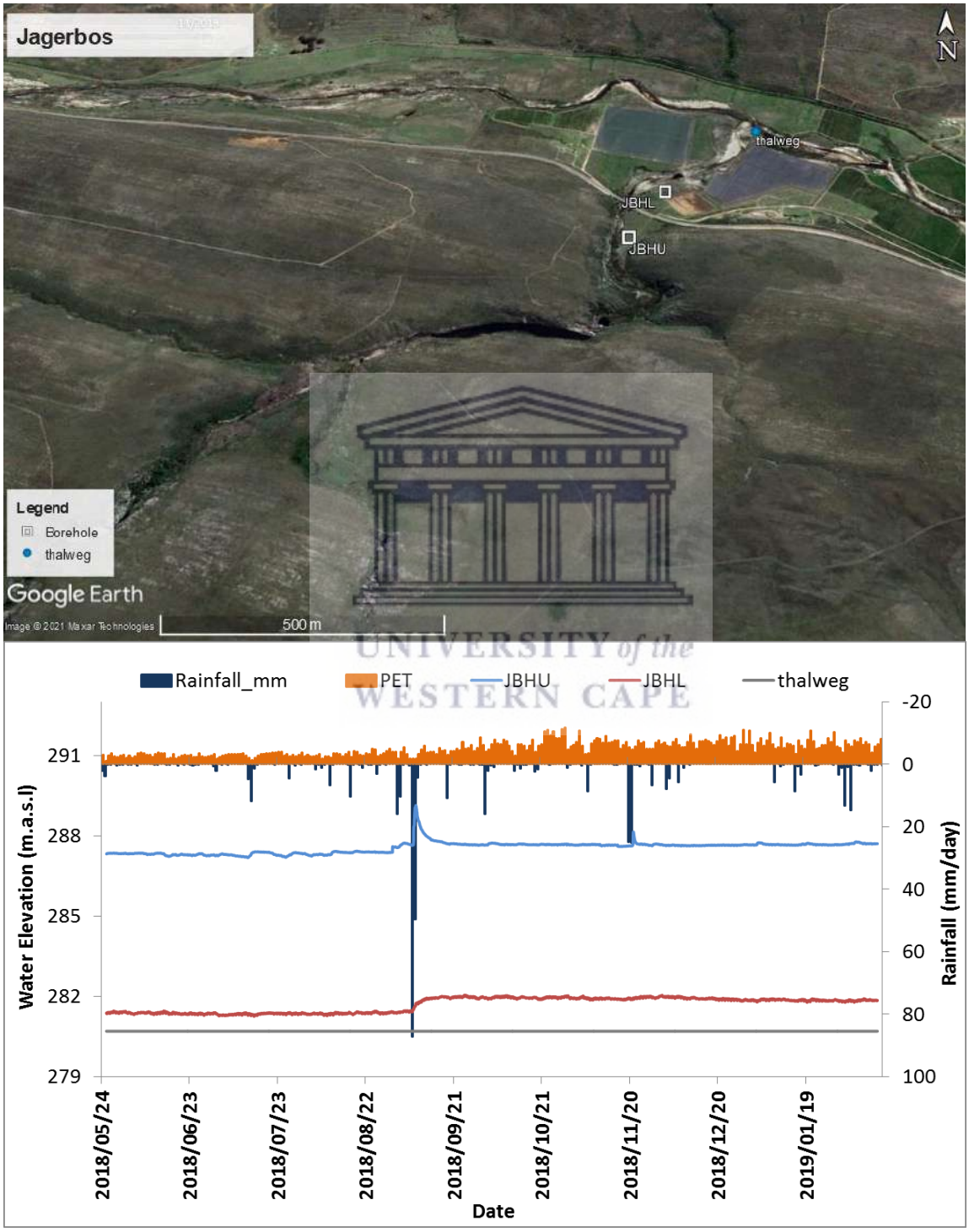

Figure 4.13: Deep groundwater level dynamics in response to rainfall and PET. Airbus Google earth image (2020 CNES/AfriGIS Pvt Ltd). JBHU and JBHL are upper and lower boreholes respectively. (JBHU) is located at the mouth of the narrow incised valley of a tributary while the lower (JBHL) borehole is in the main valley floodplain.

The two boreholes are approximately 300 m apart and drilled in different geological materials. The upper borehole (297 m.a.s.l) is in the quartzitic sandstone of the Nardouw group (~30 m deep) whilst the lower borehole (286 m.a.s.l. at least 100 m deep) is likely in the feldspathic layers of the Nardouw which underlie the main valley alluvial deposit. The water table at the upper borehole (JBHU) fluctuated between 7 and 8 m below ground and between 4 and 5 m at the lower borehole (JBHL) (Figure 4.13).

The water table at both boreholes maintained steady levels throughout the monitoring period only showing notable response to events greater than 10 mm/day at JBHU and greater than 20 mm/day at JBHL (Figure 4.13). Following the occurrence of 134 mm of rainfall in 2 days on the 7th and 8th September 2018, the water table at the lower borehole (JBHL) responded within 24 hours of the event and increased by 100 mm and then by 200 mm the following day. At the upper borehole (JBHU), the water table rose on the second day of the storm, rising by 440 mm and by 260 mm on the 3rd day. Although there were minor differences in their peak timings, the responses to this storm event showed quick responses to precipitation inputs implying direct recharge of the mountain bedrock aquifer. In general the upper borehole had relatively small sharp peaks (i.e. 11 mm rise in water level on 14 July 2018 and 25 mm on 20 November 2018) compared to the lower borehole that had steady increments (Figure 4.13). Due to the location of JBHU (upslope and adjacent to a tributary), the borehole gained subsurface water from the quartzitic sandstone of the Nardouw group and probably contributions from quartzitic sandstones of the Peninsula group higher up the catchment. The lower JBHL is located in the floodplain, where it could have been getting constant contributions therefore water levels rose slowly and stayed elevated. Groundwater from the alluvial aquifer could have been interacting with groundwater from the bedrock aquifer surrounding and beneath it.

4.5.7.3 Temporal variation in surface and subsurface water levels at the mid catchment site, Hudsonvale

Figure 4.14 shows water levels in the main river at HV (midcatchment) and two tributaries discharging into the river at this site: HVPK tributary originates from the Suuranys Mountains on the north side of the main valley while the Witels comes from the Tsitsikamma in the south. HVPK shows relatively constant water levels which indicate a steady supply of water. Witels is highly responsive to most events (Figure 4.14), however the record stops in 08-2018 as the instrument was lost in a flood. The main channel is highly responsive as expected due to the size of its contributing area as well as the alluvial storage it drains from. Most of the tributaries are perennial and mountain streams and seeps were observed even during the drought in 2016 (scoping trips) and 2017 (when monitoring commenced). Seeps discharging into tributaries and wetlands were observed on the high plateaus in both the two mountains suggesting that surface flow in these tributaries was recharged by groundwater from the bedrock aquifer.

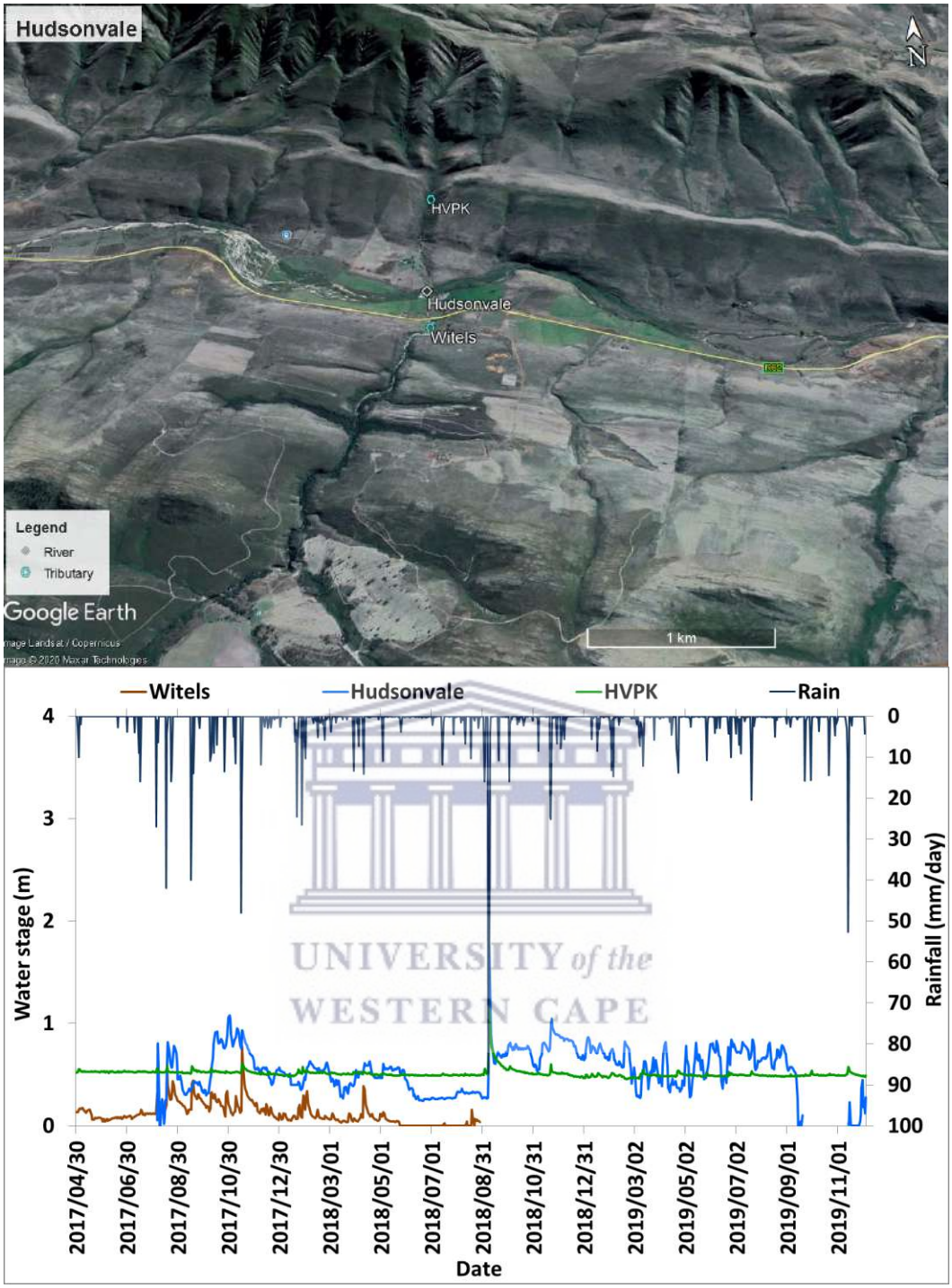

Figure 4.14: Temporal variations of surface water responses to rainfall from 2017 to 2019.

Variations of rainfall, water table and river levels at Hudsonvale from Sept 2017 to Dec 2019 are shown in Figure 4.15. Along the main river at Hudsonvale (Figure 4.15), the water table of the alluvial aquifer was consistently above the river stage suggesting that the river was gaining at this reach. The catchment was relatively dry when monitoring began (April 2017), but the water table increased steadily in response to several rainfall events less than<10 mm/day. The water table at PM PZ1 and PM PZ2 located inside the wetland increased significantly after receiving a cumulative rainfall of 172 mm during the period from May to July 2017, then remained relatively constant. After this initial level rise, there was no decline in the water table (Figure 4.15) which

suggests that there was continued recharge of groundwater or no ET losses, unlike GS PZ3 and GS PZ4 that showed declines after events due to storage depletion in the alluvial aquifer.

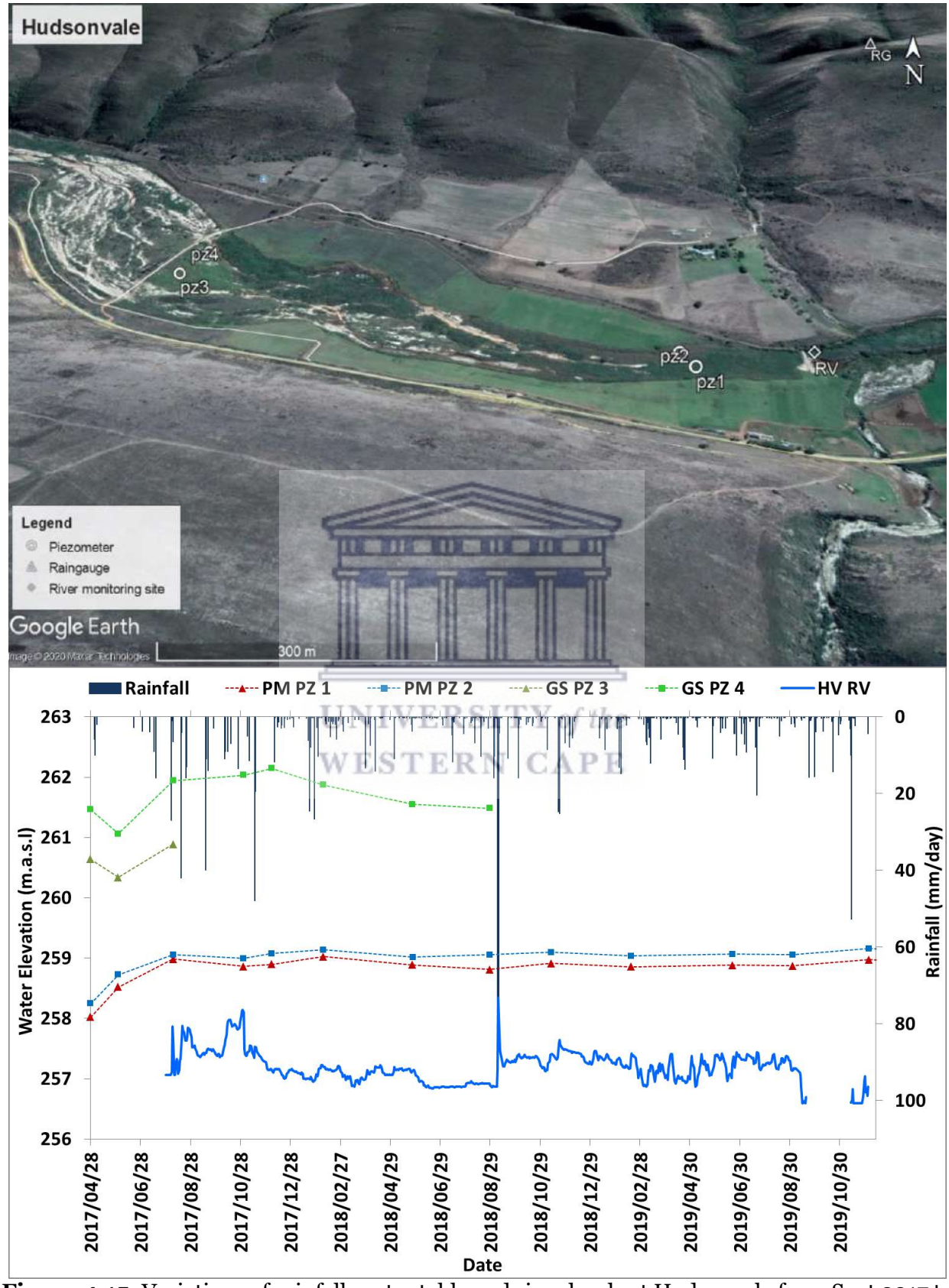

Figure 4.15: Variations of rainfall, water table and river levels at Hudsonvale from Sept 2017 to Dec 2019 (middle part of the catchment). GS and PM represent piezometers in sites dominated by grass and palmiet respectively. Airbus Google earth image (2020 CNES/AfriGIS Pvt Ltd)

Due to fine, organic soils, subsurface flow out of the wetland was likely slower (PM PZ1 and PM PZ2) than other parts of the alluvial aquifer (GS PZ3 and GS PZ4).

The palmiet slows surface flows coming in along the main channel and promotes recharge. The wetland at this site receives water flowing down the main channel as well as inflow from the alluvial aquifer on the sides depending on the slope of the water table. Similar observations to the upper wetland (shown in Figure 4.12) are also observed at this site where subsurface flow from the tributary catchment comes through the alluvial fan and recharges the floodplain alluvial aquifer resulting in a groundwater gradient towards the wetland.

4.5.7.4 Temporal variation in surface and subsurface water levels at the lower catchment site, Willowvale site from 2017-2019.

Water levels (in m.a.s.l) for adjacent river and the alluvial aquifer at Willowvale site were plotted together (Figure 4.16) to determine when the water table was above or below the river thalweg or river water level. Since monitoring commenced at the Willowvale site, water table responses were observed at the grass and palmiet dominated areas, while piezometers in the wattle site remained dry for most of the monitoring period (water table was below the depth of installed piezometers). Following the September 2018 rain event, the water table rose sharply at all locations (grass, palmiet, and wattle) as well as the stream levels (Figure 4.16). Peaks were within hours to a day of effective rainfall.

The Kromme River has perennial flow at this site and the water table at the grassland and palmiet sites was generally above adjacent river thalweg (Figure 4.16). However, in some cases, the water table dropped below piezometer depths, particularly during extended dry periods (from April to August 2017 and June to August 2018 as well as between September to December 2019). Data gaps at groundwater sites (Figure 4.16) indicate that the water table was below the piezometer depth except at PM PZ 4 where automated data collection only began in May-2018 (Figure 4.16).

The water table at the grassland area which was monitored at GS PZ7 piezometer was always above the river bed, which suggests that groundwater had the potential to discharge into the river at this site (Figure 4.16). At the other grassland site, GS PZ 6 (Figure 4.16), the water table rarely responded to rainfall events (maximum of 50 mm rise observed) with water levels dropping below the piezometer depth during dry periods. The water table monitored at PM PZ4 inside the palmiet wetland showed quick responses to rainfall events. Water levels never dropped below the piezometer depth at this site. The water table monitored at piezometers located downstream of the surface water monitoring site, (WT PZ1 and WT PZ3) remained below piezometers depths (up to 3 m below the surface) except for a brief period following the 7 and 8

September 2018 flood event (134 mm) (Figure 4.16). The water table was lowest at WT PZ1 and WT PZ3 located inside a dense wattle stand.

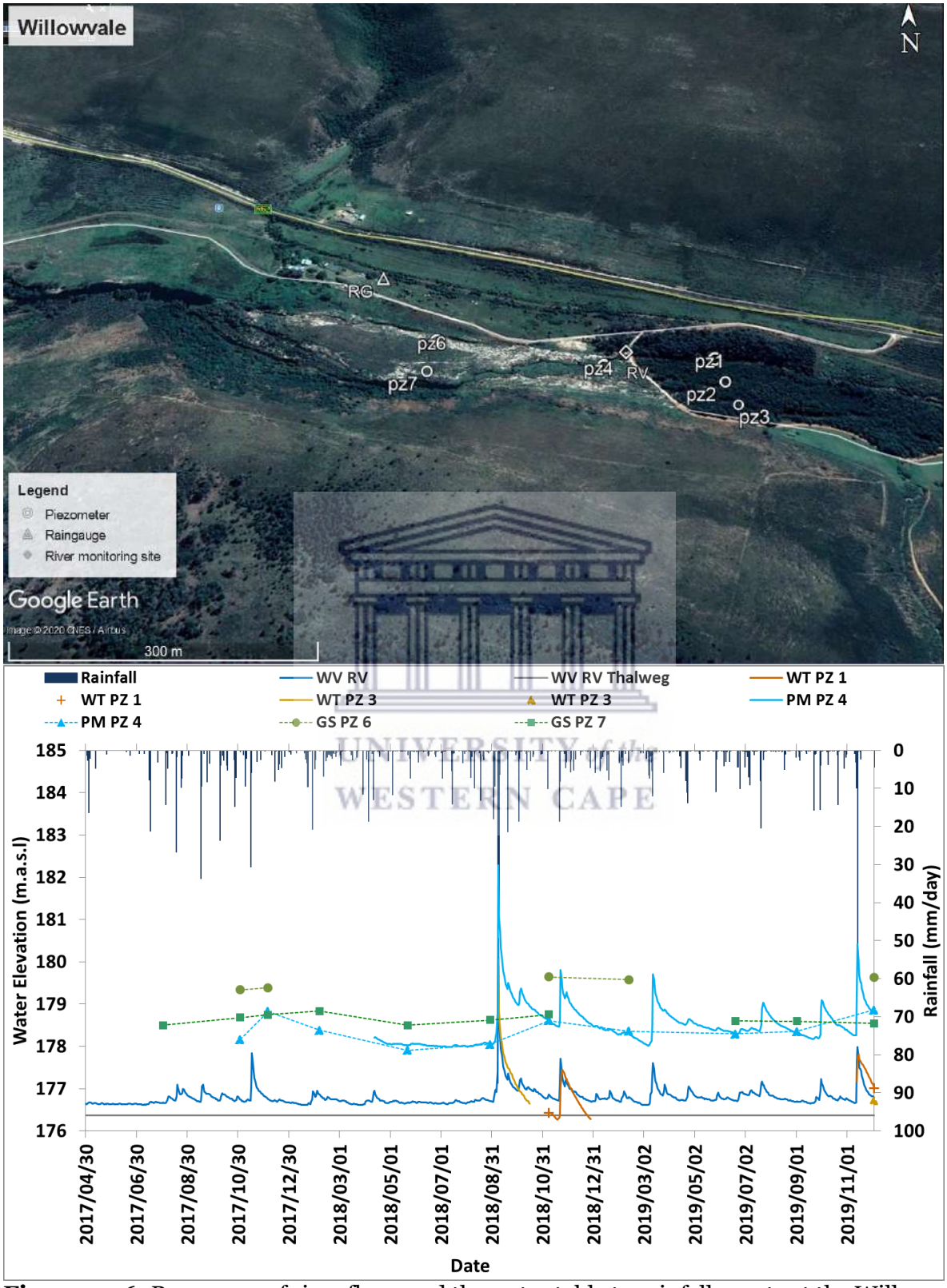

Figure 4.16: Responses of river flows and the water table to rainfall events at the Willowvale site (WV). WT, PM and GS represent piezometers in wattle, palmiet (manual and automated observations) and grass locations. Airbus Google earth image (2020 CNES/AfriGIS Pvt Ltd).

A summary of results from the hydrometric observations in this chapter is given in Table 4.6. Results are given for different scales monitored.

Table 4. 6: Summary of observed results in the Kromme catchment from 2017-2019

Scale	Flowpath/process	Analyses	Results and Interpretation
Tributary	Groundwater flow contribution into tributaries	Seeps were observed in tributary valleys and wetlands even during the drought	Most tributaries observed had perennial flow from contributions from the bedrock aquifer through seeps.
Alluvial aquifer/River	Water exchange between the floodplain alluvial aquifer and the main channel	Comparison of floodplain Groundwater elevation vs. river thalweg elevation	Alluvial aquifer groundwater elevation was consistently above river thalweg at most monitored river reaches in the floodplain showing that alluvial aquifer groundwater discharges into the main channel, even during dry periods.
Bedrock aquifer	Deep groundwater recharge	Groundwater level change after a rainfall event	Groundwater levels increased notably indicating local recharge through direct infiltration, percolation and flow to the site after storm events (i.e 25 mm/day in November 2018, 46 mm/day and 87 mm/day in September 2018).
Alluvial aquifer	Shallow groundwater recharge	Groundwater level peak timing after storm events at different locations	Dominance of recharge was indicated by minimal peak delays after rainfall events at the different locations.
Catchment	Contributions of quick and slow flowpaths	Numerical filter applied to hydrograph	Relative dominance of quick (surface and fast shallow subsurface) and slow subsurface flowpaths. Baseflow was highly variable in some tributaries and main river sites indicating variable aquifer storage.
Catchment	Runoff vs precipitation received	Calculated average annual runoff coefficients	Low ratios (0.07-0.09) indicated large ET withdrawals from the dominant flowpaths in the catchment and/or storage in inactive groundwater
Catchment	Flow recession after peak	Recession analysis (constant value) per site	High recession constants (0.7-0.9) at all sites indicated the dominance of fast interflow and/or floodplain drainage during event recession periods

4.6 DISCUSSION

Analyses of streamflow and groundwater data revealed response patterns to precipitation inputs indicative of various flowpaths such as flow from alluvial aquifer into the main channel and bedrock discharge into tributaries. This was used to guide the development of a conceptual model for the Kromme catchment (Figure 4.17). The hydrometric data showed linkages between the river, TMG groundwater, and the floodplain alluvial aquifer. The results indicated that groundwater from bedrock aquifers discharged into tributaries which in turn recharged the floodplain aquifer. Surface flows from mountains also discharged into tributaries and infiltrated into alluvial deposits in tributaries and on the floodplain. Surface and subsurface flows from perennial tributaries were important in recharging the floodplain alluvial aquifer as well as maintaining channel flows and supporting floodplain wetlands even in drought conditions. Tanner et al. (2019) investigated surface and groundwater interactions and reported similar observations in the upper Kromme. Their results showed that the wetland and river flows were sustained by groundwater discharge from the surrounding bedrock aquifers. Flows were sustained by subsurface water (both interflow and groundwater) through the alluvial fans and tributaries. Many of the large tributaries in the Kromme have perennial flow thereby sustaining river flows in the main channel. Similar flowpaths were also reported in other TMG studies where uplands and valleys were connected by baseflows originating higher up in the mountains (Glenday, 2015).

After storms, infiltration in the floodplain alluvium causes push-through of soil water into the river. Higher up in the mountains, water also infiltrates and percolates through the soil to recharge the shallow fractured rock layer and possibly pushes through old water in this layer to the channel (where mountain streams intersect rock) and some water flow to the alluvial aquifer then to the channel. Similar linkages and flowpaths have also been reported in other catchments with similar settings in the Cape Fold Belt such as the Hex (Rosewarne, 2002) and Baviaanskloof (Glenday, 2015) catchments. A comparison of the Kromme catchment to the neighbouring Baviaanskloof catchment (Glenday, 2015) shows major differences in responses despite the two catchments having many similar attributes; geology, drainage patterns, narrow valleys bordered by steep hillslopes. However, the Baviaanskloof has a drier climate (approximately 300 mm/year) than Kromme and its mountain tributaries do not have perennial flows, unlike those in the Kromme. The Baviaanskloof had a dynamic losing and gaining system (Glenday 2015); the Kromme River on the other hand was consistently gaining during the monitoring period despite the drought conditions. With reference to the channel, the depth of the floodplain water table in Baviaanskloof is at a lower level whilst in the Kromme the water table is relatively higher hence the Kromme has perennial flows in general with floodplain alluvial aquifer levels consistently supporting large permanent wetlands.

Most mountainous catchments have limited alluvial aquifers due to small floodplain areas, therefore the contribution of alluvial aquifers to storage and catchment outflow in mountainous areas is often assumed negligible (Käser and Hunkeler, 2016). The Kromme catchment has a sizeable floodplain with alluvial aquifers that make notable contributions to catchment storage and outflows. Throughout the monitoring period, the Kromme channel was gaining from the alluvial aquifer (water table largely above surface water level), and mountain bedrock through tributary flows. Other studies have reported similar results where groundwater discharge from TMG quartzitic sandstones plays an important role in sustaining river flows and wetlands (Colvin et al., 2003; Glenday, 2015; Martinez et al., 2017; Pulley et al., 2017). Seeps in the catchment were observed discharging into tributaries during drought, indicating consistent contributions from the bedrock aquifer to river flows and wetlands. The presence of wetlands and seeps recharged by bedrock aquifers and faster interflow in different parts of the catchment which were observed in the Kromme were also reported in other TMG studies (Roets et al., 2008; Xu et al., 2002). Seeps in this catchment were formed where Peninsula or Nardouw formations intersects with less permeable shale layers. Peninsula seeps are perennial whilst Nardouw seeps have been reported to be intermittent (Xu et al., 2009). The Peninsula outcrop makes up the high mountains where it rains more than in the valley resulting in increased recharge of the bedrock aquifer. Outflows from the Peninsula occur higher up the mountains and flow across in tributaries to get to the main valley.

Steep and rocky areas that make up much of the Kromme catchment resulted in notable flood peaks after high-intensity storms. Large contributions of quick flows to river flows were observed after heavy storms with lag times of less than 24 hours. In tributaries, a general lag of 1 or 2 days for peak flow response after events implied surface runoff and/or push-through subsurface flow dominates hydrographs during storms. Runoff coefficients ranged between 0.09 (main channel sites) to 0.26 (tributary) which were low but not unusual for semi-arid catchments based on results from studies in similar settings (James and Roulet, 2009; Penna et al., 2011; Glenday, 2015). In the main valley, average annual runoff coefficients were low implying large ET withdrawals from dominant flowpaths and/or storage in inactive groundwater. At the mid-catchment site (Hudsonvale), streamflow appeared to be recharged dominantly by faster flowpaths from storm events, shown in the quick peak and quick decline of the hydrograph, whilst further downstream (Willowvale), both fast and slow flowpaths appeared as key contributors to the storm response, shown in the quick peaks but slow recessions. Prolonged elevated flows weeks after events indicated flow contributions from deep, slow subsurface flowpaths whilst delayed contributions of a few days could have been from faster interflow. Overall, sharp hydrograph peaks indicated surface and shallow subsurface flow dominance in the storm response of the catchment. Antecedent soil moisture and spatial rainfall

controlled runoff and peak flow responses similar to results reported in other semi-arid catchments (James and Roulet, 2009; McGuire and McDonnell, 2010; Merz and Blöschl, 2009).

Overall the catchment streamflow was estimated to be sustained by baseflow for more than 60% of the time. As expected, baseflow from different storages i.e. bedrock and /or alluvial aquifer sustains streamflow in the absence of surface flow during dry periods (Roy and Hayashi, 2007; Glenday, 2015). Recession patterns showed that the channel is receiving flow from different storages and flowpaths at different rates with maximum recession days up to 22 days indicative of interflow dominance and also drainage of elevated alluvial aquifer. Variability in recession characteristics was therefore attributed to differences in local conditions, storages and topographic properties (Käser and Hunkeler, 2016; Smakhtin, 2001). The study also highlighted the importance of mountain bedrock aquifer discharge to the water levels in the alluvial aquifer and outflows in the Kromme River.

4.7 CONCEPTUAL MODEL

Using patterns gathered from field data, a conceptual model of different flowpaths dominant during the monitoring period was developed for the Kromme Catchment (Figure 4.17).

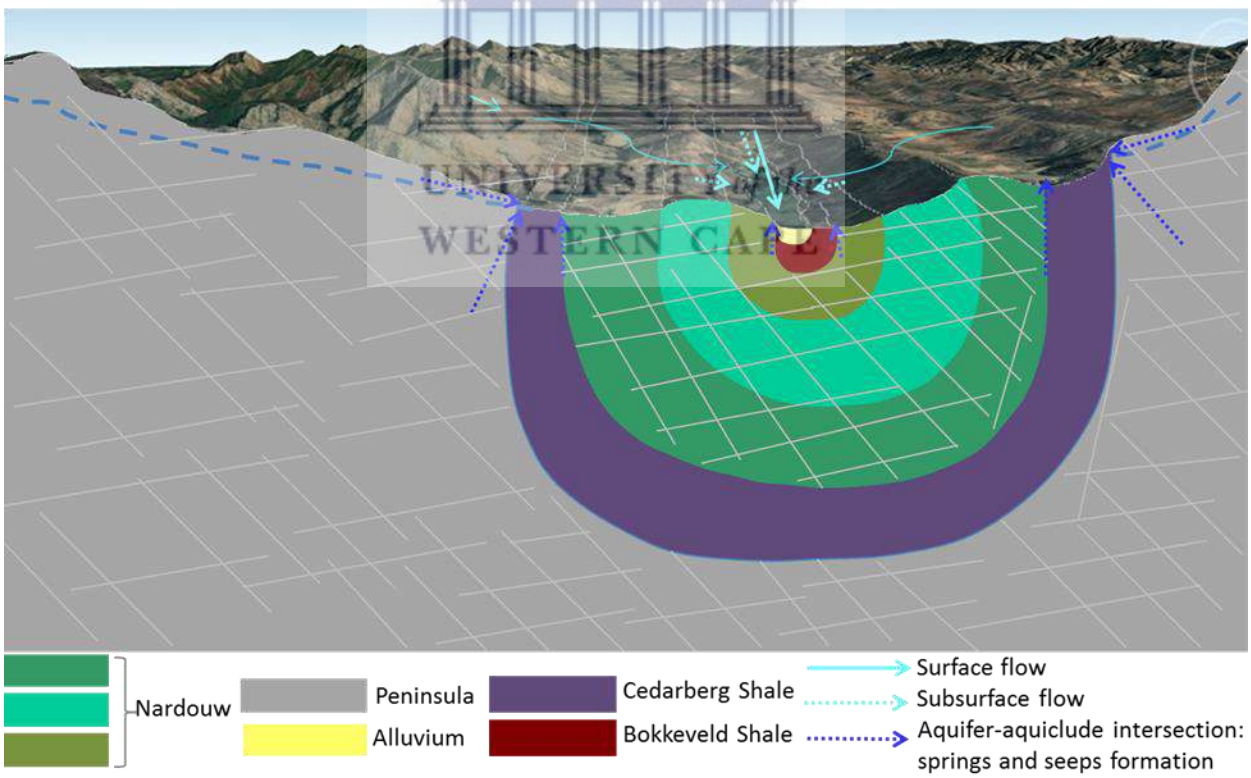

Figure 4.17: Proposed conceptual model showing the dominant flowpaths for the Kromme Catchment (Adapted from Cornelius et al., 2019).

Dominant processes observed in the catchment and inferred from the data are interception by plants, infiltration through the shallow soils and percolation into the highly fractured bedrock to

recharge the bedrock aquifer. Surface runoff after storm events dominates for short periods before it gets lost to ET or infiltration. Surface flow from mountains potentially becomes tributary flow and some infiltrates into alluvial deposit in the mountain or on the floodplain alluvial aquifer then to the river and some of it is lost to ET along the flowpath. Groundwater flow from bedrock aquifer into tributaries appeared constant; seeps were observed flowing consistently into tributaries even during the drought. Most tributaries had water flowing directly into the channel but some tributaries formed alluvial fans at the toe slopes due to deposition of alluvial materials. Flows from these tributaries got to the main river as subsurface flow through the alluvial fan and alluvial aquifer. Alluvial fans in the floodplain acted as buffers and enabled groundwater-surface water interactions.

The alluvial aquifer also received water from the bedrock aquifer and was also recharged by direct precipitation. Subsurface flows from the floodplain alluvial aquifer and mountain bedrock aquifer into the river maintained baseflows. Surface runoff was assumed minimal in the floodplain due to the presence of large sandy alluvial fill/storage. Infiltration and percolation to the alluvial aquifer raised the level of the floodplain water table resulting in increased alluvial aquifer flow to channel. Infiltration in the alluvium also caused push-through of old soil water into river after storm events. In mountains, infiltration and percolation through the thin soils recharged the bedrock aquifer and older water in the shallow fractured rock layer is pushed to the channel where mountain streams intersect the bedrock and some flows to the alluvial aquifer first then to the river.

Conclusion

Hydrometric methods proved invaluable in the general conceptualisation of flowpaths in this catchment however, there are some limitations associated with their application. The occurrence and/or dominance of certain responses and flowpaths were inferred by checking for particular patterns in the data. The conceptualised responses and flowpaths need to be quantified, i.e. quantifying how much groundwater from the bedrock gets to the alluvial aquifer and eventually to the main channel and what proportion of groundwater from the alluvial aquifer contributes to streamflow and how these contributions vary at a temporal scale. Knowledge gathered in this chapter and developments made in subsequent chapters will be used to make decisions about a numerical catchment model structure, calibration and selection of model parameter values to improve the prediction of vegetation impacts on processes.

CHAPTER 5: TEMPORAL VARIATIONS OF WATER TABLE AND SOIL WATER CONTENT UNDER A FLOODPLAIN BLACK WATTLE TREE STAND; PALMIET WETLAND AND GRASSLAND COVER TYPES.

5.1 ABSTRACT

Mountainous catchments are important freshwater sources that sustain surrounding ecosystems, agriculture, domestic and industrial uses. Invasions of floodplains by alien woody species replacing predominantly herbaceous indigenous vegetation have altered the hydrological and ecosystem functioning in these catchments particularly in semi-arid regions. Although existing studies have examined and provided evidence of changes in river flows following the establishment or clearing of alien woody vegetation, our understanding of impacts on soil water content and groundwater remains poor. As such, this work compares temporal and spatial variations in soil water content and groundwater levels at three locations with different vegetation types: invasive black wattle (*Acacia mearnsii*) trees, palmiet (*Prionium serratum*) wetland, and grass (dominated by *Pennisetum clandestinum spp*), within a floodplain site in the Kromme Catchment in the Eastern Cape Province of South Africa.

Soil water content and shallow groundwater levels (< 4m below ground) were monitored from August 2017 to December 2019 using soil moisture probes and piezometers. Rainfall, vegetation type and antecedent conditions were identified as the major factors controlling variations in soil water content and water table fluctuations. On average, soil water content and water retention were significantly higher ($p<0.05$) at the palmiet site, whilst the wattle site had the lowest among the three sites. Across all sites, shallow soils at 0-20 cm had significant responses to light and medium rainfall events (5-20 mm/day). However, soil water content responses of soils at 50-60 cm depths were dependant on the magnitude of the event and antecedent conditions, and varied significantly across the three sites. At the grassland site, soils at 50-60 cm depths responded significantly after rainfall events of at least 30 mm/day whilst the palmiet and wattle sites responded after at least 25 and 11 mm/day respectively. At the wattle site, the water table was below the depth of installed piezometers (3 m) for more than 90% of the time, only rising to this depth following heavy storms greater than 40 mm/day likely due to increased transpiration rates by the woody alien trees. The results of this study can support ecological restoration programmes and contributes to the body of literature showing influences of land cover types on soil water content and shallow groundwater.

5.2 INTRODUCTION

Water scarcity is a global phenomenon that is projected to increase particularly in arid and semi-arid regions. Therefore considerable efforts to improve water supply continue being made worldwide. Land use and land cover types, their location within a catchment and changes thereof are some of the factors that control and alter hydrological responses of catchments (Awotwi et al., 2015; Berihun et al., 2019). One major issue in many countries is the encroachment of riparian zones by alien woody species. Some of the problematic species are willows (*Salix spp*) in Australia, salt cedar (*Tamarix spp*) in America, and the black wattle (*Acacia mearnsii*) in South Africa (Doody et al., 2011; Huxman et al., 2005; Rebelo et al., 2015). Woody trees typically use more water than herbaceous plants and seasonally dormant grasses (Calder and Dye, 2001). Several studies have quantified reductions in river flows from areas with woody alien plant invasions and/or changes in streamflow patterns after clearing (Albhaisi et al., 2013; Doody et al., 2011; Dye and Jarmain, 2004; Galatowitsch and Richardson, 2005; Görgens and Van Wilgen, 2004; Huxman et al., 2005; Le Maitre et al., 2015; Warburton, 2012). Other studies have focused on variations in soil water conditions under different land uses and land cover types (She et al., 2010; W. Yang et al., 2019). However, there are limited studies characterizing the dynamic variations in both soil water content and groundwater levels in areas with contrasting vegetation types, particularly in semi-arid areas (Jacobs et al., 2013; Niu et al., 2015)

Knowledge of soil water content is important because soil water affects various ecohydrological processes in the soil-plant-atmosphere continuum (Hou et al., 2018; Ries et al., 2015; Xiaodong et al., 2013). Soil water exerts control on rainfall partitioning into infiltration, runoff and plant transpiration (Legates et al., 2011; J. Yang et al., 2019). It affects runoff generation as well as the structure and organization of vegetation. Characterizing available soil water, therefore, offers unique insights into soil water status, depletion and recharge (Ries et al., 2015) which are all essential for understanding vegetation impacts on hydrological processes.

In South Africa, the Australian black wattle predominantly invades riparian areas where soil water is readily available (Dye and Jarmain, 2004) and competes aggressively with the native vegetation such as fynbos, palmiet and grass. Black wattle alters the catchment's hydrological regime and ecosystem function by increasing rates of transpiration resulting in lowering of water table and recharge rates leading to reductions in stream flows (Dye and Jarmain, 2004; Galatowitsch and Richardson, 2005; Görgens and Van Wilgen, 2004; Le Maitre et al., 1999). Previous work has shown considerably higher water use by *Acacia* species invasions compared to

the indigenous fynbos, grass and palmiet they often replace, particularly in riparian zones (Dye and Jarmain, 2004; Le Maitre et al., 2015; Rebelo et al., 2015). Black wattle has shallow lateral roots (Le Maitre et al., 2015), but can also grow long tap roots depending on availability of soil water (Clulow et al., 2011). Field measurements and estimates of transpiration rates for black wattle ranges from 740-1500 mm/year (Clulow et al., 2011; Dye and Jarmain, 2004; Meijninger and Jarmain, 2014), 600-900 mm/year for grassland (Calder and Dye, 2001; Dye and Jarmain, 2004), 600-950 mm/year for fynbos(Calder and Dye, 2001) , and 695 mm/year for palmiet (Rebelo, 2012). Clearing of alien woody species has been observed to increase groundwater recharge and river flows (Albhaisi et al., 2013; Moyo et al., 2009; Scanlon et al., 2005). Schilling (2009), in the USA, found that the water table rose higher in areas with grass compared to areas with woody tree species following rainfall events indicating the variability of riparian water depths under different vegetation types.

It is important to investigate the impacts of black wattle on soil water dynamics but there is also need to compare the impacts to the vegetation types it replaces. In the eastern and southern parts of South Arica, black wattle replaces different vegetation types including the rare palmiet plants (Crous et al., 2019; Railoun, 2018). Palmiet (Figure 5.1) is endemic to South Africa, often found in valley bottom areas (Rebelo, 2012). Palmiet is regarded as an ecosystem engineer due to its extensive, fibrous, and thick root system (can grow up to 2 m) that traps sediment and slows down the velocity of streamflow during flood events, thereby stabilizing and filling in channels (Rebelo et al., 2019, 2015; Sieben, 2012).

Figure 5.1: Palmiet root system (a), dead palmiet under a canopy of a wattle stand (b))

However, in many areas, palmiet is considered undesirable by landowners who claim that it clogs rivers and impedes streamflow (Boucher and Withers, 2004; Job and Ellery, 2013; Rebelo, 2012). For this reason, palmiet wetlands are threatened by agricultural development (Rebelo et al., 2019), in addition to invasions by alien plants. Palmiet does not survive competition when invaded by woody species because of the intolerance to full shade from the dense cover (Figure 5.1) (Boucher and Withers, 2004; Rebelo, 2012).

The Working for Water Programme in South Africa has been clearing invaded alien plant species (IAPs) since 1995 (Galatowitsch and Richardson, 2005; McConnachie et al., 2012) to eliminate their adverse effects on water resources. It is already known that when transpiration rates increases, river levels decrease but the same cannot be assumed for soil water content and groundwater. Temporal variation in soil water content and groundwater responses helps to better understand processes leading to streamflow response. Water use of a vegetation type can vary considerably with its setting (soil, climate conditions, landscape position) and, therefore it can be difficult to compare findings for vegetation types across different individual studies. This study compares soil water content and groundwater across different vegetation types in a similar setting. The existing literature suggest that black wattle uses more water (Calder and Dye, 2001; Clulow et al., 2011; Dye and Jarmain, 2004; Le Maitre et al., 2015) than palmiet (Rebelo, 2012) and grass (Calder and Dye, 2001). However, studying palmiet vs. wattle and grass in the same conditions has never been done. Furthermore, monitoring of these vegetation types is being done in a different catchment setting and topographic position than is often done (floodplain in the middle of a meso-scale mountainous catchment). Given these gaps, it is hypothesized that at large catchment scales, such as the entire Kromme catchment, the effects of wattle expansion will result in decreased flow peaks and the subsequent palmiet wetland loss will result in increased overbank flooding as flow peaks are normally dampened and buffered by the presence of palmiet wetlands and large floodplains respectively. Rebelo (2012) analysed long-term estimated streamflow in the Kromme catchment and found evidence of change in rainfall-runoff relationship correlating with increased coverage of black wattle. This means that the clearing of black wattle could potentially result in an overall increase in catchment water yield through a decline in ET. This study did not do direct ET measurements but differences in soil water content and groundwater responses in the same setting were appropriate indicators of possible impacts and to make recommendations for future work.

This chapter assess impacts of alien woody plant invasion on soil water content and water table responses in areas dominated by herbaceous indigenous vegetation. Soil water content variation (0-60 cm) and shallow groundwater levels (up to 3 m deep) were monitored at sites with different vegetation types (grass, palmiet and wattle) for different rainfall events within a floodplain site in the Kromme catchment. The selected site is a reach of the Kromme River in the Eastern Cape Province of South Africa where one area has been cleared of black wattle and the other has not yet been cleared (Figure 5.2), providing an opportunity to investigate the impact of clearing invading alien woody species in riparian areas dominated by herbaceous indigenous vegetation.

5.3 MATERIALS AND METHODS

5.3.1 Study site: Willowvale, Kromme River

The Kromme River catchment's location, geology and land use description have been presented in Chapter 3. The work presented in this chapter is based on data collected at Willowvale, a site in the lower part of the Kromme catchment (Figure 5.2). Additional photos have been added on the figure to show the three different vegetation types at this site.

The Willowvale site presented an opportunity to monitor soil water content and shallow groundwater across multiple vegetation types in close spatial proximity to one another. The Working for Water Programme cleared IAPs in riparian zones in the catchment moving from upstream to downstream of the Kromme River. However clearing of (IAPs) at the Willowvale site was not completed, with the floodplain area to the west of a road crossing having been cleared in 2014 and the area to the east retaining solid black wattle cover (Figure 5.2).. The site has invaded and uninvaded areas which therefore vary in vegetation cover: dense wattle stand, recovering palmiet and grassland after black wattle clearing. The different sub-sites can be assumed to experience similar rainfall and temperature as well as adjacent streamflow and groundwater inputs from the upper catchment and surrounding mountains due to their close proximity (approximately 150 m apart) (Figure 5.2). Furthermore, soil properties were also similar across the three sites; differences in soil water content between the sites can largely be attributed to the differences in vegetation cover.

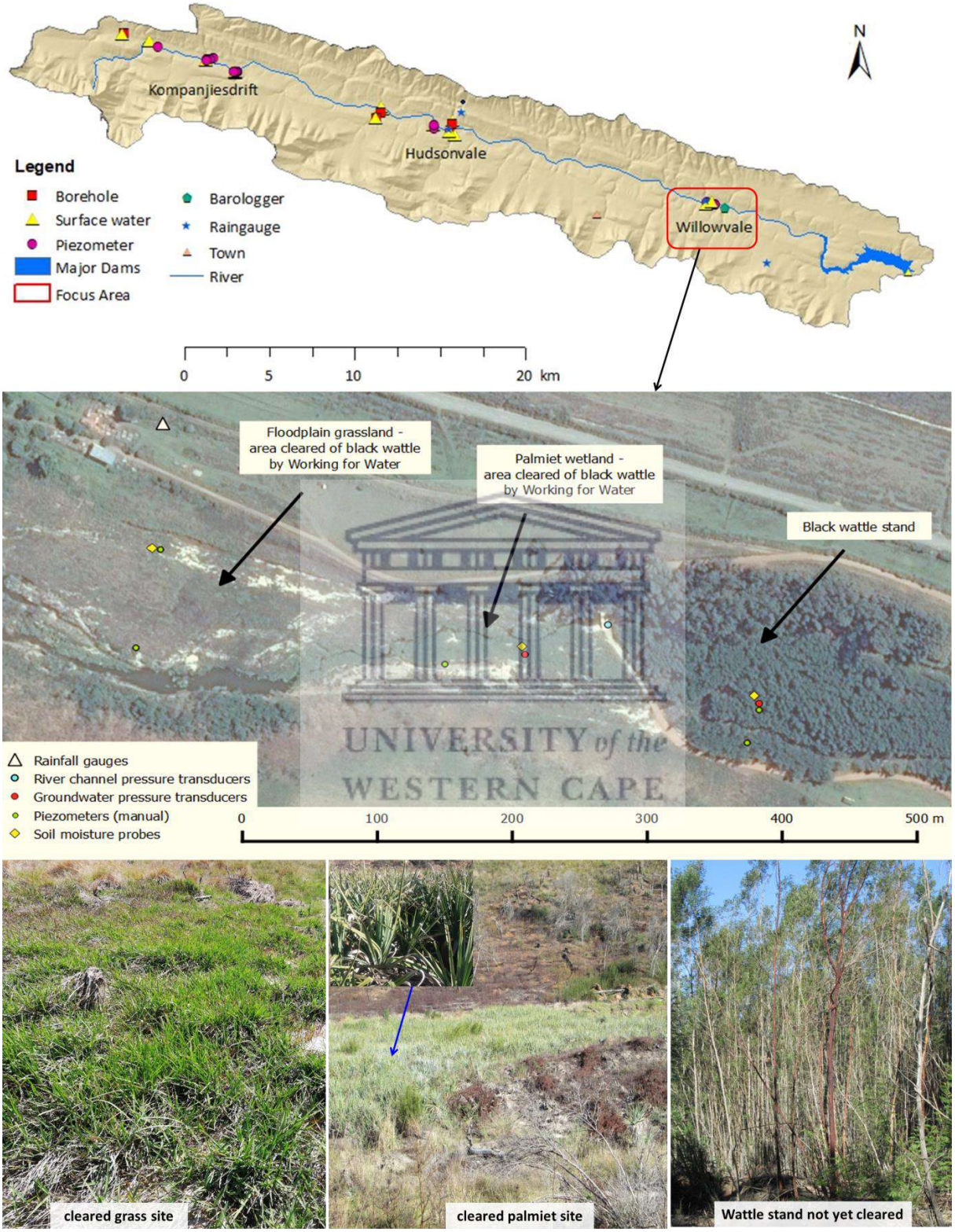

Figure 5.2: Soil water content and water table logging sites across three vegetation types.

5.4 Monitoring and data collection procedures

Changes in soil water content and shallow groundwater levels (<4 m) were monitored to assess how they vary between the invaded black wattle site and cleared sites with indigenous herbaceous vegetation (grass and palmiet). To monitor variation in shallow groundwater levels, piezometers were installed at the wattle, palmiet, and grass sites (Figure 5.2). Three piezometers were installed at the wattle site (1, 1.6 and 3.1 m depths) approximately 50 m apart. Two piezometers were installed at the palmiet site (1.1 and 2.6 m) approximately 50 m apart. At the grass site, two piezometers (1.9 and 3.1 m) were installed approximately 100 m apart. Table 5.1 shows piezometer depths and elevations (m.a.s.l).

Table 5.1: Piezometer depths and mean elevations above sea level

Piezometer Name	Site	Piezometer depth (m)	Surface elevation (m.a.s.l)	Bottom elevation (m.a.s.l)
WT PZ1	Wattle	3.1	179.2	176.1
WT PZ2	Wattle	1.0	177.9	176.9
WT PZ3	Wattle	1.6	178.2	176.6
PM PZ4	Palmiet	2.6	180.5	177.9
PM PZ5	Palmiet	1.11	182.1	181
GS PZ6	Grass	2.0	181.2	179.3
GS PZ7	Grass	3.2	181.6	178.4

WT-Wattle, PM-Palmiet and GS-Grass

The layout of piezometers was intended to give information regarding groundwater gradient across and down the floodplain. Two piezometers, one at the wattle site and one at the palmiet site, were equipped with pressure transducers (Solinst Levellogger) logging at 30-minute intervals. Piezometers were augured to a depth of refusal which was due to either reaching rock or a layer of dry, unconsolidated sand (repeated collapsing of soil inside the augured hole). Water levels in the river at a site between the palmiet and wattle monitoring points were also measured using a Solinst Levellogger logging at 30-minute intervals to compare variations between the groundwater and surface water levels. Herein, shallow groundwater refers to subsurface water monitored in piezometers (<4 m) whilst deep groundwater refers to bedrock subsurface water monitored from boreholes.

To investigate changes in soil water content, capacitance probes (DFM Technologies), were used which measure soil water content as percent saturation. The probes were installed 2 m away from piezometers in the wattle, palmiet and grass sites (Figure 5.3). The probes have six sensors at 100 mm intervals to a depth of 600 mm. Soil samples were collected at each horizon where piezometers were installed for texture and particle size analysis using the sedimentation method. Soil samples were collected for texture analyses by layer according to their stratigraphy when there were any marked changes, i.e. colour and texture, down the profile.

A tipping bucket rain gauge calibrated to 0.2 mm was installed in the floodplain, approximately 100 m from the grass piezometer, for the measurement of event-based rainfall. Temperature was recorded hourly by a HOBO temperature-event logger at the rain gauge. The monitoring of soil water content and water table responses was done from August 2017 to December 2019. Field visits were made every 2-3 months to download data and manual sampling.

Figure 5.3: Soil probe (green circle) and piezometer (pink circle) installed at the wattle site to measure subsurface soil water content and the level of the water table.

5.5 Data Analysis

Rainfall events were classified and assessed according to sizes presented in Table 5.2.

Table 5.2: Rainfall event size classification

Class	Event size (mm/day)
Light	i<9.99
Moderate	10<i<19.99
Heavy	20<i<39.99
Very heavy	i>40

To assess the variability in soil water content and water table responses across sites with different vegetation cover types, a systematic analysis of the soil water content and groundwater level time-series data was performed (Table 5.3). Soil water content (SWC) responses at each depth were calculated using Equation 5.1

$$\Delta SWC_{d,t} = SWC_{d,t} - SWC_{d,t-1} \quad (5.1)$$

$\Delta SWC_{d,t}$ is soil water content in percent saturation at depth d, for timestep t.

A SWC response in this work is a 10% increase in soil water content over a 24 hour period. Daily and hourly time steps were used for analyses to better understand the field processes. All increments of change described in the results are given as magnitude changes in units of % of saturation (because soil probes used record soil water content change in % of saturation), rather than proportional changes (% change vs. previous value). For analyses of responses to rainfall events over short time periods (<48 hours), an event was defined from when it started raining e.g. if it rained from 10 pm to 3 am, this was not regarded as two events because it was spread over two calendar days but as one event because the rainfall event was continuous. Calendar days were used for analyses of responses to events over long time periods (weeks, months, and seasons).

Large events in which the river flooded the monitoring points could be identified from the piezometer pressure transducer water level logs and this additional input was considered when interpreting the SWC responses.

To get insights on water retention with depth, exceedance probability percentages were calculated for each observed depth across the three sites to show the amount of time in which soil water content values were equalled or exceeded. To infer on the relative wetness of the area prior to an event, the antecedent precipitation index (*API*) was calculated using Equation 5.2.

$$API_t = \sum_{i=1}^{d} P_{t-i} k^i \qquad (5.2)$$

Where API_t is the API value on day t, *d* is the number of antecedent days considered, P_{t-i} is the rainfall amount on day *t-i* where *i* ranges from 1 to d, and *k* is a decay factor. A value of 0.9 was used as the decay factor selected from the range of 0.8 to 0.98 proposed by Hong et al. (2007).

Descriptive statistics were used to provide a quantitative summary of soil water content at the three sites. Analysis of variance (ANOVA) was used to test the influence of different vegetation types on mean soil water content (averaged over the 60 cm depth) over the sampled period, applying a threshold of $p < 0.05$ to determine statistical significance). T-tests were performed to check for differences between means for vegetation type site pairs.

Mean values of all data for each season during the monitoring period calculated for each site (grass, palmiet and wattle). Seasons were split into: Summer (December, January and February), Autumn (March, April and May), Winter (June, July and August) and Spring (September, October and November).

Table 5.3 summarises additional data analyses performed on the soil water content and groundwater level data across the sites. Analyses included checking soil water content increase and drainage as well as shallow groundwater level changes at the different sites. Water retention within soils after rainfall events of varying intensities was also analysed for the three sites. Other analyses as summarised in Table 5.3 were also performed to indicate the occurrence of particular processes. Atmospheric demand for evapotranspiration (ET), as reference potential ET (PET), was estimated from temperature data using the Hargreaves and Samani (1985) method. The correlation between daily PET and soil water content decline were assessed for periods of recession to assess ET influences on soil water depletion.

Table 5.3: Analyses performed to indicate the occurrence of processes-Adopted from McMillan et al. (2012) and Glenday (2015).

Spatial Scale	Data	Data analysis	Process interpretation
Floodplain	SM	Time to peak response (not saturation necessarily) and recession speed after event.	Increase in moisture can be due to direct recharge, lateral flows Decrease in moisture can be to either drainage and/or water use by the plants.
Floodplain	SM	Time to decline after storm peak	Fast decline to pre-event level (less than two days) indicates dominant vertical drainage
Main Channel	SW, P, SM	Comparing local groundwater level to the river water elevation	River gaining or losing to the alluvial aquifer
Alluvial aquifer	GW, P	Groundwater level change after a rain event	Responsiveness indicates notable recharge and no response indicates net recharge is not significant. Greater responsiveness to similar event sizes in colder conditions or across different vegetation types are indicative of ET impacts on recharge.
Alluvial aquifer	GW, P	Peak timing after storm event at different locations	Similar peak timing in water level changes indicates notable direct recharge. Delayed response can indicate recharge elsewhere and flow toward the measurement site.
Alluvial aquifer	GW,P, PET	Groundwater level decline correlated with PET	Groundwater level decline strongly correlated with PET indicates water use by plants and that plant roots can reach the water table.

SM – soil moisture, SW - surface water, P - precipitation, GW groundwater, PET- potential evapotranspiration

5.6 RESULTS

5.6.1 Rainfall variation at Willowvale from 2017-2019

The total amount of rainfall received at Willowvale in 2017, 2018 and 2019 was 451, 555 and 416 mm/year respectively. All three years fall below MAP of the catchment, which is approximately 650 mm/year (Cornelius et al., 2019). The whole catchment was monitored during a relatively dry period. During the monitoring period, antecedent precipitation index (API) was highest following the large September 2018 and November 2019 storms which triggered pronounced soil water and hydrometric responses, while series of smaller rain events in succession produced some relatively high values in April and September-November 2017 (Figure 5.4).

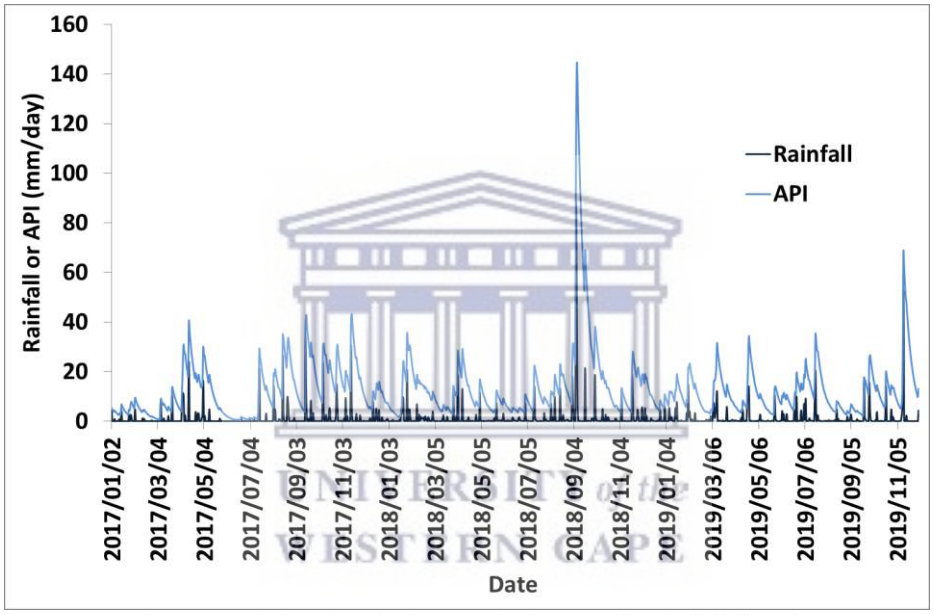

Figure 5.4: Antecedent precipitation index and observed rainfall for the 2017-2019 period

5.6.2 Soil texture

Results of the soil texture analyses from the three sites (grass, palmiet and wattle) are presented in Table 5.4. All sites have similar sandy texture (89% sand) in the 0-20 cm soils.

Table 5. 4: Soil textural classes by layer for the (a) wattle, (b) palmiet and (c) grass sites

Site	Depth (cm)	Sand (%)	Silt (%)	Clay (%)	Texture Class
Wattle	20	89	6	5	Sand
	100	89	6	5	Sand
	160	87	8	5	Loamy sand
Grass	20	89	6	5	Sand
	70	83	10	7	Loamy sand
	180	87	6	7	Loamy sand
Palmiet	20	89	6	5	Sand
	160	89	6	5	Sand
	240	89	6	5	Sand

In the B horizon (Table 5.4), soils are generally sands to loamy sands (sand fractions ranging between 83-89%, silt and clay fractions ranging between 5-10%). The horizons where soil moisture probes were installed (0-60 cm) were sandy across the three sites. Given the similarities in soil texture at the three sites, observed differences in soil water content responses to rainfall will therefore, be attributed to impacts of vegetation.

5.6.3 Spatio-temporal variations of soil water content under three contrasting vegetation types

Significant differences in soil water content responses to rainfall from August 2017 to December 2019 were observed at different depths among the black wattle, palmiet and grassland sites. Based on visual analysis (Figure 5.5), marked fluctuations of the soil water content were observed in response to rainfall events of ≥10 mm/day in general.

Soil water content of shallow soils (0–10 cm) at all three sites increased after light events (<10 mm/day) with maximum % saturation increases of approximately 10, 15 and 40 at the grass, palmiet and wattle sites respectively. At the wattle site, notable responses to light rainfall were observed at the 10-20 cm soils. No pronounced changes were observed at 30-60 cm soils following light events. Surface soil water increments in response to light events were notable (peak response) from August 2017 to August 2018, however, after the September 2018 storm, notable increments were only observed in response to medium (10-19 mm/day) to heavy (20-40 mm/day) events. Possible explanation could be that after wet periods, plants will grow leaves thereby resulting in increased ET as well as increased canopy interception.

At the grass site, notable responses to light events were only observed in shallow soils; however, for some events (>20 mm/day), deeper soils responded more than shallow. Deeper soils had larger soil water content changes compared to the shallow soils for some rainfall events i.e. on the 16th of August 2017 and 20th of July 2019, after events of 26 and 20 mm/day respectively, soils between 40-60 cm had high SWC increases (>15% saturation) whilst 20-30 cm had less than 2% saturation increase. This could have been due to a rise in the alluvial aquifer water table recharged by subsurface flow generated further up or around the contributing catchment, such that the lower soil layers at this site were influenced by the capillary fringe. For most rainfall events greater than 30 mm/day, SWC at all soil depths increased significantly (>10% proportional increase) except for the soils at 30 cm depth which seldom responded at this grass site. The site is dominated by *Pennisetum clandestinum* (Kikuyu) grass with root depths between 20-40 cm (Heuze et al., 2015), therefore the lower SWC and small responses at 30 cm may be attributed to active root water uptake at this depth.

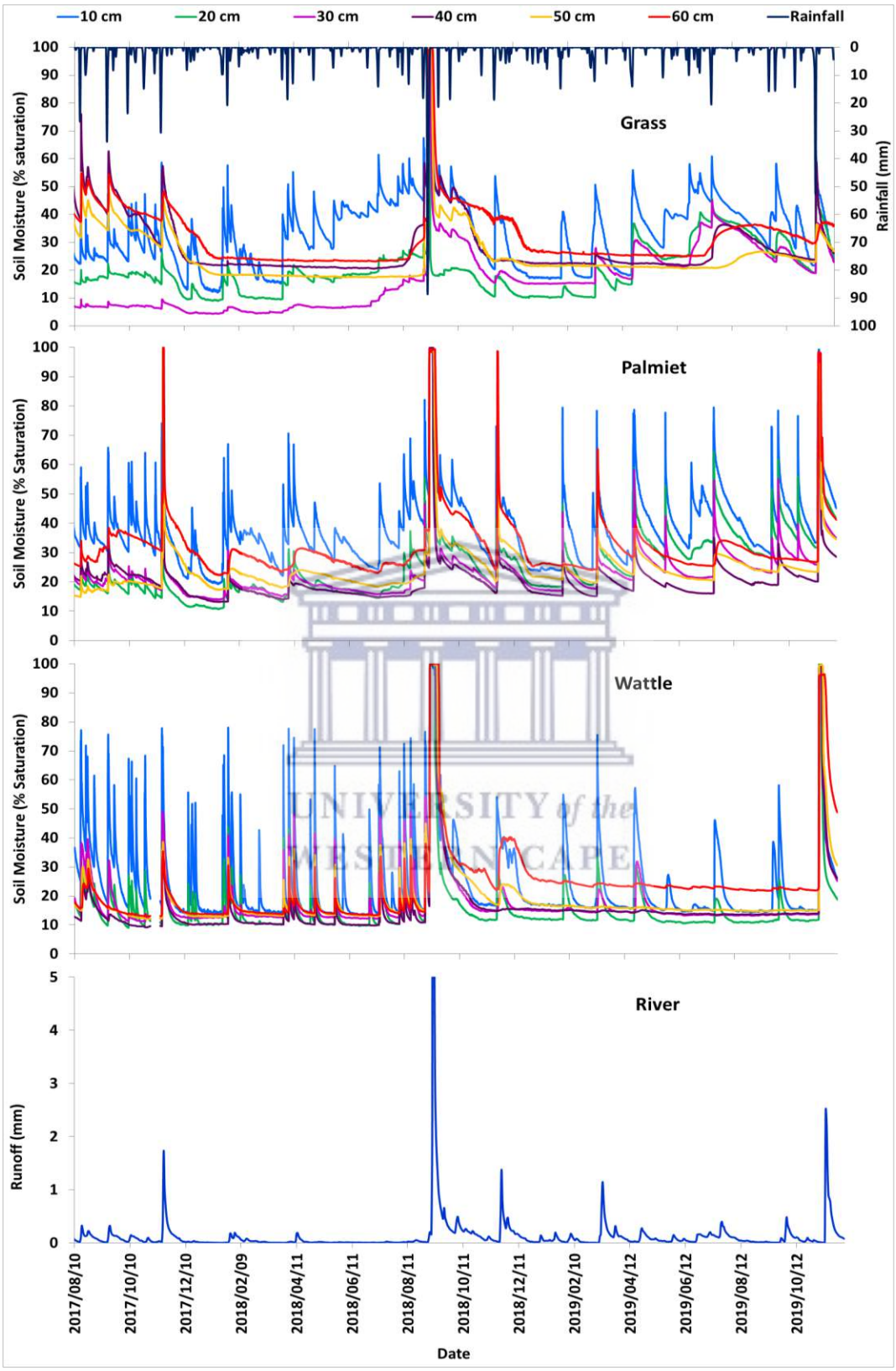

Figure 5.5: Observed temporal variation of soil water content under grass, palmiet and wattle sites and flow response from August 2017 to December 2019 at Willowvale. 10 cm to 60 cm show SWC at the respective depths

Soil water content changes in response to moderate to heavy events (10 mm< i<40 mm) were notably different in response times across the three sites. On average, shallow soils (0-10 cm) at the grassland site responded in less than 24 hours after moderate events, soils at 20-30 cm depths responded in 24 to 36 hours and the deeper 40-60 cm soils responded in 24 to 48 hours. At the palmiet site, notable soil water content changes to moderate rainfall events were observed at the 10-30 cm soil layers. However, for some events, i.e. after an event of 19 mm on the 20th of November 2018, the 40-60 cm soils had the most significant change in water content (increases in % saturation of 25, 73 and 74% respectively). In general, responses to moderate rainfall events often yielded changes in soil water content ranging between 15-55% saturation increments for the 10-30 cm soils. At deeper soils (40-60 cm), water content responses varied depending on antecedent conditions. The general responses at the palmiet site after moderate to heavy events were that shallow soils responded within 24 hours (>10% saturation increase) whilst the 40-60 cm soils responded after 24 to 48 hours (>30% saturation increase).

At the wattle site, soil water content varied significantly with depth for most moderate to heavy rainfall events. In 2017, most responses to rainfall events were observed in the 10-20 cm soil layers (i.e. 33.8 mm and 23 mm on 15 September and 8 October respectively). In 2018, for most moderate events, increment amount of soil water content in soils at 10 cm depth was between 45 to 75% saturation whilst the 50-60 cm soils increased by 14-20% saturation. From September 2018 to November 2019, significant responses were observed in the 10-20 cm soil layers for rainfall events up to 20 mm/day. The 40-60 cm soils maintained constant water content after the September 2018 storm (134 mm in 48 hours) only showing notable responses to rainfall events greater than 20 mm/day. This suggests that this could be the field capacity for this layer (between 15-25% saturation) and/or there is enough water in other layers such that the ET demand does not deplete soil water in this layer over time. Depending on the magnitude of the rainfall event, the general trend observed at this site shows responses within 24 hours after an event in the 10-20 cm soils and a lag time of more than 24 hours in the 30-60 cm soils. Overall, events less than 10 mm/day resulted in soil water content responses only in the shallow 10-20 cm depths and in other cases at 30 cm depths at all sites. Deep layers exhibited long lags or no responses to most of these events. This was due to low quantities of effective rainfall that made it past canopy and litter interception but not enough for recharge and also a function of rainfall event size and antecedent wetness before each event. Events of 25 mm/day or more resulted in full profile response indicating local recharge particularly when the 60 cm depth water content stayed elevated (at 25% saturation on average) assuming that the groundwater table was close enough to impact the capillary fringe.

5.6.4 Comparison of the advance of the wetting front in response to storm events under grass, palmiet and wattle sites

To analyse the advance of the wetting front, moderate and heavy rainfall events, which occurred on 21/11/2018 (18 mm) and 19-20/07/2019 (moderate) and (7-8th September 2018 (134 mm) and the 13th of November 2019 (53 mm), were used (Figure 5.6 and Figure 5.7). Analyses of the moderate events (Figure 5.6) show the shallow 10 cm soils responded to the November 2018 event at all sites. At the grass and wattle sites, only the 10-20 cm soils responded whilst at the palmiet site, water infiltrated down to the 30 cm soils. Analysis of the July 2019 event (Figure 5.6) shows responses at the palmiet site (10-40 cm soils responded and a slight delayed increase at 50 cm soils). At the grass site, incremental responses were observed in the 10-30 cm soils.

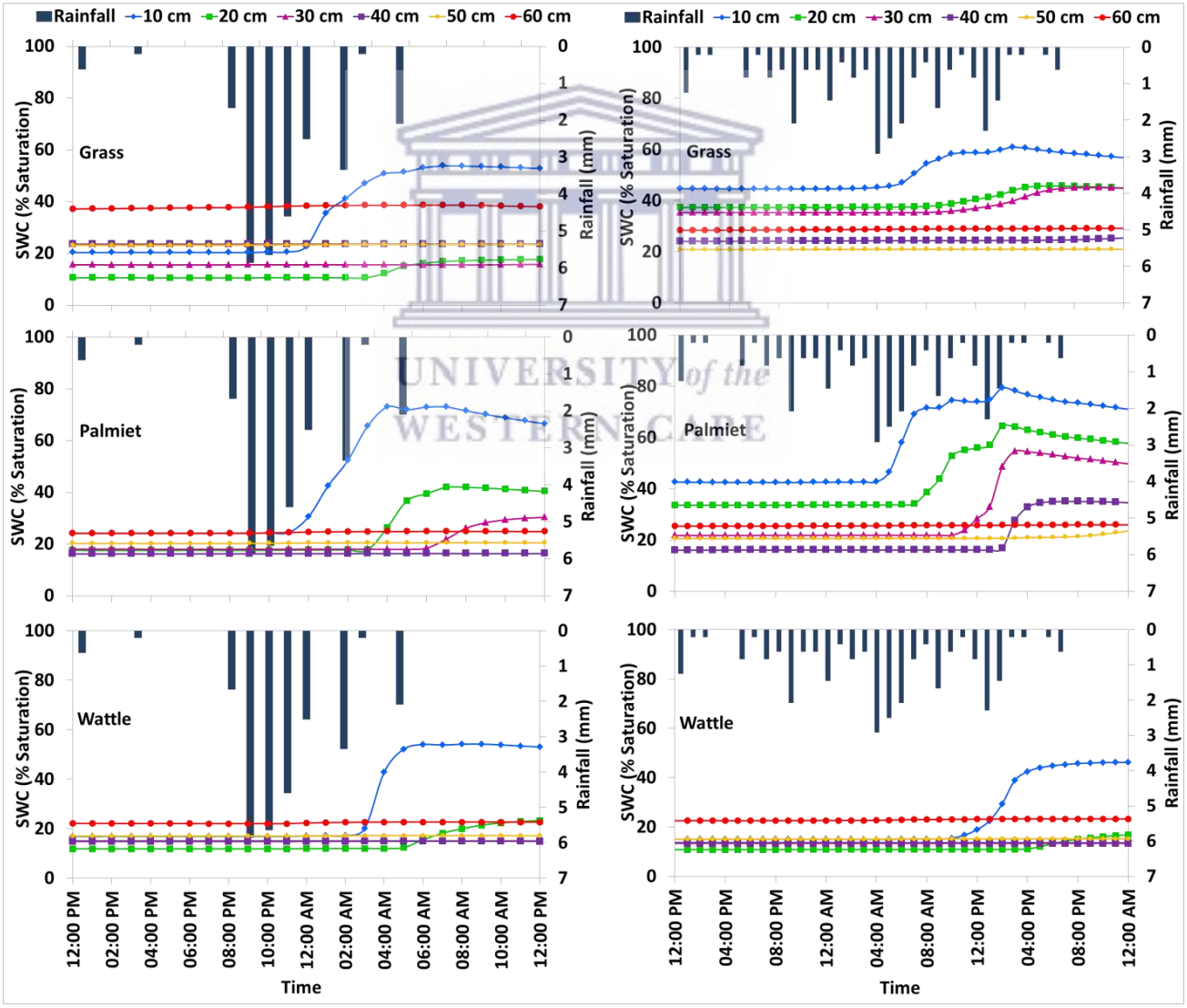

Figure 5.6: Soil water content responses to moderate rainfall events (18 mm) on 21/11/2018 (left) and (20 mm) on 19-20/07/2019 (right). 10 cm to 60 cm show SWC at the respective depths

At the wattle site, only the shallow 10 cm soils showed a significant response whilst the underlying 20 cm soils showed a slight delayed response which could have been due to high canopy and litter interception reducing the amount of water that reaches the soil layers. The advance of the wetting front down the profile is influenced by rainfall intensity, and amount of canopy and litter interception. When the top layer exceeds field capacity, water then starts moving down the profile assuming there is no preferential flow through macropores. For the two events, water moves down the profile sequentially however, the deep layers (40-60 cm) at all sites seldom responded to these light to moderate events. This means that the wetting front required more rainfall to infiltrate to deeper layers and saturate the soils. A comparison of responses from the two events shows that the palmiet site is more responsive which could be due to their root system increasing the soil porosity and increased soil water content.

Figure 5.7 shows the wetting front under heavy storm events. After the heavy storm on the 7th-8th of September 2018, the wetting front took approximately 5 hours from the onset of precipitation to increase notably at 10 cm depths across all sites (5 mm cumulative rainfall) (Figure 5.7). However, the increase was quicker at the wattle site compared to the other two sites which increased gradually. The sites reached saturation at least 23 hours after the onset of the rainfall (89 mm cumulative rainfall). Similar to the moderate events responses, the profiles at all sites show water moving down sequentially. However, at the palmiet and wattle sites (September 2018 event), the deeper 60 cm soils reach saturation before some of the upper layers. This could be groundwater recharged by lateral subsurface flows rising and saturating the deeper soils before the wetting front reaches that horizon shown in Figures 5.7 and 5.12.

All soils reached and maintained saturation for several days across the three sites which was due to overbank flooding. At the grassland site, the deeper layers remained saturated for longer (50 and 60 cm). Soil water content at 30 cm started decreasing 72 hours after rainfall stopped by 23 %, 40 cm soils decreased by 26% whilst 50-60 cm layers decreased by 22 % after 120 hours (5 days). At the palmiet site, the soils at 10-40 cm started showing decreasing soil water content in the range of 25-40% saturation in 48 hours, whilst 50-60 cm SWC decreased below saturation five days (120 hours) after the storm. At the wattle site, 10-20 cm soils started decreasing after 144 hours (6 days), 30-40 cm soils decreased after 168 hours (7 days) by 16 and 37% respectively. The 50 cm and 60 cm soils started decreasing on the 8th day (192 hours) and on the 10th day (240 hours) respectively. This longer delay in soil water content decrease is likely also a function of the topography of the site. The monitored position is downslope therefore could be receiving lateral subsurface flow from upslope.

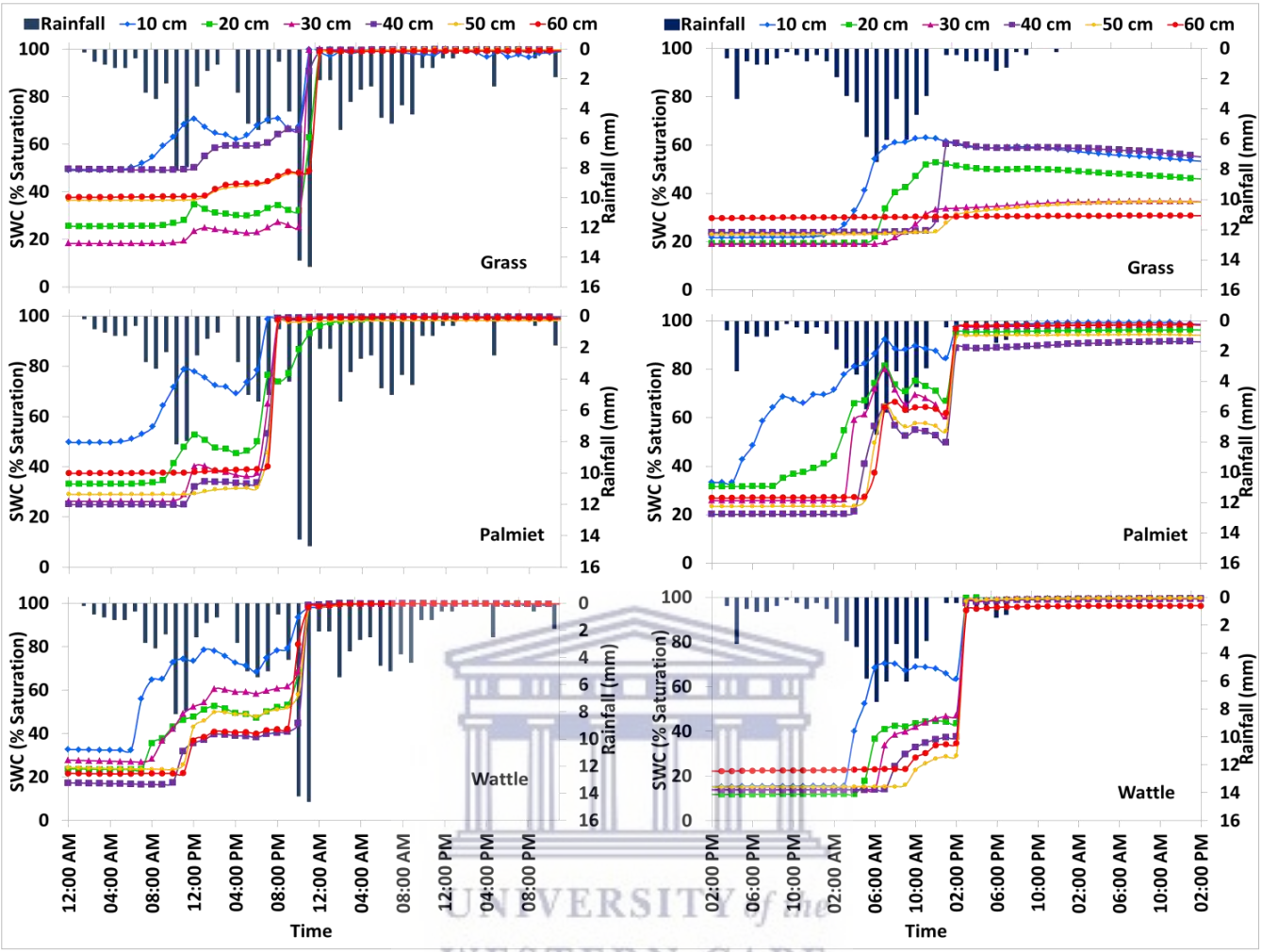

Figure 5.7: Soil water content responses to storm events on 07-08 September 2018 (134 mm) (left) and 12-14 November 2019 (53 mm) (right) at Willowvale site. 10 cm to 60 cm show SWC at the respective depths

In response to the storm event on the 13th of November 2019 (53 mm, Figure 5.7), the shallow 10 cm soils at the palmiet site responded within three hours from the onset of the rainfall (4 mm cumulative rainfall). The wetting front at the grass and wattle sites progressed much slower reaching the 10 cm soils after 10 hours from the onset of the rainfall. This could be due to the antecedent soil moisture conditions. Grass and wattle had low soil water content compared to soils at the palmiet wetland. At the grass site, soils at 10-50 cm depths responded significantly within 24 hours except for soils at 60 cm which showed less than 1% saturation increase. At the palmiet site, all soils responded significantly within 6-18 hours (ranging from 40-85%). The wattle and palmiet soils reached saturation 11 hours from the onset of the rainfall but the soils at the grassland site did not reach saturation in response to this storm event. The saturation at the palmiet site could be linked to alluvial aquifer rise as shown in Figure (5.12), the shallow groundwater level rose to 11 cm below the ground surface at this site. The soil water content at

the palmiet and grass sites had actually started declining before the sharp increase to saturation and there was very little rain by this time. Therefore, river and alluvial aquifer contributions could be probable factors associated with this final increase. All layers at the palmiet and wattle sites show a sharp increase in the same hour which is not what would be expected if additional lighter rainfall was creating another wetting front that was moving down. The shallow (10-30 cm) soil layers at the palmiet started decreasing 12-15 hours after peak soil water content whilst deep (40-60 cm) soils decreased after 24-38 hours. At the wattle site, soil water content started decreasing 72 hours after peak soil water content at the 10-30 cm soil layers, 96-120 hours for soils at 40-60 cm depth.

Figure 5.8 shows variation of soil water content with depth for selected storm events. Values are plotted for a day's average soil water content with depth (day before an event, day of event and the day after the event). The three profiles show distinct vertical response patterns to both storm events. The wattle site had the least water content before presented events except for the 30 cm soils at the grass site in January and September 2018. The 30 cm soils at the grass sites are in the active root depth, therefore more water will be extracted by the roots of grass in this layer.

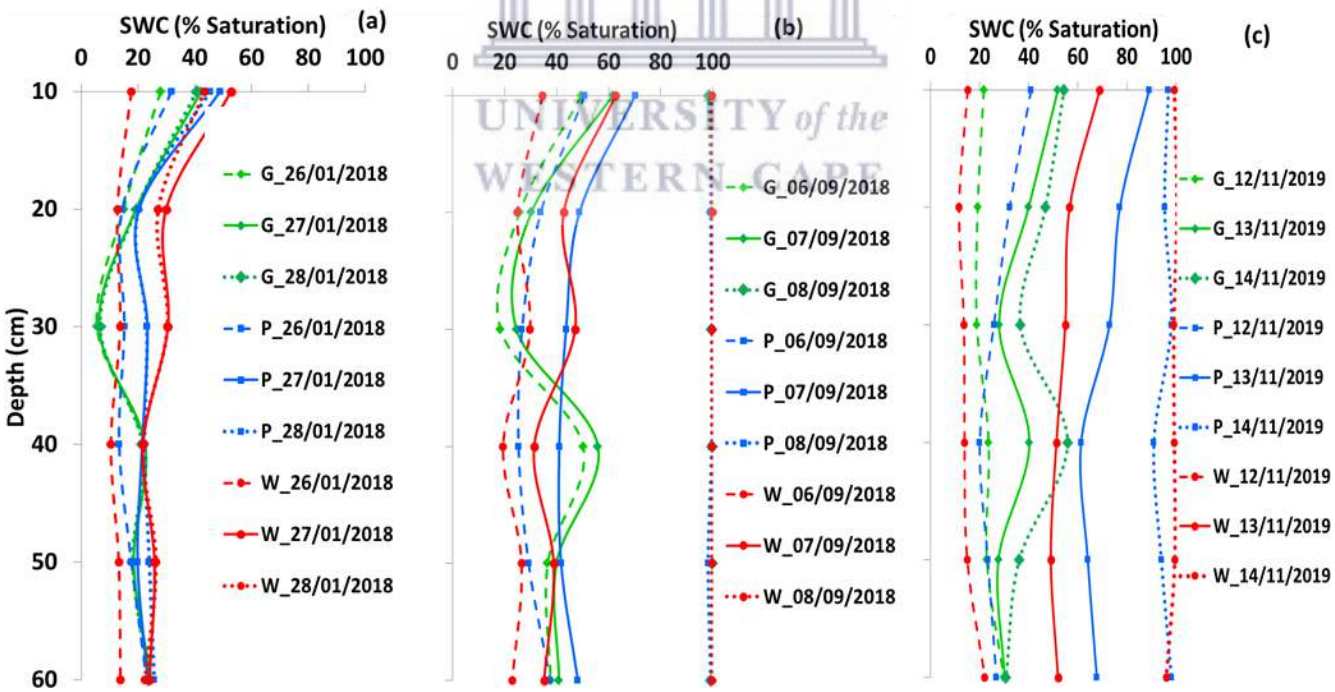

Figure 5.8: Soil water responses to events in (a) January 2018 (20 mm in 11 hours) (b) September 2018 (134 mm in 50 hours) and (c) 13 November 2019 (53 mm in 31 hours) respectively at 10-60 cm depths at the Willowvale site. For the curves, G=grass, P=palmiet and W=wattle.

For the average January 2018 event (Figure 5.8a), the grass site did not show notable changes in comparison to the responses observed at the palmiet and wattle sites. However, soil water content decrease was not quick by the next day compared to the September 2018 and November 2019 events. All profiles at the three sites reached saturation in response to the September 2018 storm (Figure 5.8b). However, in November 2019 (Figure 5.8c), only the soils at the wattle and site reached saturation. The palmiet soils did not reach saturation but all soils got to more than 90% saturation. At the grass site, soils only got to approximately 60% saturation. For all events (Figure 5.8), the 40 cm depth at the grass site shows relatively more water content than other depths. A potential explanation for the 40 cm bulge in the grass profile could be some lateral subsurface flow contributions in that horizon.

Seasonal variations in soil water content with depth at the different sites for the sampling period are shown in Figure 5.9 and Appendix Figure 5A1. Distinct vertical patterns in soil water content were observed across the three sites. Highest water contents were observed across all sites in spring likely due to the low evapotranspiration during this season (Figure 5.9). However, winter would also have low ET therefore, the high average for spring was highly influenced by the September 2018 event.

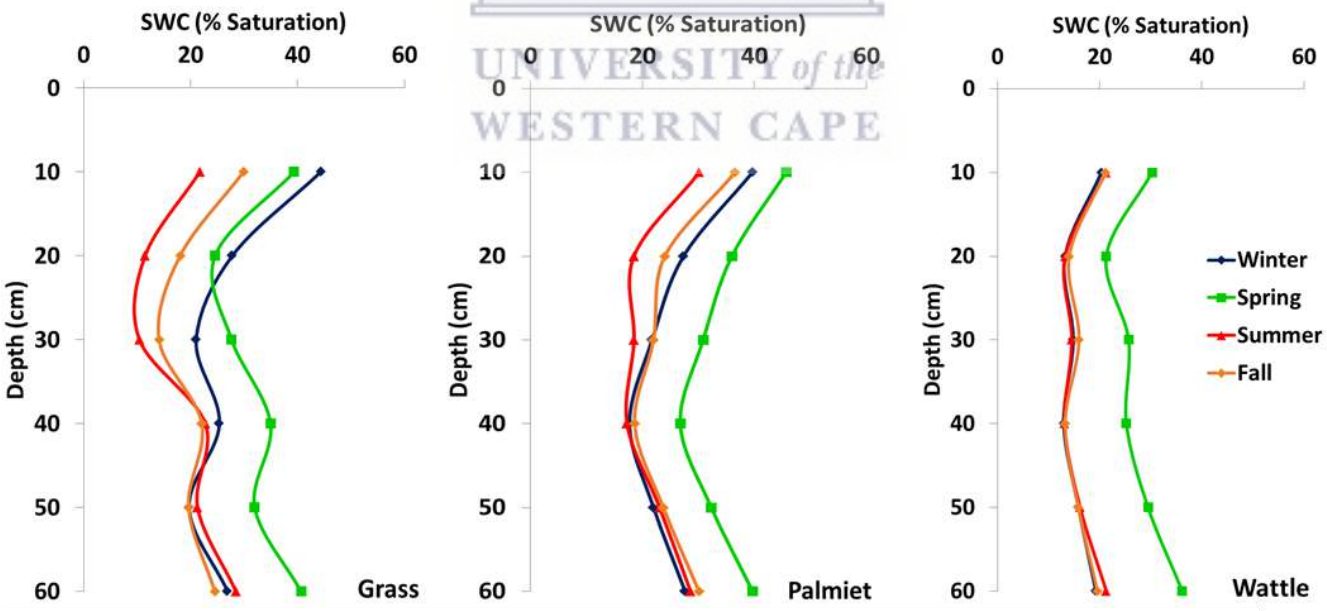

Figure 5.9: Seasonal variations in soil water content at the grass, palmiet and wattle sites

Given the lack of rainfall seasonality and the high inter-annual variability, different patterns maybe observed in a long term average. The least soil water content was observed in summer at all sites. No notable differences were observed at the wattle site in winter, summer and fall of the

sampling period (Figure 5.9). At the palmiet site, there were no significant differences in soil water content at deep (40-60 cm) soil layers. During summer and spring, soils at the palmiet site (0-40 cm) had relatively higher water content compared to grass but at deep (50-60 cm) layers, the two sites had relatively similar soil water content (Figure 5.9).

5.6.5 Frequency analysis of soil water content at the three sites

Exceedance probability curves for the observed soil water content responses to rainfall showed significant differences in soil water retention capacity among the three sites under different vegetation communities (Figure 5.10). Each exceedance curve shows the frequency of different soil water content levels at each depth per site during the sampled period (August 2017-December 2019). The distribution of soil water content across the sampling period displayed using exceedance curves was a result of rain events (assumed to be the same at all sites due to their close proximity), how much water made it to the soil surface due to canopy interception (assumed to be different across all sites), and infiltration rates (soils had similar properties so infiltration was assumed to be relatively similar) as well as overbank flooding and the depth of the water table. The amount available to infiltrate was assumed to differ due to canopy interception, as were the ET rates (different for all sites with an expected difference in the distribution of withdrawals with depth), vertical drainage, groundwater depth and capillary rise at each site.

All three sites exceeded or equalled 100 % saturation for less than 2 % of the sampled period. This was achieved after an 88 mm/day storm. The wetting pattern suggested that the whole floodplain became flooded with water flowing from upstream of the river which is shown by river stage of up to 4 m above ground (Figure 5.12). At 50% exceedance, the shallow soils were at approximately 40% saturation at the grass and palmiet but low (< 20% saturation) at the wattle site (Figure 5.10). This could be an indication that the wattle trees were drawing the soil water below field capacity more quickly and more regularly at 10-20 cm depths than the other vegetation types. Furthermore, the soils at the wattle site were not getting as wet for small events as other sites, which may be due to higher canopy losses. The soils could have been draining fairly quickly by gravity back to field capacity after wetting up and then ET continued to draw it down thereby remaining dry for long periods. No significant variation was also shown at deeper soils between grass and palmiet at 50% exceedance. Intermediate soils (30-40 cm), however showed relatively similar soil water contents between wattle and grass at the 50% exceedance (Figure 5.10).

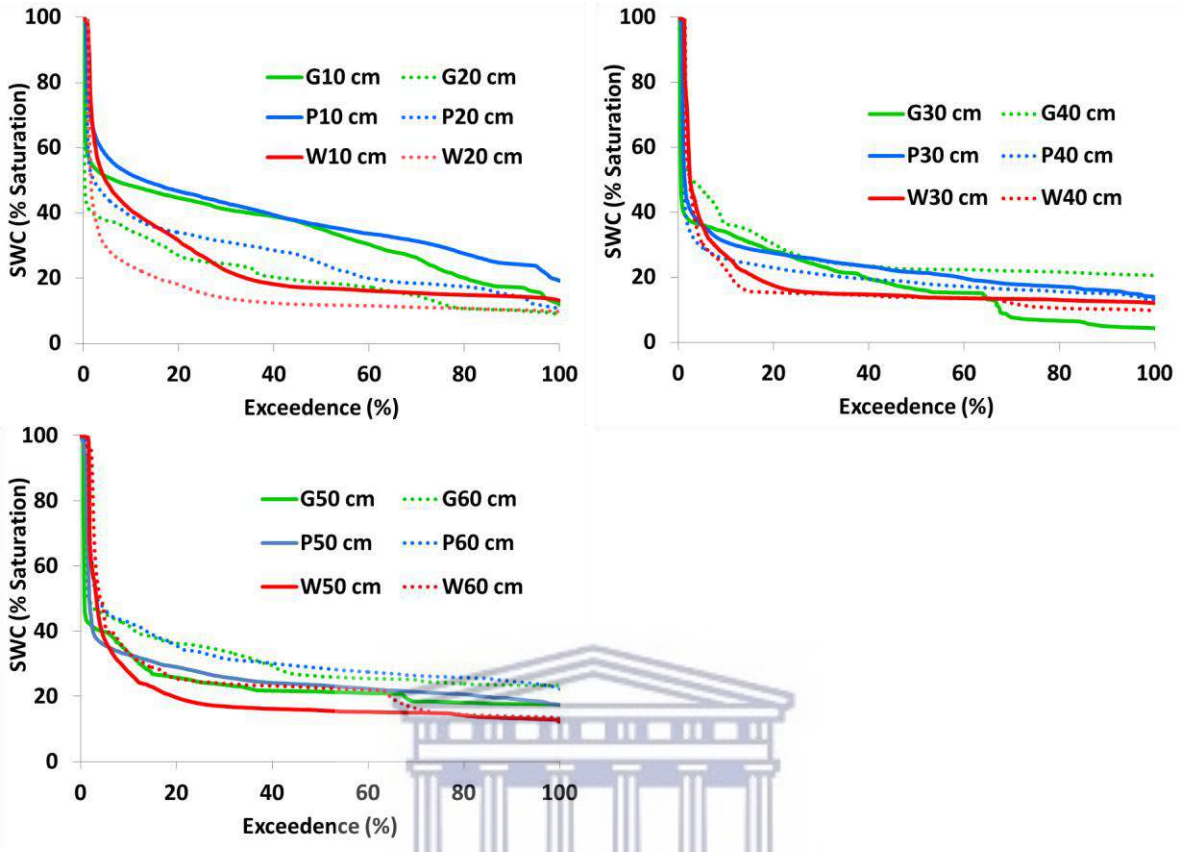

Figure 5.10: Soil water content exceedance probability for the grass, palmiet and wattle site.

Variations in soil water content and means for the sampled period are shown in Figure 5.11 and Appendix Figure 5A2. The vegetation cover types displayed differences in the observed full profile average soil water content (Figure 5.11). The palmiet site had overall soil water content ranging from 20 to 38% saturation with a full profile average % saturation value of 27. The grass site had a soil water content range of 16-33 % saturation and a profile average of 25. The wattle site had the lowest mean soil water content, ranging from 15 to 24, with a full profile average % saturation value of 19. The wattle site showed the least variation in soil water content for the whole 0-60 cm profile compared to the grass and palmiet sites. Furthermore, the wattle site also showed the lowest mean soil water content among the three sites. Average soil water content at the three land cover types revealed that the palmiet site had significantly ($p<0.05$) higher water content than the wattle site. The grass site had relatively higher soil water content in deep soil layers than palmiet and wattle (Appendix Figure 5A2).

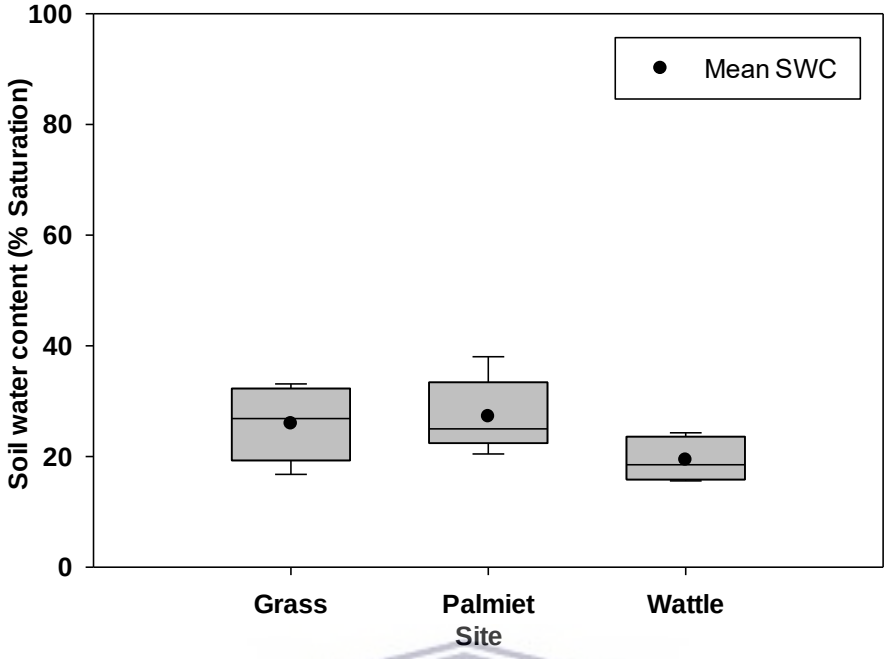

Figure 5.11: Variation in full profile (0-60 cm) mean soil water content across the three sites.

5.6.6 Water table responses in areas under grass, palmiet and wattle vegetation types

The study also described variability in water table responses under the three contrasting vegetation types, and facilitated the description of subsurface flow regime at the floodplain site. Shallow groundwater levels showed notable differences across the three sites (Figure 5.12). Important to note is that when monitoring began in April 2017, the water table was below all installed piezometer depths. Analyses of soil properties with depth showed similar sandy soil dominated profiles (Table5.4) across the three sites therefore differences in shallow groundwater level dynamics was largely attributed to differences in above ground vegetation cover types. Significant water table fluctuations were observed at the grassland site from April 2017 to December 2019 (GS PZ6 and GS PZ7). The water table was higher at GS PZ6 at most times compared to GS PZ7 during periods when there was a measurement at both locations. At GS PZ6 the water table was below 2 m (the piezometer depth), on most sampling dates whilst at GS PZ7 the water table was above 3 m (piezometer depth) on all days sampled (Figure 5.12).

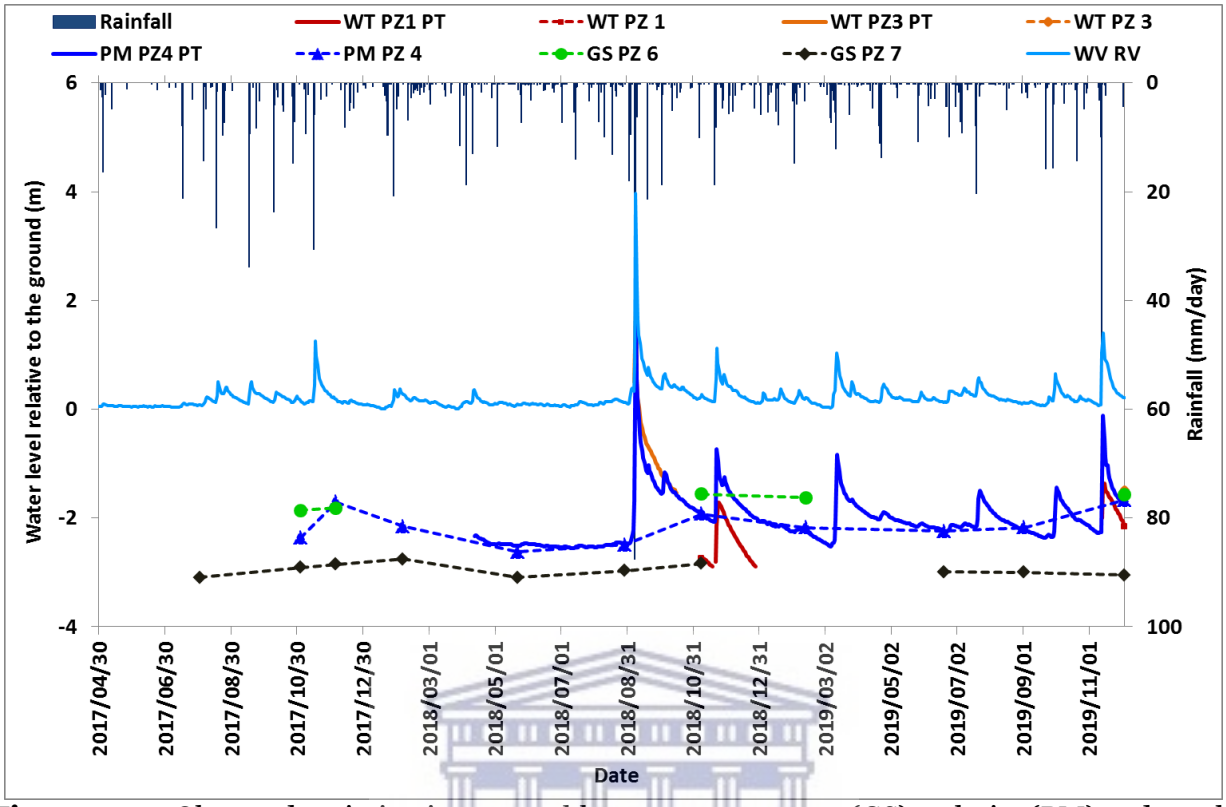

Figure 5.12: Observed variation in water table responses at grass (GS), palmiet (PM) and wattle (WT) sites. WV RV is the observed water level at Willowvale. Solid lines represent continuous data whilst dotted lines are only for visualisation purposes for manual dip meter measurements taken during field trips.

At the palmiet site, the initial pressure transducer malfunctioned therefore continuous data recorded is only from April 2018 to December 2019. Water table depths typically ranged between 2.1 to 2.5 m below the ground surface from April 2017 to December 2019 except during and after large storm events. In September 2018, after 53 mm of rainfall in 19 hours, the water table rose from 2.2 m below ground surface to 2.08 m, then in the 20th hour since the onset of the event after 54 mm of rainfall the water table rose from 2.08 m below ground surface to 0.5 m above the ground surface in one hour indicating overland flow/flooding from the river flows exceeding channel low flow banks (Figure 5.12). Before the storm, the water table was below the piezometer depth (2 m) at the wattle site (in which all wattle piezometers were dry, including the deepest 3 m WT PZ1). By 20 hours since the rain started, the water table had risen to within a 2 m depth (1.998 m below ground). In the 21st hour, the water level rose steadily to 1.5 m below ground then changed rapidly to 0.3 m above the ground showing overbank flooding from the river. The water level reached a maximum of 2.5 m above the ground whilst the palmiet reached a maximum of 2.4 m indicating that the floodplain was inundated. The overland flow lasted for 81 and 90 hours (more than 3 days) at the palmiet and wattle site respectively.

After the September 2018 storm, the streamflow was likely maintained primarily by surface flow and interflow. However during the recession, some of the river flow contributions could have been water draining out of the floodplain. The elevation of water (m.a.s.l.) in the river relative to the piezometer water levels at the palmiet site showed that the elevation of the floodplain aquifer water table was always higher than the river indicating a gaining system shown in m.a.s.l on Figure 4.16 in Chapter 4.

At the wattle site, the water table was below 3.2 m depth, (the three installed piezometers at this site were dry for most of the monitoring period) (Figure 5.12). The water table rose to within 2 m of the ground following the September 2018 rainstorm of 134 mm in 48 hours, 20 mm in November 2018 and 53 mm in November 2019. Sharp decreases were observed four to five days after the storm for both the wattle and palmiet sites. However, the water table at the wattle site dropped quicker than at the palmiet site. At the palmiet site, the decrease was more gradual and the water table remained at levels higher than levels observed prior to the September 2018 rainstorm but at the wattle site, the water table dropped to levels below the installed piezometer depths. In general, the groundwater table only rose significantly across the area following the September 2018 and November 2019 rainstorms (Figure 5.12). An analysis of the shallow groundwater level time series at the palmiet site showed other significant responses also, however, some of these responses were not significant enough to rise to the 60 cm depth.

The events in November 2018, March, July, August and October 2019 showed notable peaks that coincided with river peaks (Figure 5.12). For all these events, shallow groundwater at the wattle site only rose to within 3 m of the surface in response to the November 2018 and November 2019 events. This shows that the groundwater table at the wattle was dropping faster than at the palmiet or grass sites. The soil water content responses to these events, showed the wetting front moving down the profile to the deep layers at the palmiet site for the November 2018, March and July 2019 events. In July 2019, the wetting front reached the deep soils only at the grass and palmiet sites. For most rainfall events in 2019 the wetting front did not move down the profile at the grass and wattle sites. At the wattle and grass sites, there was a peak response in the surface layers, but the 40 cm soils did not respond to the November 2018 event however, the 50 and 60 cm soil water content increased showing subsurface lateral flow contributions rather than local recharge from a wetting front. At all sites, the deep soil layers stayed relatively constant and elevated after the September 2018 storm probably implying that the water table rose and the soils were maintained by the capillary fringe or subsurface lateral flows from the surrounding area.

5.8 DISCUSSION

This study measured soil water content under some of the typical land cover types (grass, palmiet and wattle) in the Kromme catchment. Rainfall events of different intensities were observed during the monitoring period. The land cover types influenced soil water content dynamics. Similar to other studies in semi-arid environments, the magnitudes soil water content changes varied depending on differences in magnitudes of precipitation events, antecedent conditions (Gao et al., 2014), duration of dry interval preceding each rainfall event (He et al., 2012; Heisler-White et al., 2008; Wilcox, 2010) , and above ground vegetation cover type (Niu et al., 2015; Wang et al., 2013; Yang et al., 2019). Variation of subsurface water levels were influenced by above ground land cover types and changes thereof (Molina et al., 2007; Wahren et al., 2009).

The observed results suggested that events greater than 30 mm/day played a key role in increasing soil water storage at all sites. Similar to other semi-arid landscapes, precipitation (light to medium rainfall events) was the main source of replenishment in the shallow soils (0-20 cm) however, recharge and storage in deeper 50-60 cm soils required continuous rainfall (high antecedent soil water) or heavy rainfall (Berihun et al., 2019; Hou et al., 2018; Yang and Shang, 2012). This has also been shown in other studies where smaller events merely caused fluctuations in the topsoil due to wetting and drying by evaporation (Berihun et al., 2019; Heisler-White et al., 2008). Events equal or greater than 25 mm/day were needed to get through canopy and litter interception and for a wetting front to move down the profile to the deep 60 cm soil layers. Furthermore, periods of dry spells also affected recharge of soils at greater depths as more precipitation was required to replenish the soils (Niu et al., 2015). Same results were observed by He et al. (2012) in the Qilian Mountains in northern China where soils at 50-60 cm depths were effectively recharged by continuous (increasing antecedent conditions) and/or larger amounts of precipitation.

Soil water content responses varied across sites due to the different vegetation types. A comparison of the overall variation of soil water content indicated that shallow soils (0-10 cm) had pronounced responses to most of the rainfall events at all three sites. At the grassland site, the shallow soils (20-30 cm) showed low soil water content as this layer was the root zone depth of the dominant kikuyu grass. The soils at 40-60 cm generally showed high water content, however, there was no discernible change in soil water content in the same layers from November 2017 to August 2018 and from December 2018 to August 2019. Rainfall events during this period ranged from 0.2-31 mm/day but the soils maintained constant soil water content.

This could have been due to localized lateral subsurface flow contributions. On average, the water table at this site was approximately ≥1.8 m below ground surface or lower when the 40-60 cm soils had relatively constant values therefore the capillary fringe could not have influenced the soil water content during these periods.

At the palmiet site, soil water content responses were highly dynamic with depth. The soils at 60 cm show high soil water content which rose during the sampling period from August 2017 to December 2019. This was attributed to increased local recharge shown by the wetting front moving down the profile to deep layers in response to most rainfall events compared to the grass and wattle sites. Palmiet plants promote recharge due to their fibrous root system (Rebelo et al., 2015). The root systems influenced the movement of water down the profile probably through the creation of preferential flowpaths from the root structures (Wahren et al., 2009). Pronounced fluctuations were not as quick as the wattle site as there was a lag in responses after rainfall events and water content decline after peak responses was gradual compared to the other two sites. Soil water content gradually increased at deeper layers and in some cases without direct rainfall inputs which could have been an indication of localized contributions from subsurface soil water or capillary rise. Another potential factor was the general rise of the water table in the alluvial aquifer in response to rainfall events and subsurface inputs at the floodplain margin and main river bed. Palmiet traps sediment and reduces water velocity in channels due to the clonal nature of its extensive root system (Job, 2014; Rebelo et al., 2015), therefore, subsurface water was retained for longer periods in palmiet dominated areas and recharge of deeper soil horizons was promoted (Crous et al., 2019; Railoun, 2018; Rebelo et al., 2019; Sieben, 2012). These results highlight the importance of the indigenous herbaceous palmiet plants in promoting groundwater recharge through its fibrous root system (Rebelo, 2012).

At the wattle site, the responses of soil water content after rainfall events were quick (reaching peak water content in one or two hours on average after the onset of events). The soil water content at the wattle site showed the highest peaks in shallow soils (10 cm) from August 2017 to August 2018. The wattle site had sharp soil water content decrease after peak responses resulting in the least water retention across the three sites. This is an indication of rapid water use by the black wattle trees. Wattles have coarse and shallow roots that may influence preferential flow (Wahren et al., 2009) hence the sharp peaks after rainfall events and they are also capable of accessing soil water in both shallow and deep soils depending on its accessibility. Soil water content increased in general at the 40-60 cm after the September 2018 storm and constant levels were maintained which means the water table rose higher at this site after the storm.

Seasonal patterns in soil water content for the different vegetation cover types were analysed. On average, there were notable difference in soil water content between spring and other seasons across all sites. All the large storm events occurred in spring thereby increasing the mean soil water content at all sites compared to other seasons. All sites had low mean soil water content in summer , compared to spring and winter indicating the importance of ET in summer (drying out soils and lowering water tables) such that little recharge occurs. Water levels under wattle vegetation cover remained below piezometer depths only to respond to high intensity events (> 40 mm/day). In areas without black wattle trees (palmiet and grassland), shallow groundwater levels remained within 2 m of the ground surface for prolonged periods. A possible explanation was the difference in root distribution and evapotranspiration rates of the different vegetation types (Li et al., 2017), particularly due to greater transpiration by the wattle trees as reported by other studies (Bulcock and Jewitt, 2012; Clulow et al., 2011; Dye and Jarmain, 2004). Soils at the black wattle site were drier and the alluvial groundwater table was also lower at this site as expected given differences in transpiration rates for these species measured elsewhere in the literature (i.e. Calder and Dye, 2001; Doody et al., 2011; Le Maitre et al., 2015; Rebelo, 2012).

The spatial and temporal variation of soil water content were significantly influenced by rainfall event size and intensity (Fan et al., 2016), as well as by the above ground structure of the land cover types (Molina et al., 2007; Niu et al., 2015). Temporal variations of soil water content in different land cover types were not always consistent with rainfall event sizes due to differences in the dry sequence duration preceding events (Gao et al., 2014; Niu et al., 2015). In many semi-arid landscapes, alien invading woody species have been shown to have increased transpiration rates particularly in riparian areas where water is readily available consequently reducing river flows and groundwater levels in the floodplain (Doody et al., 2011). All monitoring wells were dry when they were installed as it was during a dry period but shallow groundwater levels rose in areas with palmiet and grass but remained below piezometer depths under the wattle invaded site. Removal of invading species and replacing or allowing the regrowth of native herbaceous species may result in improved subsurface hydraulic processes (i.e. water retention and infiltration rate), reduced ET rates and consequent increase in groundwater supplies (Doody et al., 2011; Kellner and Hubbart, 2016; Niu et al., 2015; Wahren et al., 2009) as shown by the results of this study. Rainfall that could recharge the floodplain alluvial aquifer may be lost to ET by the alien vegetation. The floodplain alluvial water table can have an impact on catchment outflow and water yield particularly in large catchments, therefore alien invasion in floodplains can have detrimental effects on overall outflow and catchment water yield particularly in catchments that have sizeable floodplains such as the Kromme.

5.9 CONCLUSION

This study characterized spatial and temporal soil water content dynamics and shallow groundwater levels across three sites under contrasting vegetation types (black wattle, grass and palmiet) at a floodplain site in a semi-arid catchment. Rainfall event magnitude, antecedent wetness and vegetation type were identified as the major factors controlling soil water content dynamics and shallow groundwater levels. Deep 50-60 cm soils were generally recharged by rainfall of magnitudes 30 mm/day or higher. On average, soil water content was higher at the palmiet and grass sites compared to the wattle invaded site possibly due to higher transpiration rates by the woody alien species. The groundwater table at the palmiet and grass sites was sometimes observed to rise without local recharge. Contributions were possibly from mountain runoff infiltrating and coming through the subsurface or lateral or groundwater flow down the valley elevation gradient. However, following some heavy events, groundwater was observed to rise to levels within the root zone at the palmiet and wattle sites affecting the soil water content directly from the capillary fringe. In general, the water table at the wattle site was below the depth of installed piezometers (3 m) for more than 90% of the time only responding to rainstorms greater than 40 mm/day.

Given the relative importance of floodplain landscapes particularly in arid and semi-arid catchments, as well as the global increase in land use and land cover changes particularly alien invasions in riparian landscapes, quantitative studies of this kind are therefore imperative regarding impacts of contrasting land cover types on floodplain hydrology as well as to guide vegetation recovery and restoration efforts (Gao et al., 2014; Ziadat and Taimeh, 2018). Soil water varies at both spatial and temporal scales, therefore understanding these variations becomes critical particularly in arid and semi-arid landscapes for water resource management and vegetation restoration (He et al., 2012; Wang et al., 2013; Ziadat and Taimeh, 2018).

The results of this study can therefore guide restoration works as well as to build capacity through science communication regarding the impacts of black wattle on subsurface processes as well as the ecological and hydrological importance of palmiet in river systems. Soil moisture plays a very important role on water cycling and vegetation growth in arid and semi-arid catchments. Furthermore, studying soil water content variation under different land cover types adds to the knowledge and foundation of effective water resource management and ecological restoration in semi-arid systems particularly in areas where woody alien species have invaded.

CHAPTER 6: HYDROLOGICAL PROCESS UNDERSTANDING FROM THE SPATIO-TEMPORAL VARIATION OF WATER PHYSICO-CHEMISTRY AND ISOTOPE TRACER PATTERNS IN A SEMI-ARID MESO SCALE MOUNTAINOUS CATCHMENT.

6.1 ABSTRACT

Understanding hydrological processes in semi-arid meso scale mountainous catchments requires a multi method approach for better conceptualization of catchment processes. The objective of this work was to improve hydrological process understanding from the spatio-temporal variability of water physico-chemistry and environmental tracer patterns in the Kromme catchment (Eastern Cape Province of South Africa). Samples of chloride and stable isotopes ($\delta^{18}O$ and $\delta^{2}H$) in rainfall, surface and groundwater were collected between August 2017 and February 2019. Physico-chemical parameters such as electrical conductivity (EC), temperature and pH were measured in-situ. This study also used chemical source component separation and end member mixing technique to improve the understanding of flowpaths and sources in the catchment.

Tracer data indicated groundwater contribution to surface flows in the main channel and tributaries. Isotopic evidence demonstrated that the $\delta^{18}O$ and $\delta^{2}H$ compositions in the Kromme River exhibited spatial and temporal variability from the upper to lower reaches. Water samples generally became enriched along the river length moving downstream. Overall, although water samples were increasingly enriched downstream, some locations were depleted indicating influences of depleted mountain tributaries and groundwater from the bedrock aquifer contributing to the channel therefore suggesting mixing. Tributary samples were more isotopically depleted than main river samples indicating effects of evaporative enrichment in the main channel, whilst the tributaries are receiving from depleted groundwater from the bedrock aquifer. Tracer compositions in groundwater reflected sources and mechanisms of recharge.

EC values generally increased along the length of the river, likely due to evaporation. Surface water sampled had low EC values (<350 μS/cm) suggesting contributions from subsurface flowpaths of short travel times with little time for mineral dissolution. Groundwater from the bedrock aquifer had low EC in general (EC <1000 uS/cm) which was associated with the fractured sandstone formations characteristic of the TMG regions that are not associated with high salinity. Three component source separations for the snapshot samples collected showed the importance of pre-event source components, particularly groundwater from the alluvial aquifer, highlighting the role of groundwater in sustaining river flows with some estimated proportions of greater than 90%. In general, surface water appeared to receive groundwater contributions from both the alluvial and bedrock aquifers in the catchment which was in agreement with hydrometric data showing that the main river was a consistently gaining system. Results of this study contribute to a process-based understanding of the complex interactions of water from different sources and flowpaths in meso scale semi-arid mountainous settings.

6.2 INTRODUCTION

Mountainous watersheds worldwide serve as water towers for surrounding ecosystems and downstream communities. An understanding of their hydrological processes is therefore important for sustainable management of water resources (Viviroli et al., 2011; Zhang et al., 2018). Flowpaths, water sources and streamflow characteristics in mountainous catchments vary in space and time depending on climatic variations, topography, vegetation cover and subsurface storage (Cowie et al., 2017; Zhang et al., 2018). The knowledge of runoff generation processes, i.e. flowpaths and sources, is crucial for prediction of water quantities such as catchment yield, and streamflow characteristics such as floods and low flows in a catchment (Eckhardt, 2005; Wenninger et al., 2008). Understanding these processes particularly in mountainous catchments with complex topography, highly fractured geology, high rainfall variability, and a mix of land cover types poses significant challenges to conceptualize and quantify processes (Hoeg et al., 2000; McDonnell and Tanaka, 2001). Direct measurement of discharge components continuously at sufficient number of locations is practically impossible. Multiple techniques are therefore needed to address uncertainties and get a holistic understanding of processes.

Hydrometric data has been widely used to gain insights into the hydrological functioning of catchments (McGuire and McDonnell, 2010; Munyaneza et al., 2012; Riddell et al., 2020; Uhlenbrook et al., 2002; van Tol et al., 2010). Other than using hydrometric data alone, environmental tracers were introduced to complement other hydrological methods to offer insights into catchment processes. Studies have successfully utilized isotopes in different environments such as mountainous catchments (Xing et al., 2015; Yang and Shang, 2012; Zhou et al., 2015), rainforests (Goller et al., 2005) and glaciers (Zhou et al., 2015). Environmental tracers and physico-chemical techniques have been very useful around the globe in providing insights into hydrological functioning of catchments such as recharge (Camacho Suarez et al., 2015; Hao et al., 2019), flowpaths (Cartwright et al., 2014; Wenninger et al., 2008) and water sources (Lambs, 2000; Wenninger et al., 2008). Zhou et al. (2015) identified runoff components and their temporal variation using deuterium and ^{18}O in the Qilian Mountains in China. Li et al. (2007) traced soil water and recharge dynamics in a semi-arid Taihang Mountain catchment (China). Isotopic compositions have been used to ascertain various sources contributing streamflow in meso scale semi-arid catchments (Camacho Suarez et al., 2015; Saraiva Okello et al., 2018) and mountainous catchments (Hoeg et al., 2000; Zhang et al., 2018). Natural tracers such as ^{18}O and deuterium are conservative therefore they can be used to trace flowpaths as their composition is not affected or changed by interactions with rock minerals and other aquifer materials, thereby allowing the determination of sources in a river (Vitvar and Aggarwal, 1998). Isotope tracer studies have also been integrated with physico chemical parameters (e.g. EC, pH, and temperature) as well as geochemical tracers such as chloride and silica to identify runoff sources and flowpaths (Hao et al., 2019; Maurya et al., 2011; Penna et al., 2015). Variability of tracers at a

temporal scale can be used to estimate old and new water proportions to stream flow as well as groundwater-surface water interactions (Song et al., 2006).

Tracer hydrology has received lots of attention at smaller scales (Colvin et al., 2009; Hao et al., 2019; Hood and Hayashi, 2015; Wenninger et al., 2008), but little has been documented at larger spatial scales due to logistical and financial constraints (Mul et al., 2009). Furthermore, a few studies have used tracer data to characterize processes in large scale semi-arid mountainous catchments (Li et al., 2007; Penna et al., 2015; Zhou et al., 2015). The objective of this work is therefore, to improve the conceptualization and quantification of processes in a semi-arid mountainous Kromme catchment (Eastern Cape Province of South Africa) using environmental tracers and physico-chemical parameters. The Kromme is a semi-arid, meso-scale mountainous catchment with sizeable floodplains. For large scale mountainous catchments, multiple features and processes contribute to their hydrological functioning. A diversity of flowpaths may be dominant at different spatial and temporal scales as heterogeneous underlying geology and complex topographic properties give rise to different response characteristics in various locations (Savenije, 2010). Isotopes (^{18}O and deuterium) can be useful tools for integrating hydrological information across scales (Ala-aho et al., 2018).

Most studies in high elevation mountainous catchments have focused on the influence of snow in sustaining river flows (Brauchli et al., 2017; López-Moreno and García-Ruiz, 2004; Lucianetti et al., 2020). However, river flows in most high-elevation mountainous catchments are sustained by subsurface water sources throughout the year (Stoelzle et al., 2019), and these sources are influenced by the magnitudes, and types of recharge mechanisms, as well as subsurface storage capabilities (Cowie et al., 2017). Meteorological patterns in these catchments are influenced by physiographic features such as high elevation peaks and deeply incised narrow valleys. All these characteristics result in different processes, response patterns and potential pathways that could produce similar streamflow patterns. However, even though response patterns could be similar, they can be distinguished by their tracer signatures.

Previous chapters have highlighted possible flowpaths and groundwater, surface water interactions between the mountain, floodplain and channel as well as possible water sources contributing to streamflow in this catchment. Previous hydrometric analyses have indicated that the mountain bedrock aquifer discharges into tributaries (seeps observed and consistent flow in tributaries even during a drought). The alluvial aquifer also receives contributions from the bedrock aquifer indirectly via the subsurface and is also recharged by direct precipitation and river flood events. Water table elevations in the alluvial aquifer were found to be continually above the adjacent river channel at several floodplain sites, suggesting that it could be a consistent source supporting baseflow in the main channel. Baseflow recession analyses provided insights into storage-discharge relationships at

catchment and sub catchment scales in the Kromme, however, these approaches could not fully quantify the source contributions. Isotope data would therefore help to confirm the occurrence of conceptualised flowpaths, sources and to quantify proportional contributions from each source and/or flowpath.

The Kromme is located in the Cape Fold Belt region of South Africa which comprises a series of mountain ranges primarily made up of the Table Mountain Group (TMG) geologic formations (Diamond, 2014). Previous isotope studies in some parts of the TMG have indicated that groundwater can be discharged through valley bottom wetlands, seeps, springs, and as baseflow in river channels, indirectly via alluvial aquifers or where the river channels cut directly into bedrock (Colvin et al., 2009; Xu et al., 2009). Most of these studies in the TMG region have indicated that runoff was mainly generated from groundwater contributing between 64-98% (Diamond, 2014; Smith and Tanner, 2019). Several other studies in semi-arid mountainous catchments have also shown the dominance of groundwater in sustaining river flows using tracers (Camacho Suarez et al., 2015; Gibson et al., 2016; Guo et al., 2017; Uhlenbrook et al., 2004).

This study employed the combined use of tracers from rainfall, groundwater and streamflow at multiple locations in the Kromme catchment to assess spatiotemporal variability of tracer compositions in surface and subsurface water and identify likely pathways contributing to streamflow. The information gained was used to infer potential connectivity, source contributions and streamflow changes which is critical knowledge for the optimal protection of surface and groundwater resources given the current changing land use and climatic conditions and to update and improve the conceptual model of the catchment

6.3 Materials and methods

6.3.1 Study site

Detailed descriptions of location, geology, land use, and other physiographic characteristics of the Kromme catchment are presented in Chapter 3. Figure 6.1 shows locations for isotopes, chloride sampling and in-situ monitoring of physico-chemical properties of water from different sources.

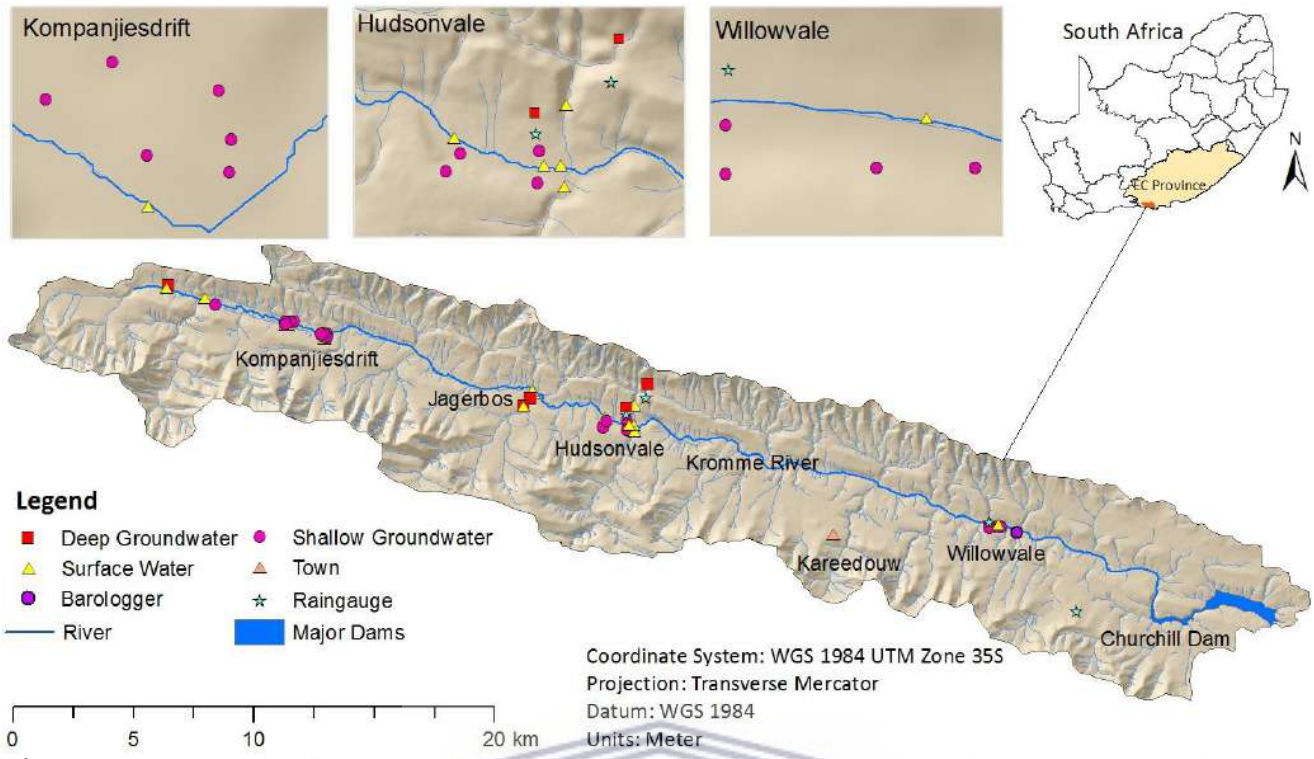

Figure 6.1: Location of water quality surface and groundwater sampling sites (Kromme catchment).

6.3.2 Data Collection Procedures

Spatio-temporal variability of physico-chemistry and tracer patterns was assessed to improve the conceptualization and quantification of processes in the Kromme catchment. A quantitative approach was used in this study to explore and characterize groundwater and surface water interactions as well as to determine various runoff components in the catchment. A total of eight sampling campaigns were done every 2-3 months from April 2017 to December 2019. The samples were collected directly from the sources using the grab sampling method. During each sampling campaign, samples were collected from three tributaries (two north facing and one south facing), eight main river points, ten piezometers for shallow groundwater (alluvial aquifer) and four boreholes, and 1 seep for deep groundwater sites (bedrock aquifer) (Figure 6.1). Herein, alluvial aquifer (shallow groundwater) and bedrock aquifer (bedrock groundwater) refers to subsurface water monitored in piezometers (<4 m) and boreholes (>4 m) respectively.

Monitoring site names and codes used in the study are given in Chapter 3, Table 3.1 and 3.2. Measurements of EC, pH and temperature were done in situ at various surface and groundwater sites using a YSI Pro-Plus Multi-parameter probe. From the rain gauge, tributaries, river sites, piezometers, boreholes and seep, a total of two hundred and eleven samples were collected for stable isotopes of O^{18} and deuterium analyses during the monitoring period. Two hundred and eleven water samples for chloride analyses were also collected but only one hundred and ninety six were analysed due to laboratory issues. Two hundred and forty three measurements of EC, pH and temperature

were done in situ at the above mentioned sources. A 50 ml bottle was rinsed three times using the water from the source then a sample was collected. The bottle was sealed tightly making sure that no air was present then stored at a temperature of not more than 4°C. Turbid samples were filtered through a 0.25 mm filter membrane.

Rainfall samples were collected by a volunteer resident of the area and stored in a refrigerator. Rain samples were collected for individual rain day events (lumped sample for the day). The day samples were not lumped further, each sample was analysed individually. For each stream and groundwater sampling campaign, the rain sample concentration values from preceding 2-3 month period have been plotted for comparison. It is important to note that not all sites could be sampled in all trips as some were dry or inaccessible during the field visit.

6.4 Data Analysis

Collected samples were analyzed for $\delta^{18}O$ and $\delta^{2}H$ isotopic compositions at the University of the Western Cape and iThemba laboratories using the liquid water isotope analyzer (Los Gatos Research Inc.). Chloride composition in samples was analysed using the Mercuric Thiocyanite method (Hach DR 6000 spectrophotometer). A standard solution method was used to validate the analysis procedure, instrument and the reagents used with a precision at 95% confidence level.

The concentration of the isotopes is expressed as a ratio of the mass balance in relation to the Vienna-Standard Mean Ocean Water (VSMOW) (Equation 6.1).

$$\delta\ (‰) = (R_s/R_{st}-1)*1000 \qquad (6.1)$$

R_s and R_{st} are ratios of isotopic compositions (i.e. $R = {}^{18}O/{}^{16}O$ for oxygen and ${}^{2}H/{}^{1}H$ for hydrogen) in the sample (s) and the standard (st) respectively.

Isotope signatures of $\delta^{18}O$ and $\delta^{2}H$ were analysed to assess how they vary across different sources. Values were plotted against the local and global meteoric lines to determine their relationship with the meteoric origin. The global meteoric water line (GMWL) defined by Craig (1961) (Equation 6.2) and the local meteoric water line (LMWL) defined by Diamond (2014) (Equation 6.3) are ratios of heavy oxygen and hydrogen expected in the rainwater before evaporation.

Global Meteoric Water Line	$\delta^{2}H = 8\delta^{18}O + 10$ ‰	(6.2)
Local Meteoric Water Line	$\delta^{2}H = 6.5\delta^{18}O + 10$ ‰	(6.3)

The LMWL and GMWL are empirical relationships between $\delta^{18}O$ and $\delta^{2}H$ of precipitation used to detect evaporative enrichment (fractionation) of different water samples. Water samples plotting on

the meteoric line are assumed to be of atmospheric origin and not altered by other processes such as open water evaporation and mixing with other rock minerals. Sources of water can be deduced by analysing where they plot in relation to the meteoric water line. If a sample plots on or close to the line similar to that of precipitation, it therefore means the sample is of meteoric origin (Dansgaard, 1964). In this study, the LMWL was generated by Diamond (2014) using precipitation data acquired from the Lentelus rainfall station approximately 50 km from the Kromme catchment. The global meteoric water line (GMWL) used was developed by Craig (1961).

The local evaporation line (LEL) was also generated to determine if evaporation processes have occurred in any of the sampled water sources particularly open water sources as well as shallow groundwater. The LEL was described by Edwards et al. (2007) and is defined by generating a regression line through surface water and shallow groundwater samples. The isotopic ratios $\delta^{18}O$ and $\delta^{2}H$, physico-chemical and geochemical tracers were also used for source component separation to distinguish between time source components (event and prevent water) in the catchment using the three component separation mass balance method to account for possible end members by extending the standard two component equation as follows:

$$Q_t = Q_{dr} + Q_{sg} + Q_{dg} \quad (6.4)$$

$$C_t Q_t = C_{dr} Q_{dr} + C_{sg} Q_{sg} + C_{dg} Q_{dg} \quad (6.5)$$

Where Q_t is the total flow, Q_{dr} is the contribution from direct runoff/ event water, Q_{sg} represents shallow groundwater and Q_{dg} represents deep groundwater. C_{sg} and C_{dg} are values representing tracer compositions of shallow groundwater and deep groundwater respectively. C_t and C_{dr} represent the tracer compositions of streamflow, event/direct runoff and pre-event water Rain samples from a most recent preceding rainfall event before the sampling was used. Samples from boreholes and springs were used for deep groundwater and samples from piezometers were used for shallow groundwater.

Deuterium excess (d) can be used as a proxy for isotopic fractionation process indicative of condensation or evaporation effects in water (Wu et al., 2012; Ala aho et al., 2019). Deuterium excess (d) was calculated using Equation (6.6) by Dansgaard (1964):

$$d = \delta^{2}\mathrm{H} - 8\delta^{18}\mathrm{O} \quad (6.6)$$

A d-excess value of 10 plots on the GMWL whilst d-excess values greater than 10 plot above the GMWL meaning the samples are depleted and can also be indicative of cooler moisture sources, while values less than 10 mean that samples are isotopically enriched and can indicate warmer moisture sources. D-excess values in relation to the GMWL are indicative of the source ocean, season and

weather system type responsible for the rain event. In this chapter d-excess is used as additional index to analyse and differentiate evaporated and non-evaporated samples from various sources monitored

Basic descriptive statistics of central tendency and variability were calculated for the measured variables by site and site type, and correlation analyses were used to describe the relationship between measured variables. To assess the spatial variability of tracer compositions and physico-chemical parameters, t-tests were performed on the data. Data was analysed at a 0.05% confidence level. Data was tested for normality and transformed before running statistical tests. ANOVA was used to test for variations in tracer patterns at a temporal scale. Principal component analysis (PCA) was done to identify patterns in the data sets and cluster analysis to classify similar samples into groups (Clarke and Gorley, 2006).

The cluster analysis was performed using normalized data and Euclidean distance resemblance measure. Parameters assessed were pH, EC, ^{18}O, ^{2}H, Cl ORP, D-excess and temperature using the mean values for each parameter per site over the sampling period. The same set of sampling events for a given parameter was used for all the sites included in the analyses to have a fair comparison.

6.5 RESULTS

6.5.1 Spatial and temporal variations of environmental tracer patterns.

6.5.1.1Spatial and temporal variations in isotopic compositions of rainfall, streamflow and groundwater.

Isotopic signatures for all sampled water types (river, groundwater, rain and springs) are described in terms of spatial and temporal variability in δ^2H and $\delta^{18}O$. D-excess values in relation to the Global Meteoric Water Line (GMWL) are also discussed. Samples collected in August and December 2017 represented a dry period, while those collected in February, August and November 2018 represented a relatively wet period. There was a prolonged dry period in 2017 from August to July (average of 0.5 mm/day). The year 2018 was also relatively dry particularly in winter (May to August) (Section 6.5.1.3, Figure 6.3). However, due to a large storm event in September (134 mm in 48 hours) and some wet months in between, the average rainfall for the year 2018 was close to the long term average. Both the years 2017 and 2018 had their wettest periods during spring (September to November) (Section 6.5.1.3, Figure 6.3).

The isotopic compositions of Kromme River water samples exhibited marked spatial variations (Table 6.1; Figure 6.2). Marked variations in isotopic compositions are shown between 2017 and 2018 samples (Figure 6.2). Tracer compositions were depleted (Table 6.1) at upper parts of the catchment (-28.19‰ for δ^2H; -4.79‰ for $\delta^{18}O$) getting slightly enriched lower catchment (-15.16‰for δ^2H; -3.55‰ for $\delta^{18}O$), likely due to evaporative enrichment of water in the main channel along the river length.

Table 6.1: Descriptive statistics of isotopic compositions in main river surface water samples

Main river			**δ^2H ‰**			**$\delta^{18}O$‰**		
	Number of sites	Samples (*n*)	Mean	Min	Max	Mean	Min	Max
Upper catchment	3	14	-22.08	-28.19	-15.66	-4.79	-5.95	-3.12
Midcatchment	3	18	-16.96	-23.76	-10.5	-3.73	-5.23	-2.66
Lower catchment	1	8	-15.16	-20.88	-9.72	-3.55	-4.55	-2.42

The local evaporation lines (LEL) for surface water and shallow groundwater samples in the catchment showed slopes ranging from 5.8 to 8.3 (Figures 6.2 and Appendix Figure 6A1). These slopes show that both surface and shallow groundwater experienced evaporative enrichment. Increased evaporative enrichment in main river samples was shown in August and November 2017 where the majority of samples plotted between -20 for δ^2H and -4 for $\delta^{18}O$ (Figure 6.2). In November 2018, most river water samples were depleted (plotting between -30 for δ^2H and -6 for

δ¹⁸O) due to the dilution effect by rainfall. From the large storm in September 2018 (134 mm in 48 hours), a series of rainfall events (some greater than 20 mm/day) occurred until the sampling in November 2018 hence the depleted surface water samples (Figure 6.2).

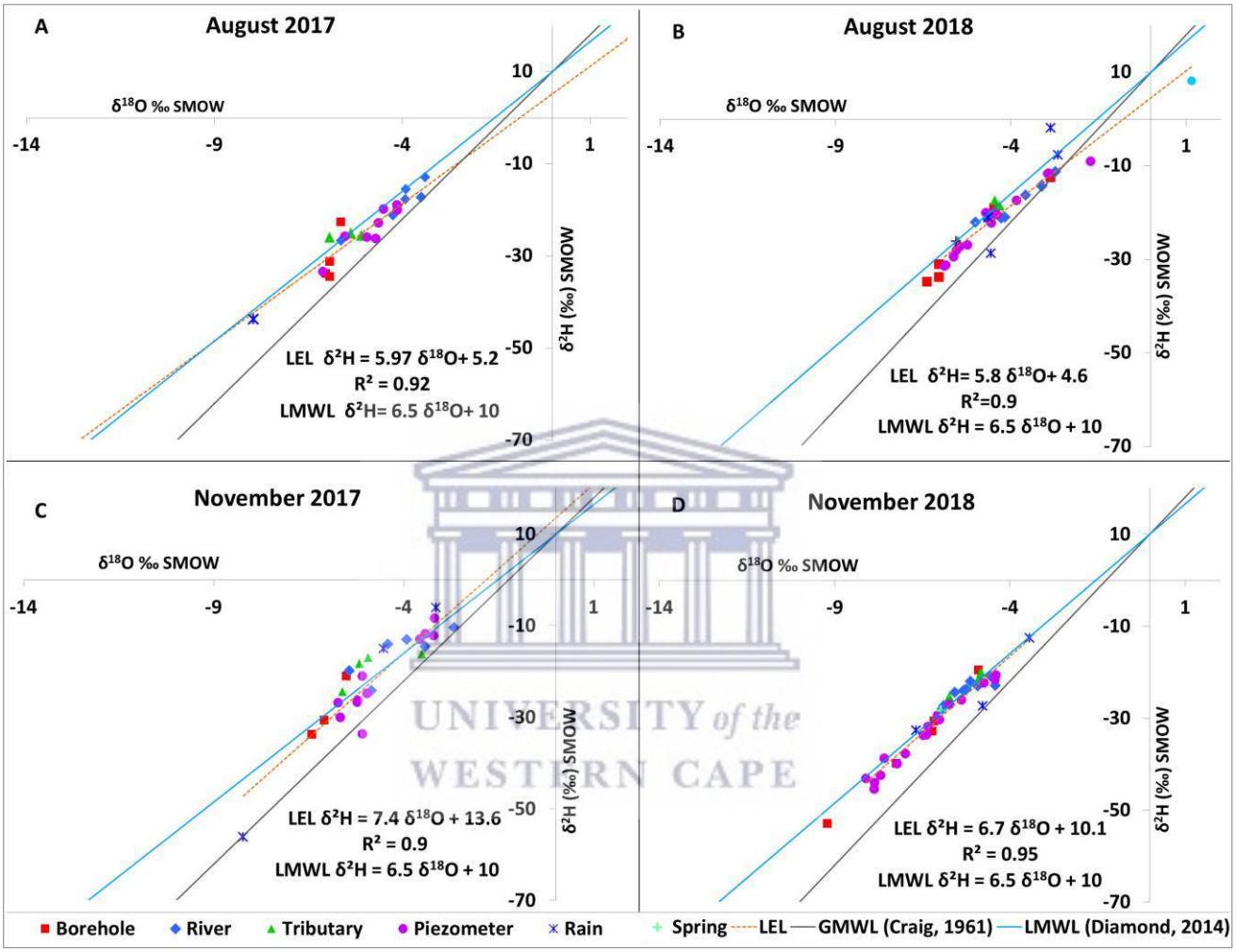

Figure 6.2: δ²H (‰) vs. δ¹⁸O (‰) for Kromme catchment 2017 and 2018 samples. All rain samples in each graph were collected from events that occurred before each sampling. LEL - Local evaporation line, LMWL - Local meteoric water line and GMWL - Global meteoric water line

Isotopic compositions of other sampled sources (rainfall, tributaries, and groundwater from alluvial and bedrock aquifers) are also shown in Figure 6.2 and summarised in Table 6.2. Variations were observed between the different sources (Figure 6.2). In general, tracer compositions showed depletion of groundwater in the alluvial aquifer at the upper catchment sites (-28.48‰ for δ²H; -5.51‰ for δ¹⁸O) getting slightly enriched downstream (-18.03‰ for δ²H; -4.06‰ for δ¹⁸O). This was due to enriched surface water infiltrating and recharging the alluvial aquifer at lower catchment sites. Isotopic compositions of groundwater from the bedrock

aquifer showed depletion at all monitored upstream and midcatchment sites (Table 6.2). Tracer compositions in groundwater ranged between minimum values of -53‰ to-31‰ for $\delta^{2}H$; -9‰ to-6‰ for $\delta^{18}O$ and maximum values between -32‰ to -18‰ for $\delta^{2}H$; -6‰ to -4‰ for $\delta^{18}O$ with an average of -33.3‰ for $\delta^{2}H$ and -6.1‰ for $\delta^{18}O$ for most of boreholes (Tables 6.2). This was due to recharge of the deep groundwater by depleted sources. Samples from the tributaries were depleted showing average isotopic compositions of -20.54 for $\delta^{2}H$ and -4.72 for $\delta^{18}O$. Deep groundwater samples were more depleted than tributary samples (Table 6.2). Deep groundwater discharges and sustains tributary flow and water in tributaries experience evaporative enrichment to an extent hence the slight differences in their isotopic compositions. Deep groundwater was more depleted than water from tributaries, main channel and shallow groundwater. This implied quick recharge of deep groundwater by water that had not been influenced greatly by ET which can be expected in fractured rock mountains. The spring/seep samples showed no significant differences at a temporal scale with compositions ranging from -24‰ to -28‰ for $\delta^{2}H$ and -5.1‰ to -5.9‰ for $\delta^{18}O$ with a mean of -26‰ for $\delta^{2}H$ and -5‰ for $\delta^{18}O$ implying a constant source of groundwater discharge.

Table 6.2: Descriptive statistics of isotopic compositions in rainfall, tributary and groundwater

				$\delta^{2}H$ ‰			$\delta^{18}O$‰		
Source	**Location**	Sites (*n*)	Samples (*n*)	Mean	Min	Max	Mean	Min	Max
Rainfall		2	12	-23.76	-82.73	24.60	-4.95	-12.96	1.83
Tributaries		4	24	-20.54	-26.10	-10.63	-4.72	-5.92	-3.04
Shallow GW	**Upper catchment**	8	36	-28.48	-42.45	-17.48	-5.51	-7.68	-3.71
	Midcatchment	3	19	-16.56	-23.60	-9.09	-3.70	-5.08	-1.73
	Lower catchment	2	10	-18.03	-31.46	-8.30	-4.06	-5.89	-1.88
Deep GW	**Upper catchment**	1	5	-33.25	-34.60	-32.34	-5.97	-6.22	-5.82
	Midcatchment	3	21	-29.31	-52.89	-12.49	-5.75	-9.21	-2.87

There were no significant variations in isotopic variations of deep groundwater (KDBH vs. JBHU, *P=0.56*) and (KDBH vs. PKBH, *P=0.76*) except samples from the floodplain borehole (JBHL) (Appendix table 6A1). Groundwater samples from the floodplain borehole (JBHL) were significantly different in isotopic compositions in comparison to groundwater from the high elevation boreholes (*p=0.02* and *p=0.03* against KDBH and JBHU respectively). Similarities in groundwater samples from upper and midcatchment boreholes (KDBH vs. JBHU) could have been due to recharge from high up in the mountains where elevation effects on the isotopic composition of precipitation was a factor. Groundwater at the floodplain borehole (JBHL) had an average isotopic composition of -19.42‰ for $\delta^{2}H$ and -4.8‰ for $\delta^{18}O$ showing relatively similar

isotopic signatures as shallow groundwater from the floodplain alluvial aquifer as well as some surface water samples from the main channel (Appendix Tables 6A2-6A5). This indicated that groundwater in the floodplain was influenced by enriched surface and shallow subsurface water sources.

6.5.1.2 Spatial and temporal variation of d-excess from various sources

Calculated d-excess values for water sampled from the various sources in the Kromme catchment are given in Table 6.3. D -excess in rainfall samples ranged between 6 to 28‰. Mean D-excess values for rainfall were between 8‰ to 19‰. The lowest mean d-excess value of 8‰ in rainfall was recorded in May 2018, indicating high evaporation.

Table 6. 3: Summary of d-excess values for different sources

		D excess (‰)				
Date		Rainfall	Deep groundwater	Shallow groundwater	River	Tributary
	Mean	**20**	**16**	**14**	**13**	**18**
08-2017	Min		13	11	10	15
	Max		22	18	16	21
	Mean	**15**	**20**	**15**	**17**	**19**
11-2017	Min	10	18	7	11	12
	Max	21	23	20	23	23
	Mean	**17**	**18**	**15**	**13**	**19**
12-2017	Min	10	15	12	10	18
	Max	28	22	18	17	19
	Mean	**14**	**15**	**14**	**13**	**15**
02-2018	Min	10	15	8	9	14
	Max	16	16	16	17	17
	Mean	**8**	**16**	**13**	**12**	**15**
05-2018	Min	6	14	6	9	14
	Max	10	17	16	16	18
	Mean	**15**	**15**	**14**	**13**	**17**
08-2018	Min	7	10	5	10	16
	Max	20	17	17	18	18
	Mean	**19**	**19**	**18**	**18**	**19**
11-2018	Min	15	17	14	12	18
	Max	20	21	22	20	20

D-excess of deep groundwater from monitored boreholes (n=4) show mean values between 15‰ to 20‰ (Table 6.3). Deep groundwater samples were largely above 10‰ showing that water was not subjected to evaporation. High d-excess values in groundwater also indicated recharge from sources not influenced by enriched meteoric water. High d-excess in deep groundwater (23‰) was recorded in November 2017 and lowest (10‰) was recorded in August 2018 (Table 6.3). Shallow groundwater samples showed marked variations in d-excess values throughout the

monitoring period (August 2017-December 2018) (Table 6.3). At some sites, high and low d-excess values were observed in different piezometers which implied different recharge sources of groundwater within the alluvial aquifer. Lowest calculated d-excess values in shallow groundwater ranged between 5-8‰ indicating a strong evaporation influence. Low d-excess values in shallow groundwater correspond to low values in precipitation which implied recharge and the influence of more enriched rainfall events. River water samples showed mean d-excess values ranging between 12‰ and 18‰. This implied depletion, however there were low d-excess values also recorded i.e. in February and May 2018, showing signs of enrichment. All low d-excess values recorded in the main channel were at the lower catchment site (Willowvale) which implied evaporation of water as it flowed along the length of the river. Tributary samples showed high d-excess and consistent little variation which implied a constant source (Table 6.3). Overall, the most non-evaporated samples at all water sources (rainfall, surface water, and groundwater) were observed in November 2018 (Table 6.3) which was due to storm events prior to sampling which were depleted.

6.5.1.3 Streamflow responses and $\delta^{18}O$ variation in various sources

Streamflow responses and $\delta^{18}O$ variation in rainfall, surface and groundwater samples are shown in Figure 6.3. Rainfall $\delta^{18}O$ compositions fluctuated during the monitoring period with increased depletion observed after large events (Figure 6.3). For example, compositions of -83 ‰ for $\delta^{2}H$ and -13 ‰ for $\delta^{18}O$ (depleted), were observed for the large storm event on 2018/09/07-08 (134 mm), then got slightly enriched in subsequent days with an average of -50 ‰ for $\delta^{2}H$, -9 ‰ for $\delta^{18}O$ (n=3).

At the upper catchment sites, groundwater samples (KD BH) were more depleted than all river samples (KD RV, KG RV and KMP RV) (Figure6.3). At the midcatchment site, tributary and borehole samples (i.e. HVPK in Figure 6.3) were depleted and less variable over time. Furthermore, deep groundwater monitored at other boreholes at the midcatchment site (JBHL and JBHU) also showed consistent depletion in isotopic composition (Figure 6.3). Groundwater from the bedrock aquifer discharges into tributaries hence the similarities in isotopic compositions (Figure 6.3) and d-excess values (Table 6.3). It is therefore, reasonable to assume that the flow contribution into the main river from the tributary sub-catchments consists predominantly of groundwater. Deep groundwater was however more depleted than water from the tributary because water in the tributary gets slightly enriched as it flows.

At Hudsonvale (midcatchment) and Willowvale (lower catchment) sites, river and shallow groundwater isotopic compositions showed marked variations over time (Figure 6.3). There were no consistent patterns between the river and shallow groundwater isotopic compositions. Sometimes the surface water in the river was more depleted than groundwater in the alluvial aquifer and vice versa in other cases (Figure 6.3). Similarities in isotopic compositions between surface and shallow groundwater samples indicated interactions between the two sources (i.e. November 2017 and November 2018 at Hudsonvale and Willowvale sites) (Figure 6.3). Periods of low flows and little or no rainfall, isotopic signatures of river water were groundwater dominated (i.e. August 2017 and August 2018). Although, isotopic signatures in river water were variable at both spatial and temporal scales, samples at the lower catchment site were generally more enriched in comparison to river samples at upper and midcatchment sites (Figure 6.3).

Overall deep groundwater at all sites was depleted and less variable over time. The most depleted $\delta^{18}O$ compositions in all sources were observed in November 2018 because prior to the November 2018 sampling, the catchment received some notable rainfall events (sum of 252 mm from September 2018) and significant streamflow responses. Therefore, the catchment was relatively wet compared to previous sampling campaigns. Observed results show similarities in isotopic compositions of some rain, river, and groundwater from alluvial and bedrock aquifers indication groundwater and surface water interactions (Figure 6.3).

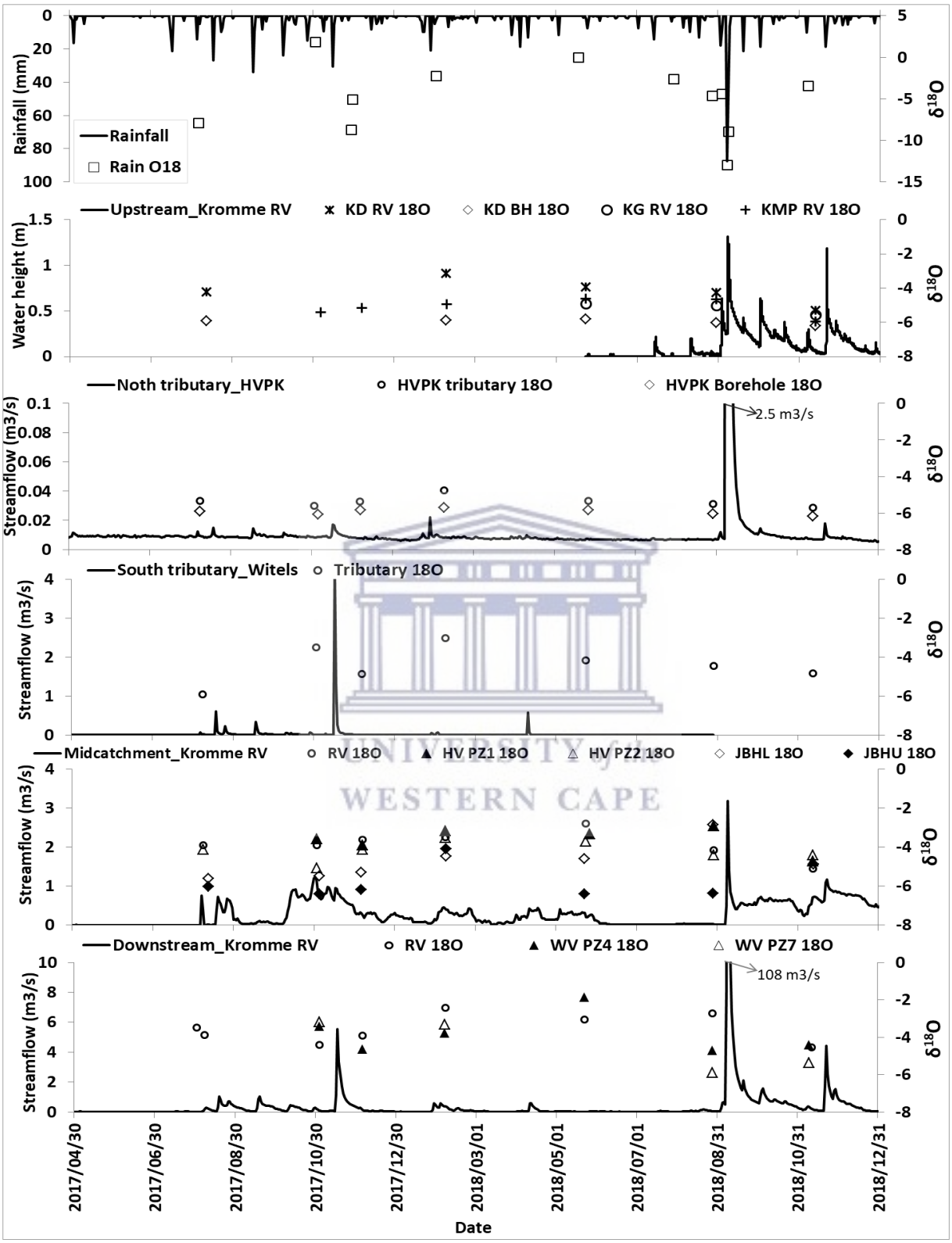

Figure 6.3: Variation of $\delta^{18}O$ and discharge at main river sites and tributaries from April 2017 to December 2019. RV-River, BH-Borehole, KD, KG and KMP are upper catchment sites, HV PZ1 and 2-piezometers at Hudsonvale, WV PZ4 and 7- piezometers at Willowvale, JBHU and JBHL are midcatchment boreholes.

6.5.2 Spatial and temporal variations in water physico-chemical parameters.

6.5.2.1 Variations in electrical conductivity (EC) and chloride (Cl)

Measured electrical conductivity (EC) and chloride (Cl) results are presented in Figures 6.4 to 6.7. The scatter plot (Figure 6.4) shows a strong relationship between EC and Cl in the catchment (R^2=0.88). EC values for surface water ranged from 115-500 uS/cm, 263-1732 uS/cm for shallow groundwater and 88-1210 uS/cm for deep groundwater in the catchment. Cl values ranges were 9-256 mg/L for surface water, 68-1527 mg/L for shallow groundwater and 17-519 mg/L for deep groundwater. High EC values and Cl compositions are observed in groundwater from the alluvial aquifer due to mineralization. Most samples of deep groundwater and surface water plot at low EC and Cl compositions indicating low salinity in this catchment (Figure 6.4).

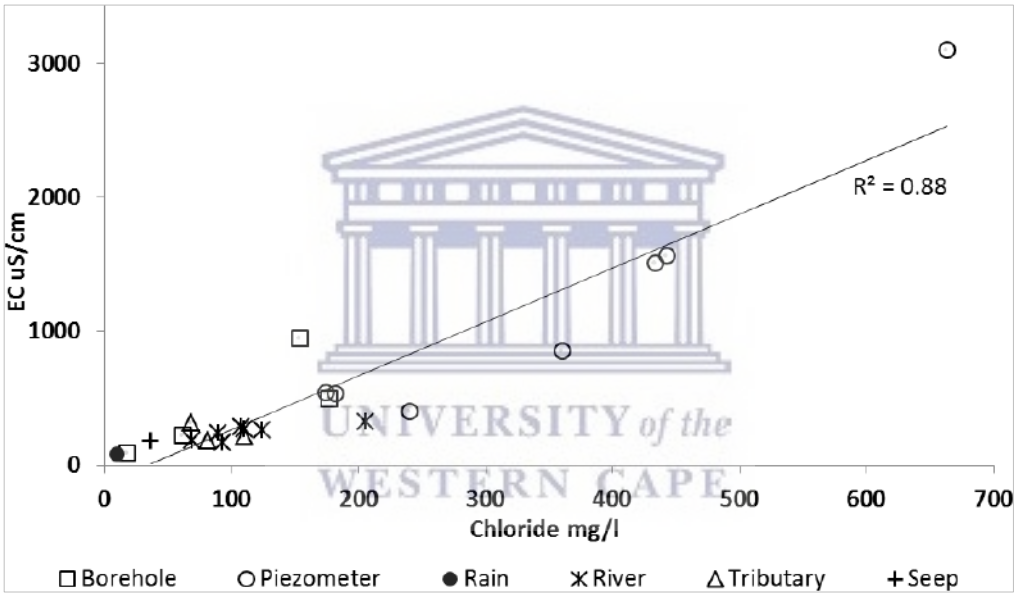

Figure 6.4: Relationship between EC and chloride from different sources (2017-2019)

EC increased from upper to lower catchment sites along the river with mean values ranging from 249 (µS/cm) upstream to 358 (µS/cm) downstream (Table 6.4). Mean Cl compositions also increased similarly. However, Cl compositions were not significantly different between upper and midcatchment sites with mean values of 111 and 112 mg/L respectively (Table 6.4).

Table 6.4: Descriptive statistics for EC and chloride compositions of surface water

Main river	**EC (µS/cm)**					**Chloride mg/L**				
	Mean	SD	Min	Max	Samples (*n*)	Mean	SD	Min	Max	Samples (*n*)
Upper catchment	248.6	93.8	114.7	419	18	111.1	78.9	9.2	256.1	13
Midcatchment	285.5	70.9	195.8	500	24	112.7	64.8	14.7	248.3	16
Lower catchment	358.4	60.3	258.2	480	10	133.0	47.7	69.1	205.5	8

Box plots of observed mean EC values and Cl compositions in surface water and, shallow and deep groundwater from April 2017 to December 2018 are shown in Figure 6.5. Surface water samples had low mean EC values and Cl compositions in general (200-400 uS/cm and <300mg/L respectively).

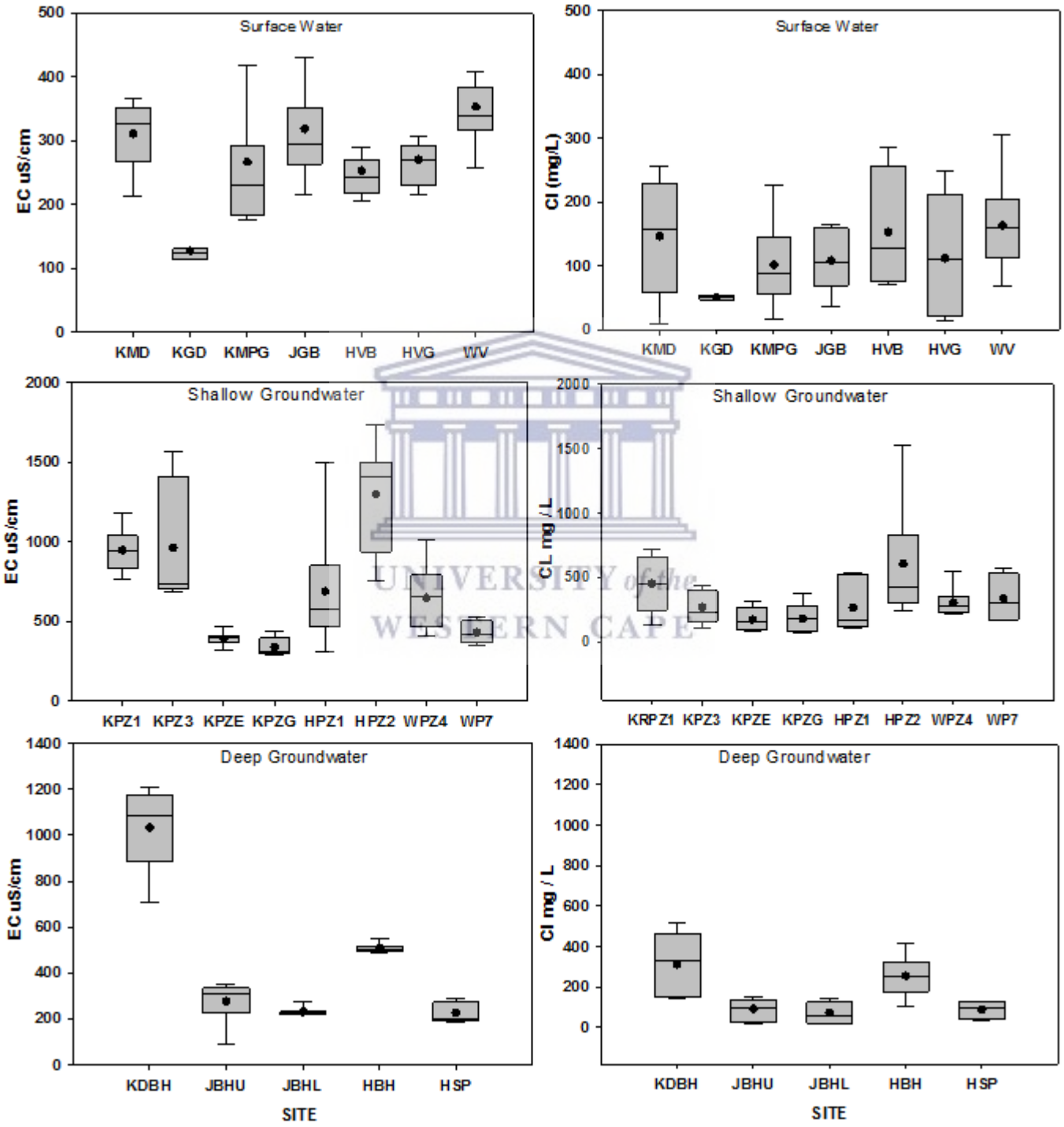

Figure 6. 5: Variation of EC and chloride from surface water or groundwater sites (2017-2019)

Surface water EC and Cl show relatively similar ranges as groundwater from the bedrock aquifer except for groundwater measured at one borehole (KDBH) in the upper catchment (Figure 6.5). Groundwater EC at this borehole was consistently higher (1033 uS/cm average) than EC at other boreholes in the catchment *(P=<0.001;* mean ranging from 200-400 uS/cm*)* as well as in comparison to the adjacent river site (KMD) *(P=<0.001)*. This borehole (KDBH) is located at the interface between shale and sandstone which may have contributed to the high EC, as the Bokkeveld shale is characterised by high salinity (Greeff, 1994). EC was also notably high in shallow groundwater at most sites ranging from 263 uS/cm to 1732 uS/cm. Cl concentration was also high in shallow groundwater ranging from 68 mg/L and 1527 mg/L with a mean of 340 mg/L. Highest values in EC and CL of shallow groundwater were all measured at the same site (HPZ2) in a midcatchment wetland (Figure 6.5). Spikes in EC values and Cl compositions in groundwater inside wetlands can be attributed to evapotranspiration from soil and wetland plant species as some species exclude/lose salts during the process (Smith, 2019).

6.5.2.2 Variations in streamflow responses and EC variation in various sources

Figure 6.6 shows streamflow responses to rainfall and the corresponding temporal variation of EC at various sites in the catchment. Observed streamflow exhibited marked spatial and temporal variability at the different sites (Figure 6.6). EC values fluctuated at all sites increasing progressively as the catchment got dry suggesting the effects of evaporation (i.e. August 2017 and June 2018). EC values also decreased during wet periods possibly due to dilution effects after the November 2017 event i.e. HVPK tributary and borehole, Willowvale river and WV PZ4 (Figure 6.6). However, shallow groundwater at some sites (i.e. HV PZ2-midcatchment), did not show a decrease in EC values after rainfall events.

In general, EC was highly dynamic, fluctuating along the profile but with a general increase in values spanning the river length. Surface water EC was therefore, significantly high at Willowvale (lower catchment site), compared to all upper catchment surface water sites *(P =0.002)*. However, in general, EC in the main channel and tributaries was consistently lower than in shallow groundwater.

Significant differences were shown in EC values between deep groundwater (HVPK borehole) and tributary samples (HVPK tributary) (Figure 6.6). Groundwater from the bedrock discharges into the tributaries therefore slight differences between the two sources were expected, however these results imply that groundwater from HVPK borehole was in a different substrate than groundwater that was discharging into the HVPK tributary.

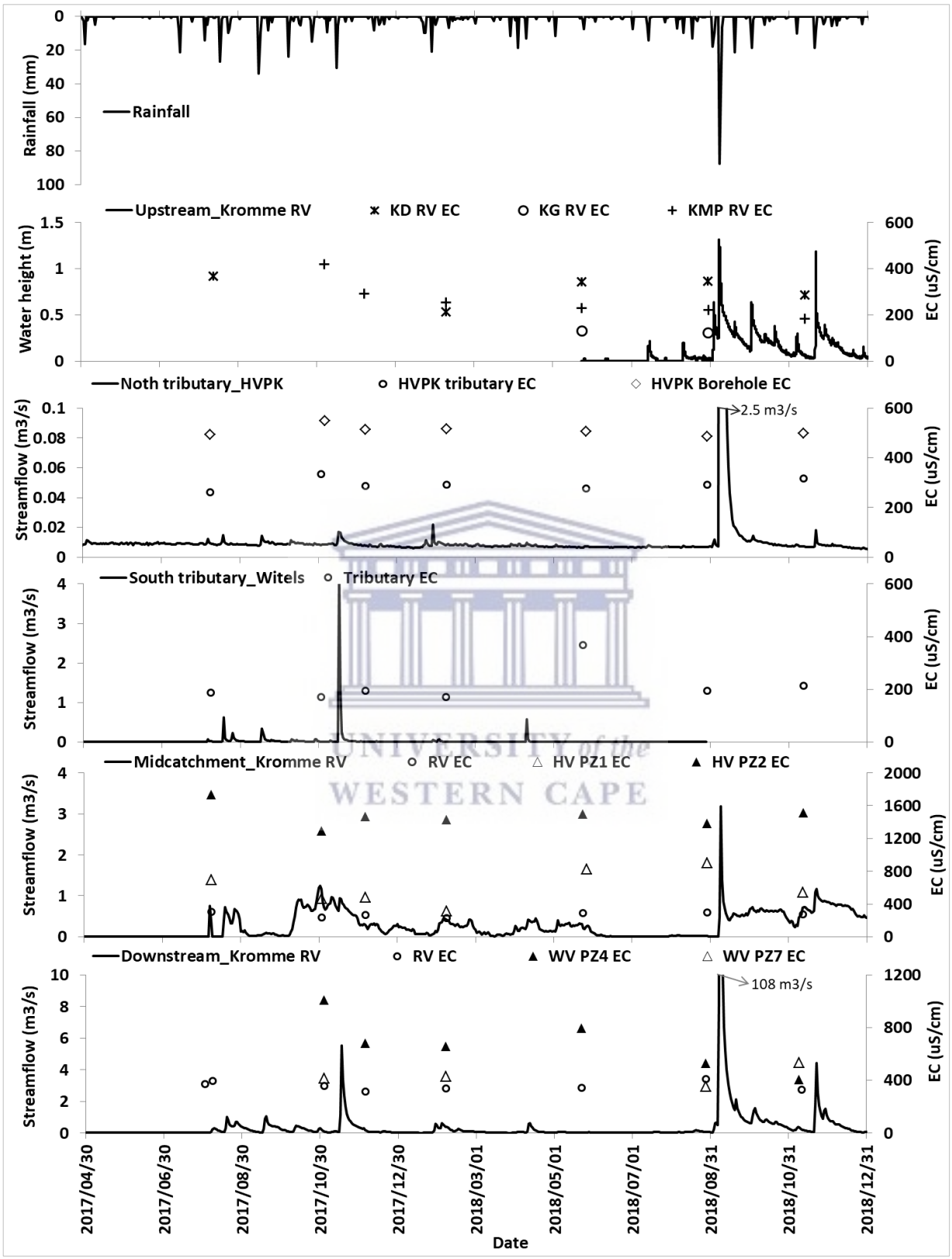

Figure 6. 6: EC and discharge variation at main river sites and tributaries from April 2017 to December 2019 RV-River, BH-Borehole, KD, KG and KMP are upper catchment sites, HV PZ1 and 2-piezometers at Hudsonvale, WV PZ4 and 7- are piezometers at Willowvale.

6.5.2.3 Spatio-temporal variations in EC in relation to the underlying geology

Spatial maps on Figure 6.7 show the spatio-temporal variation of EC in the Kromme catchment during the 2017 -2018 period at various sites. Similar to isotope results, EC in surface water showed an increase along the length of the river moving downstream. However, the surface water EC values were generally low (<350 (µS/cm) throughout the monitoring period. There were no discernible trends in groundwater EC spatially, as values varied per site.

At the upper catchment site, Kompanjiesdrift (Blue in Figure 6.7), river EC remained low throughout (<200 uS/cm). Shallow groundwater EC at this site was generally constant until November 2018 when values decreased significantly (Figure 6.7) due to dilution from recharge. At the second upper catchment site (green in Figure 6.7), EC in the river decreased from between 401-600 uS/cm in 2017 to 50-200 uS/cm range in November 2018 becoming much fresh. EC in shallow groundwater (KPZG and KPZH) was generally constant implying a constant source except at KPZE where EC alternated between the ranges 200-400 µS/cm and 400-600 µS/cm suggesting the influences of other factors.

At the midcatchment site, Jagerbos (purple in Figure 6.7), water in the river was more saline than in the water in the tributary that get discharge from the peninsula aquifer which is associated with low salinity (Smart and Tredoux, 2002). Groundwater at the floodplain borehole (JBHL) at this site remained constant (between 200-400 µS/cm), whilst groundwater EC at the upper borehole (JBHU) fluctuated between 50-400 µS/cm implying different recharge sources. At the second midcatchment site, Hudsonvale (red in Figure 6.7), EC in deep groundwater at HVPK BH maintained a constant range between 500-600 µS/cm and EC in the main channel also remained constant between 200-300 µS/cm. EC from the two tributaries at this site was also constant. Water from tributaries and boreholes from the northern Suuranys mountain range had higher EC than tributaries and boreholes from the Tsitsikamma mountain range. Differences in rainfall distribution between the two mountain ranges could be the contributing factor. The Tsitsikamma Mountains receives more rainfall resulting in increased dilution of water therefore low EC. Isotope results of these tributaries and deep groundwater did not show significant differences, most samples were depleted which revealed information about recharge only, therefore differences shown by EC data revealed some information about substrate influences and recharge magnitudes.

EC in shallow groundwater at the Hudsonvale site was constant at HPZ2 throughout but fluctuated significantly at HPZ1 although in close proximity to HPZ2 implying different sources contributing to the alluvial aquifer storage at this site.

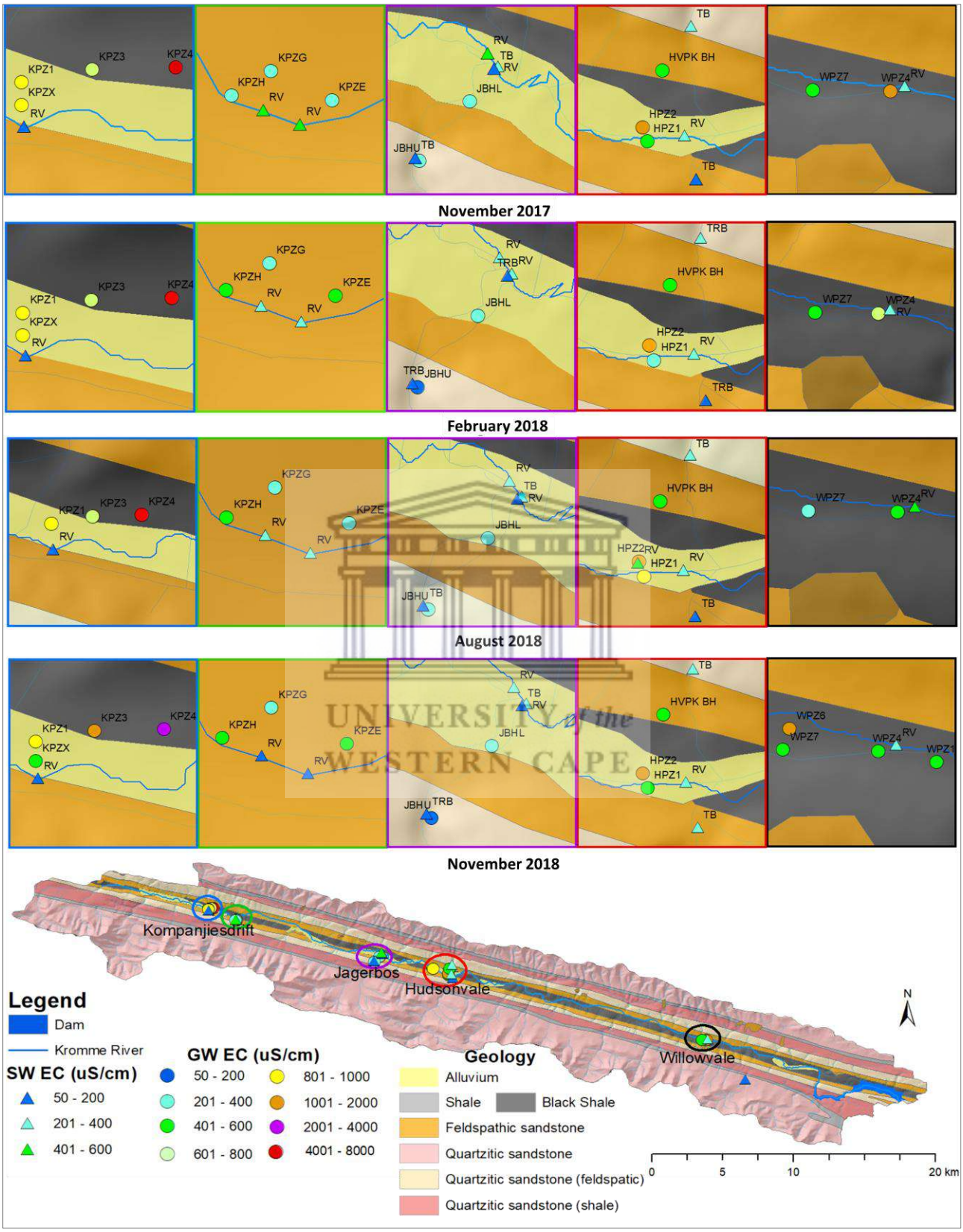

Figure 6. 7: Spatial variations of EC in surface water (SW) and groundwater (GW) during sampling campaigns (2017-2018) in the Kromme catchment. Map abbreviations RV–river, TB–tributary, PZ–piezometer and BH–borehole. All piezometers are in valley alluvial deposit.

At the lower catchment site, EC did not show consistent trends and fluctuated at both the river and shallow groundwater sites because this site receives contributions from a large contributing area and a mix of various sources with different levels of salinity.

6.5.2.2 Spatial and temporal variations of pH in water from various sources

Observed pH values for surface and groundwater are presented in Table 6.5. Minimum and maximum pH values for surface water were 4.5 and 7.4 respectively for main channel water samples. Water from tributaries ranged from 4.9 to 7. Mean values were 5.96 and 5.89 for river and tributary samples respectively. There was no consistent increasing or decreasing trend in pH along the river.

Table 6.5: Measured pH levels at different water sources in the Kromme catchment (2017-2019)

	pH					
Source	Sites (*n*)	Samples (*n*)	Mean	Std. Deviation	Min	Max
River	8	82	5.96	0.55	4.45	7.38
Tributary	3	36	5.89	0.54	4.88	7
Shallow groundwater	13	97	5.66	0.44	4.62	6.71
Deep groundwater	4	31	6.06	0.49	5.01	7.28
Seep	1	5	6.63	0.60	5.99	7.23

The pH of groundwater from deep groundwater ranged from 5 to 7.3 (Table 6.5). PH in the acidic range of 4.6 to 6.7 occurred in shallow groundwater which is associated with leachates from the fynbos vegetation dominating the hillslopes (Table 6.5). The mean pH of all water sources in the catchment was below 6.6 which is associated with the quartzitic sandstones of the TMG that dominate the catchment. The pH results show the influence of the dominating underlying lithology and above ground land cover.

6.5.3 Patterns of similarity and variation in water chemistry data from different sources in the Kromme catchment

To assess patterns of similarity in water quality data, the PCA and cluster analyses results for average values for each site/source are presented in Figure 6.8. PC1 and PC2 have eigenvalues above two thereby accounting for the largest combined percentage variance in the data set (60% total percentage variance). PC1 has a positive loading of 0.5 for $\delta^{2}H$ and $\delta^{18}O$ and accounted for 35% of the variance across samples with an eigenvalue of 2.8. PC2 has similar positive loadings of 0.5 for EC and Cl and accounted for 25% of the variance with an eigenvalue of 2 (Table 6.6).

The positive loadings for both EC and Cl indicate the influence of salinity within the data set. PC3 and 4 have positive loadings of 0.6 and 0.8 for ORP and temperature respectively. The high loadings and eigenvalues in PC1 and PC2 show the influence of Cl, EC, $\delta^{2}H$ and $\delta^{18}O$ in explaining the variation in water chemistry across the sites compared to the other properties measured in the catchment.

Table 6. 6: Results from PCA of water quality data from Kromme river monitoring sites

PC	Eigenvalues	%Variation	Cumulative % Variation		
1	2.77	34.6	34.6		
2	2.03	25.4	60		
3	1.21	15.1	75.1		
4	1	12.5	87.6		
5	0.66	8.3	95.9		
Variable	**PC1**	**PC2**	**PC3**	**PC4**	**PC5**
EC	-0.37	**0. 5**	0.17	-0.11	-0.28
pH	0.30	-0.13	-0.44	-0.29	-0.76
Temp	-0.03	0.17	-0.4	0.84	-0.2
2H	**0.50**	0.22	0.36	-0.01	-0.14
O18	**0.52**	0.29	0.25	0.02	-0.03
D-Ex	-0.36	-0.42	0.22	-0.12	-0.34
Cl	-0.35	**0.52**	0.15	-0.05	-0.27
ORP	0.02	-0.35	**0.6**	0.43	-0.32

The PCA and cluster analyses produced almost similar resulting clusters shown on dendogram and PC1 vs. PC2 axes (Figure 6.8a and Figure 6.8b). The results show three distinct clusters of water samples with similar parameter compositions (Figure 6.8). The first cluster consists of six sites; three upper catchment main river sites, two midcatchment tributary sites and a midcatchment mountain seep forming a tributary headwater. The upper catchment river sites are in close proximity therefore most likely influenced by the same hydrological processes. The seep (HVPK SP) discharges into the tributary (HVPK TB), hence the similarities in parameter compositions. Tributaries HVPK TB and JTBU are in the same cluster although they are located on opposite sides of the valley. This suggests similar pathways discharging into tributary flows in both mountain ranges, likely linked to the dominant Peninsula formation. However sampling along the tributaries appeared to impact the sampled properties, particularly their isotopic composition. Samples collected upstream in the narrow valleys of tributaries (JBTU and HVPK TB in cluster 1) were depleted whilst samples collected close to the tributary confluences with the main channel (JBTD and Witels in cluster 2) were enriched.

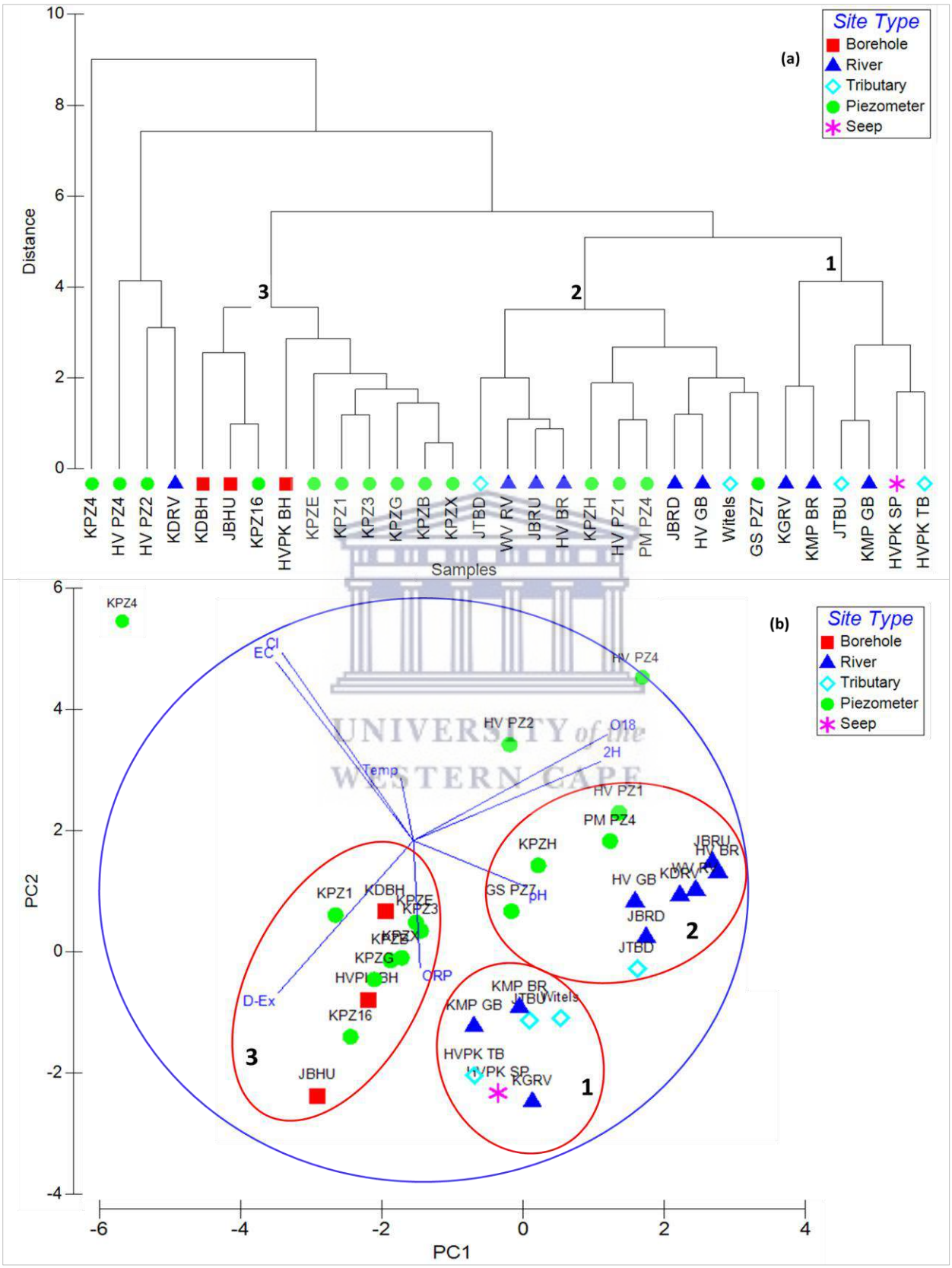

Figure 6.8: PCA and dendrogram results showing patterns of similarity in water quality data from various sources monitored in the Kromme catchment from 2017-2018.

JBTU and JBTD are samples from the same tributary but samples collected at different locations and fell into different clusters. Enrichment of the more downstream samples may be due to evaporation from the channel over the reach and/or addition of more enriched water into the tributary channels as they flow across/through alluvial fans at their terminus.

Cluster two consists of 11 sites; four groundwater sites, two tributary sites and five main channel samples. All the groundwater samples from the alluvial aquifer in this cluster are located in wetlands except for KPZH which is located just outside a wetland therefore probably getting similar subsurface water contributions from the wetland.

Cluster three consists of ten sites which are all subsurface samples; seven shallow groundwater samples and three deep groundwater samples. All the shallow groundwater samples are from upper catchment sites. All deep groundwater samples measured in the catchment fall into this cluster and most of these samples have relatively saline subsurface water (Figure 6.8).

6.5.4 Tracer based source components separation

Using combinations of $\delta^{2}H$, $\delta^{18}O$ and Cl values from different sources, Table 6.7 shows results from a three component tracer-based source component separation done. The selected end member components for this separation were direct runoff and baseflow from shallow and deep groundwater. Direct runoff in this separation is water contributing to streamflow immediately after rainfall events, in addition to rainfall, this water can also include overland flow and displaced old water from the saturated and unsaturated zone (Cartwright et al., 2014). Baseflow is water which sustains streamflow between rainfall events particularly during dry periods such as groundwater from the alluvial aquifer and groundwater from bedrock aquifer.

In some cases the streamflow samples did not fall within the range of values defined by the three end-member samples used for potential water sources, hence the blanks in the results (Table 6.7). This meant that the samples used did not fully represent all the sources contributing to streamflow at the time of sampling. In other cases, separations failed to work when end members for streamflow, and groundwater used were not sampled soon after the event of the rainfall sample used. When separations were valid for two or more tracer pairs and consistent across pairs, this reflected and confirmed the estimated contributions from the selected end members. From the three tracer combinations used $\delta^{2}H$ and Cl, and $\delta^{18}O$ and Cl worked best compared to $\delta^{2}H$ and $\delta^{18}O$.

All locations (headwaters, midcatchment and downstream) show variability in estimated proportions from different sources for the sampling results presented (Table 6.7). The tracer based separation showed that at the sampled times 2017, streamflow in the catchment was dominated by groundwater shown by combined shallow and deep contributions of up to 98% (Table 6.7). 2017 was a relatively dry year therefore baseflow sustained river flows. The year 2018 was relatively wet compared to 2017 and an increase in estimated direct runoff proportions was observed in 2018 (May and August).

In general, streamflow at the upper catchment sites was dominated by groundwater (combination of both shallow and deep groundwater) except for August 2018 (Table 6.7). At the mid and lower catchment sites, proportional contributions from the different sources varied but groundwater dominated the river samples in 2017 (Table 6.7).

Table 6.7: Three component tracer based separation for sites along the Kromme River.

Date	Status of the catchment	Site	Tracer Combinations	Direct runoff	Baseflow		MAE (%)
					Alluvial aquifer	Bedrock aquifer	
November 2017	Sampling was done during a recession period 7 days after a peak of 0.31 m^3/s.	Upper catchment (KMP)	$\delta^{18}O$ -Cl $\delta^{2}H$ -Cl	2%	3%	95%	1%
		Upper catchment (KMP)	$\delta^{18}O$ -Cl $\delta^{2}H$ -Cl	2%	2%	96%	1%
		Midcatchment (HV)	$\delta^{2}H$ -Cl	17%	5%	79%	2%
		Lower Catchment (WV)	$\delta^{18}O$ -Cl $\delta^{2}H$ -Cl	5%	28%	67%	3%
December 2017	Sampling was done late during a recession after a peak of 5.5m^3/s after a large event of 48 mm/day which came after a long dry period. Series of small events (<5mm) leading to 5 days before the sampling date	Upper catchment (KMP)	-	-	-	-	-
		Midcatchment (HV)	$\delta^{2}H$ -Cl	3%	96%	1%	4%
			$\delta^{2}H$ -Cl	3%	97%	1%	4%
		Lower Catchment (WV)	$\delta^{18}O$ -Cl	1%	88%	10%	2%
May 2018	The catchment received a few rainfall events (<12mm/day) in the previous weeks leading to this sampling.	Upper catchment (KMP)	$\delta^{18}O$ -Cl $\delta^{2}H$ -Cl	22%	44%	33%	3%
		Midcatchment (HV)	$\delta^{2}H$ -Cl	61%	34%	5%	4%
			$\delta^{2}H$ -Cl	62%	34%	3%	4%
		Lower Catchment (WV)	-	-	-	-	-
August 2018	The catchment received several rainfall events in the previous weeks leading to this sampling ranging from 7-13 mm/day. Samples were collected mid-recession of a 0.16 m^3/s peak	Upper catchment (KMP)	$\delta^{18}O$ -Cl	78%	19%	3%	0%
		Midcatchment (HV)	$\delta^{2}H$ -Cl	72%	26%	2%	3%
			$\delta^{2}H$ -Cl	70%	27%	3%	4%
		Lower Catchment (WV)	-	-	-	-	-
November 2018	Relatively wet period in the catchment prior to this sampling campaign. Samples collected 3 days after a peak of 0.31 m^3/s.	Upper catchment (KMP)	$\delta^{2}H$ -Cl	8%	46%	46%	1%
		Midcatchment (HV)	$\delta^{2}H$ -Cl	39%	19%	42%	2%
		Lower Catchment (WV)	$\delta^{2}H$ - $\delta^{18}O$	4%	75%	21%	1%

Blank entries means chemical compositions were outside the ranges of the potential source end member samples for those tracers.

There was no distinct trend shown in individual source contributions at each site across the samples, however, in most cases, higher proportional contributions were shown from a combination of groundwater from both the alluvial and bedrock aquifers. Results of the three component source separation therefore highlighted the importance of groundwater in sustaining river flows in this catchment particularly during low flow periods. These snapshot sample results cannot be generalised to estimate annual contribution values for these source components, but they give an idea of the variability of the flow components spatially and temporally.

6.6 DISCUSSION

Results from stable isotopes combined with geochemical tracers gave invaluable insights on flowpaths and the identification of relationships between rainfall, streamflow and groundwater in the Kromme catchment. Overall, most water samples from the different sources plotted on or slightly below the LMWL but above the GMWL indicating meteoric origin and minor evaporative enrichment in most samples as explained by Farid et al. (2013). Isotopic compositions of rainwater were generally depleted after storms. This is because rainfall isotopic signatures are influenced by temperature, season as well as continental effects (Dansgaard, 1964; Kendall and Coplen, 2001; Otte et al., 2017). River water samples generally became increasingly enriched along the river length moving downstream. Similar patterns have been observed in other catchments explained by cumulative evaporative effects (i.e. Saraiva Okello et al., 2018; J. Zhou et al., 2015). This was expected under semi-arid climatic conditions for surface water to be dominated by evaporation as reported by Kebede et al. (2009). Overall, although river water samples got enriched moving downstream of the river, some locations at river confluences with tributaries were depleted indicating influences of depleted contributions to the channel from mountain tributaries and springs. Similar results have been reported in other TMG catchments where springs from the highly fractured sandstones contributed significantly to river flows (Mokua et al., 2020). Boreholes, springs and tributary samples at high elevation locations were depleted whilst low elevation samples in the main channel were slightly enriched showing depletion with an increase in elevation as reported by Midgley and Scott (1994).

Similarities of $\delta^{18}O$ and $\delta^{2}H$ isotopic signatures observed in some surface and groundwater samples indicated mixing and interactions between the sources (Wu et al., 2018; Yeh et al., 2014; Zhang et al., 2018). The close link in isotopic composition between some groundwater and surface water samples confirmed that groundwater sustains river flows as shown by hydrometric data. Furthermore, tracer based source component separation also showed that groundwater sustained river flows particularly during low flow periods.

EC and Cl were used as additional tracers to characterize and improve the hydrological understanding of processes (Wenninger et al., 2008). Similar to the trend observed in river isotopic compositions, EC values generally increased along the length of the river with high values recorded downstream of the catchment due to evaporation. Low EC values (<350 μS/cm) were observed in surface water which is expected in most of the TMG quartzitic sandstones dominated catchments due to their low content of dissolved minerals (Hugenschmidt et al., 2014). The EC in deep groundwater was also generally low (EC <1000 uS/cm), associated with the fractured sandstone formations characteristic of the TMG regions which are not largely associated with high salinity. Mean EC values associated with Peninsula formation in this area are 100 μS/cm with maximum values of 260 μS/cm, whilst water from Nardouw formations have mean EC values of 300 μS/cm and a maximum of 1550 μS/cm (Smith et al., 2002). Low EC values in groundwater were also an indication of freshwater implying pronounced aquifer recharge by direct rainfall which was consistent with the isotope tracer results that showed meteoric origin in most of the groundwater samples. High recharge in these weathered and fractured sandstones results in dilution (Wu, 2009). Groundwater from the alluvial aquifer was more mineralized (high EC) than groundwater from the bedrock aquifer as expected because groundwater from TMG bedrock is usually less mineralized which is consistent with other TMG studies. However in comparison to other systems, groundwater from bedrock aquifers is usually more mineralized (Hamutoko et al., 2017). There were no significant differences between Cl compositions in surface water and groundwater from the bedrock aquifer. However, similar to EC observations, high Cl was observed in groundwater from the alluvial aquifer which may have been due to contact with rock minerals associated with high Cl or EC such as the Bokkeveld shales dominant in the catchment. Cl concentration in soil water also increases in the vadose zone when trapped by soils and plant roots after evapotranspiration processes (Guo et al., 2017).

TMG catchments have various arrangements of aquifer layers and different ways the river valleys have formed that will lead to different groundwater-surface water interactions. The Kromme has different arrangements compared to other TMG catchments such as the Jonkershoek (Midgley and Scott, 1994), Hex catchment (Roswarne, 2002) and many others (Xu et al., 2009), therefore interactions between groundwater and surface water may differ. The Kromme has a TMG syncline with shale (aquiclude) along the valley access. The Peninsula formation contributes bedrock groundwater to the main channel through the tributaries and springs (Figure 6.12). Similar to other studies in semi-arid catchments (Camacho Suarez et al., 2015; Hrachowitz et al., 2011; Munyaneza et al., 2012; Wenninger et al., 2008), the importance of groundwater was highlighted through different methods in this study. However, the study was carried out during

drought conditions which was useful for looking at low flow conditions and flowpaths that support baseflow. Additional work is still needed in the future i.e. storm responses and wet periods in general.

6.7 Updated Conceptual Model of the Kromme Catchment

The hydrometric data revealed the occurrence and dominance of particular flowpaths and processes in the Kromme catchment however, some of the conceptualised processes needed to be quantified. For example, subsurface flow from the floodplain alluvial aquifer and mountain bedrock aquifer into the river maintains the baseflow however the relevant quantities and how they differ between dry and wet periods remained unknown. Isotope and physico chemistry data were used to confirm and quantify some of these processes.

Most tributaries in this catchment have continuous surface flow throughout their length and contribute surface flow to the main channel (Figure 6.9). Mountain bedrock aquifer flow into tributaries was observed through seeps which are formed at the interface between the fractured rock and aquicludes (shale layers). Similarities in isotope samples of the seep and tributary water confirmed the constant groundwater contribution to tributary surface flow even during dry periods.

Tracer based source component separation showed that groundwater from both the alluvial and bedrock aquifers sustained streamflow with combined contributions of up to 98% during the dry period. Large rainfall events were needed for percolation and recharge during dry periods because the vadose zone was dry and more water was used by the plants resulting in little infiltration. However, groundwater from the bedrock aquifer still discharged into tributaries as seeps were observed in some parts sustaining surface flows. Some of the flow came along the drainage line in the tributary alluvium and entered the floodplain alluvial aquifer as subsurface flow via the alluvial fans (Figure 6.9a). Most tributaries had surface flow even through very dry periods showing the importance of groundwater from the bedrock aquifer in sustaining baseflow. Shallow groundwater within the floodplain aquifer went down over time during the dry period however, the river was still gaining from the groundwater from the alluvial aquifer (Figure 6.9a). Groundwater within the floodplain aquifer was recharged by precipitation and received some subsurface flows from the bedrock aquifer through tributaries and alluvial fans (Figure 6.9a). In general, groundwater from the alluvial and bedrock aquifers contributed significantly to river flow (> 90% in some cases).

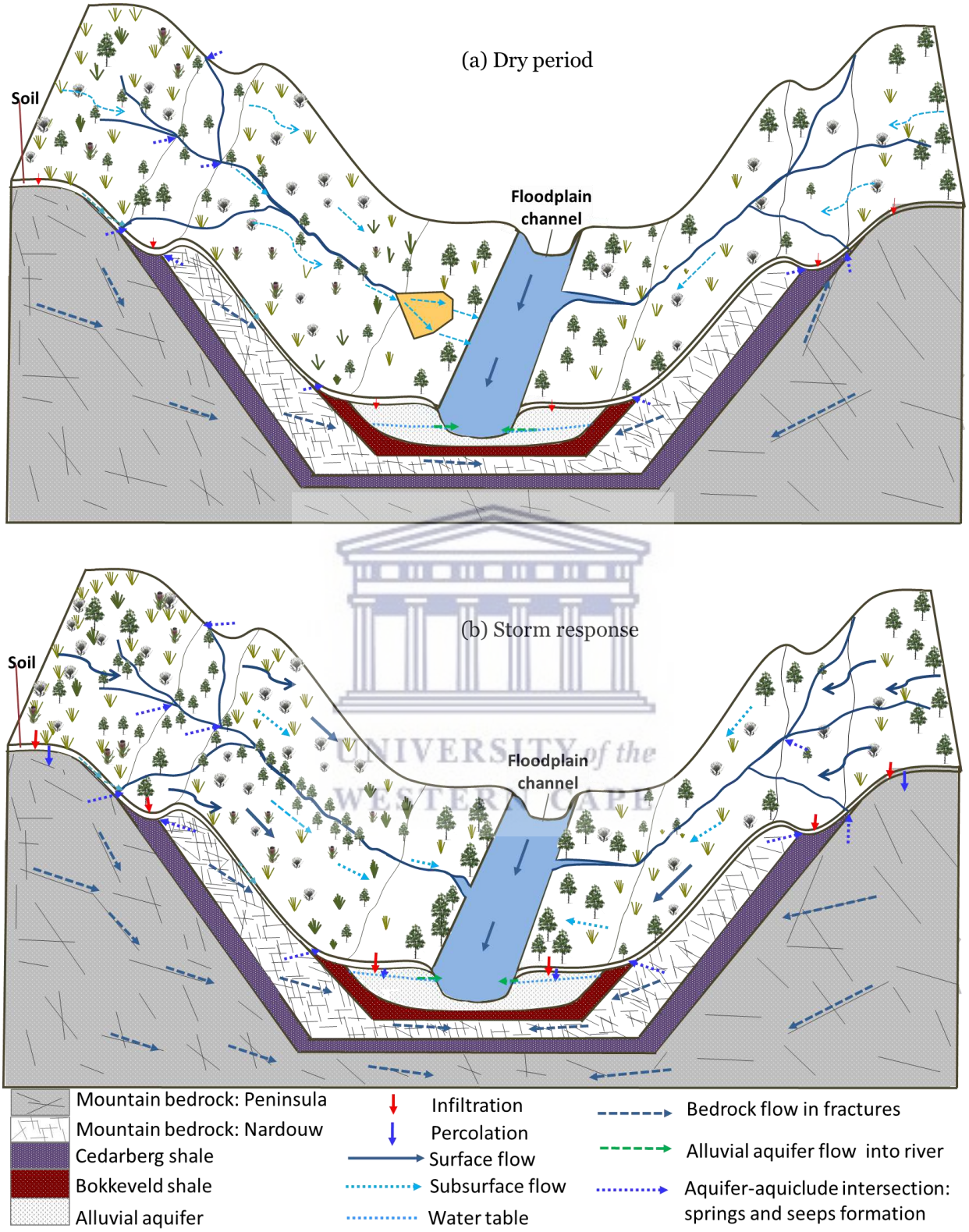

Figure 6.9: Conceptual model of flowpaths in the Kromme Catchment during (a) dry and (b) wet periods from 2017-2019 observations.

During wet periods infiltration and percolation reaches the shallow fractured rock layer and pushes older water in this layer to the channel or to the alluvial aquifer thereby raising the gradient of the floodplain water table resulting in increased alluvial aquifer flow to channel Figure 6.9b). Infiltration in the alluvium also causes causing push-through of old soil water into river channel after storm events. The main channel was gaining from the alluvial aquifer throughout the study period during both wet and dry periods (Figure 6.9).

6.8 CONCLUSION

Hydrochemical and stable water isotope approaches, coupled with statistical and hydrometric time-series data analysis were applied to assess and characterize flowpaths and sources governing streamflow generation in the Kromme catchment. The spatiotemporal variability of environmental and geochemical tracers gave valuable information about flowpaths, stream water sources and how proportions of different sources varied at both spatial and temporal scales. The combination of different methods led to the improvement of the conceptual model of flowpaths in the catchment. Coupled EC values, Cl and isotopic compositions were effective as indicators for flowpaths, sources and proportional contributions to river flows however their application alone or on individual basis in large scale, highly fractured catchments can be challenging due to low temporal variation. Tracer data reflected constant groundwater contribution to surface flow from bedrock spring discharge and from the alluvial aquifer. An important finding from this study was the high baseflow contribution to total flows during both dry and wet conditions thereby showing groundwater discharge as an essential source sustaining surface flows in semi-arid regions. Direct infiltration and percolation of rainfall in the mountains was shown to be the primary groundwater recharge source through the analysis of isotopic compositions.

The isotope and physico-chemical data proved invaluable in quantifying proportions of water from different sources into the channel and to show how these contributions vary at a temporal scale. Results of this study contribute to a process based understanding and conceptualization of flowpaths and source water contributions at meso-scale in semi-arid mountainous catchments.

CHAPTER 7: MODELLING IMPACTS OF SELECTED LAND COVER TYPES ON THE HYDROLOGICAL RESPONSES OF A SEMI-ARID MESO-SCALE, MOUNTAINOUS CATCHMENT

Abstract

Hydrological modelling has become an important tool to understand the complex interactions between climate, land cover types and hydrological processes particularly in mountainous catchments. However, in order to achieve this, there is need to balance the purpose of the modelling exercise, available data and knowledge of the catchment's hydrological processes. This chapter employed hydrological modelling to assess vegetation impacts on hydrological processes in the semi-arid Kromme catchment, South Africa. The aim was to assess potential hydrological impacts of current and other selected land cover change scenarios in a meso-scale semi-arid, mountainous catchment. A conceptual understanding of key hydrological processes in the catchment gathered from field hydrometric, isotope and hydrochemical data was used to inform the structure of a quantitative numerical MIKE SHE model. Selected scenarios of land cover change were simulated and results were assessed for water supply (streamflow and groundwater) impacts. The model was run with 15 years of climate data (2003-2018). Model outputs suggested that alien clearing resulted in significant impacts on streamflow as well as floodplain groundwater levels. Predicted results also indicated that regeneration of palmiet wetlands in the floodplain reduced flood peaks by 9 %, and groundwater levels increased by 13%. Baseflow increased by 9% and the total outflow increased by 4%. The water table was predicted to rise with alien clearing and palmiet regeneration. Predicted results also indicated that wattle trees use more water in riparian areas where it is readily available than upland areas. The proportional changes in actual ET and runoff per unit area increase in alien invasion were high in the floodplain than the upland areas. The modelling exercise highlighted potential impacts of selected vegetation types on the hydrological response of a semi-arid meso scale mountainous catchment. Results can be used to guide restoration planning in the region.

7.1 INTRODUCTION

Land cover types particularly vegetation, influences the water balance of a catchment through different processes such as transpiration, interception, infiltration and percolation (Yang et al., 2021). Most deep-rooted woody vegetation has high water use rates compared to shrubs and herbaceous plants. Therefore, invasion of grasslands and shrub land ecosystems by woody plants, particularly alien trees result in reduced dry season flows. The extent to which vegetation types influences a catchment's hydrological response depends on the density and area covered and the location of the vegetation type within the catchment (Le Maitre et al., 2015). Vegetation of the same species can have greater water use in riparian areas where water is readily available than upland areas (Le Maitre et al., 2015). The extent however, of these effects particularly in semi-arid mountainous regions is yet to be fully understood and quantified. To gain insights into the hydrological functioning of mountainous catchments and their responses to land use and land cover types and vulnerability to changes thereof, hydrological modelling has proved to be an important tool (Rangecroft et al., 2018). Studies of land cover changes have used models to assess the likely hydrological responses by simulating scenarios of land cover change (Leta et al., 2021; Rebelo et al., 2015; Sanyal et al., 2014). These models require structures that are sensitive to land cover changes and which can conceptualize and adequately represent hydrological processes (Devia et al., 2015; Glenday, 2015). This chapter employed hydrological modelling to assess potential hydrological (streamflow and groundwater) impacts of selected land cover change scenarios in the Kromme catchment, South Africa.

The Kromme catchment was selected as a case study site of semi-arid meso scale (360 km^2) mountainous catchments that is regionally important for water supply but also subjected to woody alien plant invasions. The Kromme River discharges into the Churchill and Impofu dams which are major water supply reservoirs in the region. A previous modelling study of land cover change in the catchment showed that clearing of wattle and restoration of palmiet wetlands to their previous condition in the 1950s would result in an increase in river flows by approximately 1.13 Mm^3 per year (Rebelo et al., 2015). Studies in other catchments have shown considerably higher water use by *Acacia* species invasions than indigenous fynbos and grass they often replace (Dye and Jarmain, 2004; Le Maitre et al., 2015). Field measurements and estimates of transpiration rates for black wattle ranges from 740-1500 mm/year (Clulow et al., 2011; Dye and Jarmain, 2004; Meijninger and Jarmain, 2014), compared to 600-900 mm/year for grassland (Calder and Dye, 2001; Dye and Jarmain, 2004), 600-950 mm/year for fynbos (Calder and Dye, 2001), and approximately 695 mm/year for palmiet (Rebelo, 2012). Clearing of areas invaded by black wattle and the subsequent regeneration of herbaceous plants is, therefore assumed to positively impact water supply in the catchment.

In order to evaluate water supply impacts of possible scenarios of land cover change, it is important to balance the purpose of the modelling exercise (investigative), knowledge of the catchment's hydrological processes (Hrachowitz et al., 2013; Uhlenbrook et al., 2004) and available data (Wagener et al., 2001). Hydrological modelling in mountainous catchments is challenging particularly at large spatial scales due to the inherent complexity of the intertwined processes controlling water transfer from steep headwaters and hillslopes to streams. Furthermore modelling is challenging in these catchments due to the lack of both hydrological and meteorological data to validate and force models (Camacho Suarez et al., 2015). Emerging approaches rely on existing data to understand internal processes and provide better ways to improve hydrological modelling through the use of data informed model structures. Available data can to be analysed systematically for patterns that indicate the dominance, occurrence and thresholds for the occurrence of particular flowpaths, responses and other processes (Clark et al., 2008; McMillan et al., 2011). Recommendations for the model structure decisions will then be based on the knowledge gathered from the data, i.e. annual runoff ratios can be used to infer evapotranspiration (ET) influences on the dominant model reservoirs. Ratios can also be used to balance model parameters controlling quick and slow flow production. Variability in baseflow proportions indicates outflows from different storages leading to the use of multiple reservoirs in the model to represent the different aquifer storages.

In the current conceptual model of the Kromme catchment, surface and subsurface flows from perennial tributaries play a significant role in recharging the floodplain alluvial aquifer as well as contributing to main river flows even during dry periods, as described in Chapters 4 and 6. Invasion of uplands by black wattles could reduce surface and subsurface flows from tributaries as well as reducing recharge of both the bedrock and floodplain alluvial aquifers due to increased canopy interception and transpiration.

Additionally, while lower long-term yields would be expected, it is possible that wattle invasion could increase the magnitudes of stormflow peaks. The steep and rocky areas that make up much of the catchment result in large contributions of quick flow for short periods after storms. Invasion by black wattles has been observed to result in more incised and wider channels (Pietersen, 2009), which would conduct flows more quickly creating larger peaks. However drier antecedent conditions due to increased transpiration could reduce event runoff generation, particularly from smaller events and those in drier periods. The regeneration of floodplain palmiet wetlands, on the other hand, could lead to reduced peaks due to their high surface roughness and little to no channelization, accompanied by increased delayed flows and outflows overall. At the same time, during particularly wet periods, the wetter antecedent conditions expected in palmiet wetlands compared to other cover types could reduce their capacity to attenuate floods.

The Kromme floodplain alluvial aquifer was observed to make notable contributions to river flows, particularly during dry periods.Invasion of floodplain and riparian areas by black wattles could lower the floodplain water table and therefore reduce its contributions to streamflow and reduce overall catchment yield. In contrast, regeneration of palmiet wetlands in the floodplain could increase recharge of the alluvial aquifer, and thereby increase baseflows and potentially long-term catchment outflow. Streamflow and baseflow in particular, is therefore likely to be vulnerable to landcover changes that might impact groundwater within the floodplain aquifer.

Considering these observations and hypotheses about impacts on flood peaks, baseflow, and overall yield, a model that can handle the combined mountain and floodplain landscapes which are important for assessing vegetation impacts at different locations was required. The Kromme catchment has unique topographical and geomorphological characteristics. The central valley, created by a syncline, runs between parallel mountain ranges (trellis drainage pattern) with steep, deeply incised, tributary valleys that are perpendicularly oriented to the main valley. To capture processes and these catchment characteristics, the MIKE-SHE platform was used to simulate hydrological responses to changes in land cover types in the catchment. Floodplain and valley bottom processes were modeled using a hydraulic model for the floodplain and channel processes coupled with a distributed hydrological model of the different land units connected to the central valley. This was done following previous studies that have coupled hydraulic and hydrologic models for a better representation of observed processes at large spatial scales (Glenday, 2015; Hipsey et al., 2011; Neachell, 2014). This was also done to capture the connection between the channel and the alluvial aquifer. The spatially and vertically distributed model allowed targeted analyses of the influence of alternative vegetation cover scenarios on particular flowpaths and processes at different locations in the catchment.

To assess the impacts of selected scenarios of land cover change on hydrological processes, the following questions were addressed: 1) what is the average change in flow in this particular setting under selected land cover change scenarios? 2) To what extent is the location of specific land cover within a catchment (riparian vs. upland) important to the streamflow response of that catchment? 3) How are baseflows and peak flows likely impacted by land cover change (wattle invasion or palmiet regeneration)? The modelling results were assessed in terms of surface water and groundwater impacts for each modelled land cover scenario.

7.2 MATERIALS AND METHODS

7.2.1 Study area

Figure 7.1 shows the topography, geology, land units and land cover maps used for the modelling however, detailed descriptions of the study site, monitoring locations, geology, land use, and other physiographic characteristics of the catchment are presented in Chapter 3.

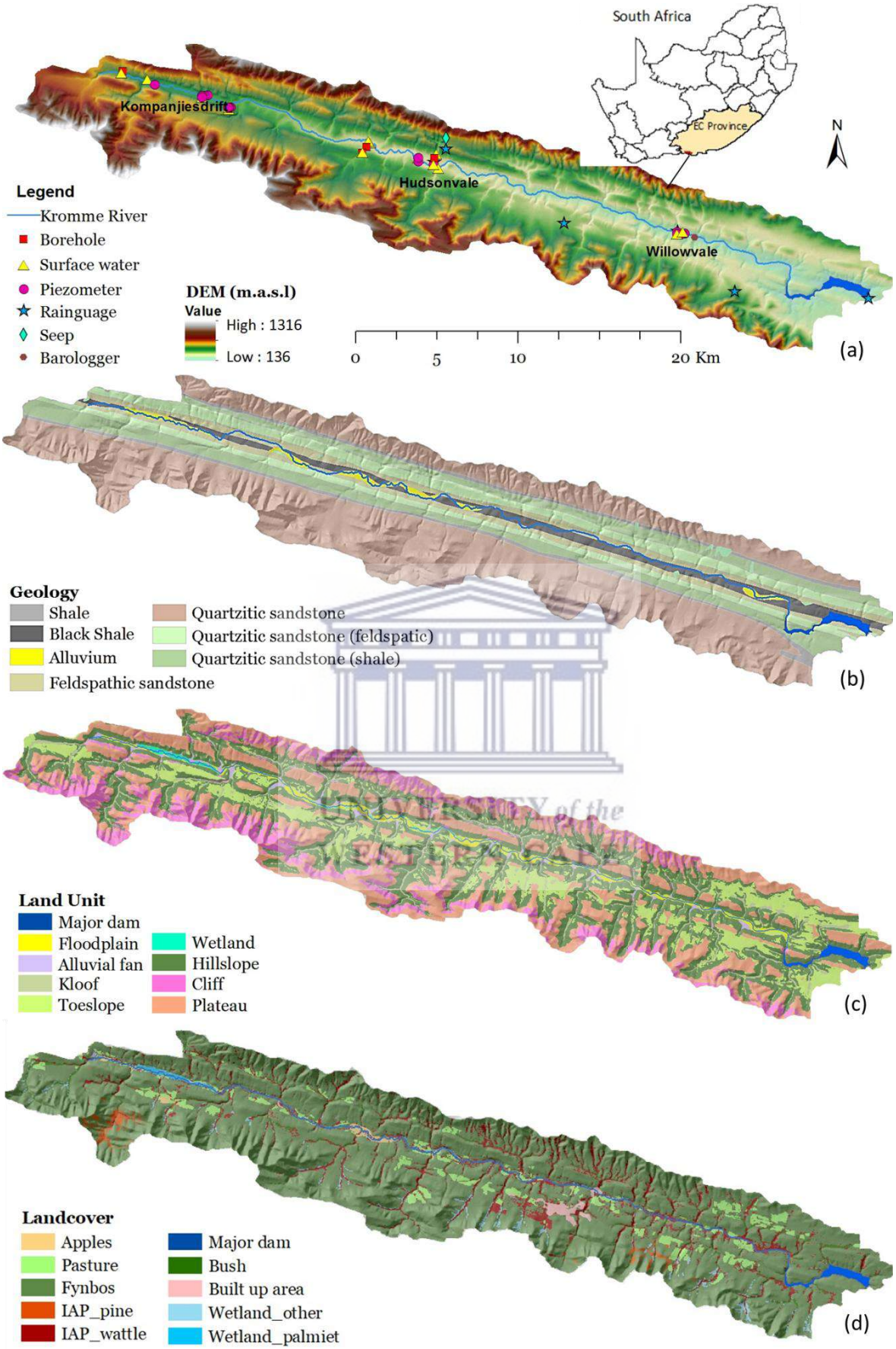

Figure 7. 1: (a) Location of the Kromme catchment in South Africa, DEM and monitoring locations (b) geological map of the catchment (c) delineated land units and (d) the dominant landcover types

7.2.2 Land unit discretization

The catchment was discretized into topographic units to allow process representation differentiated by topography and geology. Processes such as runoff responses at meso scale are influenced by the underlying geology and the complex topographic properties in mountainous catchments give rise to various response characteristics at different scales. The spatial discretization at the level of topographic landscape units was also necessary for selection of parameter ranges of the selected land cover scenarios. The Height Above the Nearest Drainage (HAND) developed by Nobre et al. (2011) was used to delineate the topographic land units. HAND relates the elevation of each point to its nearest stream and assigns values to each grid cell (Gharari et al., 2011; Savenije, 2010). Using the SU-DEM (van Niekerk, 2016) and ArcHydro tools, land units were classified using geology, slope, and HAND in ArcMap 10.2. HAND values were then combined with the slope values and set thresholds to define the topographic land units used in the modelling exercise. The landscape was broken into eight units (plateaus, cliffs, canyons, hillslopes, toeslopes, alluvial fans, floodplain and water bodies), assumed to have different characteristic hydrological responses based on field observations, land use and topography (Figure 7.1c). Table 7.1 shows the distribution and area of mapped topographic units.

Table 7.1: Distribution of mapped land units in the Kromme catchment

Topographic land unit	Area (km²)	% of catchment
Plateau	112.03	31
Cliff	45.48	13
Canyon floor	14.41	04
Hillslope	125.12	35
Toe slope	46.29	13
Alluvial fan	3.29	01
Floodplain	10.79	03
Dam	2.01	01

7.2.3 Data used

Hydrological data collected in the Kromme catchment are summarised in Table 7.2. Rainfall data were obtained from rainfall gauges provided by the South African Earth Observation Network (SAEON) and weather stations owned by the Agricultural Research Council (ARC), the South African Weather Services (SAWS), and the Department of Water and Sanitation (DWS) at Kareedouw and Cape St Francis (by Churchill dam).

Table 7.2: Hydrometric field data collection in Kromme catchments

Data	Instrument	Quantity	Data type	Frequency
Rainfall	Raingauge	4	Time series	Hourly
Groundwater	Piezometer (PT)	2	Time series	Hourly
Groundwater	Piezometer (MM)	18	Manual	2-3 months
Groundwater	Borehole (PT)	2	Time series	Hourly
RV	River (PT)	4	Time series	Hourly
SWC	Soil Probe	3	Time series	Hourly
Water Quality	YSI multi-probe	All sites	Manual	2-3 months

RV- River water stage, SWC-Soil water content, PT- Pressure transducer, MM- Manual

Piezometers and boreholes were used to monitor groundwater levels from the alluvial and bedrock aquifers respectively. Soil water content variation was monitored using soil probes at selected floodplain sites with different vegetation types. Stream water levels were monitored using pressure transducers. Water level data were then used to estimate streamflow based on rating curves. Land use and land cover data was obtained from mapped vegetation cover of the area (Euston-Brown, 2006). The topographic data were derived from the SU-DEM (van Niekerk, 2016) with a 5 m resolution aggregated to 10 m for floodplain processing and 100 m for model use. Daily data was used to force the model. Spatial rainfall and PET data for the catchment were estimated using rain gauge and temperature data from stations within the Kromme Catchment (SAEON, SAWS and ARC). PET was estimated using the Hargreaves and Samani method (1985). The data were scaled using rainfall and temperature surfaces estimated by Lynch (2004) and Schulze (2004) respectively at 2km resolutions. More details are given in Chapter 4 section 4.3.3. Calendar years (1 January to 31 December) were used in the model and model results analysis.

7.2.4 Model Set up

The MIKE SHE model was set up with a 100 m grid cell size. The model explicitly calculated canopy interception, infiltration, percolation, and ET by grid cell. Surface and subsurface flows in MIKE SHE are routed between grid cells based on the topography, hydraulic conductivity and head gradients. Spatially distributed climate time series inputs were used. The following MIKE SHE process representation options were used:

- Overland flow – was calculated across grid cells, using finite difference with distributed Manning M, and detention storage values. Initial water depth over the whole catchment was set at zero.
- Unsaturated flow – a two layer unsaturated zone was used, water content, soil profile porosity, field capacity, hydraulic conductivity parameters were assigned to grid cells using the distributed input soil map. The two layer water balance method was used, which comprises canopy interception, ponding and ET, adopted from Yan and Smith (1994). The unsaturated zone was represented by two layers in which actual ET was calculated as well as water that percolates to recharge the saturated zone. The root zone was in layer one where evapotranspiration could occur. The thickness of layer one included the root depth added to the thickness of the capillary fringe (ET surface depth in MIKE SHE). Layer two was below the active root zone in which evapotranspiration does not occur.
- ET method (Kristensen and Jensen, 1975) – evapotranspiration processes in MIKE SHE, are modelled in different steps (a) evaporation of water intercepted by vegetation canopy, (b) evaporation from ponded water and from the soil surface, (c) evaporation from the upper root zone as well as transpiration by plant roots (d) transpiration by plant roots that reach

the water table or water drawn from the saturated to the unsaturated zone by capillary forces. In the subsurface, ET calculation varies depending on the level of the water table. ET is calculated at maximum rate from the saturated zone when the water table is at/or above the bottom of the active root zone. If the water table drops below layer one, ET from the saturated zone seizes but continues to remove available water from the capillary fringe. When the water table is close to the surface, ET is also calculated at maximum rate, drawing water from the water table by capillary action. If the water table is deep, transpiration by plant roots occurs directly from the saturated zone because the plant roots can reach the capillary zone.

- Saturated flow – was calculated using the finite difference approach between grid cells and layers. The layers were configured as shown in Figure 7.2. The major bedrock aquifer layers in this catchment are Peninsula and Nardouw whilst the Cedarberg and Bokkeveld shales were assumed to be aquicludes based on literature (Colvin et al., 2007; Xu et al., 2009). The Tallus layer was added on top of the peninsula to act as an interflow layer with relatively high hydraulic conductivity compared to the Peninsula layer (Figure 7.2). In the model, the Nardouw aquifer, Cedarberg and Bokkeveld shales were set up as lenses which are regarded as discontinuous layers within geologic units in MIKE SHE. Groundwater flow from the alluvial aquifer was modelled using the finite difference 100 m grid cells with a dynamic connection between the aquifer and floodplain channel.

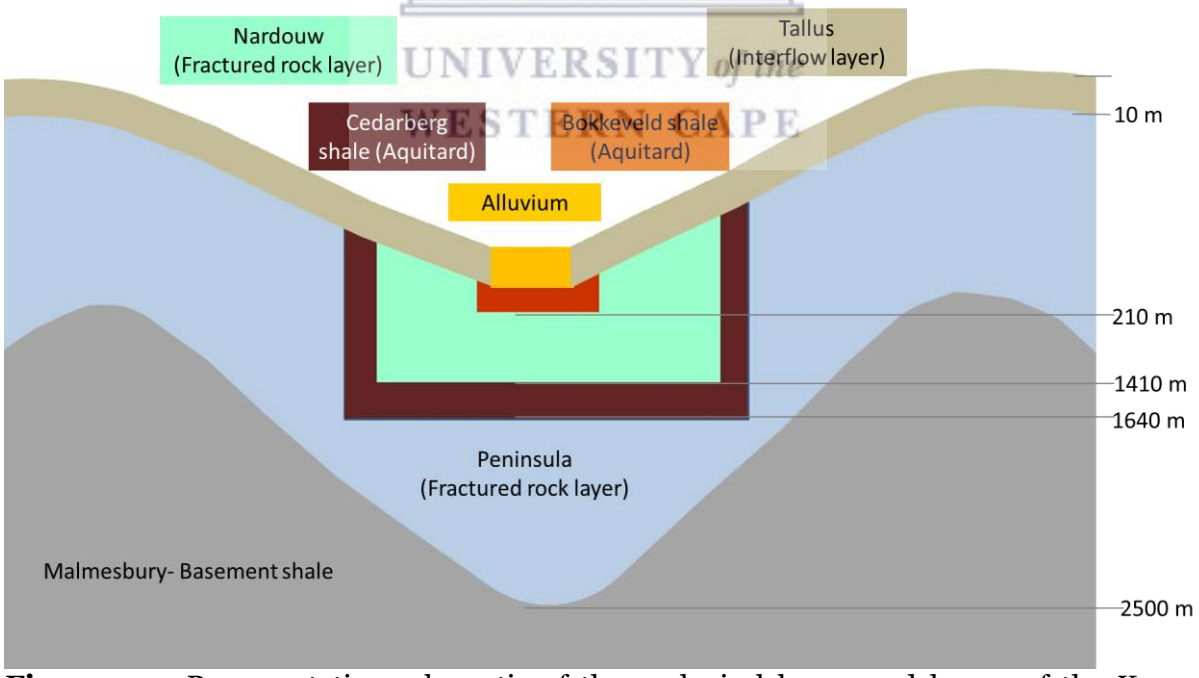

Figure 7.2: Representation schematic of the geological layers and lenses of the Kromme catchment in the MIKE SHE model.

MIKE SHE automatic calibration was carried out to try to optimize parameter sets using a range of parameter values selected for each component. Parameter ranges selected for Peninsula and

Nardouw aquifers as well as the Cedarberg and Bokkeveld aquitards were based on literature values. Initial potential heads for Tallus and Peninsula were -6 m and -20 m respectively. Vegetation parameter sets were also derived from published literature values. Model calibration was done against estimated dam inflow at catchment outlet from 2003 to 2018. The different variables and parameter sets and values used from sampling and literature (Cornelius et al., 2019; Dzikiti et al., 2014; Garcia et al., 2016; Le Maitre et al., 2015; Rebelo et al., 2015; Smith and Tanner, 2019) are presented in Tables 7.3 to 7.5.

Table 7.3: Parameters values for the upper Kromme catchment dominant vegetation types

Cover type	Max canopy interception (mm/day)	Max root depth (mm)	ET coefficient (ETk)	LAI
Palmiet wetland	1	3000	0.6	1.8
Riparian woodland	2.5	3000	0.8	3
Fynbos	1	1500	0.5	1.5
Fynbos cliff (sparse)	0.25	2500	0.15	0.35
Wattle (dense stand)	2.5	5000	1.1	5
Pine (dense stand)	2.5	5000	1	5
Fruit orchard	0.5	2000	0.8	2
Irrigated pasture	0.5	500	0.7	1

Table 7.4: Soil parameters used in the base model per land unit

Landscape unit	K (m/s)	Saturation	Field capacity	Wilting point
Floodplain	4.4E-05	0.40	0.20	0.05
Palmiet wetland	1E-04	0.60	0.30	0.10
Alluvial fan	5.4E-05	0.43	0.18	0.05
Narrow valley	9.4E-07	0.40	0.15	0.05
Toe-slope	9.4E-07	0.44	0.18	0.05
Hillslope	4.2E-08	0.42	0.20	0.08
Cliff	5E-08	0.05	0.02	0.005
Plateau	2.9E-06	0.40	0.18	0.05

Table 7.5: Hydrogeological parameters for the Kromme geological layers and lenses

Layer/lense aquifer unit	Lower level (m)	Thickness (m)	Horizontal K (m/s)	Vertical K (m/s)	Specific yield	Storage Coefficient
Alluvium	-10	10	9.7E-04	3.5E-06	0.2	1E-04
Tallus	-10	10	2.9E-08	2.3E-05	0.2	1E-04
Bokkeveld	-210	200	0	0	0.2	1E-04
Nardouw	-1410	1400	5.4E-12	2.5E-12	2.6E-04	2.95E-05
Cederberg	-1640	230	0	0	0.2	1E-04
Peninsula	-2500	1100	5.4E-12	2.5E-12	3.9E-04	3.9E-04

7.2.5 Model performance evaluation

The Nash-Sutcliffe coefficient (NSE), the regression coefficient (R^2), mean absolute error (MAE), and root mean square error (RSME) were used to evaluate model performance at a daily time step. R^2 values range between 0 and 1 (optimal), NSE values range from -∞ to 1 (optimal). For better analyses of low flows, the NSE of log transformed daily flow values was used, referred to hereafter as 'Log NSE'. To capture small differences in the performance evaluation, additional analyses were also performed on streamflow results specifically focusing on particular events (De Boer-Euser et al., 2017; Glenday, 2015). Shapes of daily hydrographs of selected events were analysed to assess the model's simulation of observed peak discharges as well as flow duration curves to evaluate low and high flows. Furthermore, a comparison of processes and patterns from hydrometry, isotopes and predicted results was done as part of the model performance and realism assessment.

7.2.6 Development of land cover change scenarios

Scenario runs were developed to assess potential impacts of possible future land cover changes. The calibrated model was run for each selected scenario with 15 years of climate data (2003-2018). The first 5 years of the model run (2003-2007) were used as a warm up period for groundwater levels. Streamflow and groundwater change analyses for each scenario were done for a 10 year period (2008-2018). Calendar years (1 January to 31 December) were used for analyses. The current land cover was used as a baseline to compare with selected scenarios of change. Single change scenarios were done in which one aspect of the current land cover was changed whilst all other aspects remained the same, to explore impacts of that type of change in land cover on streamflow and groundwater levels. Table 7.6 gives descriptions of the selected landcover change scenarios.

Table 7. 6: Selected vegetation scenario descriptions and mapping methods used

Scenario	Scenario description	Mapping description
Maximum catchment alien invasion extent	All areas that are not actively farmed both in the floodplain and in the mountains are covered with dense black wattle and pine stands	All areas except cliffs, high plateaus, orchards, pastures, or built-up areas are mapped as black wattle and pine.
Maximum floodplain black wattle extent	All areas that are not actively farmed in the floodplain are covered with dense black wattle	All other land units except the floodplain remain with the current vegetation. In the floodplain, everything is mapped as black wattle except for actively farmed areas.
Maximum floodplain palmiet extent	Black wattle IAPs are cleared in the floodplain and palmiet wetlands regenerate except on farmed areas	On the floodplain, palmiet regenerates and cover all areas that are not actively farmed (orchards, pastures). All other land units remain with the current vegetation

Tables 7.7 and 7.8 shows land cover proportions for selected scenarios (at floodplain and catchment scales respectively). The maximum catchment-wide wattle invasion scenario was considered to test landscape-scale feedbacks to assess the impact of wattle invasions in upland vs. riparian areas.

Table 7.7: Percentage floodplain cover for current and selected land covers scenarios

Vegetation type	Floodplain Cover					
	Current		Palmiet restoration		Wattle floodplain	
	Area km²	Cover (%)	Area km²	Cover (%)	Area km²	Cover (%)
Water	0.021	0	0.021	0	0.021	0
Palmiet	1.85	17	8.44	78	-	78
Forest	0.001	0	0.001	0	0.001	0
Fynbos	3.36	31	-	-	-	-
Black wattle	3.22	30	-	-	8.44	-
Orchard	0.73	7	0.73	7	0.73	7
Field	1.58	15	1.58	15	1.58	15
Bare	0.024	0	0.024	0	0.024	0

Table 7.8: Percentage catchment cover for current and selected land covers scenarios

Vegetation type	Catchment Cover							
	Current		Palmiet restoration		Wattle floodplain		Wattle Maximum	
	Area km²	Cover (%)	Area km²	Cover (%)	Area km²	Cover (%)	Area km²	Cover (%)
Water	2.51	1	2.49	1	2.49	1	2.22	1
Palmiet	6.15	2	13.73	4	3.91	1	-	
Forest	6.17	2	5.97	2	5.97	2	-	
Fynbos	249.89	70	252.51	70	252.51	70	51.12	14
Fynbos	43.46	12	39.12	11	39.12	11	43.24	12
Black wattle	27.37	8	22.34	6	32.16	9	190.93	53
Pine	3.26	1	3.16	1	3.16	1	57.79	16
Orchard	1.40	0	1.40	0	1.40	0	1.39	0
Field	18.50	5	18.50	5	18.50	5	12.53	3
Bare	0.83	0	0.83	0	0.83	0	0.83	0

The floodplain palmiet and wattle scenarios had the same spatial distribution (area and proportion of the floodplain) of 8.44 km² or 78% of the floodplain area (Table 7.7). In each scenario, the same coverage was assumed to be either wattle or palmiet with no coverage of the other type remaining. Results from the two floodplain scenarios can be directly compared to each other. The area and percentage cover changes for each scenario are shown in Tables 7.7 and 7.8, and mapped distributions are shown in Figure 7.3.

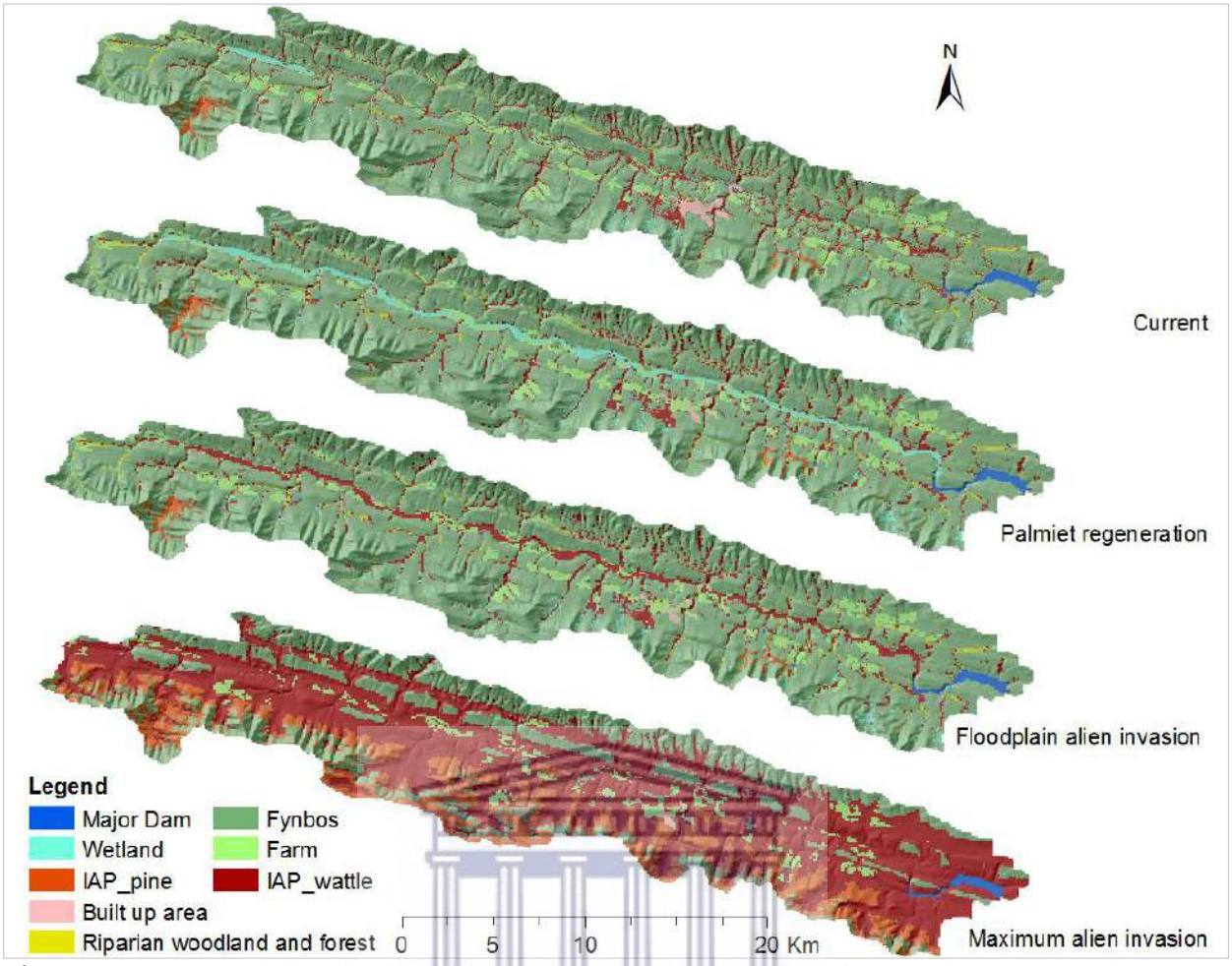

Figure 7.3: Mapped distributions of the current and selected land cover change scenarios

Parameter values were assigned by vegetation type, therefore scenarios had different Manning's roughness and detention storage in the floodplain. Relevant root depth, ET coefficient (Kc) and canopy interception values were assigned by cover type and kept consistent across all the scenarios e.g. the parameters assigned to palmiet wetland areas were the same in all scenarios. There was no need to manually work out the changes of floodplain-scale and/or catchment-scale average ET coefficient (Kc) values to represent the cover changes. The model calculated it based on the area changed. In addition to the land cover area changes, an assumption was made about the channel shape changes that would come with the vegetation cover change. The palmiet scenario was assigned a small low flow channel and a wide and rough high flow channel whilst the wattle scenarios were assigned wide and deep low flow channels and less rough high flow channels (Figure 7.4). Cross section shapes were based on field surveys done across the length of the river (Cornelius et al., 2019; Smith and Tanner, 2019). Palmiet wetland areas were assigned increased water retention to represent the peat soils of the wetland. There was a greater area of this soil type in the palmiet expansion scenario because the area of palmiet wetland was increased.

Figure 7. 4: Demonstrative conceptual cross sections of river channel in a palmiet wetland (left) and incised channel (right)

Model results were assessed against streamflow and groundwater data. Daily, monthly and annual averages of streamflow were calculated for each scenario. Furthermore, floodplain depth to groundwater under each scenario model run was also analysed and presented. All visual and statistical analyses were done to assess impacts of selected above ground land cover changes on average flows, baseflows, peak flows, storm response and other water balance components in the catchment. T-tests were performed to check for differences between means of observed vs. simulated data. Paired t-tests were done on predicted mean annual runoff (MAR) as well as high flows vs. low flows for all modelled scenarios. Data was analysed at a 0.05% confidence level. High flows were defined as flows that were above 1 mm and equalled or exceed for 5% of the time and low flows were defined as flows below 1 mm.

Proportional changes in fluxes (i.e. ET, infiltration) under the PMFP, WTFP and WTALL scenarios vs. the CRNT cover scenario were calculated as follows:

$$\text{Proportional change in flux} = \frac{\text{PMFP, WTFP or WTALL scenario flux} - \text{CRNT scenario flux}}{\text{CRNT scenario flux}}$$

To look at the landscape-scale feedbacks, the impact of the location of black wattles, and how much water they might have access to, the area increase (km^2) in black wattle coverage in the WTALL scenario vs. the CRNT and WTFP scenarios was compared to the predicted difference in mean annual runoff and ET (Mm^3 yield) vs. CRNT. This analysis was the main reason for running the WTFP and WTALL scenarios. For both scenarios, the unit runoff or ET drop (Mm^3 yield) was calculated as follows:

$$\text{Unit runoff or ET drop (Mm3)} = \frac{\text{Runoff or ET difference } (Mm^3 \text{ yield}) \text{ per area increase } (km^2) \text{ in IAP vs. CRNT}}{\text{Added cover } (km^2) \text{ of IAP vs. CRNT}}$$

7.3 RESULTS

7.3.1 Comparison of observed results to baseline model results

7.3.1.1 Observed vs. modelled streamflow in the Kromme catchment

The model performance was assessed against observed streamflow data in the catchment (Churchill Dam inflow). The baseline calibrated model for the Kromme Upper catchment achieved a relatively reasonable goodness of fit between the calibrated model results vs. observed data (Table 7.9). The Nash Sutcliffe Efficiency (NSE) values of 0.8 and 0.86 for daily and monthly average flow were obtained respectively suggesting acceptable reproduction of the observed streamflow. Most statistical parameters calculated show better model performance for the monthly scale comparisons than daily ones i.e. RMSE, R^2, and NSE values.

Table 7.9: Statistical results of observed vs. baseline calibrated model

Daily			**Monthly**		
Statistics	Observed	Modelled	Statistics	Observed	Modelled
Mean	1.23	1.17	Mean	1.23	1.17
Std. deviation	6.08	5.19	Std. deviation	2.712	2.16
Std. error	0.10	0.09	Std. error	0.25	0.20
CV	4.95	4.42	CV	2.21	1.84
Min	0.00	0.04	Min	0.01	0.04
PC10	0.001	0.06	PC10	0.05	0.08
PC25	0.06	0.12	PC25	0.13	0.17
PC50	0.27	0.26	PC50	0.32	0.47
PC75	0.78	0.72	PC75	0.91	1.10
PC90	2.17	1.98	PC90	2.96	3.01
Max	175	157.3	Max	16.46	16.25
RMSE		2.69	RMSE		1.01
MAE		0.74	MAE		0.49
NSE		0.80	NSE		0.86
NSE (LogQ)		0.35	NSE (LogQ)		0.76
R^2		0.81	R^2		0.88
Mean Error		-0.05	Mean Error		-0.05

PC-Percentiles

Daily and monthly hydrographs of observed vs. modelled streamflow are shown in Figure 7.5a and 7.5b respectively. The baseline model at daily time scale had slightly more small to medium peaks than observed data (Figure 7.5a). This showed that the model overestimated flows in some cases but the goodness of fit for most peak flow events was acceptable. The model yielded relatively comparable results at the monthly time scale for both high and low flows (Figure 7.5b). The model prediction followed trends in the observed data and deviations from the average were not high.

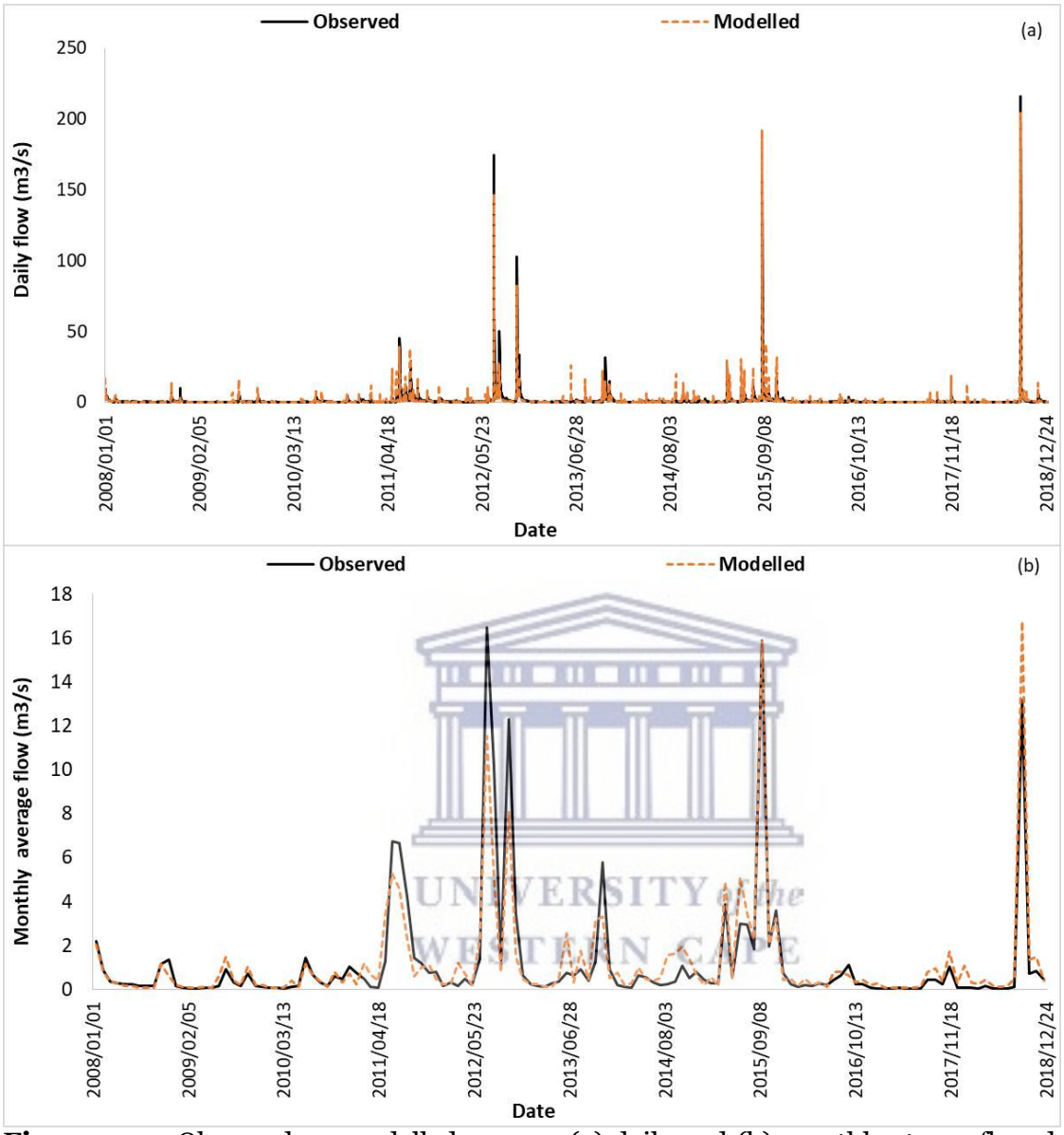

Figure 7. 5: Observed vs. modelled average (a) daily and (b) monthly streamflow data for the Kromme Upper catchment from 2008-2018

7.3.1.2 Observed vs. modelled floodplain groundwater levels

A comparison of predicted vs. observed groundwater levels is shown in Figure 7.6. This was done to compare if the simulation mimicked the observed groundwater level patterns not necessarily the exact groundwater level values. There was no automated time series groundwater data at the midcatchment site, however looking at dates with corresponding field observations, the simulated water level showed reasonable patterns compared to the observations. Simulated depths were in the range of the observation points and a temporal pattern comparable to Observed 1, 2 and 3 (Figure 7.6a).

At the lower catchment site, the model simulated the patterns of groundwater level change well in that the patterns from the simulated data were comparable to patterns from observed data, although the simulated water depth was low (Figure 7.6b). It should be noted that the simulation results were for 100 m model grid cells and were compared with point location observations therefore a close match of depths was not expected. The similar degree of rise and speed of recession are encouraging.

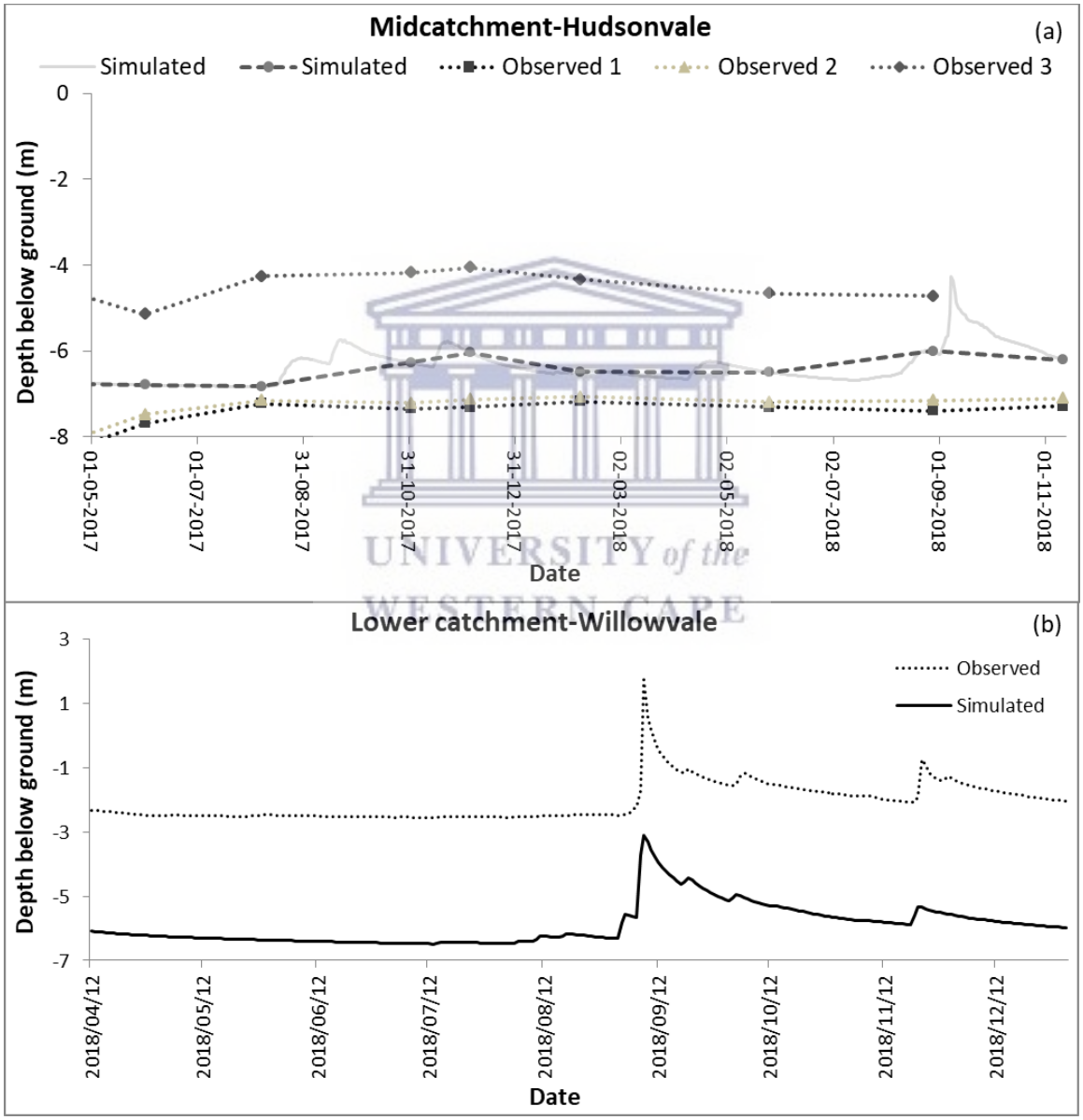

Figure 7.6: Observed vs. simulated floodplain water levels at mid and lower catchment sites

7.3.1.3 Predicted water balance components and comparison of model results vs. hydrometry and hydrochemistry results

The modelled water balance showed an average annual runoff of 38.6 Mm^3 (18% of the total precipitation), with most water lost through evapotranspiration (79% of total precipitation), and a change in storage of 6.5 Mm3 (Table 7.13 in section 7.33). To establish the relative level of reliability of the model and inevitable weaknesses, Table 7.10 shows a comparison of modelled processes to prior hydrometric and hydrochemistry observations made in the catchment. Based on reported statistics (Table 7.9), visual hydrograph and groundwater level analyses and predicted vs. observed results comparison (Table 7.10), the model was considered fit for running alternative vegetation cover scenarios presented in 7.3.2.

Table 7.10: Comparison of observed processes and patterns between hydrometry, isotopes and predicted results

Process or flowpath	Hydrometry	Hydrochemical results	Model results
Channel gaining or losing, as a whole and over different reaches, at different times	Channel gaining from the alluvial aquifer, tributary flows or mountain bedrock flows. River stage always below groundwater levels at monitored sites.	Chemical source component separation shows up to 96% contribution to river from alluvial aquifer particularly during dry periods.	Model results showed alluvial aquifer contributions of > 55% to river flows during the modelled period which may have been an underestimation.
Change in shallow groundwater levels in the floodplain	Groundwater levels in the alluvial aquifer increased notably even without precipitation inputs showing that recharge was not only influenced by direct rainfall only	Inconsistencies in geochemical compositions at different shallow groundwater sites implied different contributing sources.	Results showed more floodplain alluvial aquifer recharge from water flowing from the mountain areas (18.9 Mm^3) vs. direct recharge from rain (<7.2 Mm^3).
Groundwater flow into mountain tributaries	Seeps observed in tributary valleys and wetlands even during the drought. Linear shapes of recession plots particularly at tributary sites indicated a constant source. Most tributaries observed had perennial flow.	Similar isotopic and hydrochemical signatures in water from seeps and tributaries indicated and confirmed constant groundwater contributions from the bedrock aquifer.	Model results show proportions of water from seeps and tributaries to the river (i.e. 5 and 37 Mm^3 for 2017 and 2018 respectively). Constant outflow from the bedrock and interflow layer into the tributaries was predicted but the proportional quantities of the overall flow leaving the mountains and the catchment were small.
Main channel streamflow peak timing after storm events	Dominance of surface and shallow subsurface flows was indicated by quick time to peak.	Chemical separation showed high proportions of direct runoff during wet periods (storm events with contributions of ~61% on average)	Sharp rising limbs on predicted streamflow hydrographs shows quick peak timing after storms. 60% of total runoff from surface flow and interflow.
Contributions of quicker and slower response flowpaths	Baseflow contributions were highly variable for different events at some sites indicating variable aquifer storage and different flowpaths.	Chemical separation results quantified main sources (surface runoff, shallow and deep groundwater). Groundwater was shown to contribute highest proportions (>50%).	Model results quantified main sources and groundwater from the alluvial aquifer was shown to contribute more than other flowpaths and sources (17.6 Mm^3 average annual).
Average annual runoff coefficients	Low coefficients (0.1) indicate large ET withdrawals from the dominant flowpaths in the catchment and/or storage in inactive groundwater		Model results i.e. for the years 2017 and 2018 yielded runoff coefficients of 0.1 and 0.2 respectively (Appendix Table 7A1).

7.3.2 Impacts of selected landcover scenarios on river flows

7.3.2.1 Impacts of selected landcover scenarios on mean annual runoff

Mean annual runoff which is a key element of the water balance was computed for the modelled 10 year period (Figure 7.7). Time series of simulated annual runoff results per scenario are presented in Figure 7.7. The floodplain palmiet regeneration scenario (PMFP) generated the highest annual water yield consistently throughout the simulated period (2008-2018). Simulated annual runoff dynamics per scenario of change shows an average increase of 1.66 Mm^3/year (4%) under PMFP vs. the current cover (CRNT) scenario for the 10 year period. Mean annual runoff decreased by 1.86 and 14.85 Mm^3 (5% and 38%) under the floodplain wattle (WTFP) and maximum alien invasion (WTALL) scenarios respectively in comparison to the CRNT (Table 7.11). Predicted runoff from the palmiet scenario had the highest runoff ratio of 0.19 whilst the maximum wattle invasion generated the least ratio of 0.11 (Table 7.11). The maximum alien invasion scenario generated the least runoff throughout the modelled period (Figure 7.7).

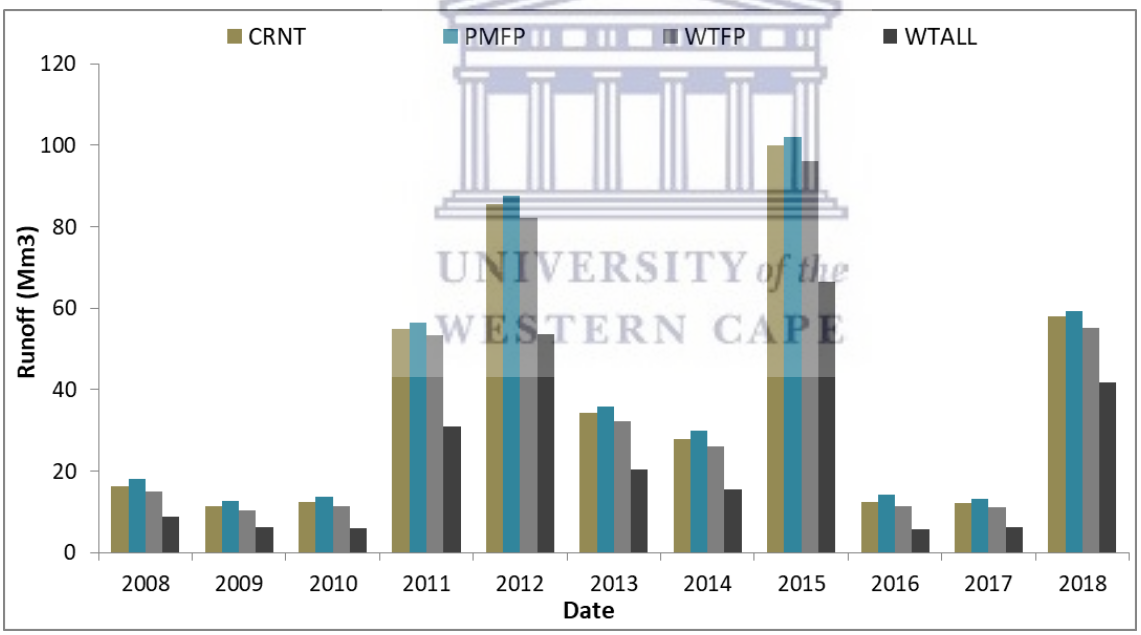

Figure 7. 7: Simulated annul runoff for the Kromme catchment under selected landcover scenarios (2008-2018)

Table 7. 11: Average annual runoff per modelled scenario of change

	CRNT	PMFP	WTFP	WTALL
Average annual runoff (Mm^3)	38.64	40.30	36.78	23.79
Change in average annual runoff vs. CRNT	-	1.66	-1.86	-14.85
% increase or decrease vs. CRNT	-	4%	-5%	-38%
Runoff ratio	0.18	0.19	0.17	0.11

7.3.2.2 Impacts of selected landcover scenarios on daily flows in m³/s

Daily streamflow hydrographs (Figures 7.8 a; b) show that the maximum catchment-wide alien invasion (WTALL) generated the least daily flows compared to the other scenarios of change, as expected given the high transpiration rates assigned to the woody alien plants in the model. The floodplain palmiet scenario (PMFP) generated increased average daily flow of 4% over the modelled period vs. the CRNT scenario. The PMFP generated average daily flows of 1.28 m³/s whilst the CRNT scenario had 1.22 m³/s.

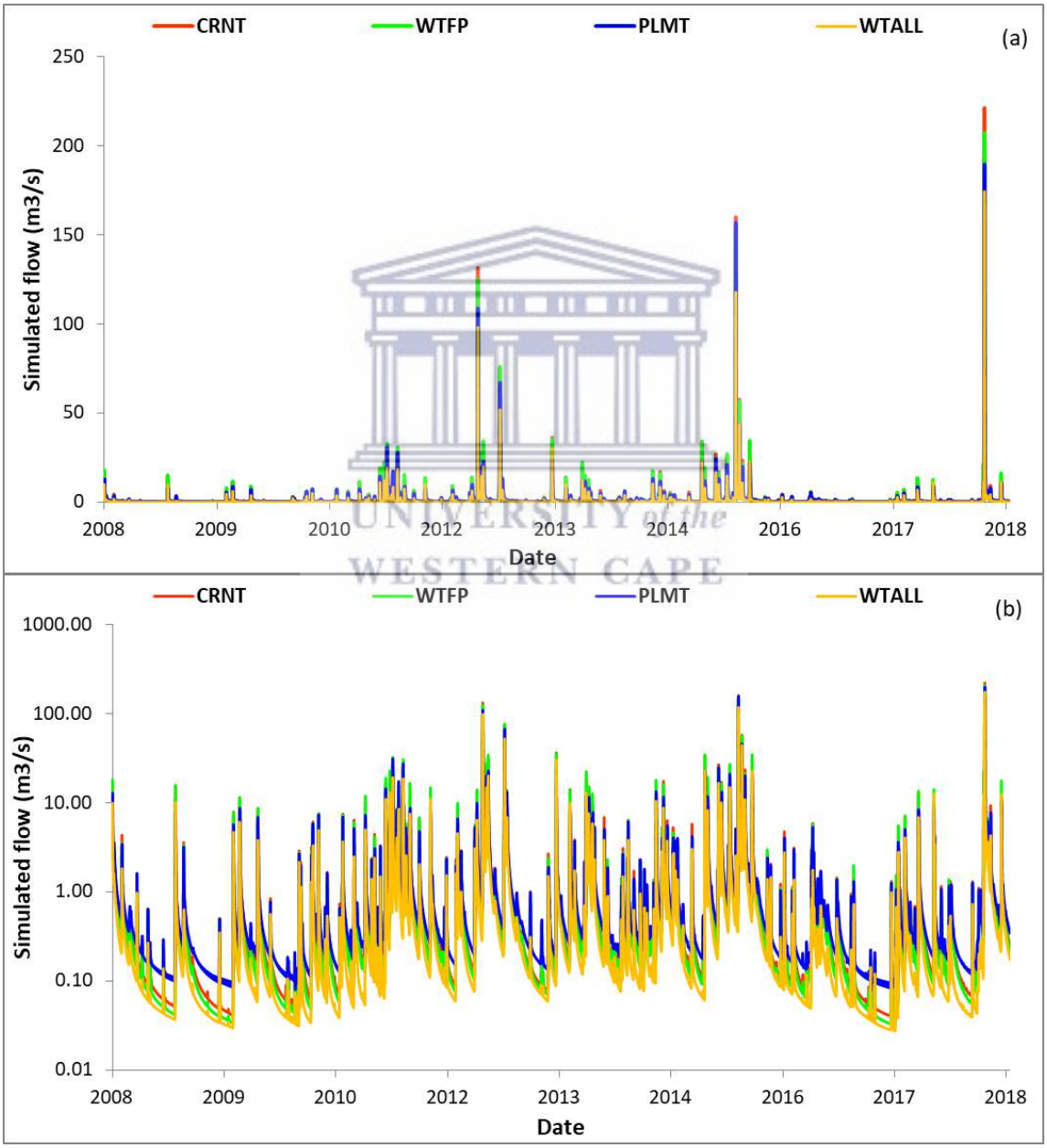

Figure 7. 8: Simulated daily streamflow for landcover scenarios in the Kromme from 2008-2018 (same data but different y-axis scales, log scale (b) for better visualisation of low flows).

The PMFP scenario had smaller peaks than the current (CRNT) and floodplain wattle (WTFP) scenarios. Although, the regeneration of floodplain palmiet scenario (PMFP) predicted reduced peaks, it had the highest magnitudes in predicted low flows compared to other scenarios, as shown clearly in the log scale hydrograph (Figure 7.8b).

The floodplain wattle scenario (WTFP) predicted high peak flows in general than other scenarios (Figure 7.8), because the floodplain channel shape was structured to have low roughness and a larger area of low hydraulic conductivity soils, hence the lower infiltration in the model. The palmiet scenario (PMFP) had a rougher floodplain and more peat soils as this would be the case if palmiet regenerates in the floodplain. This is most likely due to the physiology of palmiet root system that stabilizes channels and reduces the velocity of streamflow hence the small peaks predicted, in comparison to the wattle invasion scenarios (Figure 7.8). The WTALL scenario generated the lowest values in both high and low flows. In terms of simulated low flows, the WTALL generated the lowest baseflows consistently throughout the modelled period (Figure 7.8b). The PMFP scenario generated the highest contribution of baseflows to the streamflow (Figure 7.8b).

7.3.2.2 Daily streamflow responses in high and low flow conditions under selected landcover scenarios

Within the modelled time period (2008-2018), the calendar years 2009 and 2015 were classified as driest (407 mm) and wettest (874 mm) rainfall years. Predicted streamflow was also lowest and highest in 2009 and 2015 respectively (Appendix Table 7A.2). The majority of years within the modelled period were relatively dry having below average annual precipitation of 600 mm/year (Appendix Figure 7A2). The predicted lowest and highest streamflow years (2009 and 2015 respectively) were used to compare streamflow responses of the different scenarios of landcover change under low and high flow conditions (Figure 7.9).

In high flow conditions, model results show high peaks under WTFP and CRNT scenarios (Figure 7.9b), however streamflow yield was highest under the palmiet scenario (102 Mm^3) (Appendix Table 7A.3). During low flow periods (Figure 7.9a), the model results indicated that restoring the floodplain palmiet wetlands could result in increased baseflows which sustain streamflow particularly during dry periods. During the driest months in 2009 (January-April), the average predicted daily streamflow was highest under palmiet (0.13 m^3/s) and lowest under WTALL (0.04 m^3/s). Overall predicted streamflow yield was also highest under palmiet (12.8 Mm^3) during the driest year which was a 12% increase compared to the CRNT cover whilst

during high flows the proportional increase between the two scenarios was 2%. The largest predicted daily flow peak during a wet year was 157 m^3/s under CRNT and PMFP scenarios, whilst the largest flow peak during the dry year was 11.5 m^3/s under WTFP scenario (Appendix Table 7A.4). Observed data showed peaks of 156 and 5 m^3/s for 2009 and 2015 respectively (Appendix Table 7A.4).

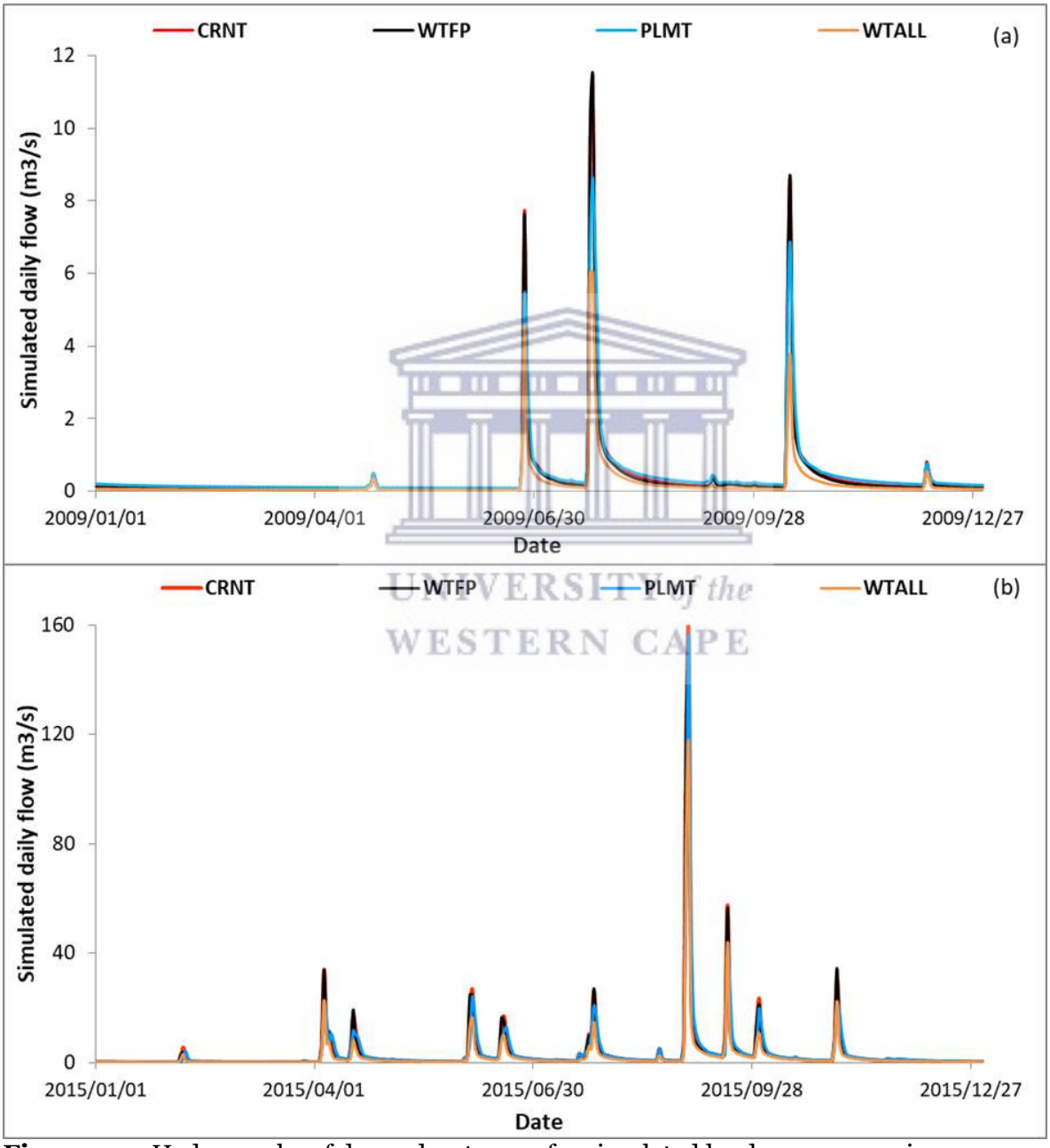

Figure 7.9: Hydrographs of dry and wet years for simulated land cover scenarios

7.3.2.3 Variation in flow duration under selected landcover scenarios

To get a comprehensive assessment of the simulated flow regimes, flow duration curves were constructed (Figure 7.10). The flow duration results indicated that overall, palmiet regeneration (PMFP), produces more runoff than other scenarios of change. Flow duration curves under predicted CRNT and other land cover scenarios plot at the low flow end (< 5 mm for greater than 95% of the time). This showed that low flows are dominant in this catchment under all predicted scenarios of change including the CRNT cover (Figure 7.10 and Table 7.12).

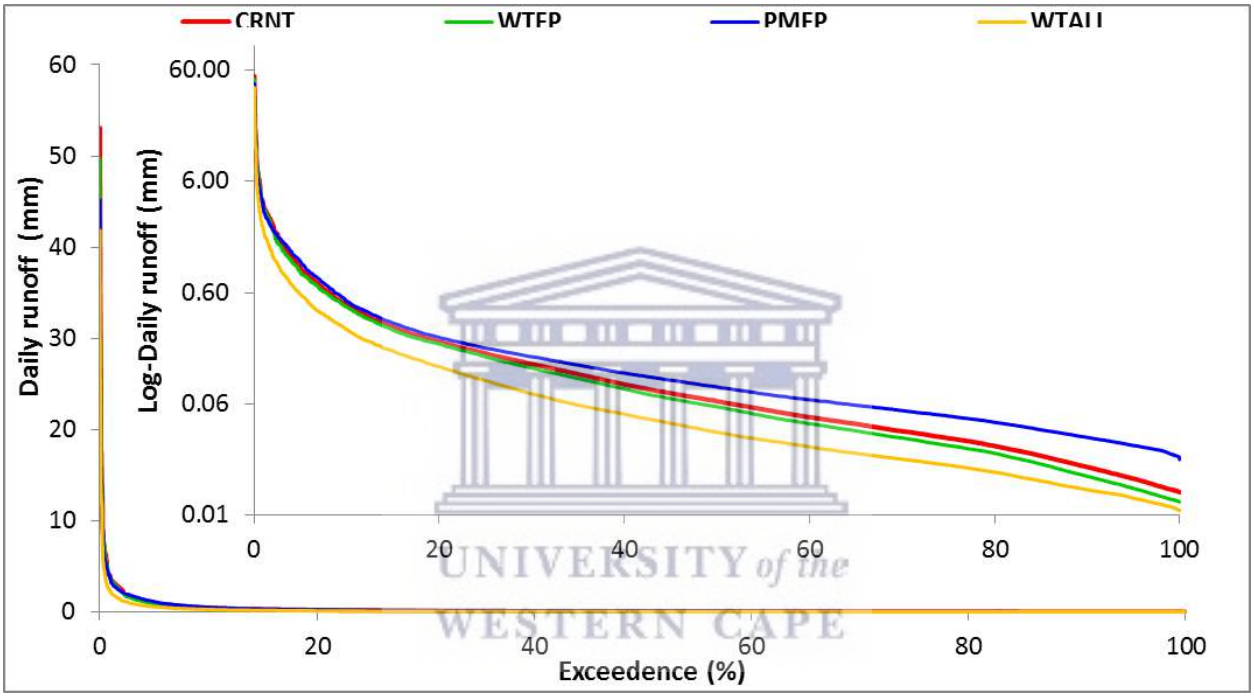

Figure 7.10: Flow duration curves for simulated daily runoff of the landcover scenarios of change in the Kromme catchment from 2008-2018.

For all model runs, high, low and average daily runoff and their corresponding exceedance percentages are given in Table 7.12. The maximum daily runoff for all scenarios ranged from 42-53 mm/day which was equalled or exceeded for 0.02 % of the time (Table 7.12). Predicted maximum runoff for the palmiet scenario (PMFP), was 15% less than the current cover scenario (CRNT), and the full wattle invasion (WTALL) was 21% less than the CRNT. Although the catchment is dominated by low flows under all scenarios of change, highest low flow magnitudes were generated under the floodplain palmiet regeneration scenario than the other two scenarios (Table 7.12).

Table 7.12: Statistical summary for simulated land cover scenarios

% exceedance	Daily runoff (mm)			
Land cover scenario	CRNT	PMFP	WTFP	WTALL
0.02	53.08	45.17	49.74	41.84
1	3.7	3.71	3.61	2.26
5	1.004	1.142	0.91	0.58
50	0.06	0.09	0.06	0.03
95	0.013	0.025	0.01	0.009
98	0.011	0.023	0.009	0.007
100	0.010	0.019	0.008	0.007

7.3.3 Variation in water balance components under scenarios of land cover change.

The average annual predicted water balance components for the 2008-2018 period are presented in Table 7.13. The PMFP and WTFP scenarios had the same land cover change at both the floodplain scale (78.2%) and catchment scale (2%). The WTALL scenario had a 61% change in cover vs. the CRNT cover scenario. Model results suggest that regeneration of floodplain palmiet (PMFP) in this catchment after clearing the floodplain invasive trees is likely to have a significant impact on the average annual runoff (4%) compared to the predicted CRNT state (Table 7.13). The PMFP scenario had a change of land cover on only 2% of the total catchment, therefore a 4% change in mean runoff is a relatively large change for such as small proportional cover change. Predicted changes in runoff between the CRNT and the two wattle invasion scenarios (WTFP and WTALL) indicate a decrease of 5% and 38% respectively (Table 7.11 in section 7.3.2.1). Under the CRNT cover and all modelled scenarios of change, most of the water in the catchment was predicted to be lost through AET (actual evapotranspiration) which accounted for more than 75% of the total precipitation across all model runs (Table 7.13).

Table 7.13: Average annual water balance components between modelled scenarios

Flux (Mm^3/year)	**CRNT**	**PMFP**	**WTFP**	**WTALL**
Precipitation (Mm^3/year)	213.04	213.04	213.04	213.04
AET (Mm^3/year)	167.87	167.72	169.71	187.45
AET (% of precipitation)	**79%**	**79%**	**80%**	**88%**
Runoff (Mm^3/year)	38.64	40.30	36.78	23.79
Runoff (% of precipitation)	**18%**	**19%**	**17%**	**11%**
Net subsurface storage change (Mm^3/year)	6.52	6.49	6.54	1.93
subsurface storage change (% of precipitation)	**3%**	**3%**	**3%**	**1%**

Statistical results for the paired t-tests done on predicted mean annual runoff (MAR) of the landcover scenarios are presented in Table 7.14. All scenario MAR results were compared to the CRNT predicted runoff (Table 7.14). Additionally, the PMFP and WTFP scenario results were also compared against each other. Differences between scenarios were considered significant if p values of the paired t-tests for the selected scenario pairs were less than 0.05. Statistics for the period 2008-2018 all show p values less than 0.05 indicating significant differences between the CRNT cover model run and the selected scenario runs (Table 7.14). Predicted mean annual runoff between PMFP and WTFP scenarios was also significantly different.

Table 7.14: Statistical summary for simulated MAR (mm/year) of land cover scenarios

t-Test: Paired Two Sample for Means-MAR (mm per year)								
	Pair 1		Pair 2		Pair 3		Pair 4	
Scenario	CRNT	PMFP	CRNT	WTFP	CRNT	WTALL	PMFP	WTFP
Mean	0.29	0.31	0.3	0.28	0.3	0.18	0.31	0.28
Variance	0.058	0.059	0.058	0.05	0.058	0.027	0.059	0.05
Observations	11	11	11	11	11	11	11	11
Pearson Correlation	0.99		0.99		0.99		0.99	
HMD	0		0		0		0	
df	10		10		10		10	
t Stat	-15.4		5.98		4.67		9.44	
P(T<=t) one-tail	1.36E-08		6.77E-05		0.00044		1.34E-06	
t Critical one-tail	1.8		1.8		1.8		1.8	
P(T<=t) two-tail	2.72E-08		0.000135		0.00088		2.7E-06	
t Critical two-tail	2.23		2.23		2.23		2.23	

HMD-Hypothesized Mean Difference, MAR- mean annual runoff

Additional statistics were calculated for the PMFP and WTFP scenarios during high and low flows (Appendix Table 7A.5). High flows were defined as flows that were above 1 mm and equalled or exceed for 5% of the time. Low flows were defined as flows below 1 mm. Results show significant differences between the floodplain palmiet and wattle scenarios during low flows ($p<0.05$). However, there were no significant differences between the two scenarios during high flows ($p>0.05$) (Appendix Table 7A.5).

7.3.4 Modelled changes in processes and flowpaths leading to streamflow changes under selected land cover scenarios

Predicted changes in particular fluxes and flowpaths due to the selected landcover change scenarios are presented in Figure 7.11 and Appendix Table 7A.7. Water from the mountains reaching the floodplain edge was the same for CRNT, PMFP and WTFP scenarios because vegetation cover changes were only done in the floodplain and the rest of the mountain areas remained the same in these scenarios except for WTALL (Figure 7.3). Model predictions of most processes across the scenarios therefore, showed the lowest fluxes of most components under the WTALL scenario as expected due to the large spatial area of cover change (Figure 7.11).

Most predicted surface flows contributing to the river were mountain sourced under all scenarios (up to 94%) (Appendix Table 7A.7). In the mountains, less of the water was subjected to ET because of fast runoff due to steep slopes therefore large quantities made it to the river. Predicted floodplain generated surface flows were minimal (up to 6% of total surface flows) (Figure 7.11). Although, floodplain surface runoff contribution to the river was generally small, the highest proportion was generated under the PMFP scenario (1.3 Mm^3) compared to WTFP and WTALL scenarios (Figure 7.11).

Model results showed that the alluvial aquifer was significantly recharged by water sourced from the mountains to the floodplain surface (Figure 7.11). Recharge on the alluvial aquifer was therefore, not all rainfall derived recharge. It comprised direct rainfall, surface runoff from the mountains which infiltrated on the floodplain as well as subsurface interflow and bedrock flows from the mountain. The mountain sourced surface water recharging the alluvial aquifer was predicted to decrease by 43% (from 12.6 Mm^3 down to 7.3 Mm^3) under WTALL compared to CRNT, and by 45% between PMFP and WTALL scenarios.

Similar to surface flows, large quantities of predicted infiltration on the floodplain surface were also mountain sourced under all scenarios (Figure 7.11). A comparison between scenarios showed a significant difference in mountain sourced infiltration on the floodplain between the CRNT and WTALL scenarios (18.9 Mm^3 vs. to 13.9 Mm^3), a proportional decrease of 24%. The increase of canopy cover from the dense wattle stands (WTALL) was expected to reduce infiltration, percolation to deeper layers, and recharge. Predicted mountain sourced interflow contribution to the main channel also decreased considerably (by 38%) under WTALL scenario compared to the CRNT.

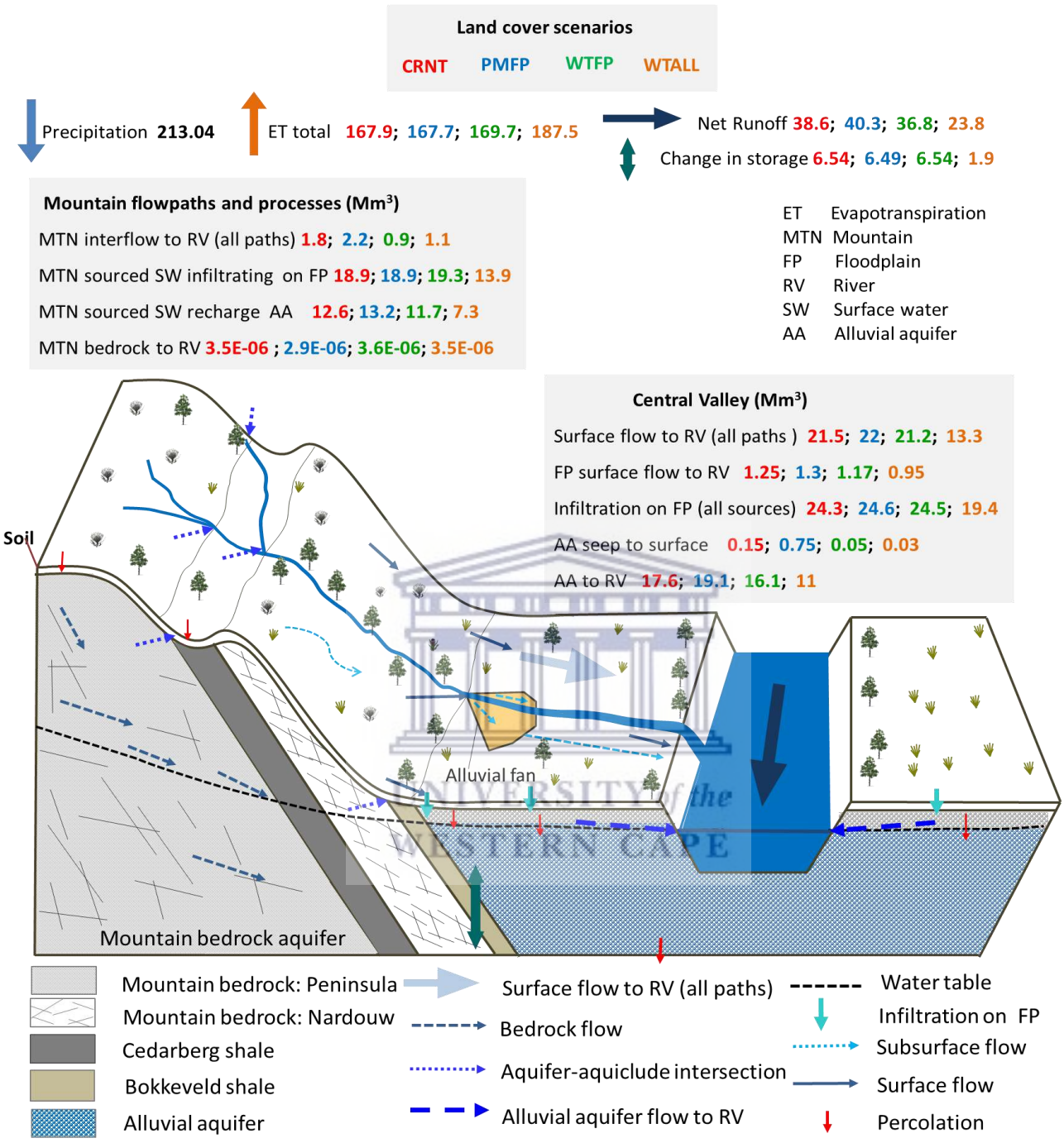

Figure 7.11: Predicted fluxes and flowpaths under different scenarios of landcover change.

Modelled proportional contributions from the alluvial aquifer to the river suggest that regeneration of floodplain palmiet (PMFP) is likely to result in the highest annual proportion of 19 Mm^3 and the least contribution of 11 Mm^3 under the WTALL scenario (Figure 7.11). Seeping water from the alluvial aquifer to the surface in the floodplain was also significantly higher under PMFP than other scenarios (Figure 7.11).

The predicted mountain and floodplain bedrock direct contribution into the river was small and almost negligible under all scenarios of change (Figure 7.11; Appendix Tables 7A.7). This was due to the structure of the geological layers as shown in Figure 7.2 (section 7.2.4), where aquicludes are in between the bedrock aquifers and the river therefore direct contribution was not expected.

7.3.5 Impact of the location of black wattle invasion on ET and runoff response

To assess the impact of location of black wattle invasion on ET and runoff response, the area increase (km²) in wattle coverage in the WTALL scenario vs. the CRNT and WTFP scenarios was compared to the predicted decrease in mean annual runoff and ET (Mm³ yield) vs. the CRNT (Tables 7.15 and 7.16). The expectation was that both scenarios (WTFP and WTALL) will not be the same in terms of water use by wattles per area of cover due to the topographic location of the trees and water availability. Wattles in the WTFP scenario would therefore have more net impact per km² than those in the WTALL.

Table 7.15: Differences in AET per unit area under riparian vs. upland black wattle invasion

Land cover scenario	Black wattle cover (km²)		Total IAP cover (wattles + pines)		Increase in wattle area vs. CRNT (km²)		Increase in IAP area vs. CRNT (km²)		**AET** (Mm³)		Change in **AET** vs. CRNT (Mm³)		Change in **AET** per unit area increase in IAP (Mm³) change÷(km² increase in IAP)	
	FP	CAT	FP	CAT	FP	CAT	FP	CAT	FP	CAT	FP	CAT	FP	CAT
CRNT	3.2	25.96	3.2	29.12					9.2	167.9				
WTFP	8.4	32.2	8.4		5.2	5.2	**5.2**	**5.2**	11	169.7	1.8	1.8	0.35	**0.35**
WTALL	8.4	190.9	8.4	241	5.2	164.9	**5.2**	**211.9**	10.4	187.5	1.2	19.6	0.23	**0.09**

Table 7. 16: Runoff differences per unit area under riparian vs. upland black wattle invasion

Land cover scenario	Black wattle cover (km²)		Total IAP cover (wattles + pines)		Increase in wattle area vs. CRNT (km²)		Increase in IAP area vs. CRNT (km²)		**Runoff** (Mm³)		Change in **Runoff** vs. CRNT (Mm³)		Change in **Runoff** per unit area increase in IAP change (Mm³) ÷ (km² increase in IAP)	
	FP	CAT	FP	CAT	FP	CAT	FP	CAT		CAT		CAT		CAT
CRNT	3.2	25.96	3.2	29.12						38.64				
WTFP	8.4	32.2	8.4		5.2	5.2	**5.2**	**5.2**		36.78		-1.86		**-0.36**
WTALL	8.4	190.9	8.4	241	5.2	164.9	**5.2**	**211.9**		23.79		-14.85		**-0.07**

The proportional change in actual ET per unit area increase in IAPs was high under the WTFP scenario (0.35 Mm^3/km^2) than the WTALL scenario (0.09 Mm^3/km^2) (Table 7.15). Similar to ET, the proportional change in runoff per unit area increase in IAPs indicated a 0.36 Mm^3/km^2 decrease in runoff under WTFP compared to a 0.07 Mm^3/km^2 decrease under WTALL (Table 7.16). The location of a specific land cover within a catchment (riparian vs. upland) therefore has greater impact on the on the hydrological response. Predicted results indicated that wattles use more in riparian areas where water is readily available than upland areas.

7.3.6 Impacts of selected landcover scenarios on floodplain grounder depth

Modelled outputs were also analysed for floodplain groundwater level changes (Figure 7.12). Predicted results indicated that regeneration of floodplain palmiet (PMFP) could result in an increase in groundwater levels in the alluvial aquifer on average (Figure 7.12). The predicted mean groundwater depths were -6.1 m under CRNT scenario, -5.3 m under PMFP, -7.02 m under WTFP and -7.2 m under the WTALL scenarios. The proportional difference in the modelled mean groundwater depths compared to the predicted CRNT cover scenario showed an increase of 13% under PMFP and decreases of 15% and 18% under WTFP and WTALL scenarios respectively.

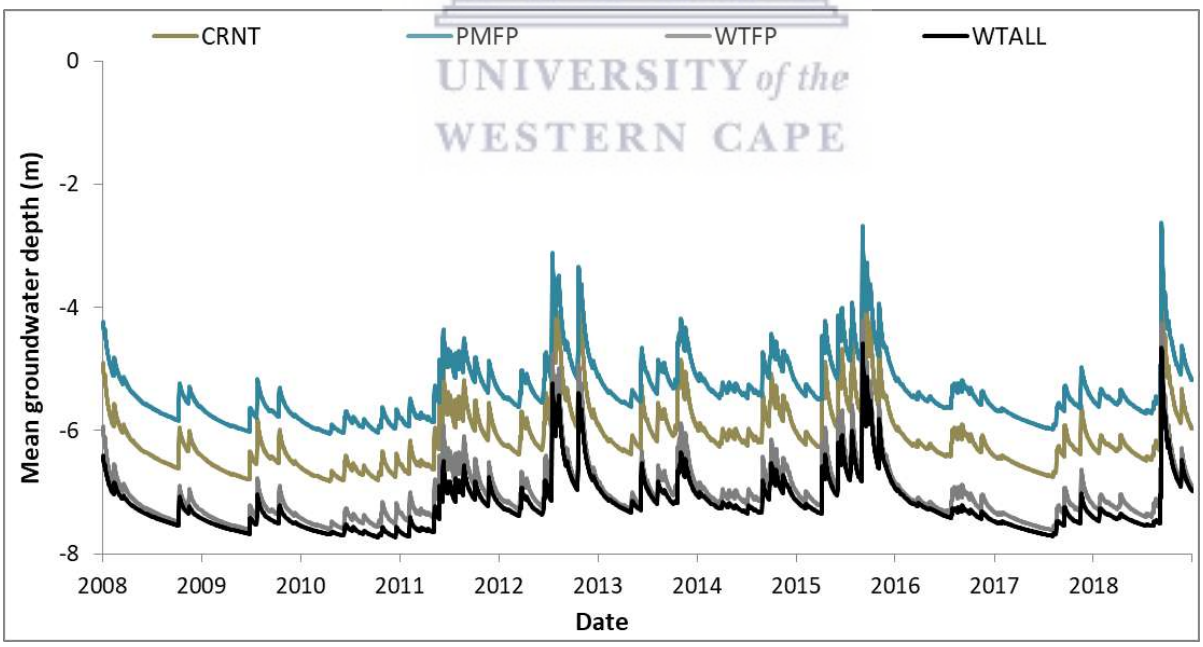

Figure 7.12: Average groundwater depth per simulated scenario of change from 2008-2018.

The predicted groundwater depth under the palmiet regeneration scenario (PMFP) fluctuated between 2.6 and 5.9 m below ground which was higher than groundwater levels under the CRNT cover and wattle invasion scenarios. This would be expected as a result of consistent recharge of

the alluvial aquifer from surface and subsurface water from the surrounding mountains in the absence of high water using alien invasive trees. Both the predicted floodplain and maximum catchment-wide alien invasion scenarios (WTFP and WTALL) resulted in reduced groundwater levels within the alluvial aquifer. The WTFP ranged from 4.2 to 7.5 m below ground whilst the WTALL fluctuated between 4.7 and 7.6 m below ground (Figure 7.12).

7.3.7 Summary of impacts of landcover on selected major hydrological components

Model results indicate that overall, clearing of woody alien invasives and allowing the regeneration of palmiet could increase baseflow by 9%, total outflow by 5% and groundwater levels in the floodplain by 13% compared to the current cover scenario. Predicted flood peaks increased under WTFP vs. PMFP and decreased under PMFP vs. CRNT (Table 7.17) which was a result of using different channel shapes associated with the different land cover types in the model.

Table 7. 17: Percentage change per scenario for dominant flowpaths and processes.

Impact	PMFP VS CRNT	WTFP VS CRNT	WTALL VS CRNT	WTFP VS. PMFP
Floodplain GW levels change	+13%	-15%	-18%	-4%
Increase in baseflow	+9%	-8%	-37%	-9%
Increase in total outflow	+4%	-5%	-38%	-16%
Flood peaks	-9%	0	-32%	+9%

Model results also provided evidence of significant reduction in both streamflow and baseflow under the two wattle expansion scenarios compared to the current state (Table 7.17). Although predicted groundwater levels were significantly lower under both invasion scenarios, results show that hydrological connectivity remained between the channel and alluvial aquifer although significantly lower compared to the current and palmiet scenarios (Figure 7.11). This is due to the associated decline in alluvial aquifer storage because of the increased water use by alien trees.

7.4 DISCUSSION

7.4.1 Model performance in streamflow calibration and realism of processes

7.4.1.1 Numerical model performance in streamflow calibration

Lumped, parsimonious, models can sufficiently simulate streamflow patterns in micro-scale catchments, (McMillan et al., 2011), however, a more spatially distributed modelling approach for meso scale catchments was assumed necessary based on results from previous modelling studies (i.e. Glenday, 2015; Rebelo, 2012). Spatial discretization also facilitated the determination of threshold controlled surface and subsurface processes (Fenicia et al., 2008; Glenday, 2015), and parameterization of the selected land cover scenarios (Torbick et al., 2006). The baseline calibrated model for the Kromme Upper catchment had slightly more small to medium peaks than observed data at daily time scale. This implied that the model overestimated flows in some cases during low flow periods, which is comparable to other modelling studies in semi-arid regions (Okello et al., 2018), but the goodness of fit for most peak flow events was acceptable.

7.4.1.2 Numerical model performance in the realism of processes

The spatially and vertically distributed model structured for the Kromme allowed targeted analyses of particular flowpaths and processes at different locations in the catchment similar to other semi-arid modelling studies (Busche, 2012; Glenday, 2015). The predicted mean annual flow for the Kromme catchment was 168 Mm^3 and most of this water emerged from surface flows from the mountains due to the steep slopes influenced by the topography and parameterisation of soils in the model. These flows were short lived after events, but made up the bulk of water leaving the mountains in the long term average in the simulation. Surface flow was predicted to be the dominant flowpath leaving the mountains in the model, however given the observed consistency of flow in some of the tributaries, the simulated proportion of quickflow in the tributaries could have been too high and not realistic. However, large quantities of the surface flow from the mountains (tributaries) infiltrated and recharged the alluvial aquifer in the model. Given the reasonable streamflow and alluvial aquifer groundwater performance of the model, it is possible that this infiltration of surface water inputs from the mountains that was simulated on the floodplain was comparable to actual infiltration of water from tributaries and alluvial fans, entering the floodplain as subsurface flow. To improve the model performance on this, more measured flows from other parts of the catchment would be needed for use in the calibration process i.e. to improve the tributary flow magnitudes.

Predicted outflow from the bedrock aquifer into tributaries was constant but the amount was a small proportion of the overall flow leaving the mountains and the catchment. The model also

predicted low proportions of interflow to the main river which would be expected in catchments characterised by low slopes and geological layers that are not highly fractured (Xu et al., 2002). The Kromme is the opposite of this, therefore high interflow rates were expected but the predicted results did not show evidence of this. Likewise, hydrometry and hydrochemical techniques showed higher contributions from the deep aquifer than the quantities predicted by the model. Highly fractured layers were expected to contribute large quantities of water (Tessema et al., 2014), therefore the low quantities predicted could imply unrealistic set-up and parameterisation of these layers in the model. In the floodplain, the model predicted large contributions from the alluvial aquifer to the river which was consistent with observed results where the river was constantly gaining from the alluvial aquifer.

Although great efforts were made in using the best available input data and process understanding in model structuring, issues of uncertainties were in the configuration of subsurface layers for deep groundwater reservoirs, the interflow layer and soils. The soil infiltration rate influenced the magnitudes of water leaving the mountains purely as surface runoff vs. interflow which may have been overestimated. Another issue of uncertainty was the estimation of the spatial rainfall which was done using the Lynch surface (Lynch, 2004) and the few rainfall stations in the catchment. This may have resulted in the over and under prediction of peak flows. Additional rainfall stations are therefore needed to improve the estimation of spatial rainfall in future modelling exercises.

7.4.2 Modelled changes in processes and flows under selected vegetation cover scenarios compared to expected responses

The calibrated base model set-up was used for the scenario runs with the same parameters values for soils, vegetation and geology from different sources available for the Kromme catchment (i.e Diamond, 2014; Euston-Brown, 2006; Lynch, 2004; Xu et al., 2009). However, channel shapes were changed to match the likely geomorphological changes associated with selected vegetation types based on field observations of channels in palmiet wetlands vs. areas that have other covers due to invasion/conversion. Other land cover scenario studies (i.e. Awotwi et al., 2015; Gyamfi et al., 2016) simulated scenarios of land cover change by only altering the vegetation cover properties in the model without considering changes in channel shapes caused by the selected vegetation types due to alterations in geomorphic processes. Channels have been reported to become wider and increasingly incised with black wattle invasion (Pieterson 2009). In wetter or small catchments, channel properties in modelling studies may be less of a concern considering that interactions between channels, aquifers and the floodplain maybe less significant (Slater

and Khouakhi, 2019). However, in semi-arid meso scale catchments such as the Kromme, channel properties per land cover scenario therefore became important. This is because interactions between the channel, floodplain and aquifers can drive the observed streamflow patterns particularly in semi-arid areas (Ochoa et al., 2013; Glenday, 2015).

Conversion of a vegetation type to another with lower or higher transpiration rates has been observed to result in a net increase or decrease in catchment yield respectively considering that ET has major influences on overall outflows (Le Maitre et al., 2000; Nosetto et al., 2011; Wang et al., 2018). Model results of wattle invasion in the Kromme catchment showed an increase in evapotranspiration rates and decrease in runoff and groundwater levels, which was consistent with findings from previous studies on wattle cover in other invaded catchments (Clulow et al., 2011; Jarmain and Everson, 2002; Everson et al.,2007). At Two streams catchment in KwaZulu Natal, South Africa, ET increased (~1200 mm/yr) due to black wattle invasion (Clulow et al., 2011). In a modelling exercise, Rebelo et al. (2015) predicted that clearing black wattle in the Kromme catchment and restoring wetlands to their condition in the 1950s resulted in a runoff increase of 1.13 Mm3/yr (3% of the supply to the Churchill dam, and 6% supply to Nelson Mandela Metropolitan). This was the modelled outcome of an 84% increase in wetlands and clearing 3.36 km^2 of wattle. Model results from this study indicated that clearing wattle from 2% of the catchment (5.03 km^2) results in average annual increase in runoff of 1.66 Mm^3 which is 5% supply to the Churchill dam (35 Mm^3 capacity).

The location of a specific land cover within a catchment (riparian vs. upland) was shown to have a greater impact on the hydrological response in this study. Predicted results indicated that wattles have greater impact per unit area of invasion in riparian areas where water is readily available (shallow water tables), than wattles in upland (dry) areas as reported by a few other studies (Everson et al. 2007; Le Maitre et al., 2015; Salemi et al., 2012; Warburton, 2012). The proportional change in actual ET per unit area increase in IAPs was high under the WTFP scenario (0.35 Mm^3) than the WTALL scenario (0.09 Mm^3). Similar to ET, the proportional change in runoff per unit area increase in IAPs indicated a 0.36 Mm^3 decrease in runoff under WTFP compared to a 0.07 Mm^3 decrease under WTALL. Everson et al. (2007), showed that clearing riparian wattle trees increased streamflow by 6.47 m^3/ha/yr, whilst clearing in dry lands increased flow by 5.62 m^3/ha/yr. Fourie et al. 2007 and Dzikiti et al., 2013b also showed that clearing riparian invasion resulted in 25 and 35 mm/ year in groundwater fluctuations respectively. Differences in water use by trees may be due to vegetation characteristics but factors such as water accessibility, depth to the water table and storage capacities also play major

roles (Funk et al., 2017; Rebelo et al., 2015). Indigenous vegetation may also have similar water use characteristics to invading species thereby offsetting the benefits of alien clearing due to little or no change in water yield (Doody et al., 2011).

The Kromme catchment was monitored during a very dry period which gave insights on the role of baseflow contributions in sustaining streamflow. Field hydrometric and hydrochemistry data showed that even during dry periods the alluvial aquifer water table remained constantly above the river channel level, thereby constantly sustaining river flows. Floodplain groundwater levels under dense wattle stands remained below piezometer depths (3 m below ground surface), while measured levels were highest in the palmiet wetlands. Model results also predicted higher floodplain groundwater levels in the palmiet scenario as expected than under wattle invasion scenarios. Wattle trees have been shown in other studies to lower the water table and soil water content (Dye et al., 2001; Everson et al., 2014), however there has been little research on the impacts of indigenous palmiet on these hydrological components (Rebelo et al., 2019). The palmiet ET rate was set low whilst the manning's n and the detention storage was set higher than other cover types based on the literature (Rebelo, 2012), and field observations. The high water table was due to the set surface roughness, lower canopy interception, and soil properties assumed for palmiet vs. wattle trees. In reality, the fibrous palmiet roots act as filters, trapping sediments in floodplain channels and reducing the velocity of flowing water thereby encouraging recharge (Rebelo, 2012; Sieben, 2012).

Although predicted groundwater levels were significantly lower under both wattle invasion scenarios (WTFP and WTALL), results of this study show that hydrological connectivity remained between the channel and alluvial aquifer although significantly lower compared to the CRNT and PMFP scenarios.

7.4.3 Implications of modelling results for hydrological process understanding and catchment management

Model results showed high levels of groundwater and surface water interactions therefore invasion by wattle trees could be critical particularly on low flows in this catchment. Furthermore, black wattle invasions were predicted to reduce water quantity in the catchment. In reality, reduced water quantity could result in reduced dilution capacity of water in the river system thereby negatively affecting the water quality particularly during periods (Saraiva Okello et al., 2018).Loss of water services resulting from alien plant invasion has been motivation for large scale restoration plans in recent years (McConnachie et al., 2012; WFW, 1995). The Kromme River catchment is one of the few sites in this country with an extensive wetland

restoration program therefore studies of this nature are aimed at assisting such programmes with scientifically informed strategies. If modelled changes were to take place in the catchment, there are potential real world consequences for i.e. local downstream and regional water supply particularly to the Port Elizabeth Metropolitan that periodically experiences severe water shortages. WTALL scenario was an extreme case of invasion, but results highlighted potential impacts in the long-term if all clearing work stopped and wattles expand in coverage. Expansion of floodplain wattle (WTFP) may occur earlier if clearing stops because wattle trees grow faster in the floodplain due to easy access to water. If the catchment's water resources are to be protected, the alien control programme should continue in the Kromme with regular follow ups considering the scale of invasions and predicted magnitudes of impacts indicated by results of this study.

Quantitative estimates of alien tree invasion for the upper Kromme catchment suggest potential impacts on water supply in the region particularly the Nelson Mandela Metropolitan. Predicted results indicated that clearing 2% of the catchment (5.03 km2) results in an average annual increase in runoff of 1.66 Mm^3 which is 5% supply to the Churchill dam (35 Mm^3). Annual yield would decrease by 14.9 Mm^3 (for 2008-2018) between the WTALL vs. the CRNT scenarios. The decrease is equal to 42% of the total volume of the Churchill Dam which supplies water to the Nelson Mandela Metropolitan.

7.5 CONCLUSION

This study used hydrologic modelling to assess the likely impacts of continued invasion of woody alien trees compared to IAPs clearing and subsequent palmiet wetland restoration on streamflow and groundwater in a semi-arid meso-scale catchment. Field data was used to answer questions on flow connectivity and selection of some parameter values to ensure the model structure met the needs of its application in terms of process representation and desired outputs. Given scenarios of further woody alien invasions, simulated model results showed a reduction in streamflow and the drawdown of storage from the alluvial aquifer due to increased transpiration rates. Model results indicated that clearing of floodplain black wattle and allowing the regeneration of palmiet increases groundwater levels in the floodplain by 13%, baseflow by 9% and total outflow by 4% in the semi-arid meso scale mountainous catchment. The hydrological impacts of vegetation cover changes on low flows, floods and overall water yield differed with vegetation type, extent and topographic location of vegetation cover change, and climate regime. Model results indicated that water use by black wattle trees was not uniformly proportional to the unit area occupied but depend greatly on the specific location of the trees within the catchment.

CHAPTER 8: CONCLUSIONS AND RECOMMENDATIONS

8.1 General Conclusions

8.1.1 Introduction

Understanding the impacts of vegetation cover changes on hydrological processes is a key part of catchment management in areas where large-scale land cover changes are occurring. The goal of this study was improve the simulation of vegetation impacts on hydrological processes in a semi-arid meso scale catchment. Field data was used to guide the development of a conceptual model of the catchment and to structure the numeric model. This was also done to ensure that the model structure met the needs of its application in terms of process representation and desired outputs. The model was used to run selected possible land cover scenarios of change. Likely impacts of alien invasion, clearing and floodplain palmiet regeneration on streamflow and groundwater in the Kromme catchment were assessed from the predicted results. Information gathered from the field data, and predicted impacts of likely alien invasion scenarios on water resources adds to the knowledge base of semi-arid systems in mountainous settings.

8.1.2 Developing a conceptual model for a semi-arid meso scale mountainous catchment based on hydrometry and hydrochemistry analyses

8.1.2.1 *Streamflow characteristics and dominant flowpaths linking landscape units in the Kromme catchment*

Precipitation, soil water content, groundwater levels, and flow data (2017-2019) were analysed both in turn and in combination, to identify patterns that indicated the occurrence and dominance of certain processes, responses, and flowpaths. Results showed how the steep and rocky areas that make up much of the catchment resulted in significant flood peaks after high-intensity storms. Large proportional contributions of quick flow to river flows were observed only after heavy storms (>15 mm/day).

The Kromme central valley runs between parallel mountain ranges (trellis drainage pattern) with steep, deeply incised, tributary valleys that are perpendicularly oriented to the main valley. Mountain bedrock aquifer flow into tributaries appeared constant as seeps were observed flowing consistently into tributaries even during the drought. Surface and subsurface flows from perennial tributaries, originating in the mountains, were significant in recharging the central valley floodplain alluvial aquifer and maintaining streamflow in the main channel even during dry periods. Furthermore, the catchment has a sizeable floodplain with large alluvial aquifers that make significant contributions to catchment storage and outflows. Measured water level

gradients between shallow groundwater and surface water in the river indicated that subsurface flow from the floodplain alluvial aquifer and mountain bedrock aquifer maintains the river baseflow. Tracer source component separation also supported this observation shown by high percentages of groundwater contribution to surface water particularly during the dry periods. Infiltration and percolation to the alluvial aquifer also raises the gradient of the floodplain water table resulting in increased alluvial aquifer flow to channel.

Recession patterns showed that the channel receives flow from different storages and flowpaths. Overall, the catchment streamflow was dominated by baseflow during the field monitoring period. Average annual runoff coefficients were low (less than 10% of precipitation became runoff), implying large ET withdrawals from dominant flowpaths and/or storage in inactive groundwater.

Hydrometric techniques highlighted possible flowpaths and groundwater surface water interactions between the mountain, floodplain and channel as well as likely sources contributing to streamflow in this catchment. Most of these flowpaths and processes were conceptualized but not explicitly quantified using hydrometric data i.e. proportional contributions of alluvial and bedrock flow into tributaries and main channel. Isotope data therefore confirmed the occurrence of some conceptualised flowpaths, sources and quantified proportional contributions from each source and/or flowpath.

8.1.2.2 Field evidence of impacts of black wattle, palmiet and grassland cover types on processes in the floodplain based on soil water content and water table data

Characterizing available soil water under different vegetation types offered unique insights into soil water status, depletion and recharge which were all essential for understanding vegetation impacts on hydrological processes. Rainfall, vegetation type and antecedent conditions were identified as the major factors controlling variations in the floodplain soil water content and water table fluctuations. Field data indicated that the wattle trees were likely using soil water for evapotranspiration at higher rates than palmiet and grass. Soils under wattle trees drained faster after events and the water table was deeper at the wattle site as it was below the depth of installed piezometers (3 m) for more than 90% of the time, only rising to this depth following heavy storms greater than 40 mm/day. This implied less flow contributions from the alluvial aquifer to river flows at this site. In areas without black wattle trees (palmiet and grassland), shallow groundwater levels remained within 2 m of the ground surface for prolonged periods constantly discharging into the river. On average, soil water content and water retention were

significantly higher ($p<0.05$) at the palmiet site, whilst the wattle site had the lowest among the three sites. Palmiet traps sediment and reduces water velocity in channels due to the clonal nature of its extensive root system (Rebelo et al., 2015; Sieben, 2012), therefore subsurface water was retained for longer periods in palmiet dominated area and recharge of deeper soil horizons was promoted. Temporal variations of soil water content under the different land cover types were not always consistent with rainfall event sizes due to differences in the dry sequence durations preceding events.

Removal of invading species and replacing or allowing the regrowth of native herbaceous species may result in increased water retention and infiltration rates, reduced ET rates and a consequent increase in floodplain groundwater levels as shown by the results of this study. Given the relative importance of floodplain landscapes particularly in arid and semi-arid catchments, as well as the global increase in land use and land cover changes particularly alien invasions in riparian landscapes, quantitative studies of this kind are therefore imperative regarding impacts of contrasting land cover types on floodplain hydrology (Gao et al., 2014; Ziadat and Taimeh, 2018).

8.1.2.3 Hydrological process understanding from the spatio-temporal variation of water physico-chemistry and isotope tracer patterns in a semi-arid mountainous catchment.

The spatio-temporal variability of water physico-chemistry and environmental tracer patterns were used to improve hydrological process understanding in the Kromme catchment. Tracer data indicated steady contribution of groundwater to surface flows in the main channel and tributaries confirming results observed through hydrometric techniques. Isotopic evidence demonstrated that the $\delta^{18}O$ and $\delta^{2}H$ compositions in the Kromme River exhibited spatial and temporal variability from the upper to lower reaches, controlled by atmospheric temperature. Water samples generally got enriched along the river length moving downstream. Overall, although water samples were increasingly enriched downstream, some locations had depleted samples in locations were tributaries join the main channel. This indicated influences of water from mountain tributaries and groundwater from the bedrock aquifer contributing to the channel.

Similar to isotope tracers, EC values generally increased along the length of the river due to evaporation. However, surface water had low EC values overall (<350 µS/cm). Deep groundwater in the catchment also had relatively low EC in general (EC <1000 uS/cm), which is associated with the fractured sandstone formations characteristic of the TMG regions that are

not associated with high salinity. Low EC in groundwater also implied pronounced aquifer recharge by direct rainfall.

From the hydrometric analyses, surface runoff was shown to dominate for short periods after storm events. Tracer source component separation from the snapshot sampling showed direct runoff contributions up to 10% from events occurring during dry periods and increasing (up to 40%) in wet periods. Mountain bedrock aquifer flow into tributaries was observed through seeps. Similarities in isotope samples of seeps and tributary water during the monitoring period confirmed the constant groundwater contribution from the bedrock aquifer to tributary surface flow even during dry periods. Source component separation showed that groundwater from both the bedrock and alluvial aquifers sustained streamflow with combined contributions accounting for up to 98% of the streamflow during the dry period. These snapshot sample results cannot be generalised to estimate annual contribution values for these source components, but they give an idea of the variability of the flow components spatially and temporally. In general, groundwater from the alluvial aquifer contributed significantly to river flow (up to 90% in some cases). The high baseflow contribution to total flows during both dry and wet conditions was also highlighted by hydrometric data which showed that the main river was a consistently gaining system. Adding isotopes and physico-chemistry data led to the improvement of the conceptual model of flowpaths in the catchment.

8.1.2.4 Hydrological methods for characterization of processes in semi-arid TMG catchments

Hydrometric data indicated the occurrence and dominance of particular processes, responses, and flowpaths. The spatiotemporal variability of environmental and geochemical tracers improved the understanding of flowpaths, stream water sources and proportions of different sources contributing to river flows. The combination of different methods led to the improvement of the conceptual model of flowpaths for the Kromme catchment. Coupled EC values, Cl and isotopic compositions were effective as indicators for flowpaths, sources and proportional contributions to river flows however their application alone or on individual basis in large scale, highly fractured catchments could be challenging due to low temporal variation in some cases. Chemical compositions of some sources were too similar to be used for source component separations. Isotopes were effective in revealing recharge mechanisms but could not be used to understand other factors influencing water quality. EC was effective in showing surface and subsurface processes influenced by evaporation, substrate materials and mineralization processes, and to some extent recharge. Water chemistry in TMG catchments has

been reported to be consistent due to the lack of marked variations (Diamond, 2014), thereby making it difficult to use a single water chemistry parameter to draw conclusive results.

8.1.3 Modelling impacts of selected land cover types on the hydrological response of a semi-arid meso-scale, mountainous catchment

Knowledge from the hydrometry and hydrochemistry analyses was important in structuring the distributed MIKE SHE model for simulation of vegetation impacts on hydrological processes in the Kromme catchment. The spatially and vertically distributed model allowed targeted analyses of the influence of alternative vegetation cover scenarios on particular flowpaths and processes at different locations in the catchment. Hydrological modelling proved invaluable in quantifying some of the conceptualised flowpaths in this catchment, i.e. quantifying how much groundwater from the bedrock gets to the alluvial aquifer and eventually to the main channel, and what proportion of groundwater from the alluvial aquifer contributes to streamflow.

Scenario runs were also developed to assess potential impacts of possible future land cover changes. Simulated model results showed a reduction in streamflow (up to 38%) and the drawdown of storage from the alluvial aquifer because of increased transpiration rates due to woody alien invasions. Results also showed that clearing of floodplain black wattle and allowing the regeneration of palmiet increases groundwater levels in the floodplain by 13%, baseflow by 9% and total outflow by 5%. The palmiet scenario was also associated with a small decrease in floodplain ET (0.02%) and a net increase in alluvial aquifer contribution to river flow of 10% compared to the current cover. Results supported the hypothesis that clearing of woody alien trees such as black wattle and allowing the regeneration of herbaceous species such as palmiet in a semi-arid meso scale mountainous catchment results in increased runoff and floodplain groundwater patterns.

Predicted groundwater levels were significantly low under both wattle invasion scenarios (WTFP and WTALL). However, results showed that hydrological connectivity remained between the channel and alluvial aquifer indicating the importance of the alluvial aquifer storage in this catchment comparable to results by Everson et al. (2014). Similar to field observations, the model succeeded in predicting high groundwater levels under palmiet vs. other land cover scenarios. The floodplain alluvial water table has an impact on catchment outflow and water yield therefore alien invasion in floodplains can have detrimental effects on overall outflow and catchment water yield particularly in large scale catchments that have sizeable floodplains. This is less of a concern in smaller catchments, however in large catchments like the Kromme, different mechanisms give vegetation access to water in the floodplain i.e. river and alluvial aquifer contributing to changes in floodplain soil water content dynamics. The alluvial aquifer

receives substantial surface and subsurface flows from the mountains, therefore floodplain invasion by black wattle impacts the floodplain water table, and overall yield as the alluvial aquifer discharges into the river.

Model results also indicated that ET and streamflow response from a specific land cover type is not uniformly proportional to the unit area occupied by the land cover but depends greatly on the specific location of the land cover type within the catchment. Alien invading woody species were shown to have increased transpiration rates and reduced runoff in riparian areas compared to drier upland areas.

8.2 Summary of knowledge contribution

This work contributes significantly to the knowledge of runoff generation processes in semi-arid meso scale mountainous catchments using a multi method approach. The Kromme catchment covers 360 km^2 and has both steep areas (mountainous terrain) and flat floodplain areas (with significant alluvial deposits) where processes vary due to the diversity of topographic characteristics, geomorphological factors and precipitation inputs. This topographic diversity would be expected at this spatial scale, particularly in mountainous regions, however the connectivity between different landscape units has rarely been studied, particularly in semi-arid areas in which thresholds of saturation are more rarely met. The study provided a case-study of how the steep hillslopes can be hydrologically connected to valley bottoms in mountainous catchments at the meso scale in a dryland setting. In this case, surface water from the mountains (bedrock outflow and surface flow from rainfall), flows in tributaries to the main river, whilst some of this water infiltrates on the floodplain recharging the alluvial aquifer. The alluvial aquifer, in turn, also discharges into the river maintaining flows. These findings provide a potential conceptual model to be considered for other catchments in the TMG region, and other semi-arid settings with similar topographic characteristics. The study also highlighted the possible impacts of black wattle invasion on streamflow and groundwater in semi-arid settings, and illustrated how the location of cover changes is likely to influence their catchment-scale impact in this type of environment. The study also highlighted the significance of palmiet wetlands on floodplain alluvial aquifer recharge and storage, and most importantly, catchment yield.

The combined use of hydrometry, isotopes and physico-chemical data has not been extensively explored in this region, therefore this study also contributes to the few studies on runoff generation that used this approach to understand processes (Smith and Tanner, 2019). Furthermore, the use of isotopes and physico chemistry for source component separation had

not been explored at the catchment scale in the Kromme. This is a new data set that can be used as a basis to explore additional water quality components and patterns in the catchment.

This study also highlighted the importance of combining modelling and a field based study for a comprehensive understanding of processes in a large meso scale semi-arid mountainous catchment. Field data helped with process understanding and structuring of the numerical model whilst the modelling helped to explore likely impacts of land cover changes in the catchment. Mapping of the topographic land units dominant in the catchment using the Height Above the Nearest Drainage (HAND) and slope, helped to understand the dominant hydrological processes controlling runoff generation in the catchment. Using different methods, this study revealed sources, flowpaths and different patterns of runoff generation and the likely impacts of particular land cover changes on water yield, and groundwater and surface water interactions.

8.3 Implications for water resources management

The findings of this thesis can be used to guide water resource protection and restoration strategies as areas of potential vulnerability to land cover changes and probable quantities of water that can be gained or lost due to palmiet regeneration or alien invasion respectively were shown. Quantitative estimates of invasion impacts for the Kromme catchment suggests potential impacts on water supply in the region. Modeled scenarios of change indicated that full expansion of IAP cover in the upper Kromme catchment could result in a 38% decrease in average annual catchment yield. Predicted annual yield decreased from 38.64 Mm^3 to 23.79 Mm^3 for 2008-2018 period, under the full expansion of IAP vs. the CRNT scenario. The predicted difference between the two scenarios (14.9 Mm^3) was equal to 42% of the total volume of the Churchill Dam (one of the dams that supply water to the Nelson Mandela Metropolitan region) which the Kromme River drains into.

Although results of this study are focused on a semi-arid catchment in South Africa, the reported findings are globally relevant as they are general hydrological principles that give ideas of the magnitudes and the direction of invasion impacts on hydrological processes in semi-arid settings.

8.4 Recommendations for future research

- Coupled EC values, Cl and isotopic compositions were effective as indicators for flowpaths and sources, however their application on individual basis in large scale, highly fractured catchments can be challenging due to low temporal variation. Additional

detailed water quality data is also required which can be obtained by using automated samplers at various points to capture variability in water quality signatures at small temporal resolutions.

- For isotope studies, additional rain stations and isotope samplers are needed. Isotope studies can also be extended to measurements of isotopic compositions from tree sap flow to identify transpiration water sources of the trees.
- The number of active rainfall stations in the catchment continues to decrease, therefore additional resources need to be dedicated for establishment of more stations and the maintenance of available ones.
- Streamflow was estimated from rating curves and flow data from a few selected points as well as dam inflow data adding to uncertainties in the comparison of observed vs. modelled results therefore a recommendation would be the construction of gauging weirs where flows can be measured directly.
- The modelling exercise shows room for model structure improvement particularly through additional knowledge on subsurface layers responsible for generation of deep groundwater in the catchment. In some instances the model over and under predicted peak flows which could be resolved by improving the spatial distribution of rainfall in the catchment i.e. more rain gauges at different elevations, testing of satellite based estimates, etc.
- Further modelling work can be done to integrate results from this work with reservoir models for water supply impacts in the catchment.
- The modelling exercise showed that black wattle trees use more water in riparian areas than upland dry areas, however more research is required to quantify water use characteristics of indigenous trees that often replace the alien trees after clearing.

CHAPTER 9: REFERRENCES

Aduah, M.S., Jewitt, G.P.W., Toucher, M.L.W., 2017. Assessing impacts of land use changes on the hydrology of a lowland rainforest catchment in Ghana, West Africa. Water (Switzerland) 10. https://doi.org/10.3390/w10010009

Ala-aho, P., Soulsby, C., Pokrovsky, O.S., Kirpotin, S.N., Karlsson, J., Serikova, S., Vorobyev, S.N., Manasypov, R.M., Loiko, S., Tetzlaff, D., 2018. Using stable isotopes to assess surface water source dynamics and hydrological connectivity in a high-latitude wetland and permafrost influenced landscape. J. Hydrol. 556, 279–293. https://doi.org/10.1016/j.jhydrol.2017.11.024

Albhaisi, M., Brendonck, L., Batelaan, O., 2013. Predicted impacts of land use change on groundwater recharge of the upper Berg catchment, South Africa. Water SA 39, 211–220. https://doi.org/10.4314/wsa.v39i2.4

Arnold, J.G., Srinivasan, R., Muttiah, R.S., Williams, J.R., 1998. Large area hydrologic modeling and assessment part i : model development ' basin scale model called SWAT (Soil and Water speed and storage , advanced software debugging policy to meet the needs , and the management to the tank model (Sugawara et al ., 1 34, 73–89.

Awotwi, A., Yeboah, F., Kumi, M., 2015. Assessing the impact of land cover changes on water balance components of White Volta Basin in West Africa. Water Environ. J. 29, 259–267. https://doi.org/10.1111/wej.12100

Bafitlhile, T.M., Li, Z., 2019. Applicability of ε-Support Vector Machine and artificial neural network for flood forecasting in humid, semi-humid and semi-arid basins in China. Water (Switzerland) 11. https://doi.org/10.3390/w11010085

Banks, E.W., Simmons, C.T., Love, A.J., Shand, P., 2011. Assessing spatial and temporal connectivity between surface water and groundwater in a regional catchment: Implications for regional scale water quantity and quality. J. Hydrol. 404, 30–49. https://doi.org/10.1016/j.jhydrol.2011.04.017

Becker, A., 2005. Runoff Processes in Mountain Headwater Catchments: Recent Understanding and Research Challenges 283–295. https://doi.org/10.1007/1-4020-3508-x_29

Berihun, M.L., Tsunekawa, A., Haregeweyn, N., Meshesha, D.T., Adgo, E., Tsubo, M., Masunaga, T., Fenta, A.A., Sultan, D., Yibeltal, M., 2019. Exploring land use/land cover changes, drivers and their implications in contrasting agro-ecological environments of Ethiopia. Land use policy 87, 104052. https://doi.org/10.1016/j.landusepol.2019.104052

Beusche H. 2012. Modeling hydrological processes in a semi-arid mountainous catchment at the regional scale. Unpublished Ph.D thesis, Rheinischen Friedrich-Wilhelms-Universität Bonn

Beven, K., 2001. How far can we go in distributed hydrological modelling? Hydrol. Earth Syst. Sci. 5, 1–12. https://doi.org/10.5194/hess-5-1-2001

Beven, K., 1982. On subsurface stormflow: An analysis of response times. Hydrol. Sci. J. 27, 505–521. https://doi.org/10.1080/02626668209491129

Beven, K., Binley, A., 1992. The future of distributed models: Model calibration and uncertainty prediction. Hydrol. Process. 6, 279–298. https://doi.org/10.1002/hyp.3360060305

Beven, K., Young, P., 2013. A guide to good practice in modeling semantics for authors and referees. Water Resour. Res. 49, 5092–5098. https://doi.org/10.1002/wrcr.20393

Blöschl, G., Reszler, C., Komma, J., 2008. A spatially distributed flash flood forecasting model. Environ. Model. Softw. 23, 464–478. https://doi.org/10.1016/j.envsoft.2007.06.010

Böhme, B., Becker, M., Diekkrüger, B., Förch, G., 2016. How is water availability related to the land use and morphology of an inland valley wetland in Kenya? Phys. Chem. Earth 93, 84–95. https://doi.org/10.1016/j.pce.2016.03.005

Bosch, D.D., Arnold, J.G., Allen, P.G., Lim, K.J., Park, Y.S., 2017. Temporal variations in baseflow for the Little River experimental watershed in South Georgia, USA. J. Hydrol. Reg. Stud. 10, 110–121. https://doi.org/10.1016/j.ejrh.2017.02.002

Boucher, C., Withers, M., 2004. Palmiet: Veld Flora, Univ. Stellenbosch 26–28.

Bracken, L.J., Wainwright, J., Ali, G.A., Tetzlaff, D., Smith, M.W., Reaney, S.M., Roy, A.G., 2013. Concepts of hydrological connectivity: Research approaches, Pathways and future agendas. Earth-Science Rev. 119, 17–34. https://doi.org/10.1016/j.earscirev.2013.02.001

Brauchli, T., Trujillo, E., Huwald, H., Lehning, M., 2017. Influence of Slope-Scale Snowmelt on Catchment Response Simulated With the Alpine3D Model. Water Resour. Res. 53, 10723–10739. https://doi.org/10.1002/2017WR021278

Bulcock, H.H., Jewitt, G.P.W., 2012. Field data collection and analysis of canopy and litter interception in commercial forest plantations in the KwaZulu-Natal Midlands, South Africa. Hydrol. Earth Syst. Sci. 16, 3717–3728. https://doi.org/10.5194/hess-16-3717-2012

Burke, A.R., 2009. A comparison of soil moisture and hillslope-stream connectivity between aspen and conifer dominated hillslopes of a first order catchment in northern Utah by Amy Burke A thesis submitted in partial fulfillment of the requirements for the degree of MASTER.

Calder, I., Dye, P., 2001. Hydrological impacts of invasive alien plants. L. Use Water Resour. Res. 1, 1–12.

Carpenter, R. C. 1999. An economic analysis of eradicating alien vegetation as an alternative to conventional water supply schemes: a case of the Krom and Kouga. MSc Thesis. Rhodes

University, Grahamstown, South Africa.

Camacho Suarez, V. V., Saraiva Okello, A.M.L., Wenninger, J.W., Uhlenbrook, S., 2015. Understanding runoff processes in a semi-arid environment through isotope and hydrochemical hydrograph separations. Hydrol. Earth Syst. Sci. 19, 4183–4199. https://doi.org/10.5194/hess-19-4183-2015

Cartwright, I., Gilfedder, B., Hofmann, H., 2014. Contrasts between estimates of baseflow help discern multiple sources of water contributing to rivers. Hydrol. Earth Syst. Sci. 18, 15–30. https://doi.org/10.5194/hess-18-15-2014

Cha, Y., Park, S.S., Kim, K., Byeon, M., Stow, C.A., 2014. Water Resources Research 5375–5377. https://doi.org/10.1002/2013WR014979.

Chamier, J., Schachtschneider, K., le Maitre, D.C., Ashton, P.J., van Wilgen, B.W., 2012. Impacts of invasive alien plants on water quality, with particular emphasis on South Africa. Water SA 38, 345–356. https://doi.org/10.4314/wsa.v38i2.19

Chapman, T., 1999. A comparison of algorithms for stream ¯ ow recession and base ¯ ow separation Abstract : 714, 701–714.

Clark, M.P., McMillan, H.K., Collins, D.B.G., Kavetski, D., Woods, R.A., 2011. Hydrological field data from a modeller's perspective: Part 2: Process-based evaluation of model hypotheses. Hydrol. Process. 25, 523–543. https://doi.org/10.1002/hyp.7902

Clark, M.P., Slater, A.G., Rupp, D.E., Woods, R.A., Vrugt, J.A., Gupta, H. V., Wagener, T., Hay, L.E., 2008. Framework for Understanding Structural Errors (FUSE): A modular framework to diagnose differences between hydrological models. Water Resour. Res. 44, 1–14. https://doi.org/10.1029/2007wr006735

Clarke, K.R., Gorley, R.N., 2006. PRIMER v6: User Manual PRIMER-E. Plymouth, UK 1–91.

Clulow, A.D., Everson, C.S., Gush, M.B., 2011. The long-term impact of Acacia Mearnsii trees on evaporation, streamflow and groundwater resources. Rep. to Water Res. Comm. Rep. No TT 505/11.

Colvin, C., Le Maitre, D., Hughes, S., 2003. Assessing terrestrial groundwater dependent ecosystems in South Africa, Water Research Commission.

Colvin, C., Maitre, D. Le, Saayman, I., Hughes, S., 2007. An Introduction to Aquifer Dependent Ecosystems in South Africa. Natural Resources and the Environment, Water Research.

Colvin, C., Riemann, K., Brown, C., Mlisa, A., Le Maitre, D., Blake, D., Aston, T., Maherry, A., Engelbrecht, J., Pemberton, C., Magoba, R., Soltau, L., Prinsloo, F., 2009. Ecological and environmental impacts of large-scale groundwater development in the Table Mountain Group (TMG) aquifer system.

Concern, A.G., 2014. Mountains and climate change: A global concern.

Cornelius, A., Le Roux, L., Glenday, J., FT, J., Sekese, S., 2019. Participatory Hydrological Modelling for Collective Exploration of Catchment Management in the western Algoa Water Supply Area.

Correa, A., Windhorst, D., Tetzlaff, D., Crespo, P., Célleri, R., Feyen, J., Breuer, L., 2017. Temporal dynamics in dominant runoff sources and flow paths in the Andean Páramo. Water Resour. Res. 53, 5998–6017. https://doi.org/10.1002/2016WR020187

Cowie, R.M., Knowles, J.F., Dailey, K.R., Williams, M.W., Mills, T.J., Molotch, N.P., 2017. Sources of streamflow along a headwater catchment elevational gradient. J. Hydrol. 549, 163–178. https://doi.org/10.1016/j.jhydrol.2017.03.044

Craig, H. (1961). Isotopic Variations in Meteoric Waters. Science, 133, 1702-1703. http://dx.doi.org/10.1126/science.133.3465.1702

Crous, C.J., Drake, D.C., Jacobsen, A.L., Pratt, R.B., Jacobs, S.M., Esler, K.J., 2019. Foliar nitrogen dynamics of an invasive legume compared to native non-legumes in fynbos riparian zones varying in water availability. Water SA 45, 103–109. https://doi.org/10.4314/wsa.v45i1.12

Dallas H and Day J (2004). The effect of water quality variables on aquatic ecosystems: a review. WRC Report No. TT 224/04. Water Research Commission, Pretoria

Dansgaard, W., 1964. Stable isotopes in precipitation. Tellus 16, 436–468.

De Boer-Euser, T., Bouaziz, L., De Niel, J., Brauer, C., Dewals, B., Drogue, G., Fenicia, F., Grelier, B., Nossent, J., Pereira, F., Savenije, H., Thirel, G., Willems, P., 2017. Looking beyond general metrics for model comparison – Lessons from an international model intercomparison study. Hydrol. Earth Syst. Sci. 21, 423–440. https://doi.org/10.5194/hess-21-423-2017

Devia, G.K., Ganasri, B.P., Dwarakish, G.S., 2015. A Review on Hydrological Models. Aquat. Procedia 4, 1001–1007. https://doi.org/10.1016/j.aqpro.2015.02.126

Diamond, R., 2014. Stable Isotope Hydrology of the Table Mountain Group. PhD. Unpublished 1–207.

Doody, T.M., Nagler, P.L., Glenn, E.P., Moore, G.W., Morino, K., Hultine, K.R., Benyon, R.G., 2011. Potential for water salvage by removal of non-native woody vegetation from dryland river systems. Hydrol. Process. 25, 4117–4131. https://doi.org/10.1002/hyp.8395

Dye, P., Jarmain, C., 2004. Water use by black wattle (Acacia mearnsii): Implications for the link between removal of invading trees and catchment streamflow response. S. Afr. J. Sci. 100, 40–44.

Dye, P., Moses, G., Vilakazi, P., Ndlela, R., Royappen, M., 2001. Comparative water use of wattle thickets and indigenous plant communities at riparian sites in the Western Cape and KwaZulu-Natal. Water SA 27, 529–538. https://doi.org/10.4314/wsa.v27i4.4967

Dzikiti, S., Jovanovic, N.Z., Bugan, R., Israel, S., Le Maitre, D.C., 2014. Measurement and modelling of evapotranspiration in three fynbos vegetation types. Water SA 40, 189–198. https://doi.org/10.4314/wsa.v40i2.1

Eckhardt, K., 2005. How to construct recursive digital filters for baseflow separation. Hydrol. Process. 19, 507–515. https://doi.org/10.1002/hyp.5675

Edwards, T.W.D., Wolfe, B.B., Gibson, J.J., Hammarlund, D., 2007. Use of water isotope tracers in high latitude hydrology and paleohydrology. Long-term Environ. Chang. Arct. Antarct. Lakes 187–207. https://doi.org/10.1007/978-1-4020-2126-8_7

Euston-Brown, D., 2006. Baviaanskloof Mega-reserve project : Vegetation Mapping Contract : Report on methodology , vegetation classification and short descriptions of habitat units . Draft report 22 September 2006 1–35.

Everson CS, Gush MB, Moodley M, Jarmain C, Govender M, Dye P. 2007. Effective management of the riparian zone vegetation to significantly reduce the cost of catchment management and enable greater productivity of land resources. Report No. 1284/1/07. Pretoria: Water Research Commission.

Everson, C.S., Clulow, A.D., Becker, M., Watson, A., Ngubo, C., Bulcock, H., Mengistu, M., Lorentz, S., Demlie, M., 2014. The long term impact of Acacia mearnsii trees on evaporation, streamflow, low flows and ground water resources. Phase II: Understanding the controlling environmental variables and soil water processes over a full crop rotation.

Fan, J., Wang, Q., Jones, S.B., Shao, M., 2016. Soil water depletion and recharge under different land cover in China's Loess Plateau. Ecohydrology 9, 396–406. https://doi.org/10.1002/eco.1642

Farid, I., Trabelsi, R., Zouari, K., Beji, R., 2013. Geochemical and isotopic study of surface and groundwaters in Ain Bou Mourra basin, central Tunisia. Quat. Int. 303, 210–227. https://doi.org/10.1016/j.quaint.2013.04.021

Fenicia, F., Kavetski, D., Savenije, H.H.G., 2011. Elements of a flexible approach for conceptual hydrological modeling: 1. Motivation and theoretical development. Water Resour. Res. 47, 1–13. https://doi.org/10.1029/2010WR010174

Fenicia, F., Savenije, H.H.G., Matgen, P., Pfister, L., 2008. Understanding catchment behavior through stepwise model concept improvement. Water Resour. Res. 44, 1–13. https://doi.org/10.1029/2006WR005563

Fourie, F., Mbatha, K., Verster, H., Van Dyk, G., 2007. The effect of vegetation (Prosopis sp.) on groundwater levels in Rugseer River, Kenhardt, South Africa. Groundw. Ecosyst. XXXV IAH Congr. 8.

Funk, J.L., Nguyen, M.A., Standish, R.J., Stock, W.D., Valladares, F., 2017. Global resource acquisition patterns of invasive and native plant species do not hold at the regional scale in Mediterranean type ecosystems. Biol. Invasions 19, 1143–1151. https://doi.org/10.1007/s10530-016-1297-9

Galatowitsch, S., Richardson, D.M., 2005. Riparian scrub recovery after clearing of invasive alien trees in headwater streams of the Western Cape, South Africa. Biol. Conserv. 122, 509–521. https://doi.org/10.1016/j.biocon.2004.09.008

Gao, H., Hrachowitz, M., Fenicia, F., Gharari, S., Savenije, H.H.G., 2014. Testing the realism of a topography-driven model (FLEX-Topo) in the nested catchments of the Upper Heihe, China. Hydrol. Earth Syst. Sci. 18, 1895–1915. https://doi.org/10.5194/hess-18-1895-2014

Gao, X., Wu, P., Zhao, X., Wang, J., Shi, Y., 2014. Effects of land use on soil moisture variations in a semi-arid catchment: Implications for land and agricultural water management. L. Degrad. Dev. 25, 163–172. https://doi.org/10.1002/ldr.1156

Garcia, M., Portney, K., Islam, S., 2016. A question driven socio-hydrological modeling process. Hydrol. Earth Syst. Sci. 20, 73–92. https://doi.org/10.5194/hess-20-73-2016

Gharari, S., Hrachowitz, M., Fenicia, F., Gao, H., Savenije, H.H.G., 2014. Using expert knowledge to increase realism in environmental system models can dramatically reduce the need for calibration. Hydrol. Earth Syst. Sci. 18, 4839–4859. https://doi.org/10.5194/hess-18-4839-2014

Gharari, S., Hrachowitz, M., Fenicia, F., Savenije, H.H.G., 2011. Hydrological landscape classification: Investigating the performance of HAND based landscape classifications in a central European meso-scale catchment. Hydrol. Earth Syst. Sci. 15, 3275–3291. https://doi.org/10.5194/hess-15-3275-2011

Gibson, J.J., Yi, Y., Birks, S.J., 2016. Isotope-based partitioning of streamflow in the oil sands region, northern Alberta: Towards a monitoring strategy for assessing flow sources and water quality controls. J. Hydrol. Reg. Stud. 5, 131–148. https://doi.org/10.1016/j.ejrh.2015.12.062

Glenday, J. (2015). Modeling the Hydrologic Impacts of Vegetation and Channel Network Change for a Semi-arid, Mountainous, Meso-scale Catchment: the Baviaanskloof, South Africa. PhD dissertation. University of California Santa Barbara.

Goller, R., Wilcke, W., Leng, M., Tobschall, H.J., Wagner, K., Manosalvas, C., Zech, W., 2005.

Tracing Water Paths through Small Catchments Under a Tropical Montane Rain Forest in South Ecuador by an Oxygen Isotope Approach. J. Hydrol. 308, 67–80. https://doi.org/10.1016/j.jhydrol.2004.10.022

Gonzales, A.L., Nonner, J., Heijkers, J., Uhlenbrook, S., 2009. Comparison of different base flow separation methods in a lowland catchment. Hydrol. Earth Syst. Sci. 13, 2055–2068. https://doi.org/10.5194/hess-13-2055-2009

Görgens, A.H.M., Van Wilgen, B.W., 2004. Invasive alien plants and water resources in South Africa: Current understanding, predictive ability and research challenges. S. Afr. J. Sci. 100, 27–33.

Gou, J., Qu, S., Shi, P., Li, D., Chen, X., Wang, Y., Shan, S., Si, W., 2018. Application of stable isotope tracer to study runoff generation during different types of rainfall events. Water (Switzerland) 10, 1–14. https://doi.org/10.3390/w10050538

Graham, C.B., Van Verseveld, W., Barnard, H.R., McDonnell, J.J., 2010. Estimating the deep seepage component of the hillslope and catchment water balance within a measurement uncertainty framework. Hydrol. Process. 24, 3631–3647. https://doi.org/10.1002/hyp.7788

Grande, E., Visser, A., Moran, J.E., 2020. Catchment storage and residence time in a periodically irrigated watershed. Hydrol. Process. 34, 3028–3044. https://doi.org/10.1002/hyp.13798

Greeff, G.J., 1994. Groundwater Contribution to Stream Salinity in a Shale Catchment, R.S.A. Ground Water 32, 63–70.

Guo, X., Tian, L., Wang, L., Yu, W., Qu, D., 2017. River recharge sources and the partitioning of catchment evapotranspiration fluxes as revealed by stable isotope signals in a typical high-elevation arid catchment. J. Hydrol. 549, 616–630. https://doi.org/10.1016/j.jhydrol.2017.04.037

Gyamfi, C., Ndambuki, J.M., Salim, R.W., 2016. Hydrological responses to land use/cover changes in the Olifants Basin, South Africa. Water (Switzerland) 8. https://doi.org/10.3390/w8120588

Haigh, E. A., P. L. Grundling, and P. M. Illgner (2002), Report on the scoping study on the status of the Kromme river peatland complex and recommended mitigatory measures. Department of Water Affairs and Forestry Project X832633.

Haigh, L., Illgner, P., Wilmot, J., Buckle, J., Kotze, D., Ellery, W., 2008. WET-OutcomesEvaluate. WET-OutcomeEvaluate Wetl. Rehabil. Proj. Kromme River Wetl. East. Cape WRC Report, 109–169.

Hamutoko, J.T., Wanke, H., Koeniger, P., Beyer, M., Gaj, M., 2017. Hydrogeochemical and isotope study of perched aquifers in the Cuvelai-Etosha Basin, Namibia. Isotopes Environ.

Health Stud. 53, 382–399. https://doi.org/10.1080/10256016.2016.1273913

Hao, S., Li, F., Li, Y., Gu, C., Zhang, Q., Qiao, Y., Jiao, L., Zhu, N., 2019. Stable isotope evidence for identifying the recharge mechanisms of precipitation, surface water, and groundwater in the Ebinur Lake basin. Sci. Total Environ. 657, 1041–1050. https://doi.org/10.1016/j.scitotenv.2018.12.102

Hargreaves, G.H., Samani, Z.A., 1985. Reference Crop Evapotranspiration From Ambient Air Temperature. Pap. - Am. Soc. Agric. Eng. 96–99.

He, Z., Zhao, W., Liu, H., Chang, X., 2012. The response of soil moisture to rainfall event size in subalpine grassland and meadows in a semi-arid mountain range: A case study in northwestern China's Qilian Mountains. J. Hydrol. 420–421, 183–190. https://doi.org/10.1016/j.jhydrol.2011.11.056

Heisler-White, J.L., Knapp, A.K., Kelly, E.F., 2008. Increasing precipitation event size increases aboveground net primary productivity in a semi-arid grassland. Oecologia 158, 129–140. https://doi.org/10.1007/s00442-008-1116-9

Heuzé V., Tran G., Boval M., 2015. Kikuyu (Pennisetum clandestinum). Feedipedia, a programme by INRAE, CIRAD, AFZ and FAO. https://www.feedipedia.org/node/398 Last updated on July 13, 2015, 16:11

Hipsey, M.R., Vogwill, R., Farmer, D., Busch, B.D., 2011. A multi-scale ecohydrological model for assessing floodplain wetland response to altered flow regimes. MODSIM 2011 - 19th Int. Congr. Model. Simul. - Sustain. Our Futur. Underst. Living with Uncertain. 3712–3718. https://doi.org/10.36334/modsim.2011.i7.hipsey

Hishinuma, S., Takeuchi, K., Magome, J., 2014. Défis de l"analyse hydrologique pour le développement des ressources en eau dans les régions montagneuses semi-arides: Étude de cas en Iran. Hydrol. Sci. J. 59, 1718–1737. https://doi.org/10.1080/02626667.2013.853879

Hoeg, S., Uhlenbrook, S., Leibundgut, C., 2000. Hydrograph separation in a mountainous catchment - combining hydrochemical and isotopic tracers. Hydrol. Process. 14, 1199–1216. https://doi.org/10.1002/(SICI)1099-1085(200005)14:7<1199::AID-HYP35>3.0.CO;2-K

Hong, Y., Adler, R.F., Hossain, F., Curtis, S., Huffman, G.J., 2007. A first approach to global runoff simulation using satellite rainfall estimation. Water Resour. Res. 43, 1–8. https://doi.org/10.1029/2006WR005739

Hood, J.L., Hayashi, M., 2015. Characterization of snowmelt flux and groundwater storage in an alpine headwater basin. J. Hydrol. 521, 482–497. https://doi.org/10.1016/j.jhydrol.2014.12.041

Hou, G., Bi, H., Wei, X., Kong, L., Wang, N., Zhou, Q., 2018. Response of soil moisture to

single-rainfall events under three vegetation types in the Gully Region of the Loess Plateau. Sustain. 10. https://doi.org/10.3390/su10103793

Hrachowitz, M., Bohte, R., Mul, M.L., Bogaard, T.A., Savenije, H.H.G., Uhlenbrook, S., 2011. On the value of combined event runoff and tracer analysis to improve understanding of catchment functioning in a data-scarce semi-arid area. Hydrol. Earth Syst. Sci. 15, 2007–2024. https://doi.org/10.5194/hess-15-2007-2011

Hrachowitz, M., Clark, M., 2017. HESS Opinions: The complementary merits of top-down and bottom-up modelling philosophies in hydrology. Hydrol. Earth Syst. Sci. Discuss. 1–22. https://doi.org/10.5194/hess-2017-36

Hrachowitz, M., Savenije, H.H.G., Blöschl, G., McDonnell, J.J., Sivapalan, M., Pomeroy, J.W., Arheimer, B., Blume, T., Clark, M.P., Ehret, U., Fenicia, F., Freer, J.E., Gelfan, A., Gupta, H. V., Hughes, D.A., Hut, R.W., Montanari, A., Pande, S., Tetzlaff, D., Troch, P.A., Uhlenbrook, S., Wagener, T., Winsemius, H.C., Woods, R.A., Zehe, E., Cudennec, C., 2013. A decade of Predictions in Ungauged Basins (PUB)-a review. Hydrol. Sci. J. 58, 1198–1255. https://doi.org/10.1080/02626667.2013.803183

Hugenschmidt, C., Ingwersen, J., Sangchan, W., Sukvanachaikul, Y., Duffner, A., Uhlenbrook, S., Streck, T., 2014. A three-component hydrograph separation based on geochemical tracers in a tropical mountainous headwater catchment in northern Thailand. Hydrol. Earth Syst. Sci. 18, 525–537. https://doi.org/10.5194/hess-18-525-2014

Hughes, D.A., 2007. Modelling semi-arid and arid hydrology and water resources: The Southern African experience. Hydrol. Model. Arid Semi-Arid Areas 9780521869, 29–40. https://doi.org/10.1017/CBO9780511535734.004

Huxman, T.E., Wilcox, B.P., Breshears, D.D., Scott, R.L., Snyder, K.A., Small, E.E., Hultine, K., Pockman, W.T., Jackson, R.B., 2005. Ecohydrological implications of woody plant encroachment. Ecology 86, 308–319. https://doi.org/10.1890/03-0583

Iddi, S., 1998. Eastern Arc Mountains and Their National and Global Importance. J. East African Nat. Hist. 87, 19–26. https://doi.org/10.2982/0012-8317(1998)87[19:eamatn]2.0.co;2

Islam, Z., 2015. A Review on Water Resources Management Modeling on Water Resources Management Modeling Submitted by Zahidul Islam Department of Civil and Environmental Engineering University of Alberta April , 2011. https://doi.org/10.13140/2.1.4544.5924

Jackson, B., Wheater, H., McIntyre, N., 2008. Upscaling runoff from hillslope to catchment scale: a case study in an upland Welsh catchment. BHS 10th Natl. Hydrol. Symp. 268–274.

Jacobs, S., Naude, M., Slabbert, E., Kambaj, O., Fourie, M., Esler, K., Jacobs, K., Mantlana, B.,

Rozanov, A., Cowan, D., 2013. Identifying Relationships Between Soil Processes and Biodiversity to Improve Restoration of Riparian Ecotones Invaded by Exotic Acacias.

James, A.L., Roulet, N.T., 2009. Antecedent moisture conditions and catchment morphology as controls on spatial patterns of runoff generation in small forest catchments. J. Hydrol. 377, 351–366. https://doi.org/10.1016/j.jhydrol.2009.08.039

Jarmain C, Everson C. 2002. Comparative evaporation measurements above commercial forestry and sugar cane canopies in the KwaZulu-Natal Midlands. Report to Department of Water Affairs and Forestry, Division of Water, Environment and Forestry Technology. Pietermaritzburg: CSIR.

Jeelani, G., Bhat, N.A., Shivanna, K., 2010. Use of δ18O tracer to identify stream and spring origins of a mountainous catchment: A case study from Liddar watershed, Western Himalaya, India. J. Hydrol. 393, 257–264. https://doi.org/10.1016/j.jhydrol.2010.08.021

Job, N., Ellery, F., 2013. Policy brief: Halting degradation of Southern Cape peatlands in agricultural landscapes. POLICY BRIEF, Rhodes Univ. NUMBER 8 1–8.

Jovanovic, N.Z., Clercq, W.P. De, 2012. Burgan Study Area 38, 201–212.

Käser, D., Hunkeler, D., 2016. Contribution of alluvial groundwater to the outflow of mountainous catchments. Water Resour. Res. 52, 680–697. https://doi.org/10.1002/2014WR016730

Katsuyama, M., Tani, M., Nishimoto, S., 2010. Connection between streamwater mean residence time and bedrock groundwater recharge/discharge dynamics in weathered granite catchments. Hydrol. Process. 24, 2287–2299. https://doi.org/10.1002/hyp.7741

Kebede, S., Travi, Y., Rozanski, K., 2009. The d 18 O and d 2 H enrichment of Ethiopian lakes. J. Hydrol. 365, 173–182. https://doi.org/10.1016/j.jhydrol.2008.11.027

Keene, A., Bush, R., Erskine, W., 2007. Connectivity of stream water and alluvial groundwater around restoration works in an incised sand-bed stream. Management 187–192.

Kellner, E., Hubbart, J.A., 2016. Continuous and event-based time series analysis of observed floodplain groundwater flow under contrasting land-use types. Sci. Total Environ. 566–567, 436–445. https://doi.org/10.1016/j.scitotenv.2016.05.036

Klaus, J., McDonnell, J.J., 2013. Hydrograph separation using stable isotopes: Review and evaluation. J. Hydrol. 505, 47–64. https://doi.org/10.1016/j.jhydrol.2013.09.006

Kendall, C., Coplen, T.B., 2001. Distribution of oxygen-18 and deuteriun in river waters across the United States. Hydrol. Process. 15, 1363–1393. https://doi.org/10.1002/hyp.217

Kinoti, I.K., 2018. Integrated hydrological modeling of surface and groundwater interactions in Heuningnes catchment (South Africa).

Kohler, T., Maselli, D., 2009. Mountains and Climate Change: From Understanding to Action. Publ. by Geogr. Bernensia with Support Swiss Agency Dev. Coop. (SDC), an Int. team Contrib. Bern.

Kurth, A.M., Schirmer, M., 2014. Thirty years of river restoration in Switzerland: Implemented measures and lessons learned. Environ. Earth Sci. 72, 2065–2079. https://doi.org/10.1007/s12665-014-3115-y

Kurth, A.M., Weber, C., Schirmer, M., 2015. How effective is river restoration in re-establishing groundwater-surface water interactions? - A case study. Hydrol. Earth Syst. Sci. 19, 2663–2672. https://doi.org/10.5194/hess-19-2663-2015

Lambs, L., 2000. Correlation of conductivity and stable isotope 18O for the assessment of water origin in river system. Chem. Geol. 164, 161–170. https://doi.org/10.1016/S0009-2541(99)00140-0

Laudon, H., Seibert, J., Köhler, S., Bishop, K., 2004. Hydrological flow paths during snowmelt: Congruence between hydrometric measurements and oxygen 18 in meltwater, soil water, and runoff. Water Resour. Res. 40. https://doi.org/10.1029/2003WR002455

Le Maitre, D.C., Gush, M.B., Dzikiti, S., 2015. Impacts of invading alien plant species on water flows at stand and catchment scales. AoB Plants 7. https://doi.org/10.1093/aobpla/plv043

Le Maitre, D.C., Scott, D.F., Colvin, C., 1999. A review of information on interactions between vegetation and groundwater. Water SA 25, 137–152.

Le Maitre, D.C., Versfeld, D.B., Chapman, R.A., 2000. The impact of invading alien plants on surface water resources in South Africa: A preliminary assessment. Water SA 26, 397–408.

le roux, P.A.., Hensley, M., Lorentz, S.A., van Tol, J.J., van Zijl, G.M., Kuenene, B.T., Bouwer, D., Freese, C.S., Tinnefeld, M., Jacobs, C.C., 2015. HOSAH (Hydrology ofSouth African Soils and Hillslopes).

Legates, D.R., Mahmood, R., Levia, D.F., DeLiberty, T.L., Quiring, S.M., Houser, C., Nelson, F.E., 2011. Soil moisture: A central and unifying theme in physical geography. Prog. Phys. Geogr. 35, 65–86. https://doi.org/10.1177/0309133310386514

Leta, M.K., Demissie, T.A., Tränckner, J., 2021. Modeling and prediction of land use land cover change dynamics based on land change modeler (Lcm) in nashe watershed, upper blue nile basin, Ethiopia. Sustain. 13. https://doi.org/10.3390/su13073740

Li, F., Song, X., Tang, C., Liu, C., Yu, J., Zhang, W., 2007. Tracing infiltration and recharge using stable isotope in Taihang Mt., North China 52. https://doi.org/10.1007/s00254-007-0744-4

Li, J., Liu, D., Wang, T., Li, Y., Wang, S., Yang, Y., Wang, X., Guo, H., Peng, S., Ding, J., Shen, M.,

Wang, L., 2017. Grassland restoration reduces water yield in the headstream region of Yangtze River. Sci. Rep. 7, 1–9. https://doi.org/10.1038/s41598-017-02413-9

Lin, L., Jia, H., Xu, Y., 2007. Fracture network characteristics of a deep borehole in the Table Mountain Group (TMG), South Africa. Hydrogeol. J. 15, 1419–1432. https://doi.org/10.1007/s10040-007-0184-y

López-Moreno, J.I., García-Ruiz, J.M., 2004. Influence of snow accumulation and snowmelt on streamflow in the central Spanish Pyrenees / Influence de l'accumulation et de la fonte de la neige sur les écoulements dans les Pyrénées centrales espagnoles. Hydrol. Sci. J. 49. https://doi.org/10.1623/hysj.49.5.787.55135

Lucianetti, G., Penna, D., Mastrorillo, L., Mazza, R., 2020. The role of snowmelt on the spatio-temporal variability of spring recharge in a dolomitic mountain group, Italian alps. Water (Switzerland) 12. https://doi.org/10.3390/w12082256

Lutz, S.R., Krieg, R., Müller, C., Zink, M., Knöller, K., Samaniego, L., Merz, R., 2018. Spatial Patterns of Water Age: Using Young Water Fractions to Improve the Characterization of Transit Times in Contrasting Catchments. Water Resour. Res. 54, 4767–4784. https://doi.org/10.1029/2017WR022216

Lynch, S., 2004. Development of a raster database of annula, monthly and daily rainfall for southern Africa. Water Res. Comm. 108.

Lyne, V., 2015. Stochastic Time-Variable Rainfall-Runoff Modeling.

Madlala, T., Kanyerere, T., Oberholster, P., Xu, Y., 2019. Application of multi-method approach to assess groundwater–surface water interactions, for catchment management. Int. J. Environ. Sci. Technol. 16, 2215–2230. https://doi.org/10.1007/s13762-018-1819-3

Mander, M., Blignaut, J., Van Niekerk, M., Cowling, R., M, H., D, K., Mills, A., Powell, M., Schulze, R., 2010. Baviaanskloof - Tsitsikamma Payment for Ecosystem Services: a Feasibility Assessment 1–53.

Martinez, J.L., Raiber, M., Cendón, D.I., 2017. Using 3D geological modelling and geochemical mixing models to characterise alluvial aquifer recharge sources in the upper Condamine River catchment, Queensland, Australia. Sci. Total Environ. 574, 1–18. https://doi.org/10.1016/j.scitotenv.2016.09.029

Maurya, A.S., Shah, M., Deshpande, R.D., Bhardwaj, R.M., Prasad, A., Gupta, S.K., 2011. Hydrograph separation and precipitation source identification using stable water isotopes and conductivity: River Ganga at Himalayan foothills. Hydrol. Process. 25, 1521–1530. https://doi.org/10.1002/hyp.7912

Mazvimavi, D., Stein, A., Meijerink, A.M.J., Savenije, H.H.G., 2003. Estimation of flow

characteristics of ungauged catchments : a case study in Zimbabwe, Wageningen University PhD thesis and inernational Research Centre; Summaries in Dutch and EnglishITC Dissertation.

McConnachie, M.M., Cowling, R.M., van Wilgen, B.W., McConnachie, D.A., 2012. Evaluating the cost-effectiveness of invasive alien plant clearing: A case study from South Africa. Biol. Conserv. 155, 128–135. https://doi.org/10.1016/j.biocon.2012.06.006

Mcdonnell, J., Rowe, L., Stewart, M., 1999. A combined tracer-hydrometric approach to assess the effect of catchment scale on water flow path, source and age. IAHS-AISH Publ. 265–273.

McDonnell, J.J., Kendall, C., 1992. Isotope tracers in hydrology. Eos, Trans. Am. Geophys. Union 73, 260–260. https://doi.org/10.1029/91e000214

McDonnell, J.J., Tanaka, T., 2001. On the future of forest hydrology and biogeochemistry. Hydrol. Process. 15, 2053–2055. https://doi.org/10.1002/hyp.493

McGlynn, B.L., McDonnell, J.J., Seibert, J., Kendall, C., 2004. Scale effects on headwater catchment runoff timing, flow sources, and groundwater-streamflow relations. Water Resour. Res. 40. https://doi.org/10.1029/2003WR002494

McGuire, K.J., McDonnell, J.J., 2010. Hydrological connectivity of hillslopes and streams: Characteristic time scales and nonlinearities. Water Resour. Res. 46, 1–17. https://doi.org/10.1029/2010WR009341

McMillan, H.K., Clark, M.P., Bowden, W.B., Duncan, M., Woods, R.A., 2011. Hydrological field data from a modeller's perspective: Part 1. Diagnostic tests for model structure. Hydrol. Process. 25, 511–522. https://doi.org/10.1002/hyp.7841

Meijninger, W.M.L., Jarmain, C., 2014. Satellite-based annual evaporation estimates of invasive alien plant species and native vegetation in South Africa. Water SA 40, 95–107. https://doi.org/10.4314/wsa.v40i1.12

Merz, R., Blöschl, G., 2009. A regional analysis of event runoff coefficients with respect to climate and catchment characteristics in Austria. Water Resour. Res. 45, 1–19. https://doi.org/10.1029/2008WR007163

Midgley, J., Scott, D., 1994. Use of stable isotopes of water (d and o-18) in hydrological studies in the Jonkershoek valley.

Misra, A.K., 2014. Climate change and challenges of water and food security. Int. J. Sustain. Built Environ. 3, 153–165. https://doi.org/10.1016/j.ijsbe.2014.04.006

Mockler, E.M., O'Loughlin, F.E., Bruen, M., 2016. Understanding hydrological flow paths in conceptual catchment models using uncertainty and sensitivity analysis. Comput. Geosci.

90, 66–77. https://doi.org/10.1016/j.cageo.2015.08.015

Mokua, R.A., Glenday, J., Nel, J., Butler, M., 2020. Combined use of stable isotopes and hydrochemical characteristics to determine streamflow sources in the Jonkershoek catchment, South Africa. Isotopes Environ. Health Stud. 56, 238–259. https://doi.org/10.1080/10256016.2020.1760861

Molina, A., Govers, G., Vanacker, V., Poesen, J., Zeelmaekers, E., Cisneros, F., 2007. Runoff generation in a degraded Andean ecosystem: Interaction of vegetation cover and land use. Catena 71, 357–370. https://doi.org/10.1016/j.catena.2007.04.002

Montanari, A., Young, G., Savenije, H.H.G., Hughes, D., Wagener, T., Ren, L.L., Koutsoyiannis, D., Cudennec, C., Toth, E., Grimaldi, S., Blöschl, G., Sivapalan, M., Beven, K., Gupta, H., Hipsey, M., Schaefli, B., Arheimer, B., Boegh, E., Schymanski, S.J., Di Baldassarre, G., Yu, B., Hubert, P., Huang, Y., Schumann, A., Post, D.A., Srinivasan, V., Harman, C., Thompson, S., Rogger, M., Viglione, A., McMillan, H., Characklis, G., Pang, Z., Belyaev, V., 2013. "Panta Rhei-Everything Flows": Change in hydrology and society-The IAHS Scientific Decade 2013-2022. Hydrol. Sci. J. 58, 1256–1275. https://doi.org/10.1080/02626667.2013.809088

Morán-Tejeda, E., Zabalza, J., Rahman, K., Gago-Silva, A., López-Moreno, J.I., Vicente-Serrano, S., Lehmann, A., Tague, C.L., Beniston, M., 2015. Hydrological impacts of climate and land-use changes in a mountain watershed: Uncertainty estimation based on model comparison. Ecohydrology 8, 1396–1416. https://doi.org/10.1002/eco.1590

Morris, T.L., Esler, K.J., Barger, N.N., Jacobs, S.M., Cramer, M.D., 2011. Ecophysiological traits associated with the competitive ability of invasive Australian acacias. Divers. Distrib. 17, 898–910. https://doi.org/10.1111/j.1472-4642.2011.00802.x

Mosquera, G.M., Segura, C., Crespo, P., 2018. Flow partitioning modelling using high-resolution isotopic and electrical conductivity data. Water (Switzerland) 10, 1–23. https://doi.org/10.3390/w10070904

Moyo, H.P.M., Dube, S., Fatunbi, A.O., 2009. Impact of the removal of black wattle (*Acacia mearnsii*) in the Tsomo Valley in Eastern Cape: consequences on the water recharge and soil dynamics (an ongoing study). Grassroots Newsl. Grassl. Soc. South. Africa. 9, 38–41.

Mucina, L., Rutherford, M.C., 2006. The vegetation of South Africa, Lesotho and Swaziland. Strelitzia 19 1–30.

Mueller, M.H., Weingartner, R., Alewell, C., 2013. Importance of vegetation, topography and flow paths for water transit times of base flow in alpine headwater catchments. Hydrol. Earth Syst. Sci. 17, 1661–1679. https://doi.org/10.5194/hess-17-1661-2013

Muhar, S., Januschke, K., Kail, J., Poppe, M., Schmutz, S., Hering, D., Buijse, A.D., 2016. Evaluating good-practice cases for river restoration across Europe: context, methodological framework, selected results and recommendations. Hydrobiologia 769, 3–19. https://doi.org/10.1007/s10750-016-2652-7

Mul, M.L., Mutiibwa, R.K., Uhlenbrook, S., Savenije, H.H.G., 2008. Hydrograph separation using hydrochemical tracers in the Makanya catchment, Tanzania. Phys. Chem. Earth 33, 151–156. https://doi.org/10.1016/j.pce.2007.04.015

Mul, M.L., Savenije, H.H.G., Uhlenbrook, S., 2009. Spatial rainfall variability and runoff response during an extreme event in a semi-arid catchment in the South Pare Mountains, Tanzania. Hydrol. Earth Syst. Sci. 13, 1659–1670. https://doi.org/10.5194/hess-13-1659-2009

Mulvany, T.J., 1850. On the use of self registering rain and flood gauges. Inst. Civ. Eng. Proc. (Dublin), 4, 1-8.

Munyaneza, O., Wenninger, J., Uhlenbrook, S., 2012. Identification of runoff generation processes using hydrometric and tracer methods in a meso-scale catchment in Rwanda. Hydrol. Earth Syst. Sci. 16, 1991–2004. https://doi.org/10.5194/hess-16-1991-2012

Nathan, R.J., McMahon, T.A., 1990. Evaluation of automated techniques for base flow and recession analyses. Water Resour. Res. 26, 1465–1473. https://doi.org/10.1029/WR026i007p01465

Neachell, E., 2014. Book Review - Environmental flows: Saving rivers in the thrid millennium. River Res. Appl. 30, 132–133. https://doi.org/10.1002/rra

Nijzink, R., Hutton, C., Pechlivanidis, I., Capell, R., Arheimer, B., Freer, J., Han, D., Wagener, T., McGuire, K., Savenije, H., Hrachowitz, M., 2016. The evolution of root-zone moisture capacities after deforestation: A step towards hydrological predictions under change? Hydrol. Earth Syst. Sci. 20, 4775–4799. https://doi.org/10.5194/hess-20-4775-2016

Niu, C.Y., Musa, A., Liu, Y., 2015. Analysis of soil moisture condition under different land uses in the arid region of Horqin sandy land, northern China. Solid Earth 6, 1157–1167. https://doi.org/10.5194/se-6-1157-2015

Nobre, A.D., Cuartas, L.A., Hodnett, M., Rennó, C.D., Rodrigues, G., Silveira, A., Waterloo, M., Saleska, S., 2011. Height Above the Nearest Drainage - a hydrologically relevant new terrain model. J. Hydrol. 404, 13–29. https://doi.org/10.1016/j.jhydrol.2011.03.051

Nóia Júnior, R.D.S., Fraisse, C.W., Cerbaro, V.A., Karrei, M.A.Z., Guindin, N., 2019. Evaluation of the Hargreaves-Samani Method for Estimating Reference Evapotranspiration with Ground and Gridded Weather Data Sources. Appl. Eng. Agric. 35, 823–835.

https://doi.org/10.13031/aea.13363
Nolin, A.W., 2012. Perspectives on climate change, mountain hydrology, and water resources in the Oregon Cascades, USA. Mt. Res. Dev. 32. https://doi.org/10.1659/MRD-JOURNAL-D-11-00038.S1
Nsor, C., Gambiza, J., 2013. Land Use Changes and Their Impacts on the Vegetation Kromme River Peat Basin, South Africa. Sci. J. Environ. Eng. https://doi.org/10.7237/sjeer/166
Ocampo, C.J., Sivapalan, M., Oldham, C., 2006. Hydrological connectivity of upland-riparian zones in agricultural catchments: Implications for runoff generation and nitrate transport. J. Hydrol. 331, 643–658. https://doi.org/10.1016/j.jhydrol.2006.06.010
Ochoa, C.G., Guldan, S.J., Cibils, A.F., Lopez, S.C., Boykin, K.G., Tidwell, V.C., Fernald, A.G., 2013. Hydrologic Connectivity of Head Waters and Floodplains in a Semi-Arid Watershed. J. Contemp. Water Res. Educ. 152, 69–78. https://doi.org/10.1111/j.1936-704x.2013.03169.x
Okello, A.M.L.S., Masih, I., Uhlenbrook, S., Jewitt, G.P.W., Van der Zaag, P. V., 2018. Improved process representation in the simulation of the hydrology of a meso-scale semi-arid catchment. Water (Switzerland) 10. https://doi.org/10.3390/w10111549
Okin, G.S., De Las Heras, M.M., Saco, P.M., Throop, H.L., Vivoni, E.R., Parsons, A.J., Wainwright, J., Peters, D.P.C., 2015. Connectivity in dryland landscapes: Shifting concepts of spatial interactions. Front. Ecol. Environ. 13, 20–27. https://doi.org/10.1890/140163
Orlova, J., Branfireun, B., 2014. Surface water and groundwater contributions to streamflow in the James Bay Lowland, Canada. Arctic, Antarct. Alp. Res. 46, 236–250. https://doi.org/10.1657/1938-4246-46.1.236
Orth, R., Staudinger, M., Seneviratne, S.I., Seibert, J., Zappa, M., 2015. Does model performance improve with complexity? A case study with three hydrological models. J. Hydrol. 523, 147–159. https://doi.org/10.1016/j.jhydrol.2015.01.044
Otte, I., Detsch, F., Gütlein, A., Scholl, M., Kiese, R., Appelhans, T., Nauss, T., 2017. Seasonality of stable isotope composition of atmospheric water input at the southern slopes of Mt. Kilimanjaro, Tanzania. Hydrol. Process. 31, 3932–3947. https://doi.org/10.1002/hyp.11311
Owolabi, S.T., Madi, K., Kalumba, A.M., Alemaw, B.F., 2020. Assessment of recession flow variability and the surficial lithology impact: a case study of Buffalo River catchment, Eastern Cape, South Africa. Environ. Earth Sci. 79. https://doi.org/10.1007/s12665-020-08925-4
Penna, D., Engel, M., Mao, L., Dell'agnese, A., Bertoldi, G., Comiti, F., 2014. Tracer-based analysis of spatial and temporal variations of water sources in a glacierized catchment.

Hydrol. Earth Syst. Sci. 18, 5271–5288. https://doi.org/10.5194/hess-18-5271-2014

Penna, D., Tromp-Van Meerveld, H.J., Gobbi, A., Borga, M., Dalla Fontana, G., 2011. The influence of soil moisture on threshold runoff generation processes in an alpine headwater catchment. Hydrol. Earth Syst. Sci. 15, 689–702. https://doi.org/10.5194/hess-15-689-2011

Penna, D., van Meerveld, H.J., Oliviero, O., Zuecco, G., Assendelft, R.S., Dalla Fontana, G., Borga, M., 2015. Seasonal changes in runoff generation in a small forested mountain catchment. Hydrol. Process. 29, 2027–2042. https://doi.org/10.1002/hyp.10347

Perkins, K.S., Nimmo, J.R., Medeiros, A.C., Szutu, D.J., von Allmen, E., 2014. Assessing effects of native forest restoration on soil moisture dynamics and potential aquifer recharge, Auwahi, Maui. Ecohydrology 7, 1437–1451. https://doi.org/10.1002/eco.1469

Pinder, G., Jones, J., 1969. Determination of the ground-water component of peak discharge from the chemistry of total runoff. Water Resour. Res. 5 (2), 438–445. Pionke, H.B., Gburek, W.J., Folmar, G.J., 1993. Quantifying stormflow components in a Pennsylvania 184 watershed when 18O input and storm conditions vary. J. Hydrol. 148 (1–4), 169–187.

Pietersen, A. 2009. A fluvial geomorphological study of river rehabilitation in the Kouga region, Eastern Cape. Unpublished thesis, Master of Science. Rhodes University

Poeppl, R.E., Dilly, L.A., Haselberger, S., Renschler, C.S., Baartman, J.E.M., 2019. Combining soil erosion modeling with connectivity analyses to assess lateral fine sediment input into agricultural streams. Water (Switzerland) 11. https://doi.org/10.3390/w11091793

Powell, M., Mander, M., 2009. Baviaans- Tsitsikamma Payment for Ecosystem Services: Water Services Suppliers Report 39.

Price, K., 2011. Effects of watershed topography, soils, land use, and climate on baseflow hydrology in humid regions: A review. Prog. Phys. Geogr. 35, 465–492. https://doi.org/10.1177/0309133311402714

Prucha, B., Graham, D., Watson, M., Avenant, M., Esterhuyse, S., Joubert, A., Kemp, M., King, J., Le Roux, P., Redelinghuys, N., Rossouw, L., Rowntree, K., Seaman, M., Sokolic, F., Van Rensburg, L., Van Der Waal, B., Van Tol, J., Vos, T., 2016. MIKE-SHE integrated groundwater and surface water model used to simulate scenario hydrology for input to DRIFT-ARID: The Mokolo River case study. Water SA 42, 384–398. https://doi.org/10.4314/wsa.v42i3.03

Pulley, S., Lagesse, J., Ellery, W., 2017. The mineral magnetic signatures of fire in the Kromrivier wetland, South Africa. J. Soils Sediments 17, 1170–1181. https://doi.org/10.1007/s11368-016-1577-0

Raiber, M., Lewis, S., Cendón, D.I., Cui, T., Cox, M.E., Gilfedder, M., Rassam, D.W., 2019.

Significance of the connection between bedrock, alluvium and streams: A spatial and temporal hydrogeological and hydrogeochemical assessment from Queensland, Australia. J. Hydrol. 569, 666–684. https://doi.org/10.1016/j.jhydrol.2018.12.020

Railoun, M.Z., 2018. Impacts of the invasive tree Acacia mearnsii on riparian and instream aquatic environments in the Cape Floristic Region , South Africa 1–112.

Ramatsabana, P., Tanner, J., Mantel, S., Palmer, A., Ezenne, G., 2019. Evaluation of remote-sensing based estimates of actual evapotranspiration over (Diverse shape and sized) palmiet wetlands. Geosci. 9. https://doi.org/10.3390/geosciences9120491

Rangecroft, S., Birkinshaw, S., Rohse, M., Day, R., McEwen, L., Makaya, E., Van Loon, A.F., 2018. Hydrological modelling as a tool for interdisciplinary workshops on future drought. Prog. Phys. Geogr. 42, 237–256. https://doi.org/10.1177/0309133318766802

Raubenheimer CM and Day JA (1991) In vitro leaching of two sclerophyllous fynbos plants. Hydrobiologia 224 167–174. https://doi. org/10.1007/bf00008466

Rebelo, A.J., 2012. An ecological and hydrological evaluation of the effects of restoration on ecosystem services in the Kromme River system, South Africa. Conserv. Ecol. Fac. Agriscience MSc, 217.

Rebelo, A.J., Le Maitre, D.C., Esler, K.J., Cowling, R.M., 2015. Hydrological responses of a valley-bottom wetland to land-use/land-cover change in a South African catchment: Making a case for wetland restoration. Restor. Ecol. 23, 829–841. https://doi.org/10.1111/rec.12251

Rebelo, A.J., Morris, C., Meire, P., Esler, K.J., 2019. Ecosystem services provided by South African palmiet wetlands: A case for investment in strategic water source areas. Ecol. Indic. 101, 71–80. https://doi.org/10.1016/j.ecolind.2018.12.043

Refsgaard, J.C., Hansen, J.R., 2010. Un modèle capable de changer la lourdeur de la queue d'une fonction de distribution de probabilité. Hydrol. Sci. J. 55, 899–912. https://doi.org/10.1080/02626667.2010.505571

Riddell, E.S., Nel, J., van Tol, J., Fundisi, D., Jumbi, F., van Niekerk, A., Lorentz, S., 2020. Groundwater–surface water interactions in an ephemeral savanna catchment, Kruger National Park. Koedoe 62, 1–14. https://doi.org/10.4102/koedoe.v62i2.1583

Ries, F., Lange, J., Schmidt, S., Puhlmann, H., Sauter, M., 2015. Recharge estimation and soil moisture dynamics in a Mediterranean, semi-arid karst region. Hydrol. Earth Syst. Sci. 19, 1439–1456. https://doi.org/10.5194/hess-19-1439-2015

Rimmer, A., Hartmann, A., 2014. Optimal hydrograph separation filter to evaluate transport routines of hydrological models. J. Hydrol. 514, 249–257.

https://doi.org/10.1016/j.jhydrol.2014.04.033

Roets, W., Xu, Y., Raitt, L., Brendonck, L., 2008. Groundwater discharges to aquatic ecosystems associated with the Table Mountain Group (TMG) aquifer: A conceptual model. Water SA 34, 77–88. https://doi.org/10.4314/wsa.v34i1.180863

Rosewarne, P 2002. Case study: Hex River valley. In: A synthesis of the hydrogeology of the Table Mountain Group – formation of a research strategy (eds K. Pietersen and R Parsons), pp 178-182. Report No. TT 158/01, Water Research Commission, Pretoria

Roy, J.W., Hayashi, M., 2007. Groundwater-surface water exchange in alpine and subalpine watersheds: A review of recent field studies. IAHS-AISH Publ. 3–16.

Rupp, D.E., Selker, J.S., 2006. On the use of the Boussinesq equation for interpreting recession hydrographs from sloping aquifers. Water Resour. Res. 42, 1–15. https://doi.org/10.1029/2006WR005080

Salemi, L.F., Groppo, J.D., Trevisan, R., Marcos de Moraes, J., de Paula Lima, W., Martinelli, L.A., 2012. Riparian vegetation and water yield: A synthesis. J. Hydrol. 454–455, 195–202. https://doi.org/10.1016/j.jhydrol.2012.05.061

Sanyal, J., Densmore, A.L., Carbonneau, P., 2014. Analysing the effect of land-use/cover changes at sub-catchment levels on downstream flood peaks: A semi-distributed modelling approach with sparse data. Catena 118, 28–40. https://doi.org/10.1016/j.catena.2014.01.015

Saraiva Okello, A.M.L., Uhlenbrook, S., Jewitt, G.P.W., Masih, I., Riddell, E.S., Van der Zaag, P., 2018. Hydrograph separation using tracers and digital filters to quantify runoff components in a semi-arid mesoscale catchment. Hydrol. Process. 32, 1334–1350. https://doi.org/10.1002/hyp.11491

Savenije, H.H.G., 2010. HESS opinions "topography driven conceptual modelling (FLEX-Topo)." Hydrol. Earth Syst. Sci. 14, 2681–2692. https://doi.org/10.5194/hess-14-2681-2010

Savenije, H.H.G., 2009. HESS Opinions. Earth 157–161.

Scanlon, B.R., Reedy, R.C., Stonestrom, D.A., Prudic, D.E., Dennehy, K.F., 2005. Impact of land use and land cover change on groundwater recharge and quality in the southwestern US. Glob. Chang. Biol. 11, 1577–1593. https://doi.org/10.1111/j.1365-2486.2005.01026.x

Schilling, K.E., 2009. Hydrological processes inferred from water table fluctuations, Walnut Creek, Iowa 172.

Schulze, R. E. (1995).Hydrology and agrohydrology: a text to accompany the ACRU 3.00 agrohydrological modelling system. Pietermaritzburg, Dept. of Agricultural Engineering, University of Natal.

Schulze, R.E., 2000. Modelling Hydrological Responses to Land Use and Climate Change: A Southern African Perspective. AMBIO A J. Hum. Environ. 29, 12. https://doi.org/10.1639/0044-7447(2000)029[0012:mhrtlu]2.0.co;2

Schulze RE (2007). Climate Change and the Agriculture Sector in South Africa: An Assessment of Findings in the New Millennium. University of KwaZulu-Natal, Pietermaritzburg, RSA, School of Bioresources Engineering and Environmental Hydrology, ACRUcons Report, 55. pp71.

She, D.L., Shao, M.A., Timm, L.C., SentíS, I.P., Reichardt, K., Yu, S.E., 2010. Impacts of land-use pattern on soil water-content variability on the loess plateau of China. Acta Agric. Scand. Sect. B Soil Plant Sci. 60, 369–380. https://doi.org/10.1080/09064710903049334

Sieben, E.J.J., 2012. Plant functional composition and ecosystem properties: The case of peatlands in South Africa. Plant Ecol. 213, 809–820. https://doi.org/10.1007/s11258-012-0043-3

Singha, K., Li, L., Day-Lewis, F.D., Regberg, A.B., 2011. Quantifying solute transport processes: Are chemically "conservative" tracers electrically conservative? Geophysics 76. https://doi.org/10.1190/1.3511356

Slater, L.J., Khouakhi, A., 2019. River channel conveyance capacity adjusts to modes of climate variability. Sci. Rep. 1–10. https://doi.org/10.1038/s41598-019-48782-1

Smakhtin, V.U., 2001. Estimating continuous monthly baseflow time series and their possible applications in the context of the ecological reserve. Water SA 27, 213–217. https://doi.org/10.4314/wsa.v27i2.4995

Smart, M.C. and Tredoux, G. (2002). Groundwater Quality and Fitness for Use. In: K. Pietersen and R. Parsons (eds.) A Synthesis of the Hydrogeology of the Table Mountain Group – Formation of a Research Strategy. WRC Report No. TT 158/01, WRC, Pretoria, pp. 118-123

Smith ME, Clarke S and Cave LC (2002) Chemical evolution of Table Mountain Group groundwater and the source of iron. Proc. Conf. Ground Water Division. Sept. 2002, Somerset West, South Africa. 47-52

Smith, C., 2019. Determining the Hydrological Functioning of the Palmiet Wetlands in the Eastern and Western Cape of South Africa 1–135.

Smith, C.J., Tanner, J., 2019. Palmiet Wetland Sustainability : A Hydrological And Geomorphological Perspective On System Functioning Palmiet Wetland Sustainability : A Hydrological And Geomorphological Perspective On System Functioning Report to the Water Research Commission by JL Tan.

Somers, L.D., McKenzie, J.M., 2020. A review of groundwater in high mountain environments.

Wiley Interdiscip. Rev. Water 7, 1–27. https://doi.org/10.1002/wat2.1475

Song, X., Liu, X., Xia, J., Yu, J., Tang, C., 2006. A study of interaction between surface water and groundwater using environmental isotope in Huaisha River basin. Sci. China, Ser. D Earth Sci. 49, 1299–1310. https://doi.org/10.1007/s11430-006-1299-z

Soulsby, C., Birkel, C., Tetzlaff, D., 2016. Modelling storage-driven connectivity between landscapes and riverscapes: towards a simple framework for long-term ecohydrological assessment. Hydrol. Process. 30, 2482–2497. https://doi.org/10.1002/hyp.10862

Stoelzle, M., Schuetz, T., Weiler, M., Stahl, K., Tallaksen, L., 2019. Beyond binary baseflow separation: delayed flow index as a fresh perspective on streamflow contributions. Hydrol. Earth Syst. Sci. Discuss. 1–30. https://doi.org/10.5194/hess-2019-236

Stoelzle, M., Schuetz, T., Weiler, M., Stahl, K., Tallaksen, L.M., 2020. Beyond binary baseflow separation: a delayed-flow index for multiple streamflow contributions. Hydrol. Earth Syst. Sci. 24, 849–867. https://doi.org/10.5194/hess-24-849-2020

Tang, G., Carroll, R.W.H., Lutz, A., Sun, L., 2016. Regulation of precipitation-associated vegetation dynamics on catchment water balance in a semiarid and arid mountainous watershed. Ecohydrology 9, 1248–1262. https://doi.org/10.1002/eco.1723

Tanner, J.L. (Jane L., Hughes, D.A. (Denis A.., South Africa. Water Research Commission, 2015. Understanding and modelling surface water-groundwater interactions : report to the Water Research Commission.

Taylor, S.J., Ferguson, J.W.H., Engelbrecht, F.A., Clark, V.R., Van Rensburg, S., Barker, N., 2016. The Drakensberg Escarpment as the Great Supplier of Water to South Africa, in: Developments in Earth Surface Processes. pp. 1–46. https://doi.org/10.1016/B978-0-444-63787-1.00001-9

Tessema, A., Nzotta, U., Chirenje, E., 2014. Assessment of Groundwater Potential in Fractured Hard Rocks Around Vryburg, North West Province, South Africa.

Tetzlaff, D., Carey, S.K., Laudon, H., McGuire, K., 2010. Catchment processes and heterogeneity at multiple scales-benchmarking observations, conceptualization and prediction. Hydrol. Process. 24, 2203–2208. https://doi.org/10.1002/hyp.7784

Todini, E., 2007. Hydrological catchment modelling: Past, present and future. Hydrol. Earth Syst. Sci. 11, 468–482. https://doi.org/10.5194/hess-11-468-2007

Torbick, N., Lusch, D., Qi, J., Moore, N., Olson, J., ge, J., 2006. Developing land use/land cover parameterization for climate–land modeling in East Africa. Int. J. Remote Sens. - INT J Remote SENS 27, 4227–4244. https://doi.org/10.1080/01431160600702426

Uhlenbrook, S., Frey, M., Leibundgut, C., Maloszewski, P., 2002. Hydrograph separations in a

mesoscale mountainous basin at event and seasonal timescales. Water Resour. Res. 38, 31-1-31–14. https://doi.org/10.1029/2001wr000938

Uhlenbrook, S., Roser, S., Tilch, N., 2004. Hydrological process representation at the meso-scale: The potential of a distributed, conceptual catchment model. J. Hydrol. 291, 278–296. https://doi.org/10.1016/j.jhydrol.2003.12.038

van Griensven, A., Meixner, T., 2007. A global and efficient multi-objective auto-calibration and uncertainty estimation method for water quality catchmnt models. J. Hydroinformatics 9, 277–291. https://doi.org/10.2166/hydro.2007.104

van Tol, J.J., le Roux, P., Hensley, M., Lorentz, S.A., 2010. Soil as indicator of hillslope hydrological behaviour in the Weatherley Catchment, Eastern Cape, South Africa. Water SA 36, 513–520. https://doi.org/10.4314/wsa.v36i5.61985

Vitvar, T., Aggarwal, P.K., 1998. 12 . a Review of Isotope Applications in Catchment Hydrology. Isot. Hydrol. Sect. 1–19.

Viviroli, D., Archer, D.R., Buytaert, W., Fowler, H.J., Greenwood, G.B., Hamlet, A.F., Huang, Y., Koboltschnig, G., Litaor, M.I., López-Moreno, J.I., Lorentz, S., Schädler, B., Schreier, H., Schwaiger, K., Vuille, M., Woods, R., 2011. Climate change and mountain water resources: Overview and recommendations for research, management and policy. Hydrol. Earth Syst. Sci. 15, 471–504. https://doi.org/10.5194/hess-15-471-2011

Viviroli, D., Dürr, H.H., Messerli, B., Meybeck, M., Weingartner, R., 2007. Mountains of the world, water towers for humanity: Typology, mapping, and global significance. Water Resour. Res. 43, 1–13. https://doi.org/10.1029/2006WR005653

Viviroli, D., Weingartner, R., 2004. The hydrological significance of mountains: from regional to global scale. Hydrol. Earth Syst. Sci. 8, 1017–1030. https://doi.org/10.5194/hess-8-1017-2004

Viviroli, D., Weingartner, R., Messerli, B., 2003. Assessing the hydrological significance of the world's mountains. Mt. Res. Dev. 23, 32–40. https://doi.org/10.1659/0276-4741(2003)023[0032:ATHSOT]2.0.CO;2

von Freyberg, J., 2015. Groundwater dynamics and streamflow generation in a mountainous headwater catchment Process understanding from field experiments and modeling studies.

Vörösmarty, C.J., McIntyre, P.B., Gessner, M.O., Dudgeon, D., Prusevich, A., Green, P., Glidden, S., Bunn, S.E., Sullivan, C.A., Liermann, C.R., Davies, P.M., 2010. Global threats to human water security and river biodiversity. Nature 467, 555–561. https://doi.org/10.1038/nature09440

Wagener, T., Boyle, D.P., Lees, M.J., Wheater, H.S., Gupta, H. V., Sorooshian, S., 2001. A

framework for development and application of hydrological models. Hydrol. Earth Syst. Sci. 5, 13–26. https://doi.org/10.5194/hess-5-13-2001

Wahren, A., Feger, K.H., Schwärzel, K., Münch, A., 2009. Land-use effects on flood generation - Considering soil hydraulic measurements in modelling. Adv. Geosci. 21, 99–107. https://doi.org/10.5194/adgeo-21-99-2009

Wang, S., Fu, B., Gao, G., Liu, Y., Zhou, J., 2013. Responses of soil moisture in different land cover types to rainfall events in a re-vegetation catchment area of the Loess Plateau, China. Catena 101, 122–128. https://doi.org/10.1016/j.catena.2012.10.006

Wang, S., Fu, B.J., Gao, G.Y., Yao, X.L., Zhou, J., 2012. Soil moisture and evapotranspiration of different land cover types in the Loess Plateau, China. Hydrol. Earth Syst. Sci. 16, 2883–2892. https://doi.org/10.5194/hess-16-2883-2012

Wang, Y., Liu, Y., Jin, J., 2018. Contrast effects of vegetation cover change on evapotranspiration during a revegetation period in the Poyang Lake Basin, China. Forests 9, 1–14. https://doi.org/10.3390/f9040217

Warburton, M., 2012. Challenges in Modelling Hydrological Responses to Impacts and Interactions of Land Use and Climate Change. Challenges Model. Hydrol. Responses To Impacts Interact. L. Use Clim. Chang.

Washington, R., 1996. Mountains and climate, Geography Review. https://doi.org/10.1017/cbo9781139023924.013

Weiss, a, 2001. Topographic position and landforms analysis. Poster Present. ESRI User Conf. San Diego, CA 64, 227–245.

Welch, L.A., Allen, D.M., 2012. Consistency of groundwater flow patterns in mountainous topography: Implications for valley bottom water replenishment and for defining groundwater flow boundaries. Water Resour. Res. 48, 1–17. https://doi.org/10.1029/2011WR010901

Wenninger, J., Uhlenbrook, S., Lorentz, S., Leibundgut, C., 2008. Idenfication of runoff generation processes using combined hydrometric, tracer and geophysical methods in a headwater catchment in South Africa. Hydrol. Sci. J. 53, 65–80. https://doi.org/10.1623/hysj.53.1.65

WFW, 1995. Working for Water A South African Sustainability Case. Water Resour.

Wilcox, B.P., 2010. Ecohydrology Bearing - Invited Commentary Transformation ecosystem change and ecohydrology: ushering in a new era for watershed management. Ecohydrology 130, 126–130. https://doi.org/10.1002/eco

Wilson, J.L., Guan, H., 2013. Mountain-Block Hydrology and Mountain-Front Recharge.

Groundw. Recharg. a Desert Environ. Southwest. United States 9, 113–137. https://doi.org/10.1029/009WSA08

Wilson, J.L., Guan, H., 2004. Mountain-Block Hydrology and Mountain-Front Recharge occurs (as estimated , block system and examine hydrologic processes 9.

World Meteorological Organization, 2008. Guide to Hydrological Practices. Volume I: Hydrology–From Measurement to Hydrological Information, WMO-No. 168.

Wu, C., 2009. Groundwater Occurrence in the Table Mountain Area of Cape Town, South Africa. MPHIL Thesis. Univ. West. Cape.

Wu, H., Li, J., Song, F., Zhang, Y., Zhang, H., Zhang, C., He, B., 2018. Spatial and temporal patterns of stable water isotopes along the Yangtze River during two drought years. Hydrol. Process. 32, 4–16. https://doi.org/10.1002/hyp.11382

Xiaodong, G., Jinren, N., Zhenshan, L., Ronggui, H., Xin, M., Qing, Y., 2013. Quantifying the synergistic effect of the precipitation and land use on sandy desertification at county level: A case study in Naiman Banner, northern China. J. Environ. Manage. 123, 34–41. https://doi.org/10.1016/j.jenvman.2013.02.033

Xing, B., Liu, Z., Liu, G., Zhang, J., 2015. Determination of runoff components using path analysis and isotopic measurements in a glacier-covered alpine catchment (upper Hailuogou Valley) in southwest China. Hydrol. Process. 29, 3065–3073. https://doi.org/10.1002/hyp.10418

Xu, Y., Lin, L., Jia, H., 2009. Groundwater Flow Conceptualization and Storage Determination of the Table Mountain Group (TMG) Aquifers, Water Research Commission.

Xu, Y., Titus, R., Holness, S.D., Zhang, J., Van Tonder, G.J., 2002. A hydrogeomorphological approach to quantification of groundwater discharge to streams in South Africa. Water SA 28, 375–380. https://doi.org/10.4314/wsa.v28i4.4910

Yang, J., Chen, H., Nie, Y., Wang, K., 2019. Dynamic variations in profile soil water on karst hillslopes in Southwest China. Catena 172, 655–663. https://doi.org/10.1016/j.catena.2018.09.032

Yang, W., Wang, Y., He, C., Tan, X., Han, Z., 2019. Soil water content and temperature dynamics under grassland degradation: A multi-depth continuous measurement from the agricultural pastoral ecotone in Northwest China. Sustain. 11. https://doi.org/10.3390/su11154188

Yang, Y., Shang, S., 2012. Comparison of dual-source evapotranspiration models in estimating potential evaporation and transpiration. Nongye Gongcheng Xuebao/Transactions Chinese Soc. Agric. Eng. 28, 85–91. https://doi.org/10.3969/j.issn.1002-6819.2012.24.013

Yang, Z., Hou, F., Cheng, J., Zhang, Y., 2021. Modeling the effect of different forest types on

water balance in the three gorges reservoir area in China, with coup model. Water (Switzerland) 13, 1–15. https://doi.org/10.3390/w13050654

Yeh, H.F., Lin, H.I., Lee, C.H., Hsu, K.C., Wu, C.S., 2014. Identifying seasonal groundwater recharge using environmental stable isotopes. Water (Switzerland) 6, 2849–2861. https://doi.org/10.3390/w6102849

Zhang, Q., Knowles, J.F., Barnes, R.T., Cowie, R.M., Rock, N., Williams, M.W., 2018. Surface and subsurface water contributions to streamflow from a mesoscale watershed in complex mountain terrain. Hydrol. Process. 32, 954–967. https://doi.org/10.1002/hyp.11469

Zhang, R., Zhao, X., Zhang, C., Li, J., 2020. Impact of rapid and intensive land use/land cover change on soil properties in arid regions: A case study of Lanzhou new area, China. Sustain. 12, 1–16. https://doi.org/10.3390/su12219226

Zhao, S., Hu, H., Harman, C.J., Tian, F., Tie, Q., Liu, Y., Peng, Z., 2019. Understanding of storm runoffgeneration in a weathered, fractured granitoid headwater catchment in northern China. Water (Switzerland) 11, 1–22. https://doi.org/10.3390/w11010123

Zhou, J., Liu, G., Meng, Y., Xia, C.C., Chen, K., Chen, Y., 2021. Using stable isotopes as tracer to investigate hydrological condition and estimate water residence time in a plain region, Chengdu, China. Sci. Rep. 11, 1–12. https://doi.org/10.1038/s41598-021-82349-3

Zhou, J., Wu, J., Liu, S., Zeng, G., Qin, J., Wang, X., Zhao, Q., 2015. Hydrograph Separation in the Headwaters of the Shule River Basin: Combining Water Chemistry and Stable Isotopes. Adv. Meteorol. 2015. https://doi.org/10.1155/2015/830306

Zhou, Y., Yang, Z., Zhang, D., Jin, X., Zhang, J., 2015. Comparaison des régimes d'écoulement des bassins des rivières Hailiutu et Huangfuchuan dans le plateau semi-aride d'Erdos du Nord-Ouest de la Chine. Hydrol. Sci. J. 60, 688–705. https://doi.org/10.1080/02626667.2014.892208

Ziadat, F., Taimeh, A., 2018. Effect of rainfall intensity, slope, land use and antecedent soil moisture on soil erosion in an arid environment.

CHAPTER 10: THESIS APPENDICES

10.1 Chapter 4 supplementary material

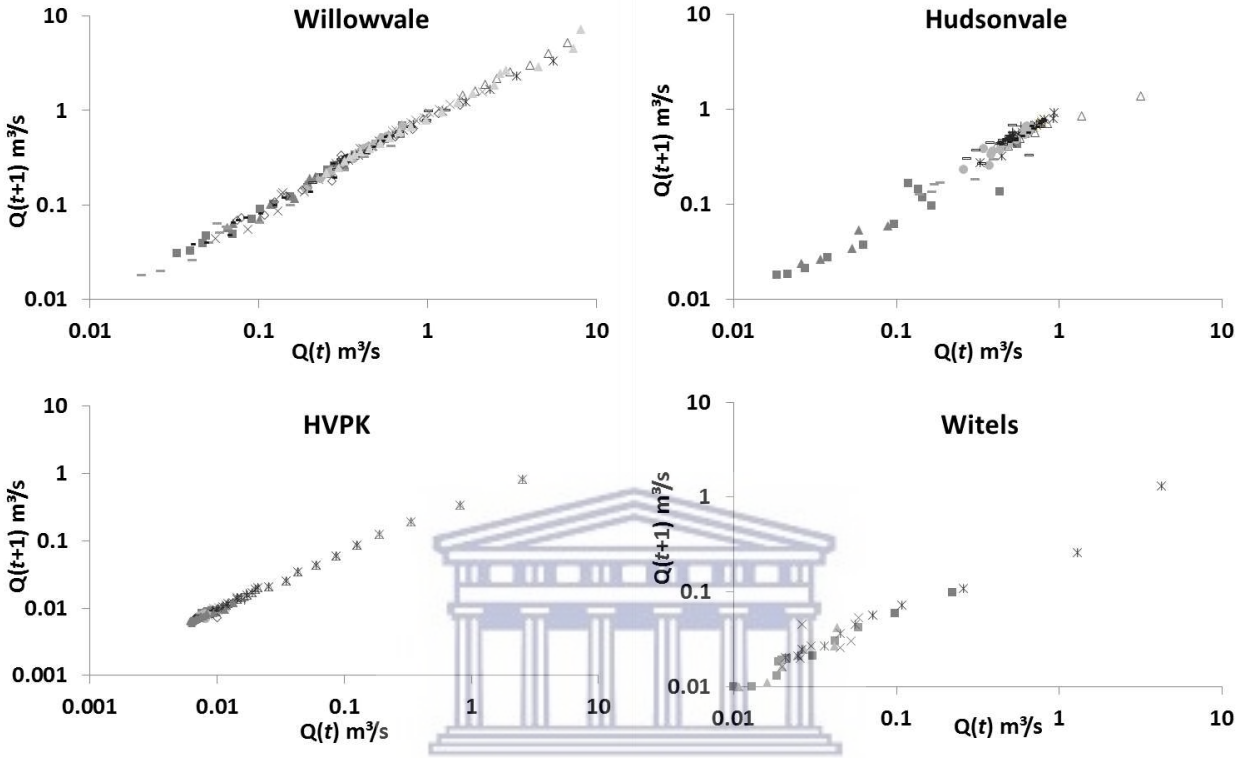

Figure 4A1: Recession patterns for different individual events at each site. The different icons per graph per site represent different recession events.

10.2 Chapter 5 supplementary material

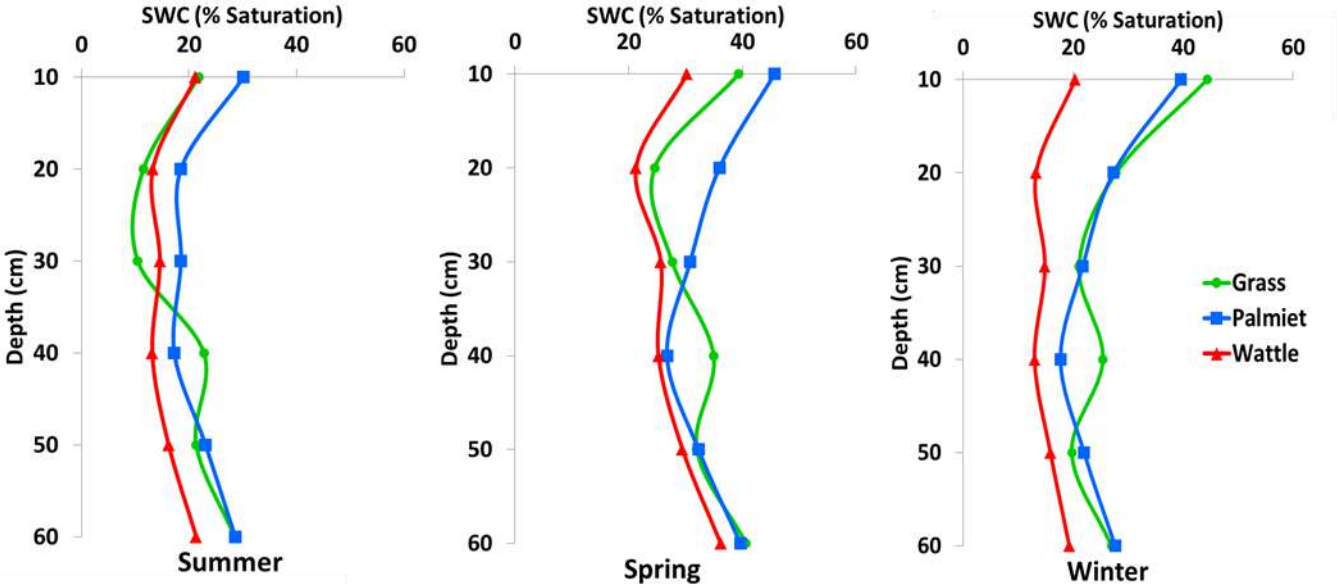

Figure 5A1: Variations in SWC responses with depth at the three sites during different seasons

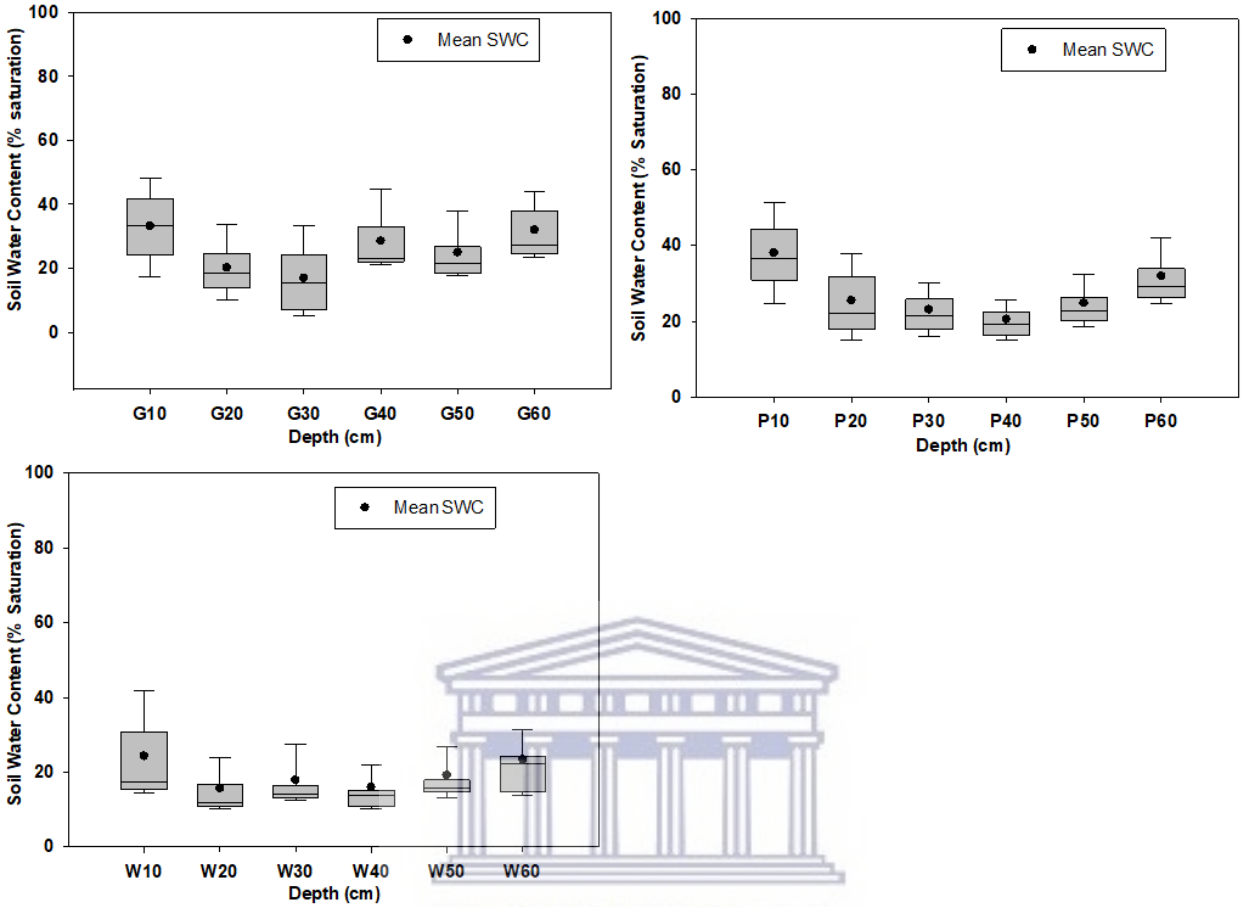

Figure 5A2: Mean soil water content variations at the grass, palmiet and wattle sites

Table 5A1: Analysis of variance between observed SWC at the three sites

Anova: Single					
Groups	**Count**	**Average**	**Variance**		
Grass	751	25.51	66.41		
Palmiet	751	27.56	87.67		
Wattle	751	19.44	143.1		
ANOVA					
Source of Variation	**SS**	**MS**	**F**	**P-value**	**F crit**
Between Groups	26805.17	13402.58	135.3042	3.25E-56	2.999724
Within Groups	222874.1	99.05516			
Total	249679.3				

Descriptive Statistics	Grass	Palmiet	Wattle
Mean	25.51	27.56	19.44
Standard Error	0.3	0.34	0.44
Median	23.88	26.05	16.07
Standard Deviation	8.15	9.36	11.96
Minimum	15.07	16.22	12.04
Maximum	99.31	99.66	99.8
Confidence Level(95.0%)	0.58	0.67	0.86

t-Test: Two-Sample Assuming Unequal Variances

	Grass	Palmiet
Mean	25.50627	27.5631
Variance	66.40531	87.66455
Observations	751	751
df	1472	
t Stat	-4.54109	
P(T<=t) one-tail	3.03E-06	
t Critical one-tail	1.645889	
P(T<=t) two-tail	6.05E-06	
t Critical two-tail	1.961577	

t-Test: Two-Sample Assuming Unequal Variances

	Grass	Wattle
Mean	25.50627	19.43778
Variance	66.40531	143.0956
Observations	751	751
df	1323	
t Stat	11.48966	
P(T<=t) one-tail	1.71E-29	
t Critical one-tail	1.646006	
P(T<=t) two-tail	3.42E-29	
t Critical two-tail	1.961759	

t-Test: Two-Sample Assuming Unequal Variances

	Palmiet	Wattle
Mean	27.5631	19.43778
Variance	87.66455	143.0956
Observations	751	751
df	1418	
t Stat	14.65818	
P(T<=t) one-tail	1.05E-45	
t Critical one-tail	1.645929	
P(T<=t) two-tail	2.1E-45	
t Critical two-tail	1.961638	

10.3 Chapter 6 supplementary material

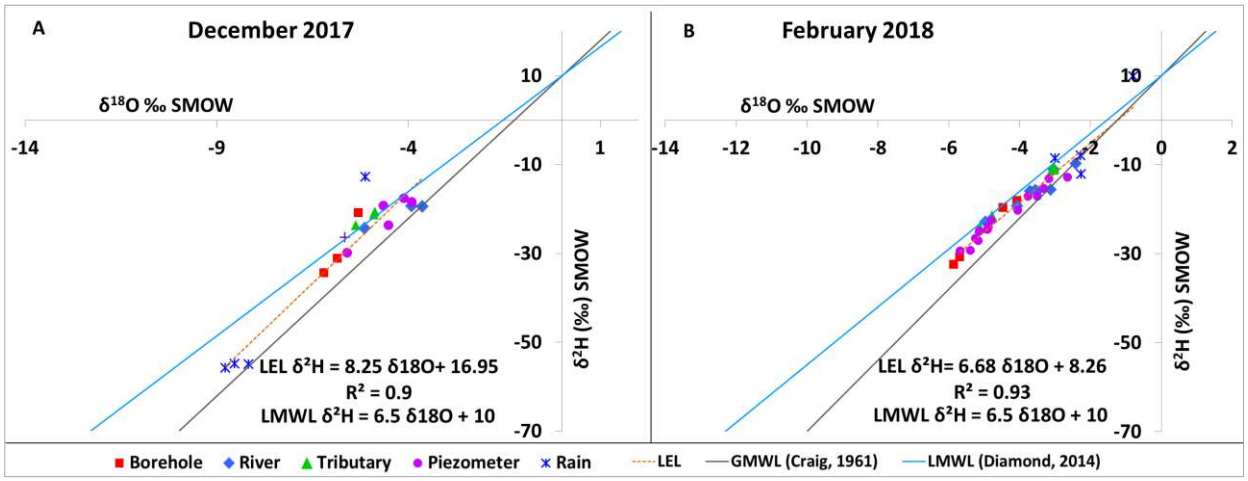

Figure 6A1: δ2H (‰) vs. δ18O (‰) for summer 2017/2018 samples in the Kromme catchment

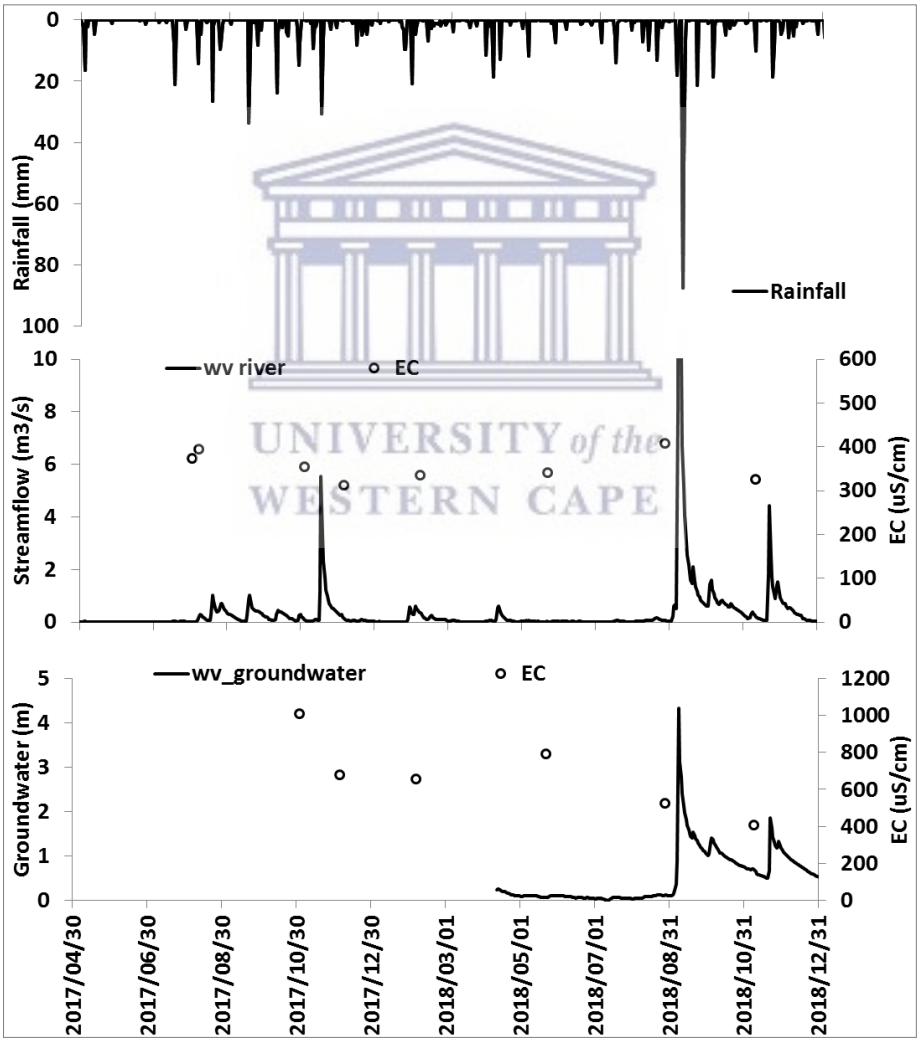

Figure 6A2: EC variation in river and groundwater downstream at Willowvale

Table 6A1. Summary of statistical analysis of EC, CL and $\delta^{18}O$ for deep groundwater samples

Sample Type	Site	Site	Variable	N	*P Value*	Significance
DG vs. SW	KD BH vs. KD RV	Upper catchment	**EC**	8	P = <0.001	SD
			CL	7	P = 0.086	NSD
			$\delta^{18}O$	7	P = <0.001	SD
DG vs. DG	KD BH vs. JBHU	Upper vs. Midcatchment	**EC**	8	P = <0.001	SD
			CL	7	P = 0.007	SD
			$\delta^{18}O$	7	P = 0.555	NSD
DG vs. DG	KD BH vs. JBHL	Upper vs. Midcatchment	**EC**	8	P = <0.001	SD
			CL	7	P = 0.004	SD
			$\delta^{18}O$	7	P = 0.018	SD
DG vs. DG	KD BH vs. PK BH	Upper vs. Midcatchment	**EC**	8	P = <0.001	SD
			CL	7	P = 0.482	NSD
			$\delta^{18}O$	7	P = 0.759	NSD

DG-Deep Groundwater, SW – Surface Water, SGW- Shallow Groundwater, RV – River, TB- Tributary, MR – Main river

Table 6A2. Mean, minimum, maximum and standard deviations of deep groundwater

		Deep Groundwater						
		EC	**pH**	**Temp (C)**	**2H**	**O18**	**Chloride**	**D-Excess**
KDBH	Mean	1033.5	6.8	18.46	-33.25	-5.97	311.6	14.52
	SD	185.6	1.3	1.07	0.94	0.16	162.69	1.52
	Min	705	6.01	17	-34.6	-6.22	145.8	12.76
	Max	1210	9.36	19.9	-32.34	-5.82	519.7	16.92
	Count	6	6	6	5	5	5	5
		EC	**pH**	**Temp (C)**	**2H**	**O18**	**Chloride**	**D-Excess**
JBHU	Mean	283.1	5.91	19.07	-34.67	-6.39	91.54	16.45
	SD	85.5	0.3	0.98	10.09	1.49	52.43	2.21
	Min	88.2	5.41	17.8	-52.89	-9.21	17.5	14.34
	Max	351.2	6.27	20.8	-18.02	-4.07	154.8	20.78
	Count	9	8	9	7	7	7	7
		EC	**pH**	**Temp (C)**	**2H**	**O18**	**Chloride**	**D-Excess**
JGBHL	Mean	236.2	6.39	19.62	-19.42	-4.75	73.09	18.62
	SD	20.76	0.31	1.13	3.25	0.94	49.93	4.45
	Min	219.5	5.93	18.1	-22.7	-5.63	16.5	10.43
	Max	272.6	6.93	21.6	-12.49	-2.87	140.7	23
	Count	9	7	9	7	7	7	7
		EC	**pH**	**Temp (C)**	**2H**	**O18**	**Chloride**	**D-Excess**
PKBH	Mean	477.2	5.81	24.49	-31.03	-5.95	255.94	16.53
	SD	94.1	0.72	7.44	0.4	0.16	102.93	1.48
	Min	230.6	5.01	14.3	-31.72	-6.17	102.6	14.84
	Max	548	7.28	34.1	-30.6	-5.69	418	18.68
	Count	9	9	9	7	7	7	7

Table 6A3. Mean, minimum, maximum and standard deviations of upstream groundwater

Groundwater from the alluvial aquifer -Upper catchment								
KMPZ E		**EC**	**pH**	**Temp (C)**	**2H**	**O18**	**Chloride**	**D-Excess**
	Mean	391.9	5.6	21.2	-31.3	-5.7	175.9	14.3
	SD	43.7	0.3	2.4	1.9	0.4	94.5	3.7
	Min	324.8	5.2	18.0	-33.7	-6.4	79.2	7.0
	Max	467.7	6.0	24.5	-29.4	-5.1	311.7	17.4
	Count	7	7	7	6	6	6	6
KMPZ G		**EC**	**pH**	**Temp (C)**	**2H**	**O18**	**Chloride**	**D-Excess**
	Mean	341.2	5.4	19.2	-30.7	-5.8	181.6	15.8
	SD	55.7	0.2	1.8	4.1	0.7	122.7	1.5
	Min	293.8	5.0	16.5	-37.8	-7.0	68.6	13.9
	Max	434.9	5.6	21.6	-27.4	-5.4	380.0	18.0
	Count	6	6	6	5	5	5	5
KMPZ H		**EC**	**pH**	**Temp (C)**	**2H**	**O18**	**Chloride**	**D-Excess**
	Mean	375.0	5.2	19.9	-20.6	-4.3	207.9	14.0
	SD	62.2	0.3	2.7	4.5	0.9	125.1	3.1
	Min	263.2	4.9	15.8	-27.1	-5.7	97.3	12.1
	Max	429.5	5.6	23.2	-17.5	-3.7	387.6	18.7
	Count	6	6	6	4	4	4	4
KPZ 1		**EC**	**pH**	**Temp (C)**	**2H**	**O18**	**Chloride**	**D-Excess**
	Mean	910.2	5.8	19.0	-31.2	-5.9	431.9	15.9
	SD	83.7	0.2	1.8	5.7	0.8	209.2	1.1
	Min	765.0	5.7	16.6	-40.0	-7.2	139.3	15.3
	Max	990.0	6.1	21.4	-26.3	-5.2	717.0	17.8
	Count	6	6	5	5	5	6	5
KPZ 3		**EC**	**pH**	**Temp (C)**	**2H**	**O18**	**Chloride**	**D-Excess**
	Mean	926.9	5.9	19.6	-27.7	-5.4	256.8	15.7
	SD	370.3	0.2	2.7	1.6	0.5	121.1	3.0
	Min	682.0	5.6	16.8	-30.3	-6.0	112.4	11.3
	Max	1564.0	6.2	23.1	-26.3	-4.7	442.5	19.0
	Count	7	7	6	5	5	6	5

Table 6A4. Mean, minimum, maximum and standard deviations of midcatchment groundwater

Groundwater from the alluvial aquifer -Midcatchment								
HVPZ 4		**EC**	**pH**	**Temp (C)**	**2H**	**O18**	**Chloride**	**D-Excess**
	Mean	804.2	6.1	18.5	-15.3	-3.2	243.5	10.4
	SD	28.0	0.2	3.5	5.4	1.0	112.7	3.3
	Min	773.0	5.7	14.4	-23.6	-4.5	114.9	4.7
	Max	846.0	6.3	23.2	-9.1	-1.7	325.5	13.5
	Count	6	6	6	6	6	3	6
HVPZ 1		**EC**	**pH**	**Temp (C)**	**2H**	**O18**	**Chloride**	**D-Excess**
	Mean	689.9	5.5	17.8	-15.3	-3.6	268.9	13.5
	SD	370.4	0.4	3.8	4.2	0.7	184.0	1.7
	Min	314.4	4.8	12.1	-22.4	-4.7	115.8	11.7
	Max	1498.0	6.0	22.6	-11.6	-2.9	531.3	15.6

	Count	8	8	8	6	6	7	6
HPZ 2		**EC**	**pH**	**Temp (C)**	**2H**	**O18**	**Chloride**	**D-Excess**
	Mean	1299.3	6.2	17.6	-18.7	-4.2	607.0	14.8
	SD	338.7	0.3	3.6	2.2	0.5	447.0	2.6
	Min	761.0	5.7	12.7	-21.0	-5.1	246.9	11.0
	Max	1732.0	6.6	22.0	-15.1	-3.5	1527.0	19.6
	Count	8	8	8	7	7	7	7

Table 6A5. Mean, minimum, maximum and standard deviations of groundwater

Groundwater from the alluvial aquifer -Lower catchment								
WVPZ 7		**EC**	**pH**	**Temp (C)**	**2H**	**O18**	**Chloride**	**D-Excess**
	Mean	432.0	5.5	19.0	-20.3	-4.4	339.0	15.3
	SD	74.8	0.5	2.0	10.4	1.4	194.5	2.8
	Min	353.2	4.9	16.3	-31.5	-5.9	174.0	11.2
	Max	533.0	6.2	21.0	-8.3	-3.2	569.0	17.1
	Count	4	4	4	4	4	4	4
WVPZ 4		**EC**	**pH**	**Temp (C)**	**2H**	**O18**	**Chloride**	**D-Excess**
	Mean	647.7	5.8	19.2	-16.5	-3.8	308.9	13.9
	SD	207.9	0.4	1.7	4.9	1.1	119.2	4.5
	Min	406.2	5.4	16.3	-21.7	-4.7	224.1	5.6
	Max	1010.0	6.4	20.9	-9.4	-1.9	547.0	18.0
	Count	7	7	7	6	6	6	6

Table 6A.6 R^2 and slope values for rainfall, surface and groundwater

	Aug-2017		**Nov-2017**		**Feb-2018**		**May-2018**		**Aug-2018**		**Nov-2018**		**n**
	R^2	**Slope**	**R^2**	**Slope**	**R^2**	**Slope**	**R^2**	**Slope**	**R^2**	**Slope**	**R^2**	**Slope**	
DG	0.89	30	0.9	14	0.99	8.3	0.96	8.7	0.97	**6.5**	0.99	7.6	4
SGW	0.84	7	0.85	7.8	0.97	5.85	0.96	5.8	0.96	5.8	0.97	**6.6**	14
RV	0.8	5.2	0.64	4.1	0.92	5.3	0.95	4.6	0.94	4.9	0.76	3.8	8
Rain			0.97	7.9	0.78	9.4	1	6.68	0.85	10.6	0.87	5.9	4
TB	0.3	0.6	0.55	**6.4**	0.99	**6.4**	0.98	5.8	0.95	6.96	0.97	5.3	4

DG-Deep Groundwater, SW – Surface Water, SGW- Shallow Groundwater, RV – River, TB- Tributary

Table 6A.7: Statistical summary of river pH values

Main river	**pH**				
	Mean	SD	Min	Max	Count
Upper catchment	6.04	0.57	5.09	7	18
Midcatchment	5.86	0.50	4.45	6.53	24
Lower catchment	6.18	0.42	5.5	6.86	10

Table 6A.8: Statistical summary of observed water quality variables in tributaries

Tributaries	EC (µS/cm)	pH	Temp (C)	2H	O18	Chloride	D-Excess
Mean	210	5.98	19.96	-20.84	-4.76	98.63	17.25
SD	67.23	0.53	5.15	4.16	0.72	73.59	2.53
Min	127.6	4.88	10.8	-26.08	-5.71	9.1	11.88
Max	340.9	7	29.7	-10.87	-3.05	269.6	22.36
Count	29	29	29	19	19	19	19

Table 6A.9 Statistical results for EC, CL and $\delta^{18}O$ for SW and GW from the alluvial aquifer samples

Sample Type	Site	Site	Variable	N	*P Value*	Significance
SGW vs. SGW	HVPZ1 vs. WVPZ4	Midcatchment vs. Lower catchment	**EC**	8	P = 0.795	NSD
			CL	7	P = 0.181	NSD
			$\delta^{18}O$	7	P = 0.696	NSD
SGW vs. SGW	HVPZ2 vs. WVPZ4	Midcatchment vs. Lower catchment	**EC**	8	P = <0.001	SD
			CL	7	P = 0.143	NSD
			$\delta^{18}O$	7	P = 0.423	NSD
SW vs. SW	HV vs. WV	Midcatchment vs. Lower catchment	**EC**	8	P = 0.002	SD
			CL	7	P = 0.636	NSD
			$\delta^{18}O$	7	P = 0.493	NSD

SW – Surface Water, SGW- Shallow Groundwater

Table 6A.10 Statistical results for EC, CL and $\delta^{18}O$ samples from all sampled water sources

Sample Type	Site	Site	Variable	N	*P Value*	Significance
DG vs. DG	JBHU vs. JBHL	Midcatchment	**EC**	8	P = 0.179	NSD
			CL	7	P = 0.513	NSD
			$\delta^{18}O$	7	P = 0.031	SD
DG vs. SW	JBHU vs. JBRU	Midcatchment	**EC**	8	P = 0.538	NSD
			CL	7	P = 0.563	NSD
			$\delta^{18}O$	7	P = 0.002	SD
DG vs. SW	JBHU vs. JBRD	Midcatchment	**EC**	8	P = 0.396	NSD
			CL	7	P = 0.367	NSD
			$\delta^{18}O$	7	P = 0.004	SD
DG vs. TB	JBHU vs. JBTU	Midcatchment	**EC**	8	P = 0.002	SD
			CL	7	P = 0.303	NSD
			$\delta^{18}O$	7	P = 0.043	SD
SW vs. DG	JBRU vs. JBHL	Midcatchment	**EC**	8	P = 0.014	SD
			CL	7	P = 0.227	NSD
			$\delta^{18}O$	7	P = 0.048	SD
DG vs. SW	JBHL vs. JBRD	Midcatchment	**EC**	8	P = 0.216	NSD
			CL	7	P = 0.150	NSD
			$\delta^{18}O$	7	P = 0.061	NSD
DG vs. DG	JBHU vs. PK BH	Midcatchment	**EC**	8	P = <0.001	SD
			CL	7	P = 0.003	SD
			$\delta^{18}O$	7	P = 0.449	NSD
DG vs. DG	JBHL vs. PK BH	Midcatchment	**EC**	8	P = <0.001	SD

				CL	7	P = 0.001	SD
				$\delta^{18}O$	7	P = 0.006	SD
DG vs. DG	PK SP	vs. PK BH	Midcatchment	**EC**	8	P = <0.001	SD
				CL	7	P = 0.030	SD
				$\delta^{18}O$	7	P = 0.039	SD
DG vs. TB	PK SP	vs. PK TB	Midcatchment	**EC**	8	P = 0.004	SD
				CL	7	P = 0.299	NSD
				$\delta^{18}O$	7	P = 0.346	NSD
DG vs. TB	PK BH	vs. PK TB	Midcatchment	**EC**	8	P = <0.001	SD
				CL	7	P = 0.040	SD
				$\delta^{18}O$	7	P = <0.001	SD
DG vs. SW	PK BH	vs. HV	Midcatchment	**EC**	8	P = <0.001	SD
				CL	7	P = 0.017	SD
				$\delta^{18}O$	7	P = <0.001	SD
MR vs. TB	HV	vs. PK TB	Midcatchment	**EC**	8	P = 0.036	SD
				CL	7	P = 0.706	NSD
				$\delta^{18}O$	7	P = <0.001	SD
DG vs. SGW	PK BH	vs. HVPZ1	Midcatchment	**EC**	8	P = 0.187	NSD
				CL	7	P = 0.874	NSD
				$\delta^{18}O$	7	P = <0.001	SD
DG vs. SGW	PK BH	vs. HVPZ2	Midcatchment	**EC**	8	P = <0.001	SD
				CL	7	P = 0.066	NSD
				$\delta^{18}O$	7	P = <0.001	SD
SW vs. SGW	HV	vs. HVPZ1	Midcatchment	**EC**	8	P = 0.006	SD
				CL	7	P = 0.066	NSD
				$\delta^{18}O$	7	P = 0.514	NSD
SW vs. SGW	HV	vs. HVPZ2	Midcatchment	**EC**	8	P = <0.001	SD
				CL	7	P = 0.014	SD
				$\delta^{18}O$	7	P = 0.341	NSD
MR vs. TB	HV	vs. WE	Midcatchment	**EC**	8	P = 0.002	SD
				CL	7	P = 0.626	NSD
				$\delta^{18}O$	7	P = 0.426	NSD
TB vs. TB	PK TB	vs. WE	Midcatchment	**EC**	8	P = <0.001	SD
				CL	7	P = 0.459	NSD
				$\delta^{18}O$	7	P = 0.006	SD

DG-Deep Groundwater, SW – Surface Water, SGW- Shallow Groundwater, RV – River, TB- Tributary, MR – Main river

10.4 Chapter 7 supplementary material

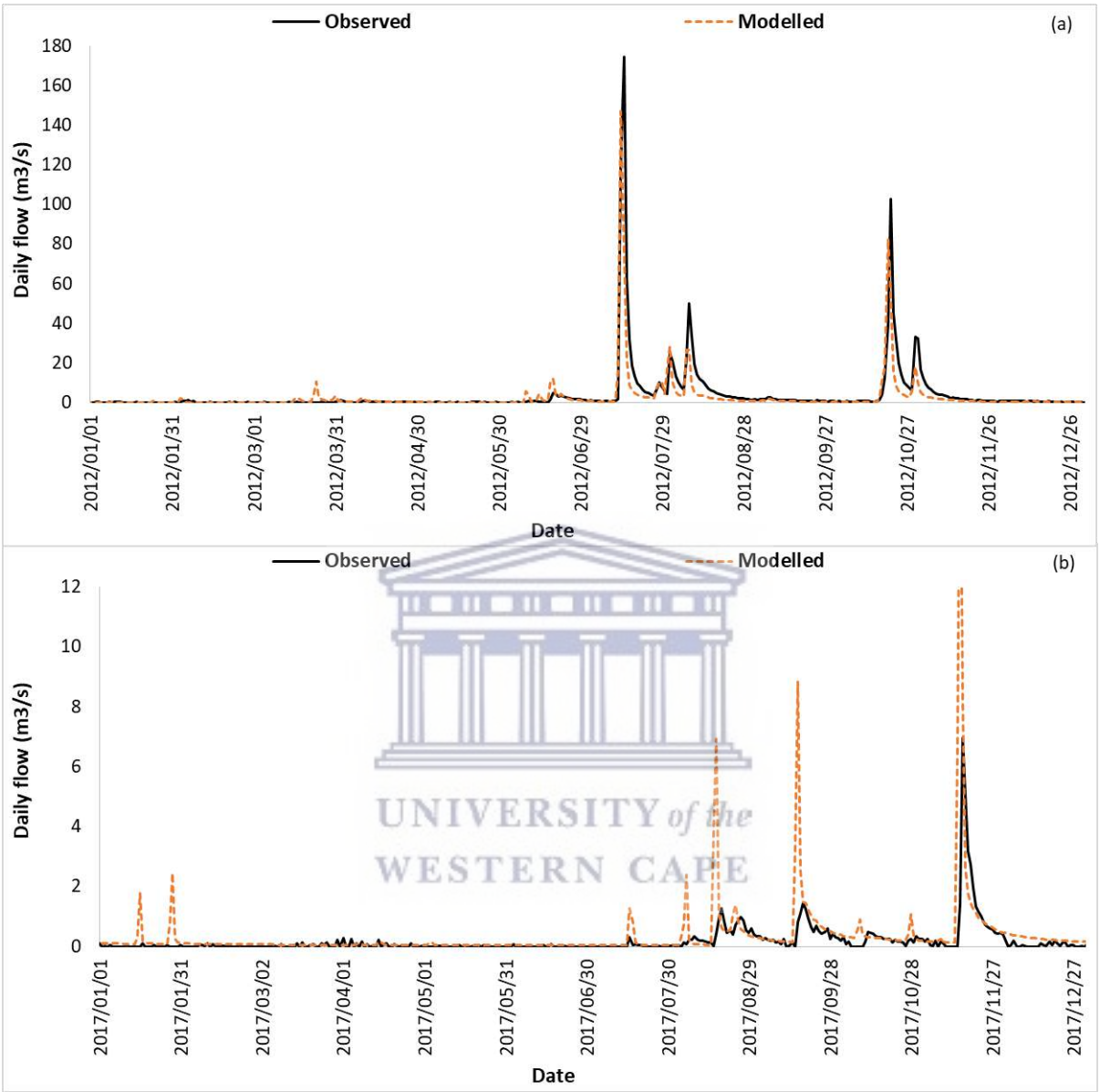

Figure 7A.1: Observed wettest (a) and driest (b) rainfall and streamflow years

Table 7A.1: Runoff ratio from the model for 2017 and 2018

Year	2017	2018
Modelled	0.1	0.2
Observed 1	0.1	0.1
Observed 2	0.1	0.1

Table 7A.2: Dry and wet streamflow and rainfall years

	Rainfall years		Streamflow	
	min	max	min	max
Observed	2017	2012	2017	2012
Modelled	2009	2015	2009	2015

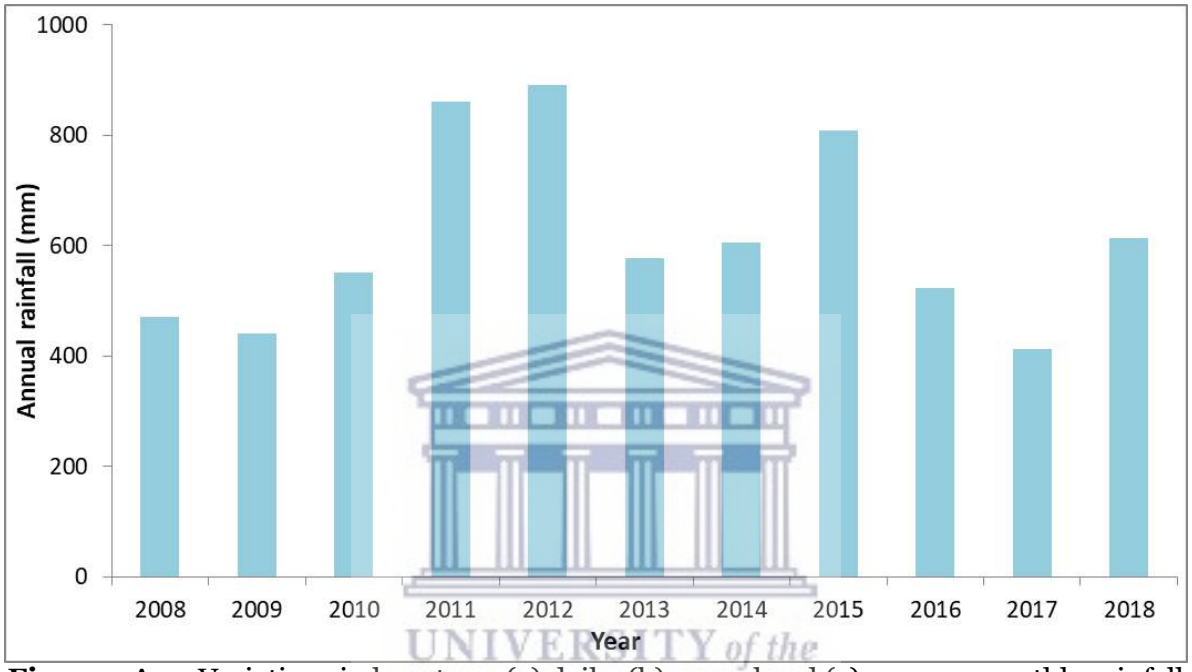

Figure 7A.2: Variations in long term (a) daily, (b) annual and (c) average monthly rainfall

Table 7A.3: Predicted streamflow yield per year in Mm^3

Date	CRNT	PMFP	WTFP	WTALL
2008	16.15	18.17	14.92	8.90
2009	**11.43**	**12.75**	**10.35**	**6.30**
2010	12.44	13.81	11.48	6.00
2011	54.97	56.49	53.29	30.97
2012	85.63	87.55	82.28	53.52
2013	34.22	35.95	32.31	20.41
2014	27.90	29.81	26.14	15.45
2015	**99.92**	**102.06**	**96.06**	**66.44**
2016	12.28	14.19	11.40	5.71
2017	12.08	13.09	11.11	6.34
2018	58.01	59.36	55.29	41.68

Table 7A.4: Variation in peak flows of observed and land cover scenarios (m^3/s)

Year	Observed	CRNT	PMFP	WTFP	WTALL	
2009	5.32	11.41	8.65	11.48	6.04	Low flows

Table 7A.5: Comparison of simulated landcover scenario differences in high vs. low flows

t-Test: Paired Two Sample for Means - Daily runoff (mm)				
	LOW FLOWS		HIGH FLOWS	
Scenario	PMFP	WTFP	PMFP	WTFP
Mean	0.15	0.12	3.36	3.58
Variance	0.05	0.03	27.34	33.04
Observations	3828	3828	190	190
Pearson Correlation	0.90		0.92	
H. Mean difference	0		0	
df	3827		189	
t Stat	23.66		-1.35	
P(T<=t) one-tail	6.8E-116		0.09	
t Critical one-tail	1.65		1.65	
P(T<=t) two-tail	1.4E-115		0.18	
t Critical two-tail	1.96		1.97	

Table 7A.6: Water balance components between modelled scenarios

Water balance components (Mean_Annual_Mm3)						
Flux general	Flux	Location-scale	CRNT	PMFP	WTFP	WTALL
Precipitation	**Precipitation**	**Catchment**	**213.04**	**213.04**	**213.04**	**213.04**
		Mountain	205.81	205.81	205.81	205.81
		Floodplain	7.23	7.23	7.23	7.23
AET total	**AET total**	**Catchment**	**167.87**	**167.72**	**169.71**	**187.45**
		Mountain	158.69	158.68	158.68	177.09
		Floodplain	9.18	9.05	11.03	10.37
Runoff	**NET Runoff (after transmission loss)**	**Catchment**	**38.64**	**40.30**	**36.78**	**23.79**
	Channel transmission loss	Catchment	0.53	0.87	0.56	0.49
Subsurface storage change	**Net SZ storage change**	**Catchment**	**6.52**	**6.49**	**6.54**	**1.93**

Table 7A.7: Predicted flowpaths and processes at the catchment, mountain and floodplain scales for the 2008-2018 period

			Mean annual Mm^3			
Flowpaths and fluxes (general)	Detailed flowpaths and fluxes	Location-scale	CRNT	PMFP	WTFP	WTALL
Surface flow to river	Surface flow entering main river (all flowpaths)	Catchment	21.54	21.96	21.15	13.26
	MTN surface flow into main river (all paths)	MTN & FP	20.29	20.66	19.98	12.31
	Direct MTN surface flow into river	Mountain	5.00	5.00	5.00	2.81
	MTN storm SRO onto FP surface and flow to river	MTN & FP	15.28	15.39	14.97	9.50
	SRO generated on FP and flow into main river	Floodplain	1.25	1.30	1.17	0.95
MTN Subsurface flow	MTN interflow to main river (all paths)	MTN & FP	1.84	2.22	0.90	1.09
	MTN interflow direct into river	Mountain	0.0054	0.0055	0.0054	0.0047
	MTN interflow seep to surface	Mountain	0.10	0.15	0.08	0.04
	MTN interflow to tributary, FP surface, recharge AA, to river	MTN & FP	1.76	1.87	0.82	1.03
	Percolation from UZ (& ponded) to MTN interflow zone	Mountain	41.93	40.10	42.02	26.84
AA flow to river	AA flow into river (all flowpaths)	Floodplain	17.56	19.14	16.13	10.99
	MTN tributary, recharge AA and contribute to river	MTN & FP	12.60	12.86	11.69	7.32
	MTN interflow into alluvial aquifer and into river	MTN & FP	0.05	0.04	0.05	0.04
	MTN bedrock to interflow zone, recharge AA and contribute to river	MTN & FP	7.8E-07	2.6E-07	9.7E-07	-3.4E-07
Floodplain and AA processes	Infiltration on FP (all paths)	Floodplain	24.30	24.61	24.53	19.35
	MTN-sourced SW infiltrating on FP	MTN & FP	18.92	18.91	19.32	13.86
	Recharge from UZ (& ponded) into alluvial aquifer	Floodplain	17.05	18.88	15.54	10.54
	MTN-sourced SW recharge alluvial aquifer	MTN & FP	12.58	13.22	11.66	7.30
	Alluvial aquifer seep to surface	Floodplain	0.15	0.75	0.05	0.03
	Main river loss into alluvial aquifer	Floodplain	0.53	0.87	0.56	0.49
	MTN interflow into alluvial aquifer	MTN & FP	0.0484	0.0457	0.0505	0.0425
Bedrock aquifer fluxes	MTN interflow into bedrock aquifer	Mountain	6.1E-05	6.1E-05	6.1E-05	4.5E-05
	MTN bedrock to MTN interflow zone	Mountain	8.3E-06	8.3E-06	8.3E-06	1.1E-05
	Bedrock aquifer direct into main river	Catchment	3.5E-06	2.9E-06	3.6E-06	3.5E-06

MTN-mountain, FP-floodplain, AA-alluvial aquifer, UZ-unsaturated zone, SRO-surface runoff. NB. The water inputs to the floodplain include precipitation, surface and subsurface flows coming from the mountains. Detailed components listed under each general flowpath or flux include water from different sources therefore do not sum up to the general flowpath of flux